Activation of the transcription factor nuclear factor kappa B in Crohn's disease.

Ellis, Richard David

Activation of the transcription factor Nuclear Factor kappa B in Crohn's disease

A thesis submitted for the degree of Doctor of Medicine

to The University of London

by

Richard David Ellis

2000

Abstract

Nuclear Factor kappa B (NFκB) is an ubiquitous primary transcription factor that plays a central regulating role in many immune and inflammatory responses.

Using immunohistochemistry, significantly increased numbers of cells positive for activated NFκB were demonstrated in all layers of inflamed Crohn's disease bowel, compared to non-inflamed bowel from controls. A significant increase in the number of positive cells was also demonstrated in the submucosa of non-inflamed areas of Crohn's disease bowel, which may therefore be the site of the first changes of Crohn's disease. Cells positive for activated NFκB were identified by morphological criteria as mostly macrophages, with some lymphocytes.

While developing a method to study activation of NFκB using *in situ* hybridisation (ISH), non-specific binding of oligonucleotide probes to eosinophils in sections of bowel was demonstrated. Binding was sequence-dependent, and was prevented by blocking agents followed by high stringency post-hybridisation washes. Hybridisation of poly-d(T) probe to mRNA was demonstrated with low stringency washes, but binding to eosinophils returned under these conditions despite blocking measures.

In vitro binding of oligonucleotide probes to eosinophilic cationic protein (ECP), isolated from eosinophil granules, was demonstrated, and this effect was shown not to be due to the unusually high pI of ECP.

Finally, a relationship between probe hydrophobicity, measured by reverse phase ion-pair high performance liquid chromatography, and *in situ* binding of individual probes to eosinophils was demonstrated. Effective tissue penetration by hydrophobic probes and subsequent strong probe-ECP interactions therefore make ISH, at least with

oligonucleotide probes, impractical in eosinophil-containing tissues, such as bowel. Previous work using oligonucleotide ISH on bowel has not recognised this difficulty and so apparently positive results are likely to have been compromised by this binding of probes to eosinophils.

In conclusion, activation of NFκB, a key event in the inflammatory response, is increased in all layers of inflamed Crohn's disease bowel and in the submucosa of non-inflamed areas, which may therefore be the site of the first changes of Crohn's disease. ECP differentially binds oligonucleotide probes during ISH and the magnitude of this binding is determined by probe hydrophobicity.

Index of contents

CHAPTER 2. MEASUREMENT OF ACTIVATION OF NFκB IN SECTIONS OF HUMAN BOWEL BY *IN SITU* HYBRIDISATION

CHAPTER 3. OLIGONUCLEOTIDE PROBES BIND TO EOSINOPHILIC CATIONIC PROTEIN

LIST OF FIGURES

Chapter 1

Chapter 2

Figure 4. Photomicrographs (above × 100, below × 400) of a frozen section of inflamed large bowel from a patient with inflammatory bowel disease (ulcerative colitis), pre-treated with RNase, with ISH using an oligonucleotide antisense probe cocktail for mRNA for IκBα, showing a similar pattern of positive cells, at reduced levels to that seen without pre-treatment with RNase (Figure 2) (appearances similar with probe cocktails for mRNA for TNFα and poly-d(T) probe).

Figure 5. Photomicrographs (above × 100, below × 400) of a frozen section of inflamed large bowel from a patient with inflammatory bowel disease (ulcerative colitis), with ISH using an oligonucleotide antisense probe cocktail for mRNA for insulin, showing a pattern of positive cells similar to that seen with all other probes; insulin mRNA should not be present in bowel, and therefore the pattern suggests binding of probes to another element.

Figure 6. Photomicrographs (above × 100, below × 400) of a frozen section of inflamed large bowel from a patient with inflammatory bowel disease (ulcerative colitis), with ISH using an oligonucleotide *sense* probe for mRNA for IκBα, showing a pattern of positive cells within the lamina propria similar to that seen with the antisense cocktail (Figure 2), but with fewer positive cells and each positive cell with fewer overlying granules. The concentrations of probe in the sense and antisense hybridisation solutions were equal.

Figure 7. Photomicrograph (x 1000) of a frozen section of inflamed large bowel from a patient with inflammatory bowel disease (ulcerative colitis) with ISH using an oligonucleotide antisense probe cocktail for mRNA for IκBα. The cell with overlying positive granules has a bilobed nucleus and granular cytoplasm, suggesting it to be an eosinophil. Many similar cells had denser overlying positive granules, but this cell was chosen for photography as the underlying cell morphology was easily seen.

Figure 8. Photomicrograph (x 400) of a frozen section of inflamed large bowel from a patient with inflammatory bowel disease (ulcerative colitis) pre-stained with eosin, with subsequent ISH using an oligonucleotide antisense probe cocktail for mRNA for IκBα; all cells with overlying positive granules, indicating binding of probes during ISH, also stained with eosin, suggesting them to be eosinophils (appearances similar with probe cocktails for mRNA for TNFα, IL-4, IL-10 and insulin, and with poly-d(T) probe).

Figure 9. Photomicrograph (x 1000) of a frozen section of inflamed large bowel from a patient with inflammatory bowel disease (ulcerative colitis) stained with 15 % carbol chromotrope for 30 minutes; only the granular cytoplasm of eosinophils stains red.

Figure 10. Photomicrograph (x 400) of a frozen section of nasal polyp from a patient with allergic rhinitis, with ISH using an oligonucleotide probe cocktail for mRNA for IκBα, showing numerous positive cells within the lamina propria (appearances similar with probe cocktail for mRNA for TNFα and insulin, and with poly-d(T) probe).

Figure 11. Photomicrograph (x 400) of a frozen section of rat cerebral cortex, with ISH using an oligonucleotide antisense probe cocktail for mRNA for IκBα, showing no positive cells (appearances similar with probe cocktails for mRNA for TNFα and insulin, and with poly-d(T) probe).

Figure 12. Photomicrograph (x 400) of a section of paraffin-embedded, inflamed large bowel from a patient with inflammatory bowel disease (Crohn's disease), with ISH using an oligonucleotide antisense probe cocktail for mRNA for IκBα, showing a pattern of positive cells within the lamina propria similar to that seen in frozen sections (appearances similar with probe cocktails for mRNA for TNFα and insulin, and with poly-d(T) probe).

Figure 13. Photomicrographs (above × 100, below × 400) of a frozen section of inflamed large bowel from a patient with inflammatory bowel disease (ulcerative colitis) pre-treated with dithiothreitol and iodoacetamide, with ISH using poly-d(T) probe, showing no positive cells, indicating successful blocking of non-specific binding of probe to eosinophils (appearances similar with probe cocktails for mRNA for TNFα and insulin, and with poly-d(T) probe).

Figure 14. Photomicrographs (above × 100, below × 400) of a frozen section of inflamed large bowel from a patient with inflammatory bowel disease (ulcerative colitis) pre-treated with dithiothreitol and iodoacetamide, with ISH using poly-d(T) probe, followed by reduced stringency washes (5 x SSC), showing positive signal overlying all cells, indicating retention of poly-d(T) probe hybridised to the poly-riboadenosine tail on all mRNA.

Figure 15. Photomicrographs (above × 100, below × 400) of a frozen section of inflamed large bowel from a patient with inflammatory bowel disease (ulcerative colitis) pre-treated with RNase, thus removing all mRNA, and then pre-treated with dithiothreitol and iodoacetamide, with ISH using poly-d(T) probe, followed by reduced stringency washes (5 x SSC), showing recurrence of non-specific binding of probe to eosinophils.

Chapter 3

Figure 1. Principle of total internal reflection. Total internal reflection at the interface between two media of different refractive indices causes an evanescent wave in the medium of lower refractive index on the non-illuminated side (adapted from BIA technology handbook (Pharmacia Biosensor, Uppsala, Sweden)).

Figure 2. Principles of biomolecular interaction analysis using a BiacoreX™ instrument.

1. SPR at the sensor chip surface results in a sharp reduction in the intensity of reflected light at a specific angle of reflection (A).

2. The angle (B) changes when analyte binds to ligand on the sensor chip surface.

3. The angles A and B are recorded as changes in 'resonance signal' in RU and plotted against time as a 'sensorgram' (adapted from BIA technology handbook (Pharmacia Biosensor)).

Figure 3. A representative example of one of five injections of antisense 1 probe over ECP and myoglobin in chip A, displayed as overlaid sensorgrams. Similar sensorgrams were plotted for the three other oligonucleotide probes. The large negative deflection of both sensorgrams that occurs at the start of injection represents a combination of the bulk refractive effect and any binding of oligonucleotide probe to ECP or the control protein, myoglobin. A smaller negative deflection of the ECP sensorgram than the control protein sensorgram is observed, due to the expected binding of oligonucleotide probe to ECP, but not to the control protein. The sensorgrams are precisely superimposed but a slower, as well as smaller, negative deflection of the ECP sensorgram is observed (see section 3.6.2 for explanation).

Figure 4. Subtracted sensorgrams (ECP–myoglobin) representing net binding to ECP in chip A for all four oligonucleotide probes. The sensorgrams are representative examples of one of five cycles of injections of probes. They were created by subtraction of the sensorgrams for injection over myoglobin from the sensorgrams for simultaneous injection over ECP for each probe, and represent on-off curves for the interaction between ECP and oligonucleotide probes. The association and dissociation rate constants were calculated using the data contained in the areas of the graphs marked 'A' and 'B' respectively, while the magnitude of binding was measured at an arbitrary point, 80 seconds after the start of injection, marked 'C'. The genesis of the initial large peak at the start of injection and the subsequent large trough at the end of injection is explained in the legend to Figure 3, and their meaning discussed in section 3.6.

Figure 5. Reproducibility of subtracted sensorgrams (ECP–myoglobin) representing five successive bindings of antisense 1 to ECP in chip A. Sensorgrams were created by subtraction of the sensorgrams for injection of probes over the control protein, myoglobin, from the sensorgrams for simultaneous injections over ECP. The graphs demonstrate that the data were highly reproducible, and that the initial large peak at the start of injection and large trough at the end of injection were conserved between injections.

Figure 6. A representative example of one of four injections of antisense 1 probe over ECP and lysozyme in chip B, displayed as overlaid sensorgrams. In contrast to Figure 5, there is no delay in the deflection of the two sensorgrams at the start and end of injection, and in this chip, the bulk refractive effect of the injection solution is negligible.

Figure 7. Subtracted sensorgrams (ECP–lysozyme) representing net bindings to ECP in chip B of all four oligonucleotide probes to ECP. Sensorgrams were created by subtraction of the sensorgrams for injection over the control protein, lysozyme, from the sensorgrams for simultaneous injections over ECP, for each probe. The curves represent *smooth* on-off curves for the interaction between ECP and the four tested oligonucleotide probes, and are the only complete cycle of injections of all four probes in chip B.

Figure 8. Graph displaying means and standard deviations of magnitudes of bindings of different oligonucleotide probes to ECP (×) and to myoglobin (•) in chip A in RU (data displayed in tabulated form in Table 2).

Chapter 5

Figure 1. Photomicrographs (magnification × 1000) of unstimulated (above) and stimulated (below) HeLa Ohio cells grown onto cover slips and immunostained for activated NFκB. Cells were stimulated with TNFα and PMA and fixed in ethanol/formaldehyde. The stimulated cell shows dense nuclear staining (brown, peroxidase-based detection system). The results show, together with results displayed in Figures 2 and 3, that the antibody binds to the nuclei of stimulated cells, which is consistent with its proposed specificity for activated NFκB.

Figure 2. Photomicrographs (magnification × 1000) of negative controls of unstimulated (above) and stimulated (below) HeLa Ohio cells grown onto cover slips and immunostained with substitution of PBS for the primary (anti-p65 NFκB) antibody (brown, peroxidase-based detection system). Cells were stimulated with TNFα and PMA and fixed in ethanol/formaldehyde. The absence of staining confirms that the staining in Figure 1, with use of the primary antibody, is not due to non-specific binding of secondary or tertiary layers of immunostaining, or due to endogenous peroxidase activity.

Figure 3. Photomicrographs (magnification × 400) of a frozen section of mouse cerebral cortex immunostained for activated NFκB (above) showing nuclear staining, and negative control (below) immunostained in the same manner with PBS substituted for the primary antibody (brown, peroxidase-based detection system) and counterstained with Mayer's haematoxylin. Neurones in mouse cerebral cortex are known to constitutively express activated NFκB, and so the results are consistent with the proposed specificity of the primary antibody.

Figure 4. Photomicrographs of the *mucosa* of a frozen section (above, magnification × 100; below, magnification × 400) of inflamed CD bowel (patient 10) immunostained for activated NFκB and counterstained with Mayer's haematoxylin, showing scattered cells positive for activated NFκB (red, alkaline phosphatase-based detection system).

Figure 5. Photomicrographs of the *submucosa* of a frozen section (above, magnification × 100; below, magnification × 400) of inflamed bowel from a patient with CD (patient 10) immunostained for activated NFκB and counterstained with Mayer's haematoxylin, showing scattered cells positive for activated NFκB (red, alkaline phosphatase-based detection system).

Figure 6. Photomicrographs of the *muscle* layer of a frozen section (above, magnification × 100; below, magnification × 400) of inflamed bowel from a patient with CD (patient 10) immunostained for activated NFκB and counterstained with Mayer's haematoxylin, showing scattered cells positive for activated NFκB (red, alkaline phosphatase-based detection system).

Figure 7. Photomicrographs (magnification × 200) of a frozen section (above, mucosa; middle, submucosa; below, muscle) of inflamed bowel from a patient with CD (patient 10) immunostained for activated NFκB with PBS substituted for the primary antibody as a negative control. The sections were not counterstained with Mayer's haematoxylin to ensure background staining was not obscured. No positive cells and minimal background staining is observed (red, alkaline phosphatase-based detection system). The results demonstrate that the positive cells in Figures 4, 5 and 6 were not due to non-specific binding of the secondary or tertiary layers of immunostaining, or due to endogenous alkaline phosphatase activity.

Figure 8. Photomicrograph of a frozen section (magnification × 100) of normal bowel from a control patient (control 6) immunostained for activated NFκB and counterstained with Mayer's haematoxylin, showing few cells positive for activated NFκB (red, alkaline phosphatase-based detection system).

Figure 9. Number of cells positive for activated NFκB per mm^2 in the three layers of normal bowel from control patients, non-inflamed CD bowel and inflamed CD bowel. The levels of significance of comparisons between groups using the Mann-Whitney test are displayed. Horizontal bars indicate median values. Red data points represent patients receiving corticosteroid therapy. The data on which these graphs are based are displayed in Appendix III. The results demonstrate significantly increased tissue-densities of positive cells in all layers of inflamed CD bowel in comparison to normal bowel from controls. In only the submucosa of non-inflamed CD bowel was there a significantly increased tissue-density of positive cells in comparison to normal bowel from controls.

Figure 10. Graph of number of cells positive for NFκB per mm^2 in the *mucosa* of CD patients against the inflammatory score of sections taken from the same biopsy specimen. Specimens taken simultaneously from non-inflamed areas of five patients were included (allocated an inflammatory score of 0) and hence in five patients there are two specimens within this graph. A regression line is fitted and the Spearman's rank correlation coefficient displayed.

Figure 11. Graph of number of cells positive for NFκB per mm^2 in the *submucosa* of CD patients against the inflammatory score of sections taken from the same biopsy specimen. Specimens taken simultaneously from non-inflamed areas of five patients were included (allocated an inflammatory score of 0) and hence in five patients there are two specimens within this graph. A regression line is fitted and the Spearman's rank correlation coefficient displayed.

Figure 12. Graph of number of cells positive for NFκB per mm^2 in the *muscle* layer of CD patients against the inflammatory score of sections taken from the same biopsy specimen. Specimens taken simultaneously from non-inflamed areas of four patients were included (allocated an inflammatory score of 0) and hence in four patients there are two specimens within this graph. A regression line is fitted and the Spearman's rank correlation coefficient displayed.

Figure 13. Photomicrographs of formaldehyde-fixed, paraffin-embedded sections of mouse cerebral cortex pre-treated by microwaving, and then immunostained for activated NFκB (above and middle), showing cytoplasmic staining of neurones within an area of the section (above, magnification × 400), and nuclear staining in another area of the section (middle, magnification × 200), (brown, peroxidase-based detection system). Negative control section (below, magnification × 200) immunostained in the same manner with PBS substituted for the primary antibody showing no positive cells. Sections were counterstained with Mayer's haematoxylin. Results are difficult to interpret, but suggest that when used in microwave pre-treated, paraffin-embedded tissue, the primary antibody is not specific for activated NFκB. Alternatively, the microwave pre-treatment may have altered cytoplasmic stores of NFκB, such that the antibody then binds to them.

Figure 14. Photomicrographs (magnification × 400) of formaldehyde-fixed, paraffin-embedded sections of HeLa S3 cells pre-treated by microwaving, and then immunostained for activated NFκB (brown, peroxidase-based detection system). Cells treated with PMA to activate NFκB (above) show nuclear staining most likely to represent artefact, as suggested by the irregular contour of the nuclear staining and difficulty in reproducing these appearances. Unstimulated cells (middle) show cytoplasmic staining, but no nuclear staining. Negative control section (below) of stimulated cells immunostained in the same manner, but with PBS substituted for the primary antibody, showing no staining. Sections were counterstained with Mayer's haematoxylin.

Figure 15. Photomicrographs (magnification × 400) of formaldehyde-fixed, paraffin-embedded sections of inflamed small bowel from a patient with CD, pre-treated by microwaving and then immunostained for activated NFκB (above), showing cytoplasmic staining of large mononuclear cells, but no nuclear staining (brown, peroxidase-based detection system). Exclusive cytoplasmic staining suggests that in sections of bowel prepared in this way, staining of cells containing nuclear-translocated, activated NFκB did not occur. Negative control section (below) immunostained in the same manner with PBS substituted for the primary antibody showing no positive cells. Sections were counterstained with Mayer's haematoxylin.

Chapter 6

Figure 1. An example of a dotplot of forward scatter versus side scatter characteristics of HeLa cells, showing a gated area, R1, that is designated as representing whole cells. Similar dotplots were obtained for Jurkat T cells.

Figure 2. An example of a DNA histogram. A plot of number of nuclei versus PI fluorescence for a suspension of HeLa cell nuclei. A region, M1, is gated and used for subsequent analysis. Similar histograms were obtained for Jurkat T cell nuclei.

Figure 3. An example of a histogram of number of HeLa cells versus log FITC-fluorescence. Population A is stained with anti-p65 NFκB antibody (Boehringer Mannheim) and population B with isotype control antibody. The region M1 represents fluorescence intensity above the 95th centile of fluorescence intensity of the isotype control antibody-stained population. Similar histograms were obtained for whole Jurkat T cells and suspensions of nuclei of both cell types.

Figure 4. Overlaid histograms of number of cells versus FITC-fluorescence intensity for Boehringer Mannheim anti-p65 NFκB antibody staining of stimulated and unstimulated suspensions of nuclei from HeLa cells prepared and fixed by fixation method A and stained by immunostaining method 1.

Figure 5. Graph displaying integrated percentage of the total analysed population of stimulated and unstimulated suspensions of nuclei from HeLa cells, prepared and fixed by fixation method A, and stained by immunostaining method 1, versus the FITC-fluorescence intensity of anti-p65 NFκB antibody staining. Subtraction of these curves results in the graph displayed in Figure 6.

Figure 6. Graph displaying the result of subtraction of the curve for unstimulated nuclei from the curve for stimulated nuclei in Figure 5. Thus, difference in cumulative percentage of nuclei is plotted against FITC-fluorescence intensity of anti-p65 NFκB antibody staining. The curve may represent measurement of activation of NFκB (see section 4.2).

Chapter 7

Figure. Measured hydrophobicity (retention time in RP-IP HPLC columns in minutes) versus calculated hydrophobicity score of the four oligonucleotide probes for IκBα. Correlation coefficient (r) calculated by Pearson's method.

Appendix I

Figure. Establishing regeneration conditions. Effect of different volumes of regeneration solutions A to C (regeneration injections 1-20, see Table) on the magnitude of binding (displayed in black in RU) of oligonucleotide 1 to ECP (above) and myoglobin (below), and on regeneration of the dextran-ligand surface, as assessed by change in the sensorgram from before injection of probe to after regeneration (displayed in red in RU). The data plotted in these graphs are also displayed in the Table: the graphs allow easy identification of trends, particularly the approximately exponential decay in magnitude of binding of probe to ECP with successive bindings, at least until regeneration solution C is used (starting at regeneration injection 9), while the numerical data in the Table explain conclusions drawn below. Regeneration injections 12-20 are repeated injections of the same volume of the same regeneration solution to verify its properties.

LIST OF TABLES

Chapter 1

Chapter 2

Chapter 3

Table 2. Magnitudes of bindings of different oligonucleotide probes to ECP and to myoglobin in chip A (data displayed in graphic form in Figure 8). In each cycle, each probe was injected once, and the order of injections was changed between cycles. Means and standard deviations of magnitudes of bindings of each oligonucleotide probe are displayed in RU.

Table 3. Differences in magnitude of binding of oligonucleotide probes to ECP and myoglobin (termed net bindings to ECP) in chip A.

Table 4. Magnitudes of bindings of antisense 1 and sense oligonucleotide probes to ECP and to lysozyme in Chip B. In each cycle, antisense 1 and sense probes were injected once. Means and standard deviations of magnitudes of bindings for each oligonucleotide probe are displayed in RU.

Table 5. Rate and equilibrium constants for the interaction between oligonucleotide probes and ECP in chip A (k_a in M^{-1} s^{-1}, k_d in s^{-1} and K_D in M).

Table 6. Rate and equilibrium constants for the interaction between oligonucleotide probes and ECP in chip A. Comparison of sense and antisense oligonucleotide probes.

Chapter 4

Table. Retention times of individual IκBα oligonucleotide probes in IP-RP HPLC columns.

Chapter 5

Table 1. Clinical details of patients from whom operative resection specimens were collected for immunostaining of frozen sections.

Table 2. Clinical details of control patients from whom operative resection specimens were collected for immunostaining of frozen sections.

Table 3. Scanning system for histological assessment of biopsy specimens. An inflammatory score was calculated by adding the scores from four categories, namely enterocytes, mononuclear cells, crypts and neutrophils. Four sections from each biopsy specimen were examined and scored, and the mean of these scores allocated as the final inflammatory score for the specimen.

Table 4. Conversion of histological scores to grades, and categorisation into inflamed and non-inflamed specimens.

Chapter 6

Table 1. Results of experiment where whole *HeLa* cells were fixed in 70 % ethanol (fixation method B) and then immunostained with anti-p65 NFκB antibody (Boehringer Mannheim) and isotype control antibody (immunostaining method 3, two-layer technique). MFIs are displayed. None of the different types of analysis of the data (far left column) produced the expected order of ranking of magnitude for different cell treatments, and it was therefore concluded that the protocol had not resulted in successful staining of activated NFκB.

Table 2. Results of experiment where whole *Jurkat T* cells were fixed in 100 % methanol (fixation method C) and then immunostained with anti-p65 NFκB antibody (Boehringer Mannheim) and isotype control antibody (immunostaining method 3, two-layer technique). MFIs are displayed. None of the different types of analysis of the data (far left column) resulted in the expected order of ranking of magnitude for different cell treatments, and it was therefore concluded that the protocol had not resulted in successful staining of activated NFκB.

Table 3. Results of experiment where whole *HeLa* cells were fixed in 100 % methanol (fixation method C) and then immunostained with anti-p65 NFκB antibody (Boehringer Mannheim) and isotype control antibody (immunostaining method 3, two-layer technique). MFIs are displayed. None of the different types of analysis of the data (far left column) resulted in the expected order of ranking of magnitude for different cell treatments, and it was therefore concluded that the protocol had not resulted in successful staining of activated NFκB.

Table 4. Results of experiment where whole *HeLa* cells were fixed in PFA/Triton-X (fixation method D) and then immunostained with anti-p65 NFκB antibody (Boehringer Mannheim) and isotype control antibody (immunostaining method 2). MFIs are displayed. None of the different types of analysis of the data (far left column) resulted in the expected order of ranking of magnitude for different cell treatments, and it was therefore concluded that the protocol had not resulted in successful staining of activated NFκB.

Table 5. Results of experiment where whole *Jurkat T* cells were fixed in Triton-X/PFA (fixation method E) and then immunostained with anti-p65 NFκB antibody (Boehringer Mannheim) and isotype control antibody (immunostaining method 3, two-layer technique). MFIs are displayed. None of the different types of analysis of the data (far left column) resulted in the expected order of ranking of magnitude for different cell treatments, and it was therefore concluded that the protocol had not resulted in successful staining of activated NFκB.

Table 6. Results of experiment where whole *HeLa* cells were fixed in Ortho Permeafix (fixation method F) and then immunostained with anti-p65 NFκB antibody (Boehringer Mannheim) and isotype control antibody (immunostaining method 3, two-layer technique). MFIs are displayed. None of the different types of analysis of the data (far left column) resulted in the expected order of ranking of magnitude for different cell treatments, and it was therefore concluded that the protocol had not resulted in successful staining of activated NFκB.

Table 7. Results of experiment where whole *Jurkat T* cells were fixed in Ortho Permeafix (fixation method F) and then immunostained with anti-p65 NFκB antibody (Boehringer Mannheim) and isotype control antibody (immunostaining method 3, two-layer technique). MFIs are displayed. None of the different types of analysis of the data (far left column) resulted in the expected order of ranking of magnitude for different cell treatments, and it was therefore concluded that the protocol had not resulted in successful staining of activated NFκB.

Table 8. Results of experiments where *HeLa* cells were fixed and enucleated in 100 % methanol (fixation method A) and then immunostained with anti-p65 NFκB antibody (Boehringer Mannheim) and isotype control antibody (immunostaining method 1, three-layer technique). MFIs are displayed. All the analyses (far left column) of the data from experiment A, except the '% positive cells' analysis, are consistent with the expected order of ranking of magnitude for different cell treatments. However, when the experiment was repeated in B, the order was no longer as expected, with the largest MFI being the 'inhibited' cell population (see section 3.2).

Table 9. Results of experiments where *Jurkat T* cells were fixed and enucleated in 100 % methanol (fixation method A) and then immunostained with anti-p65 NFκB antibody (Boehringer Mannheim) and isotype control antibody (immunostaining method 1, three-layer technique). MFIs are displayed. The experiment was repeated four times (A, B, C and D), but none of the different types of analysis of the data (far left column) consistently resulted in the expected order of magnitude for different cell treatments, and it was therefore concluded that the protocol had not resulted in successful staining of activated NFκB.

Table 10. Results of experiment where *HeLa* cells were fixed and enucleated in 100 % methanol (fixation method A) and then immunostained with anti-p65 NFκB antibody (Santa Cruz) and isotype control antibody (immunostaining method 1, three-layer technique). MFIs are displayed. None of the different types of analysis of the data (far left column) resulted in the expected order of ranking of magnitude for different cell treatments, and it was therefore concluded that the protocol had not resulted in successful staining of activated NFκB.

Appendix I

Table. Establishing regeneration conditions. Effect of injection of different volumes of regeneration solutions A to C on the magnitude of binding, in RU, of oligonucleotide 1 to ECP and myoglobin in chip A, and on regeneration of the dextran-ligand surface in each cell of the chip. Magnitude of binding is calculated as the change in the level of the sensorgram from before injection of probe to 80 seconds after injection. Regeneration is assessed by change in the baseline sensorgram from before injection to after regeneration. The results represent a step-wise evolution of the constitution of the regeneration injection, where the constitution of the next regeneration injection (see section 3.5, Chapter 3 for constitution of solutions A, B and C) to be tested was chosen after assessing the results obtained from the previous regeneration injection. Injections 12-20 are repeated injections of the same volume of the same regeneration solution to verify its effects. Conclusions drawn from these data are discussed below, and the same data are displayed in graphs in the Figure, to allow easy identification of trends.

Appendix III

Table I. Number of hits counted per mm^2 using a Lennox graticule on sections of *inflamed* bowel immunostained for activated NFκB (+ve) and the negative control with PBS substituted for the primary antibody (-ve). In patients with CD, the differences between these counts (Δ) are displayed in a scattergram in Figure 9, Chapter 5.

Table II. Number of hits counted per mm^2 using a Lennox graticule on sections of *non-inflamed* bowel immunostained for activated NFκB (+ve) and the negative control with PBS substituted for the primary antibody (-ve). The differences between these counts (Δ) are displayed in a scattergram in Figure 9, Chapter 5.

Table III. Number of hits counted per mm^2 using a Lennox graticule on sections of bowel from control patients immunostained for activated NFκB (+ve) and the negative control with PBS substituted for the primary antibody (-ve). The differences between these counts (Δ) are displayed in a scattergram in Figure 9, Chapter 5.

Appendix IV

Table. Assessment of reproducibility of counts of cells immunostaining positive for activated NFκB.

Appendix V

Table. Hydrophobicity scores calculated from sequences for oligonucleotide antisense and sense probes used in previous publications.

Appendix VI

Table. Mean percentage nucleotide base content of human liver, sperm and thymus.

Abbreviations and common names

A	adenine
AIDS	acquired immunodeficiency syndrome
BSA	bovine serum albumin
C	cytosine
CD	Crohn's disease
CD	cluster differentiation factor
DEPC	diethylpyrocarbonate
DNA	deoxyribonucleic acid
DNase	deoxyribonuclease
DTT	dithiothreitol
ECP	eosinophil cationic protein
EDTA	ethylenediaminetetraacetic acid
FITC	fluoroscein isothiocyanate
g	gram
G	guanine
HBS	HEPES-buffered saline
HEPES	N-2-hydroxyethylpiperazine-N-2-ethanesulphonic acid
HIV	human immunodeficiency virus
IBD	inflammatory bowel disease
ICAM	intercellular cell adhesion molecule
IEL	intraepithelial lymphocyte
IL	interleukin
IL-2R	interleukin-2 receptor

IFN	interferon
Ig	immunoglobulin
iNOS	inducible nitric oxide synthase
IP-RP HPLC	ion-pair reverse-phase high performance liquid chromatography
ISH	*in situ* hybridisation
KCl	potassium chloride
kDa	kiloDaltons
KOH	potassium hydroxide
l	litre
LPS	lipopolysaccharide
LPMNC	lamina propria mononuclear cell
μ	micro-
m	metre
m	milli-
M	molar
MFI	mean fluorescent intensity
MHC	major histocompatibility complex
min	minute
mRNA	messenger ribonucleic acid
MW	molecular weight
n	nano-
NaCl	sodium chloride
NaOH	sodium hydroxide
NFκB	nuclear factor κ of B cells

NHS/EDC	hydroxysuccinimide and N-ethyl-N'-(dimethylaminopropyl)carbodiimide
PBS	phosphate buffered saline
PC	personal computer
PCR	polymerase chain reaction
PDTC	pyrrolidine dithiocarbamate
pI	isoelectric point
PI	propidium iodide
PMN	polymorphonuclear leucocyte
PMA	phorbol 12-myristate 13-acetate
RNA	ribonucleic acid
RNase	ribonuclease
ROI	reactive oxygen species
rpm	revolutions per minute
RPMI	Roswell Park Memorial Institute
RU	resonance units
SD	standard deviation
SPR	surface plasmon resonance
T	thymidine
TCM	tissue culture medium
TGF	transforming growth factor
TNFα	tumour necrosis factor α
IL	interleukin
SSC	standard saline citrate

UC	ulcerative colitis
UK	United Kingdom
VCAM	vascular cell adhesion molecule
$ZnCl_2$	zinc chloride

Acknowledgements

My thanks to members of The Gastrointestinal Laboratory, The Rayne Institute:

- Dr RPH Thompson for his continuous support, advice and supervision of this project
- Dr N Punchard for proposing the project, for much helpful advice and support, and for review of manuscripts
- Dr JJ Powell for his enthusiastic appraisal and suggestions
- Miss S Majid for her help as a laboratory assistant
- Miss A Rhodda for secretarial help

My thanks to:

- Dr GA Limb of The Department of Immunology, The Rayne Institute for her tuition of the technique of *in situ* hybridisation
- Dr R Poulsom and Mr G Elia of The Imperial Cancer Research Foundation at Lincoln's Inn Fields for their tuition of the technique of immunohistochemistry and their critical appraisal of the results of *in situ* hybridisation experiments
- Dr S Jones of The Retinitis Pigmentosa Laboratory, The Rayne Institute for his help with design of oligonucleotide probes for *in situ* hybridisation experiments
- Dr R Evans and Dr C Janneau of The Department of Biochemistry, United Medical and Dental School of Guy's and St. Thomas' Hospitals for access to use of the BiocoreX™ instrument, and advice on the experiments performed
- Dr P Taylor of Transgenomics Incorporated for performing ion-pair reverse-phase high performance liquid chromatography in Chapter 4
- Professor P Venge of The University of Uppsala for donating purified eosinophilic cationic protein used in Chapter 3

and particular thanks to my wife, Diana, for her long-standing support, to whom I dedicate this thesis.

Aims of the thesis

The initial aim of this thesis was to develop a method of detecting *in situ* activation of the transcription factor NFκB within cells in sections of tissue, and to use this method to study the activation of NFκB in normal and diseased bowel. No such method existed at the start of the work, and it would be used to determine whether activated NFκB is expressed within cells in normal bowel, and whether activation of NFκB is increased in inflammatory bowel disease. In addition, the site of activation within the bowel wall, for instance, surrounding the vasculature or within Peyer's patches, would be investigated, and the cell type containing activated NFκB determined.

Study would be particularly focused on apparently normal, non-inflamed areas of bowel taken from patients with Crohn's disease, to use the properties of NFκB, which is a factor that plays a central, early role in co-ordinating gene expression of numerous inflammatory mediators in response to many pathological stimuli, to determine the site and nature of the first inflammatory events in Crohn's disease. This should improve understanding of the pathophysiology of the disease, and perhaps provide clues to its cause. Furthermore, a potential potent target for new treatments of Crohn's disease would be identified.

Summary of main findings

The main findings of this thesis are:

1. Oligonucleotide probes non-specifically bind to eosinophils within sections of bowel during *in situ* hybridisation (ISH).

2. Non-specific binding of oligonucleotide probes to eosinophils is blocked by pre-treating sections with dithiothreitol and iodoacetamide in ISH experiments using high stringency post-hybridisation washes that remove probe hybridised to target mRNA.

3. Non-specific binding of oligonucleotide probes to eosinophils is not blocked by pre-treatment with dithiothreitol and iodoacetamide when the stringency of post-hybridisation washes is reduced to a level that allows retention of oligonucleotide probe bound to target mRNA. This strongly suggests that the successful blocking of non-specific binding to eosinophils using dithiothreitol and iodoacetamide in ISH experiments with *high* stringency washes was in part due to the effect of high stringency washes removing probe bound to eosinophils.

4. The magnitude of oligonucleotide probe binding to eosinophils varied with probes of differing sequences.

5. Oligonucleotide probes bind *in vitro* to eosinophilic cationic protein (ECP), but not to control proteins. The property of ECP that is responsible for this effect is not its unusually high isoelectric point (pI), as probes did not bind to a control protein with a similar pI.

6. The dissociation constant at equilibrium, indicating affinity, of the interaction between oligonucleotide probes and ECP is of the order 10^{-6} M, indicating moderate affinity, although the interaction is likely to be of high capacity because of the abundance of ECP.

7. Measured parameters of the *in vitro* interaction between individual oligonucleotide probes and ECP, namely magnitudes of binding, association rate constants, dissociation rate constants and dissociation constants at equilibrium, did not explain differential magnitudes of *in situ* binding of the same probes to eosinophils.

8. Hydrophobicities of individual probes, measured by ion-pair reverse-phase high performance liquid chromatography, correlated with differential magnitudes of *in situ* binding of the same probes to eosinophils. Hydrophobicity of oligonucleotide probes limits tissue penetration and so limits the amount of probe available to bind to ECP in eosinophils in sections of bowel during ISH.

9. Cells containing activated NFκB were demonstrated by immunohistochemistry in the lamina propria of normal bowel from control patients.

10. The tissue-density of cells containing activated NFκB was significantly increased in all layers of inflamed bowel from patients with Crohn's disease (CD) compared to normal bowel from controls.

11. The tissue-density of cells containing activated NFκB was significantly increased in only the submucosa of macroscopically and microscopically non-inflamed bowel from patients with CD compared to normal bowel from controls, which suggests that the apparently non-inflamed bowel in CD may be more immunologically active than completely normal bowel from controls, and that the first molecular inflammatory events of CD may occur in the submucosa.

12. Activation of NFκB was restricted mainly to large mononuclear cells, morphologically suggestive of macrophages, suggesting these to be a major cell-type involved in propagating inflammation in CD.

13. Activation of NFκB may be measured in large populations of cells using flow cytometry with a protocol using fixation in 100 % methanol followed by immunostaining with a triple layer technique.

Chapter 1. General introduction

Part A: The NFκB and IκB proteins

1. Discovery of NFκB

In 1986, Sen and Baltimore (1) described a B cell nuclear factor that bound to a site in the immunoglobulin κ enhancer, and this later became known as NFκB. NFκB was soon demonstrated in other cell types (2) and is now known to be ubiquitous (3). Binding sites were found in the promoters and enhancers of many genes, most of which were not B-cell specific, but were generally involved in immunological processes, inflammatory reactions and cell growth and death. In addition, multiple factors were demonstrated to activate NFκB, and so NFκB was identified as a transcription factor that played a central, orchestrating role in many inflammatory and immunologically-mediated events. Activation of NFκB does not require protein synthesis (2), because NFκB exists in a pre-formed state bound to an inhibitory molecule, IκB, within the cytoplasm and is hence described as a 'primary' transcription factor. Several subtypes of NFκB are now recognised that, together with many levels of control of activation and interaction with other transcription factors, allow it to play multiple, diverse roles.

2. Molecular Biology of NFκB

The active forms of human NFκB are dimers, most commonly of a protein of 50 kDa, termed p50, and a protein of 65 kDa, termed p65 or Rel A, which both bind to DNA.

Both subunits contain the same DNA-binding domain of 300 amino acids that are called the NRD domain (4) (NFκB/Rel/dorsal, as it is also found in the related Rel oncoproteins and Drosophila factor, dorsal) or Rel homology domain (5). p50 contains little additional sequence, but p65 contains three independent transcription activating domains that bind with high affinity to decameric consensus sequences in the target genes (commonly 5'-GGGACTTTCC-3', although multiple other similar sequences with reduced affinity are described (6)), usually leading to transcription of the gene.

Both subunits can be independently transported into the nucleus and contain a cluster of positively charged amino acid residues within the NRD that serve as nuclear location signals (NLS).

p50 exists also as a precursor molecule, p105 (also termed NFκB-1), which is essentially a p50 molecule joined to an IκB molecule (7). In addition, three other subunits of NFκB have been described: NFκB-2 (p100), which consists of a p52 subunit, with similar properties to p50, joined to an IκB-like molecule (8); Rel B, which appears to be an alternative to p65 (Rel A) (9), and c-Rel which appears also to be an alternative to p65, but with reduced transcription activating potential (10). Various hetero- and homo-dimers of these subunits have been described, but the most common and most important is the p50-p65 heterodimer (3).

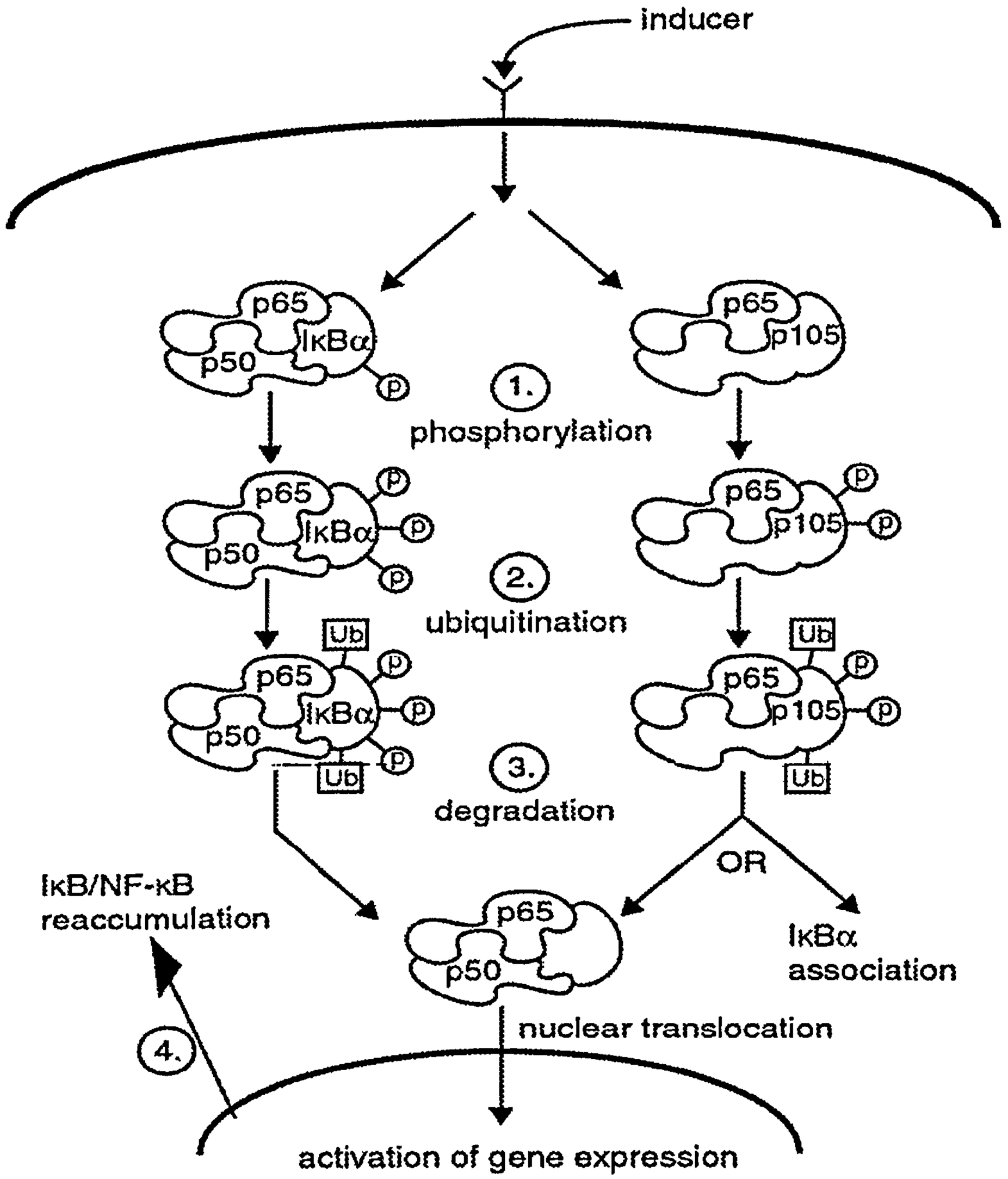

Figure 1. Generalised scheme of activation of NFκB. Following exposure of a cell to an inducer of activation of NFκB, IκB (IκBα, IκBβ or one of the precursor proteins with IκB-like activity, such as p105) is phosphorylated (step 1) by an IκB kinase. IκB is then ubiquitinated (step 2), and finally degraded by the proteasome (step 3). In the case of p105, the degradation is partial, yielding p50. NFκB then translocates to the nucleus (step 4), where it activates a variety of genes (Table 1) including IκBα and p50/p105 (with permission from the Annual Review of Immunology (5). Copyright 1996 by Annual Reviews).

3. Regulation of activation of NFκB

The mechanism of activation of NFκB, and its regulation, are described below and summarised in Figure 1.

3.1 Regulation of activation of NFκB by accessory proteins

Cytoplasmic NFκB is bound to an inhibitory protein, IκB, that prevents its nuclear translocation (11) and transcription activating capacity (12) by direct protein-protein interactions that sterically inhibit interaction of the NLS and NRD domains with their receptors. Furthermore, IκB can dissociate nuclear NFκB-DNA complexes (13) by an allosteric, rather than competitive, mechanism, and removes NFκB from the nucleus. An amino acid sequence that is responsible for its export from the nucleus, termed the 'nuclear export sequence', has been discovered in IκBα (14). Although the predominant form of NFκB, p50-p65 (RelA), is exclusively cytoplasmic until activated, there is evidence that other forms of NFκB may be found constitutively within the nucleus: NFκB-1 (p105) homodimers are found at low levels within the nucleus of many cell types in the unstimulated state (although there is conflicting evidence about the transcription activating potential of this homodimer), and nuclear p50-c-rel heterodimers are found in mature B-cell lines (15).

3.2 Subtypes of IκB

Two main, similar forms of IκB have been described in humans: IκBα (16), a 37 kD protein previously known as MAD-3, and IκBβ, a 46 kD protein (17) that is immunologically distinct. However, both contain the distinctive motif of IκB proteins of multiple, closely adjacent, homologous 33 amino acid sequences called 'ankyrin

repeats'. As described below in more detail, as soon as NFκB is activated, there is a rapid response in transcription of the IκB genes, and newly-synthesised IκB enters the nucleus, removes activated NFκB from DNA and transports the complex back into the cytoplasm. IκBα is produced when cells are stimulated with TNFα and phorbol 12-myristate 13-acetate (PMA), but IκBβ is produced when cells are stimulated with IL-1 or lipopolysaccharide (LPS) (5).

A third IκB protein, IκBγ (18), appears to be limited to mouse B-cells.

Finally, as described above, p105 (NFκB-1) and p100 (NFκB-2), the precursor molecules for p50 and p52 respectively, contain IκB-like sequences that appear to be functionally active in cytoplasmic retention and prevention of activation of transcription.

3.3 Post-transcriptional regulation of activation

Activation of NFκB, described below, is primarily post-transcriptional and, indeed, post-translational.

NFκB is activated when IκB dissociates from NFκB in the cytosol, allowing nuclear translocation of the activated form. The first evidence for this came from a study that demonstrated *in vitro* activation of cytosolic NFκB by treatment with a dissociating agent, the detergent desoxycholate (19) and, from another study, when deactivation of NFκB occurred when purified IκB was added to a preparation of activated NFκB.

Dissociation of IκB occurs by proteolytic degradation, suggested by the rapid disappearance of IκB on stimulation of cells with agents known to activate NFκB, with a half-life for IκB, in these circumstances, of 1.5 minutes. In contrast, in cells in which IκB is experimentally over-expressed, and are not stimulated with agents known to

activate NFκB, the half-life of IκB is over two hours (20). Thus, IκB disappears from cells in which NFκB is activated at a greatly increased rate, which can only be due to proteolytic degradation. Furthermore, a proteolytic enzyme for IκBα has now been identified and found to be a non-lysosymal, ATP-dependent 26S proteolytic complex composed of a 700 kDa proteasome (21-23).

3.4 Proteolytic degradation of IκB is preceded by its phosphorylation and then ubiquitination

The event that initiates eventual activation of NFκB appears to be phosphorylation of IκBα (and probably IκBβ) (24), and in particular, phosphorylation of two serine residues at the N-terminus of IκBα, ser32 and ser36 (25). Phosphorylation of these residues is followed by ubiquitination (addition of a short polypeptide termed 'ubiquitin') of two nearby lysine residues, presumably because phosphorylation results in a change in secondary or tertiary structure that exposes the lysine residues to ubiquitination (26). Ubiquitination of IκBα is followed by its proteolytic degradation (20).

3.5 Control of phosphorylation of IκBα

The events that connect signals at the cell surface to phosphorylation of IκB are the subject of intense investigation. Several protein kinases that control phosphorylation of IκBα in response to different stimuli have been identified, but more may exist:

- Double-stranded RNA activated kinase phosphorylates IκBα *in vitro* (27), and *in vivo* inactivation of this kinase inhibits the ability of double-stranded RNA to activate NFκB (28), but does not block activation of NFκB by TNFα;
- Casein kinase II has also been demonstrated to phosphorylate the C-terminus of IκBα (29,30), and
- mammalian mitogen activated protein 3 kinase-related kinase (MAP3K-related kinase) has recently been shown to participate in the phosphorylation of IκBα in response to stimulation of some TNFα receptors (CD120a and b, also known as p55 and p75 respectively) and type 1 IL-1 receptor (31).

Thus, in response to different stimuli, different kinase cascades may participate in phosphorylation of IκBα, which explains how, perhaps together with other mechanisms as yet unknown, a single transcription factor can play multiple, diverse roles in mammalian cells.

3.6 Role of reactive oxygen intermediates in the activation of NFκB

Initially, reactive oxygen intermediates (ROIs) were thought to be one of the 'final common pathways' by which different NFκB-activating stimuli activated NFκB, perhaps by causing an intracellular rise in hydrogen peroxide, which in some way led to activation of protein kinases. Evidence to support this hypothesis came from the ability of micromolar quantities of hydrogen peroxide to activate NFκB (32), and from inhibition of NFκB activation by certain antioxidants, such as N-acetyl-L-cysteine (33) and pyrrolidine dithiocarbamate (34). This property of antioxidants was conserved despite use of different activators of NFκB.

However, there is evidence that casts doubt on this theory of ROIs as a final common pathway, as in tumour cell lines, experimental over-expression of catalase, which degrades hydrogen peroxide, does not block PMA- and TNFα-induced activation of NFκB (35,36). In addition, the discovery of IκB kinases sensitive to differing NFκB-activating stimuli argues against the existence of a 'final common pathway' preceding the phosphorylation of IκB.

3.7 Transcriptional regulation of activation of NFκB

3.7.1 Transcription of the IκBα gene

Although activation of NFκB is primarily by a post-translational mechanism, deactivation of activated NFκB occurs by re-synthesis of IκB protein, which then displaces activated NFκB from its binding sites to DNA, and transports it back into the cytoplasm. Surprisingly, the transcription of the IκBα gene is primarily controlled by activated NFκB itself, and when IκBα is subsequently translated, a negative feedback loop is completed. Evidence for control of IκBα transcription by activated NFκB comes from four sources:

- IκBα mRNA is constitutively expressed at only very low levels in human T-cells and monocytes, and levels are strongly enhanced by stimuli that activate NFκB (37);
- genetically-coded over-expression of p65 (which is the major transcription activating subunit of NFκB), but not p50 (which has little transcription activating potential), increases levels of IκBα mRNA (37,38);
- inhibitors of activation of NFκB, such as pyrrolidine dithiocarbamate (PDTC), prevent an increase in IκBα mRNA (38), and

- activation of the promoter of the porcine IκBα gene is dependent on the presence and integrity of two κB sites to which activated NFκB can bind (39).

3.7.2 Transcription of the genes encoding the subunits of NFκB

As stated above, transcriptional regulation of IκBα by activated NFκB controls *deactivation* of NFκB. However, there is also evidence that *maintenance* of NFκB activation is dependent on transcription, in this case of the subunits of NFκB itself. In a study in T-cells (40), continued activation of NFκB required new protein synthesis, suggesting that proteolysis of NFκB subunits is a further way in which activated NFκB is deactivated. It is therefore of interest to review how transcription of the genes encoding the various subunits of NFκB are regulated.

p105 (p50) and p100 (p52)

The genes for p105 (p50) and p100 (p52) are constitutively expressed, but levels of their mRNAs rise in response to agents that activate NFκB (41); as with the gene for IκB, there are two κB binding motifs in the promoter of the gene for p105 (42), and similar findings are expected for the promoter of the gene for p100 (3), and so activated NFκB appears to play a major role in regulating production of its subunits. Furthermore, transcription of the subunits of other types of NFκB, such as c-rel and Rel B, are also controlled by activated NFκB (9,43).

p65 (Rel A)

In contrast, the gene for p65 (Rel A) is not under transcriptional regulation by activated NFκB, as agents that activate NFκB do not cause a rise in the level of its mRNA (44), and there is simply a low-level constitutive expression of its mRNA, and hence protein. As stated previously, p65 is the most potent transcription-activating subunit of NFκB, and this continuous, constitutive, low-level expression of its mRNA renders its transcription-activating potential easily controlled by the rapidly-induced IκB, and, to a lesser extent, by p105 and p100, which have IκB-like activity (3).

3.8 Summary of regulation of activation of NFκB

In summary, NFκB is kept in an inactive, dormant state in the cytosol as a pre-formed complex bound to an inhibitory protein, IκB, and control of its activation occurs at both the transcriptional and post-translational levels, which is unique amongst transcriptional activators (3).

4. Genes activated by NFκB

The target genes of NFκB are numerous (Table 1) and most share the common feature of being quickly induced in response to extracellular stimuli. Furthermore, NFκB is activated in response to many different agents (see section 5), and so a rise in activated NFκB is not necessarily informative about a program of gene expression in response to a particular inducing agent. Most of the target genes are involved in immunological activity, and the roles of NFκB in particular contexts have been extensively studied, and are discussed below.

Table 1. Genes activated by NF-κB (6)

CLASS	TARGET GENES
Viruses	Human immunodeficiency virus 1 (HIV-1) (45) Cytomegalovirus (46) Adenovirus (47) Simian virus 40 (48)
Immunoreceptors	Immunoglobulin κ light chains (2) T cell receptor β chain (49) Major histocompatibility complex class 1 (50) Major histocompatibility complex class II (51) Tissue factor (52)
Cell adhesion molecules	Endothelial leucocyte adhesion molecule-1 (53) Vascular cell adhesion molecule-1 (54) Intercellular cell adhesion molecule-1 (55)
Cytokines and haematopoetic growth factors	β-Interferon (56) Granulocyte/macrophage colony-stimulating factor (57) Granulocyte colony-stimulating factor (58) Macrophage colony-stimulating factor (59) Interleukin-2 (60) Interleukin-6 (61) Interleukin-8 (62) TNFα (63) Lymphotoxin (64)
Transcription factors and subunits	IκBα (37,38) p105 (p50) (41) p100 (p52) (41) c-rel (9) Rel B (43)
Others	NO-synthase (65)

4.1 Genes transcribed in response to activation of NFκB during T-cell activation

Over one hundred genes are transcribed in T-cells after stimulation by antigen in the context of the appropriate major histocompatibility complex molecule, or by agents that mimic this interaction (66). NFκB, in combination with other transcriptional regulators, is involved in the expression of many of these genes, especially in the early phase of the response to T-cell receptor stimulation (67).

One of the most important of these genes is that encoding IL-2, which requires NFκB activation for its transcription in response to antigen stimulation of T-cells, but not in response to other T-cell activators such as anti-CD3 (68). However, NFκB plays only one part in an ensemble of regulatory factors involved in initiation of its transcription, and the promoter for IL-2 contains binding sites for multiple transcription activating factors, including NFκB (60), nuclear factor of activated T-cells (NF-AT) (69), activated protein-1 (AP-1) (70), octamer factors (71), purine-rich binding factors (72) and a CD-28 responsive complex (73), and many of these sites must be simultaneously occupied to allow full IL-2 promoter activity (69).

The gene encoding IL-2 receptor (IL-2R) α chain is another important example of a gene whose transcription during T-cell activation is often dependent on NFκB activation. As seen with the gene for IL-2, NFκB participates in IL-2R α chain gene transcription only when T-cells are activated by some mechanisms (by antigen (74-76) and by TNFα (77)), but not by others (phorbol ester (76)).

4.2 Genes in B cells transcribed in response to activation of NFκB

NFκB was first described as a factor that activated the immunoglobulin (Ig) κ light chain gene in B cells (1), and so acquired its name 'nuclear factor κ of B cells'. It was noted that NFκB was constitutively active in mature B cells and plasma cells, but not in pre-B cells, unless stimulated with cytokines or LPS. The constitutively active, nuclear form of NFκB in mature B cells has been shown to be largely the p50-c-Rel heterodimer (15,78), and the p50-p65 form has been found at low levels only in the cytoplasm. The mechanism of this increased activity of the p50-c-Rel form is not clear, but may relate to reduced stability of IκBα and increased transcription of the c-Rel gene (78,79). The function of constitutively active p50-c-Rel and the absence of constitutively active p50-p65 is unproven, but is thought to be maintenance of the mature B cell state with capacity to produce immunoglobulin (3).

NFκB has also been implicated in the transcriptional regulation of a variety of other genes in B cells including those encoding major histocompatibility complex (MHC) class I and II molecules (50,51) and β2 microglobulin (80).

4.3 Function of NFκB in neurones

NFκB has been shown by immunohistochemistry to be constitutively activated in neurones of mouse cerebral cortex and hippocampus, and in primary neuronal cultures derived from rat cerebral cortex by gel shift assay (81). The physiological significance of this finding is unknown, but it may relate to the expression of vascular cell adhesion molecule-1 (VCAM-1), which is involved in neural differentiation and is an NFκB-controlled gene, as a correlation between expression of VCAM-1 and activation of

NFκB has been demonstrated in P19 embryonic carcinoma cell cultures, which act as a model of neural differentiation (82).

5. Agents activating NFκB

Unlike other transcription factors, such as heat shock factor or steroid receptors, which are specifically activated by only one agent, NFκB is activated by numerous agents (Table 2). Such agents can originate from different sites within the cell:

- from the cell surface, such as receptors for cytokines (e.g. IL-1 (83), IL-2 (84), TNFα (83) and lymphotoxin (85));
- from elements of second messenger pathways that are associated with events at the cell membrane, such as phorbol esters and calcium ionophores (2,86);
- from cytoplasmic events such as kinase induction by dsRNA (56) and the inhibition of protein synthesis (2), and finally
- by intranuclear proteins such as the *tax* transactivator of the human T-cell lymphotropic virus 1 (HTLV1) (87).

As discussed above in section 3, the mechanisms by which such diverse stimuli can all activate NFκB is only partially understood, but relates to the complex control of its activation. Furthermore, activation of NFκB by these stimuli does not produce a uniform response, as different types of NFκB can be activated and the eventual gene transcription often depends on interaction with other transcriptional regulators.

Table 2. Conditions activating NF-κB.

CLASS	INDUCING CONDITIONS
Bacterial products	Lipopolysaccharide (2)
Viruses	HIV-1 (88)
	Adenovirus (89)
Viral products	Double-stranded RNA (56)
	X protein of hepatitis B virus (90)
	Latent membrane protein-1 of Epstein-Barr virus (91)
	Human T-cell lymphotrophic virus tax protein (87)
Inflammatory cytokines	TNF α (83)
	Lymphotoxin (85)
	Interleukin-1 (83)
	Interleukin-2 (84)
T-cell mitogens	Antigen (84)
	Lectins (phytohaemagglutinin (2), concanavalin A (92))
	Calcium ionophores (86)
	Anti-CD2 (93)
Others	UV light (94)
	Hydrogen peroxide (95)
Drugs	Phorbolesters (2)

6. The relationship between NFκB and TNFα

TNFα is a potent and rapid activator of NFκB (40,83). Binding of TNFα to cell surface receptors activates a phoshatidylcholine-specific phospholipase C to produce 1,2-diacylglycerol, which then induces an acidic sphingomyelinase to release ceramide from sphingomyelin (96,97). Ceramide is thought to control the activity of specific protein kinases and phosphatases, which then act on mitochondrial membrane proteins and alter mitochondrial production of ROIs resulting in activation of NFκB, perhaps by induction of IκBα kinases (see section 3.5).

Conversely, activated NFκB controls transcription of TNFα (63), but its exact role is unresolved. Three sites homologous to NFκB consensus sequences can be identified in the human TNFα promoter, but are involved in TNFα transcription by only some stimulators of TNFα production. For instance, none are involved in PMA-induced TNFα transcription in human T and B cells (98) and monocytic cells (99), but all are involved in LPS- and virus-induced TNFα transcription in a B cell line (100), and LPS-induced TNFα transcription in monocytic cell lines (101).

Thus, TNFα activates NFκB, and activated NFκB controls transcription of TNFα, forming a positive feedback loop that may augment immune responses.

7. NFκB and disease

Because of its direct role in regulating responses to inflammatory cytokines and endotoxin, the activation of NFκB plays a role in the development of chronic diseases such as atherosclerosis, rheumatoid arthritis, Alzheimer's disease, HIV infection and inflammatory bowel disease (IBD), or in acute situations such as septic shock (studies

relating to rheumatoid arthritis, atherosclerosis and IBD are discussed in greater detail in Chapter 5, section 4.2). Activation of NFκB also plays a role in oncogenesis and apoptosis.

Atherosclerosis

Initiation and progression of atherosclerosis is related to the oxidation of lipids in low density lipoproteins that become trapped in the extracellular matrix of the subendothelial space and apparently activate NFκB, leading to transcriptional activation of genes involved in the inflammatory process (102). Interestingly, mice that are susceptible to atherosclerosis exhibit activation of NFκB when fed an atherogenic diet (103). Thrombin, a serine protease that serves several important roles in inflammatory cells, as well as in cells within vessel walls, stimulates the proliferation of vascular smooth muscle cells through the activation of NFκB (104), and hence may contribute to atherosclerosis. Furthermore, activated NFκB has been demonstrated by immunohistochemical methods in macrophages, endothelium and smooth muscle cells of human atherosclerotic lesions (105). Overall, these data provide substantial evidence that NFκB activation is an important contributor to events leading to atherosclerosis.

Rheumatoid arthritis

Activation of NFκB has been demonstrated by immunohistochemistry in the endothelium and cells of macrophage lineage (type A synoviocytes) in the synovial lining of patients with rheumatoid arthritis (106).

Alzheimer's disease

Alzheimer's disease may also involve chronic activation of NFκB, since the amyloid β peptide causes production of ROIs and activates gene expression through κB sites (107).

HIV infection

As described previously, NFκB plays an important role in the activation of HIV gene expression. Both HIV-1 and HIV-2 have NFκB binding sites close to their transcription start sites within the long terminal repeat (LTR) (108-110) and several studies have documented activation of HIV LTR by activation of NFκB (45,111,112). NFκB may therefore play a role, in concert with other transcriptional activators, in the induction of active viral replication that characterises progression of HIV infection from the early, latent stage to acquired immunodeficiency syndrome (AIDS).

Inflammatory bowel disease

At the start of the investigations described in this thesis, there were no published data concerning the activation of NFκB in IBD. Some studies have been published since then, and are discussed, together with the findings of this thesis, in Chapter 5, section 4.2.

Septic shock

The systemic inflammatory response associated with septic shock is initiated by LPS and other microbial products that stimulate expression of various inflammatory cytokines. It has recently been proposed that the production of nitric oxide in response to LPS regulates important aspects of septic shock (113). These experiments showed that iNOS-deficient mice were protected from septic shock. Since NFκB activates transcription of the iNOS gene (Table 1), activation of NFκB by LPS may play a role in the development of septic shock. Other activators of NFκB, such as TNFα, may also mediate septic shock and augment the inflammatory response through activation of NFκB (114).

Oncogenesis and apoptosis

Evidence for involvement of NFκB or IκB members in oncogenesis is based on several observations (3,115):

- NFκB proteins are members of a proto-oncogene family, and one of its members, v-rel is an altered transcription factor coded for by an avian retrovirus that is forcefully and consistently oncogenic (116);
- the NFκB gene and the *Bcl-3* gene, which encodes a protein with IκB-like properties, are translocated in certain lymphomas (117);
- NFκB is activated by several viral transforming proteins (Table 2) and this effect is thought to be related to the oncogenic properties of these proteins, for instance:

1. HTLV-1 *tax* that is involved in induction of leukaemia in HTLV-1 infection (87);

2. latent membrane protein-1 of Epstein-Barr virus which is implicated in the pathogenesis of Burkitt's lymphoma and nasopharyngeal carcinoma (91), and

3. the X protein of hepatitis B virus which is implicated in the development of hepatocellular carcinoma in chronic hepatitis B infection (90);

- exposure of cells to IκBα antisense results in oncogenic transformation (118), and
- antisense to RelA blocked development *in vivo* of tumours induced by HTLV-1 *tax* (119).

There is also evidence that activation of NFκB may protect against apoptosis, which may explain the oncogenic effect of some members of the NRD family. Of particular interest are recent reports that indicate that inhibiting activation of NFκB renders cell lines, which were previously insensitive, acutely sensitive to the apoptotic effects of TNFα (120,121). Furthermore, knockout mice, deficient of p65, die of massive apoptosis of hepatocytes during embryonic development (122).

8. NFκB as a target for anti-inflammatory and immunosuppressive agents

NFκB has multiple functions in immunological and inflammatory processes and is therefore an attractive target for anti-inflammatory and immunomodulatory therapy. Early experimental evidence suggests agents that prevent activation of NFκB may be effective in inflammatory disorders. A study in mice of p65 antisense oligonucleotide, administered as either a single intravenous bolus or locally via a catheter, improved 2,4,6-trinitrobenzene sulphonic acid-induced colitis as assessed by clinical signs, histological inflammation and cytokine production by isolated lamina propria macrophages (123). In another study, chronic granulomatous colitis induced by intramural injection of peptidoglycan polysaccharide was ameliorated, as judged by

macroscopic inflammatory scores, by intravenous administration of a selective inhibitor of the IκB proteasome (124).

Furthermore, agents already established in the treatment of inflammatory disorders have been found to inhibit activation of NFκB (see below).

Corticosteroids

Corticosteroids bind *in vitro* to cytoplasmic glucocorticoid receptors which directly interact with, and inhibit, activated NFκB (125,126). In addition, corticosteroids increase production of IκBα (127,128) and hence reduce activation of NFκB. These *in vitro* effects may explain their diverse anti-inflammatory effects *in vivo*.

Cyclosporin A

The immunosuppressants, cyclosporin A and tacrolimus (FK506), are known to suppress T-cell activation by inhibiting calcineurin, a calcium-dependent phosphatase, which is involved in the activation of the transcription factor, nuclear factor of activated T-cells (NF-AT). Although this is thought to be their predominant mode of action, they also block activation of NFκB (129,130), which, as described in section 4.1, is also critically involved in the activation of T-cells. This suggests that calcium-dependent mechanisms may be involved in activation of NFκB, which is consistent with the finding of activation of NFκB by calcium ionophores (Table 2).

Salicylates, aminosalicylates and gold

Salicylates inhibit the activation of NFκB at concentrations used to treat arthritis (131) and also inhibit activation of NFκB in stimulated endothelial cell cultures (132). 5-aminosalicylic acid (5-ASA) inhibits activation of NFκB in cultured CaCo-2 cells (133), an action probably mediated by the known anti-oxidant effects of 5-ASA. Furthermore, gold, used in the treatment of rheumatoid arthritis, inhibits activation of NFκB (134).

9. Methods of detecting activation of NFκB

NFκB is a primary transcription factor that is ubiquitously present in an inactive state in the cytosol, and so methods to study the functional importance of NFκB must detect only the activated, nuclear-translocated, IκB-dissociated form.

9.1 Electrophoretic mobility shift assay (EMSA) (135)

Transcription factors interact and bind to specific sequences of DNA and activate transcription of a gene. Only activated NFκB, and not inactive, cytosolic NFκB, binds to DNA, and this property is utilised in EMSAs to detect only the activated form.

In brief, protein extracts from whole cells, or from nuclear fractions of cells (an additional step that ensures only activated, nuclear-translocated NFκB is detected), are incubated with radioactively-labelled oligodeoxynucleotides of the same sequence as the DNA binding site of NFκB. Electrophoresis through a non-denaturing polyacrylamide gel separates free oligodeoxynucleotide from oligodeoxynucleotide bound to NFκB protein, which migrates more slowly and appears as a discrete band on

an autoradiograph. Use of control oligodeoxynucleotides and an excess of unlabelled probes allows confirmation of formation of sequence-specific complexes.

Furthermore, the identity of the oligodeoxynucleotide-binding protein can be confirmed by 'supershifting' the assay by addition of antibody specific to the oligodeoxynucleotide-binding protein, for instance, anti-p65 NFκB antibody. Binding of the antibody to the oligodeoxynucleotide-binding protein complex further slows migration in the gel and results in a 'supershifted band'.

9.2 Western blotting

Traditional Western blotting can detect only activated NFκB, and it requires either successful extraction of nuclear proteins (83) and use of a non-discriminating antibody, or alternatively, use of total cellular protein with an antibody that detects only the activated form of NFκB. At the start of this thesis, no such antibody existed.

9.3 Immunohistochemistry

As for Western blotting, no antibody that detects only the activated form of NFκB existed at the start of the studies contained in this thesis.

9.4 In situ hybridisation (ISH)

No studies exist that use ISH to detect activation of NFκB, but as described in Chapter 2, a method to detect activation of NFκB using ISH was explored.

Part B: Crohn's disease

Crohn's disease (CD) is a chronic inflammatory condition affecting any part of the gastrointestinal tract, but most commonly the terminal ileum and colon, that is usually characterised by a chronic remitting clinical course. Its clinical features, pathology and treatment are well documented, and in the following sections, discussion is mostly limited to areas directly relevant to this thesis.

10. Epidemiology and aetiology

CD appears to be increasing in incidence, with one study documenting a six-fold increase in incidence from the 1960s to the 1980s (136). This increase is unlikely to be accounted for solely by improved case detection or by assignment of a diagnosis of CD to patients with colitis whom may previously have been labelled as suffering from ulcerative colitis (UC).

The aetiology is unknown, but there is evidence to support a genetic component with a clear familial link demonstrated by twin and population studies. In a family with an incident case and an affected first-degree relative, the chance of a second first-degree relative developing CD is increased to between one in ten and one in fifteen, fifty times the population prevalence (137). In a study of twins, 8 of 18 individuals with an affected monozygotic twin developed CD themselves, compared to only 1 of 26 with an affected dizygotic twin (138), which is an equivalent level of concordance to that for insulin-dependent diabetes mellitus, and strongly suggests a genetic component to its aetiology.

There is additional evidence of a genetic component to the aetiology of CD with a weak human leucocyte antigen (HLA) class II association (DR1 Dqw5 (139) and DRB1*07 (140)) with no class I associations, although these associations are generally weaker than for UC. Furthermore, there are indications that chromosome 16 may bear a susceptibility locus for CD, with this site being close to that coding for several cell adhesion molecules (CD 11 integrin cluster, including complement receptor type 3, CD 19 involved in B cell function, and sialophorin involved in leucocyte adhesion) and for interleukin-4 receptor, which suggests that the specific protein coded for by the susceptibility locus, that at present is unknown, is likely to be involved in immune and inflammatory responses. However, the relative risk of this linkage is low at 1.3, and is documented only in families with multiple affected members (141). In another study of sibling-pairs with IBD, linkage at statistically significant levels was reported to marker sites at the same locus on chromosome 16, as well as at loci on chromosomes 3, 7 and 12 for both UC and CD (142).

There have been many hypotheses postulated for the aetiologies of CD, but none is proven, and some of the hypotheses currently under investigation are described below.

10.1 Hypotheses of infective aetiology

An infective cause for CD has been sought since its first description by Crohn in 1932 (143). However, there is epidemiological evidence against an infective aetiology, such as a study that examined childhood socio-economic circumstances of patients with IBD, when access to running hot water and a separate bathroom were associated with *increased* risk of CD (relative risk 5.0 and 3.3 respectively) (144). Furthermore, the

incidence and prevalence of IBD is probably reduced in developing countries compared to that in developed countries, which is contrary to the usual pattern of infectious diseases, and immigrant populations appear to acquire the same incidence as that of the general population of the resident country.

Mycobacterium parartuberculosis

Johne's disease in cattle is caused by *Mycobacterium paratuberculosis* and shares many characteristics with CD, but the bacteria are rarely detectable in CD (145). One study found 65 % of specimens from CD patients positive for *Mycobacterium paratuberculosis* DNA using polymerase chain reaction (PCR), compared to 13 % of controls, and 4 % with UC, but the study was too small for these differences to achieve statistical significance (146). Immunohistochemistry fails to detect *Mycobacterium paratuberculosis* in tissue sections of affected bowel, and serological studies have found conflicting evidence of antibodies to *Mycobacterium paratuberculosis* antigens (147,148). Furthermore, antituberculous chemotherapy has produced inconsistent results in the treatment of CD (149).

Measles

Drawing on the precedent of persistent measles virus causing subacute sclerosing panencephalitis, an hypothesis for persistent measles virus causing CD has been postulated. A study using ISH and immunohistochemistry has demonstrated measles RNA and nucleocapsid protein respectively in CD tissue (150). This finding has been linked to pathological studies that have demonstrated vascular injury, focal arteritis, fibrin deposition and arterial occlusion in the intestinal microcirculation of affected areas of CD (151), with granulomata associated with this vasculitis (152), by the

demonstration of paramyxovirus-like particles by transmission electron microscopy within these granulomata (153).

There is epidemiological data to support a link between measles infection and CD, with infants born during a measles epidemic being significantly more likely (relative risk 1.5) to develop CD in the next 30 years than those born in non-epidemic periods (154). Furthermore, in the same population, four pregnancies were complicated by clinically proven measles infection, and of the four individuals born from these pregnancies, three subsequently developed CD (155). In addition, measles vaccination may increase the risk of developing CD (156), and this has been proposed to explain the apparently conflicting observations of declining measles infections and rising incidence of CD.

10.2 Smoking

Patients with CD who smoke have more aggressive disease and suffer more frequent relapses, and there is a higher prevalence of smoking in patients with CD than in controls (157-160). Furthermore, patients with CD who stop smoking after surgery have a reduced rate of recurrent disease compared to those who continue smoking (161), and these findings provide support for the vascular aetiology of CD. Conversely, there is a reduced prevalence of smoking in patients with UC, with a particularly high incidence in ex-smokers (162,163).

11. Pathology of Crohn's disease

The pathology of CD is well described. The classic description of transmural inflammation, thickened bowel wall and narrowed lumen represents advanced disease, but the first changes of CD are more relevant to this thesis.

Originally described as the first macroscopic change, the aphthoid ulcer is an area of ulceration overlying a Peyer's patch, and with the subsequent recognition of colonic involvement in CD, also overlying colonic lymphoid patches (164). Specialised cells, termed membranous epithelial cells ('M' cells), overlie these lymphoid aggregates, and transport antigens from the lumen to the underlying lymphoid tissue, and may process and present the antigens to macrophages (165,166). This suggests that luminal antigens are important in the pathogenesis of aphthoid ulcers, which is consistent with the clinical observations of the importance of the faecal stream in the recurrence of CD (167).

More recently, endoscopy has allowed identification of more subtle early macroscopic changes that may precede aphthous ulceration, such as patchy erythema and friable mucosa (168), a 'worm-eaten' mucosal pattern (169), and pin-point haemorrhages of the size of a single villus (170). Histological examination of these areas shows inflammatory changes and granulomata suggesting that the disease process is well established at this stage (171). A study using a magnifying colonoscope demonstrated red halos surrounding colonic lymphoid patches that preceded frank aphthous ulceration in CD patients, and scanning electron microscopy of these lymphoid patches showed small erosions of the overlying specialised epithelium (172). These red halos can also be seen using a standard colonoscope in some patients with early CD (Figure 2).

Abnormalities that may reflect events which occur earlier in the pathogenesis of CD are found by histological examination of areas of bowel that are macroscopically/endoscopically normal. Indeed, microscopic inflammatory changes occur in 45 % of biopsy specimens of sigmoidoscopically normal rectum (173), and in patients with CD undergoing upper GI endoscopy, granulomata are seen in 7 % and non-specific inflammatory changes in 25 % of biopsy specimens taken from macroscopically normal gastric antrum and duodenal bulb, although some of the non-specific changes might now be attributed to *Helicobacter pylori* infection (174). Furthermore, areas of CD bowel that are passed as histologically normal on routine examination, are abnormal when studied using additional histopathological methods (see Chapter 5, section 4.2). Thus, microscopic changes often occur in macroscopically normal CD bowel, and study of early molecular events that may *precede* the first inflammatory changes, such as the activation of NFκB, should be focused on bowel that is both macroscopically and microscopically normal (see Chapter 5). In such changes may lie the aetiology of the disease.

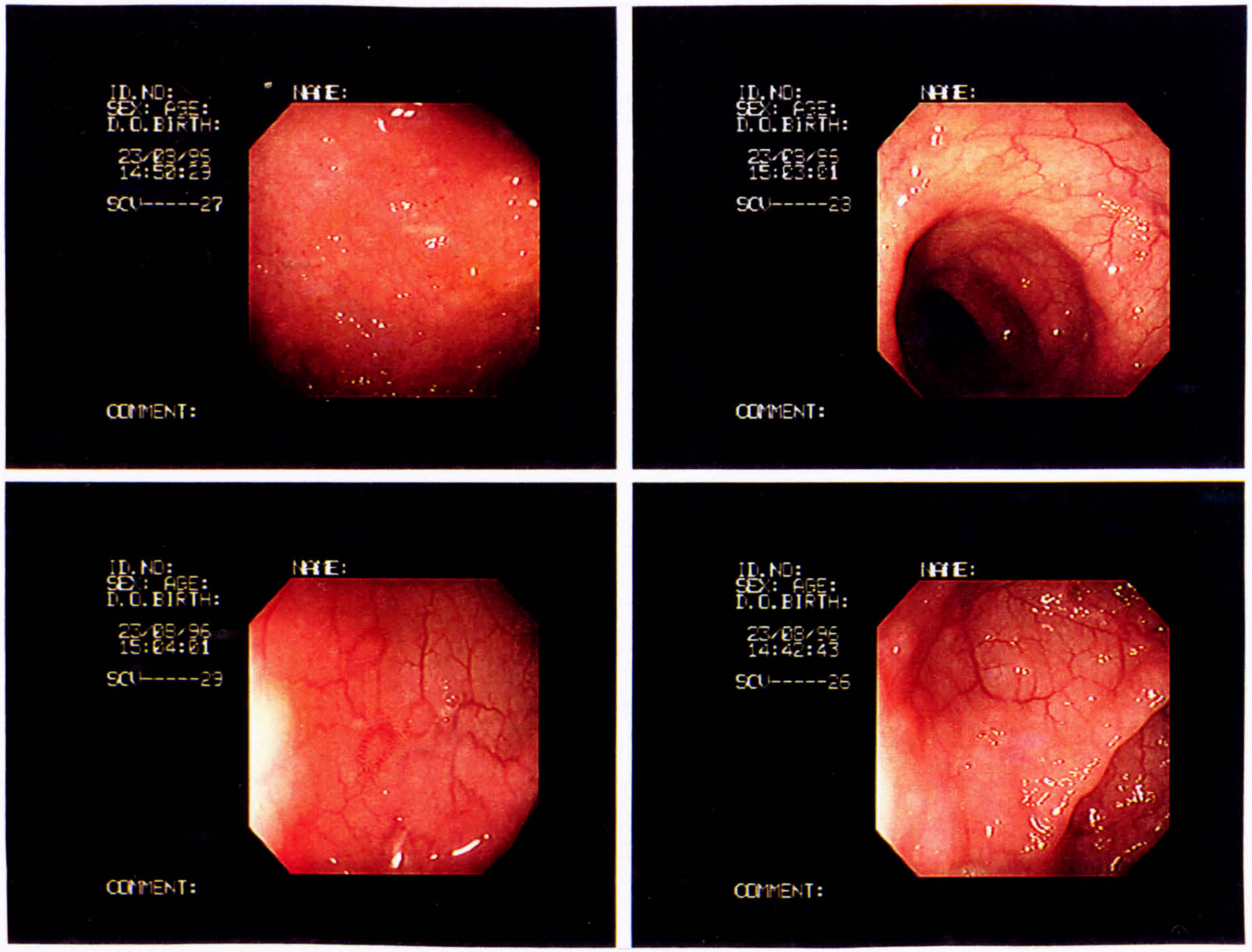

Figure 2. Early lesions of CD. Appearances of the earliest endoscopic appearances of CD, with aphthoid ulcers (top left) and ring-like areas of erythema and pin-point haemorrhages (top right and bottom left).

12. Immunology of Crohn's disease

Inflammatory bowel diseases (IBD) in general, and CD in particular, are thought to result from a complex interaction of susceptibility genes (141), environmental factors and the immune system. The immune system is the final pathway through which inflammation results, and it is possible that susceptibility genes may code for inherent alterations in the immune system that are fundamental to pathogenesis, and the extreme expression of this hypothesis is that there is an abnormal response to a 'normal' stimulus in a genetically susceptible individual (see section 1). Thus, immunological changes that occur in CD are of interest, but interpretation is hampered by the complexity of the gastrointestinal environment, where there is an abundance of food and bacterial antigens. These antigens not only result in a highly complex and brittle immunological state of tolerance in the normal bowel, but also, when the mucosal barrier is breached, may result in a profound secondary inflammatory response that may obscure the initiating abnormality. For these reasons, the immunological features of IBD, described in brief below, are difficult to interpret, and discussion is therefore often restricted to a comparison of the differences in these features between UC and CD.

12.1 Abnormalities of humoral immunity

12.1.1 Immunoglobulins and B cells

The normal protective mucosal immune response is a selective, controlled and localised response of B cells. These properties are to a large extent mediated by the immunoglobulin A response, which is the major immunoglobulin (Ig) produced by the normal intestine. IgA protects by passive aggregation and exclusion of antigen rather

than by activation of the complement cascade or by induction of an intense inflammatory response. In IBD there is a marked increase in total immunoglobulin production, with a relative increase in mucosal IgG production over IgA (175). The relative reduction of IgA production may also be associated with defective IgA function as the subtypes change from polymeric to monomeric forms, and from IgA_2 to IgA_1 (176). In CD, even histologically unaffected jejunum produces significantly less polymeric IgA compared to jejunum from patients with UC. This defect in mucosal humoral immunity may allow increased entry of antigens to the mucosa.

There are differences in the predominant subtypes of IgG produced by the mucosa in UC and CD. In UC, IgG_1 predominates, which is usually produced in response to protein antigens, while in CD IgG_2 predominates, and this is usually produced in response to carbohydrate and bacterial antigens (177), a difference that has led to speculation about environmental triggers for the two diseases.

The changes in lamina propria B cells mirror the changes in Ig production, with total numbers of cells increased in both UC and CD (178,179), but with the relative increase in IgG-producing cells greatest in UC (179).

12.1 2 Autoantibodies

There are associations between UC and several true autoimmune diseases, namely thyroid disease, haemolytic anaemia and vitiligo, and consequently there has been interest in identifying an autoantibody associated with UC. Several candidates have been proposed, but none are sufficiently disease-specific to term a true autoantibody. Epithelial cell associated component antibodies are detected in 70 % of patients with IBD compared to 8 % of controls (180), and in 50 % of healthy relatives of patients with IBD (181) and therefore may represent a marker of genetic susceptibility to IBD.

Colitis colon-bound antibody (CCA-IgG) has been identified in resected, washed UC colon in most patients, but not in CD (182). The antigen for this antibody is now known to be a 40 kD protein belonging to the tropomyosin family and is present in the skin, the eye, on colonic epithelial cells and on bile duct epithelial cells (183). Indeed, a subsequent study identified the antibody in the serum of 13 out of 14 patients with primary sclerosing cholangitis (PSC) associated with UC, but in not one control (184). Thus, this antigen and antibody may in some way be linked to the extra-intestinal features of IBD, but its significance in the aetiology of IBD is unclear.

Perinuclear anti-neutrophil cytoplasmic antibody (p-ANCA) has been identified in 20-90 % of patients with UC and less frequently in CD (185-188). It is particularly prevalent in patients with both UC and PSC (189), is rarely found in patients with UC limited to the rectum, and has been linked with a more aggressive clinical course of UC and with the occurrence of pouchitis after restorative proctocolectomy. It may also be present in a significantly increased proportion of first-degree relatives of patients with UC compared to controls, but studies are conflicting (189-191).

12.2 Abnormalities of cell-mediated immunity

12.2.1 T-cells

T-cells in intestinal lesions assessed by immunohistochemistry

In the lamina propria, the numbers of T-cells are increased in both UC and CD, but the CD4:CD8 ratio remains unchanged at 2:1, as does the proportion of cells expressing HLA-DR (192,193). The proportion expressing activation antigens such as the IL-2 receptor (CD25) (194,195), 4F2 (196) and transferrin receptor (197) is increased.

There is no increase in intra-epithelial lymphocytes (IELs) in CD or UC, except perhaps in CD ileitis (192).

Isolated lamina propria T-cells

Surprisingly few differences have been found in the proportions of subsets of isolated lamina propria T-cells from inflamed areas compared to non-inflamed areas and control specimens, perhaps because the 'normal' intestinal mucosa is in a constant state of activation, held in control by, as yet, undefined mechanisms. However, lamina propria T-cells show an activated phenotype in both UC and CD, such as expression of the IL-2 receptor, transferrin receptor (CD71) and 4F2 antigen (198).

Greater differences have been found between isolated lamina propria T-cells and circulating T-cells in IBD, but this difference may simply reflect the difficulties in isolating cells from the lamina propria, as evidenced by the wide variation in the proportions of subsets of immunological cells in lamina propria isolates in different studies.

Mucosal cytotoxic T-cells

When mucosal mononuclear cells are activated *in vitro* with IL-2, CD cells, despite producing low levels of IL-2, show equal cytotoxicity to control cells, whereas UC cells, which produce substantially less IL-2, show remarkably low cytotoxic activity (199). This suggests that although T-cells are activated in both UC and CD, this does not imply similar function.

Circulating T-cells

T-cells of γδ receptor phenotype are rare in the peripheral blood of normal controls, but are found in large numbers in normal bowel. An increase in circulating T-cells of this phenotype has been demonstrated in IBD (200), and interpreted as the appearance of 'gut-like' T-cells in the peripheral circulation. However, immunohistochemical analysis shows a reduction in these cells among IELs and lamina propria lymphocytes compared to controls (201), probably reflecting a relative increase in the alternative phenotype of αβ receptor cells in inflamed bowel.

12.2.2 Monocytes and macrophages

There is increased production of monocytes in IBD (202), probably related to increased demand for macrophages in inflamed bowel due to increased antigen stimulation because of epithelial damage, and indeed there are increased numbers of $CD68^+$, $L1^+$ monocytes in active IBD lesions, a phenotype implying recent recruitment from the circulation (203).

Normal intestinal macrophages are a heterogeneous cell population, but two main categories are identified: scavenger or mature tissue macrophages (RFD7 antibody

positive) are found predominantly below the epithelium, and interdigitating dendritic antigen-presenting cells are found predominantly in organised lymphoid tissue such as Peyer's patches. This distribution is unsurprisingly disturbed in IBD, and the heterogeneity is accentuated. Thus, there are abundant interdigitating antigen-presenting cells as well as mature tissue macrophages throughout inflamed areas in both UC and CD, and clusters of epithelioid cells are seen in CD (204).

12.2.3 Polymorphonuclear neutrophils, eosinophils and mast cells

There is marked infiltration by polymorphonuclear neutrophils (PMNs) in IBD which are the main source of ROIs and reactive nitrogen metabolites. Chemiluminescence probes detect large quantities of ROIs in the mucosa of patients with CD and UC that correlate with disease severity (205). Elevated levels of nitric oxide and synthase activity have also been demonstrated in both UC and CD colonic tissue (206), and inflamed epithelium shows expression of iNOS that is not seen in normal colonic epithelium (207). IBD mucosa is relatively depleted of antioxidant defences (208), rendering it susceptible to injury by oxidative injury, and aminosalicylates have scavenger activity for superoxide radical formation (209,210).

Increased levels of eosinophils are found both in early and in more established CD lesions (211,212). Eosinophils secrete eosinophilic cationic protein and major basic protein that, *in vitro*, are directly cytotoxic to epithelial cells (213), and secrete IL-5, which activates eosinophils and stimulates production of immunoglobulin by B cells (see section 12.3.1).

12.3 Abnormalities of cytokines

In section 4, abnormalities of cells of the immune system in IBD are described. These cells produce cytokines that activate and stimulate other inflammatory cells, and recruit further cells to the site of inflammation. Consequently, cytokine expression in IBD has been extensively studied to understand the mechanisms that initiate and propagate inflammation in IBD, to identify targets for new anti-inflammatory therapies, and to investigate for a primary abnormality of cytokine production or function that might be important in the aetiology or the mechanisms of the pathogenesis of CD. As discussed in section 4 in relation to abnormalities of *cells* of the immune system in IBD, it is difficult to interpret whether abnormal cytokine profiles are of primary importance, or whether they are simply secondary to the inflammatory process.

12.3.1 Immunostimulatory cytokines

Interleukin-1

IL-1 is a powerful pro-inflammatory cytokine that is produced predominantly by monocytes/macrophages but can be produced by a variety of immune and non-immune cell types. Two isoforms exist, a membrane-bound form, termed IL-1α, and a secreted form, termed IL-1β, and both mediate the same biological activities (214). The first study of IL-1 in IBD showed no significant increase in production as assessed by a biological proliferation assay of stimulated PBMNCs (215). However, a subsequent study, using a similar bioassay, showed increased spontaneous production by PBMNCs from CD patients (216) and this was confirmed in subsequent studies using immunoassays on stimulated PBMNCs (217,218). Furthermore, significantly

increased levels of IL-1β immunoreactivity were found in supernatants of unstimulated and stimulated lamina propria mononuclear cells (LPMNCS) taken from active lesions of both UC and CD, compared to control samples (219). The cellular source of these proteins has been shown by immunocytochemistry to be endothelial cells and colonocytes (220), but this was not confirmed in a study using ISH (221). In another study investigating IL-1 bioactivity and protein and gene expression, LPMNCs were demonstrated to be a source of IL-1 (222). As might be expected, increased levels of IL-1 are not specific to IBD and are found in other forms of gut inflammation (223).

The biological activity of IL-1 is now recognised to be determined by the balance between levels of IL-1 and its antagonist, IL-1 receptor antagonist (IL-1ra), and tissue levels of IL-1ra are elevated in IBD (224), but with a *relative* deficiency of IL-1ra in comparison to IL-1, in IBD compared to controls (225).

Interleukin-6

IL-6 has many pro-inflammatory effects and is produced by a range of cells of the immune system. Levels in peripheral blood are raised in CD but not in UC, and correlate well with other assessments of disease activity such as C-reactive protein (226). However, high levels of IL-6 mRNA in inflamed tissue were demonstrated in both UC and CD by PCR (227), with similar findings in supernatants of cultured LPMNCs (228). The significance of this difference in circulating and tissue levels between the two diseases is uncertain.

TNF α

TNFα is produced predominantly by macrophages, although it can be produced by lymphocytes and, like IL-1 and IL-6, it induces a wide range of pro-inflammatory effects and is a prime mediator of the systemic host response (229). Although it is thought to play an important role in UC and probably a larger role in CD, results of studies are conflicting. One study demonstrated significantly elevated serum levels in children with active UC and colonic CD (230), while another found no increase over normal controls (231). As with IL-1 and IL-1ra, a better assessment of TNFα activity may be made by assessing levels of both TNFα and its receptors, p55 and p75, which have neutralising capacity, and circulating levels of both receptors are elevated in CD compared to controls (232).

The concentration of TNFα in stools of children with both active CD and UC is elevated (233). TNFα mRNA measured by PCR was detected with similar frequency in mucosal biopsy specimens from patients with IBD and controls (227), but use of ISH to detect TNFα mRNA in IBD mucosa yielded positive results in macrophages in 11 of 15 patients with IBD and 4 of 9 controls (221).

Despite the conflicting evidence for involvement of TNFα in IBD, treatment of patients with refractory CD with chimeric monoclonal anti-TNFα antibody appears to be effective, although the mechanism is unclear (234).

Interleukin-5

IL-5 stimulates B cells to produce immunoglobulin and activates eosinophils. Again, evidence is conflicting concerning its role in IBD with increased levels of mRNA detected by ISH in CD (212), but no increase was found when IL-5 mRNA was

assessed by quantitative reverse transcriptase PCR performed on homogenates of mucosal biopsy specimens (235). Another study reported reduced IL-5 protein production by cultured LPMNCs in CD, and increased production in UC (236). The discrepancy in IL-5 mRNA levels measured by different techniques and IL-5 protein production in CD may be explained by, as yet, undetected methodological problems that are explored in Chapter 2.

Cell adhesion molecules

There is evidence of dysregulation of cell adhesion molecule expression in IBD with increased expression of ICAM-1 on mucosal mononuclear phagocytes (237) and increased ICAM-1, leucocyte function antigen-1 and E-selection on venules in involved mucosa (238,239). However, expression of VCAM-1 is not increased in inflamed IBD mucosa (239).

12.3.2 Immunoregulatory cytokines

Interleukin-2

IL-2 is the prototypical immunoregulatory cytokine and is produced by T-cells and modulates almost every step of T-cell function as well as function of many other cells of the immune system, and has consequently been widely studied in IBD. Circulating IL-2 is generally not detectable in health or disease, but IL-2 bioreactivity in cultures of LPMNCS was first reported to be reduced in both UC and CD (240). Subsequently, increased levels of IL-2 mRNA in active CD, but not UC, was detected by reverse-transcriptase PCR (241). Moreover, cultured T-cells from patients with UC and CD respond differently to IL-2, with a weak response in UC and a hyper-reactive response in CD. Furthermore, patients with CD given IL-2 for treatment of malignancies suffer

relapses of CD (242), and patients with AIDS often develop remission of CD, perhaps because of loss of IL-2-secreting cells (243). Consistent with the hypothesis that in UC there is IL-2 hyporeactivity and in CD, IL-2 hyper-reactivity, is the finding of a spontaneous UC-like disease in IL-2 gene knockout mice (244).

Elevated levels of soluble IL-2 receptor (sIL-2R) have also been demonstrated in IBD (245). In another study, these elevated levels correlate with LPMNC production in CD, but with PBMNC production in UC (246), and in a separate study by the same group, levels of mRNA for IL-2Rα and IL-2Rβ (subunits of the receptor) in LPMNCs were elevated in CD but not UC, supporting the concept of T-cell hyper-reactivity in CD (247).

Interferon-γ

IFN-γ is produced by T-cells and natural killer cells and mediates a wide range of immunomodulatory effects, including the induction of MHC class II molecule expression on antigen-presenting cells, a function particularly relevant to the bowel. Although initial reports suggested reduced production in IBD (248), subsequent reports suggested increased production may occur in CD, as indicated by spontaneous release of IFN-γ and increased mRNA in LPMNCs, and the presence of IFN-γ-secreting cells in inflamed mucosa (249,250). Induction of IFN-γ production is dependent on IL-12 production by monocytes/macrophages, and a recent study has shown increased spontaneous and mitogen-induced production of IL-12 by mucosal cells in CD (251), but not in UC or controls, which strengthens the hypothesis of a T helper 1-type (Th-1) cytokine pattern in CD (IL-12- and transforming growth factor β-

induced predominant production of IL-2, IFN-γ and lymphotoxin by T helper cells) (252).

Interleukin-4

IL-4 is produced by T-cells and has predominantly anti-inflammatory immunoregulatory effects on B-cells. Studies of its role in IBD are conflicting, with production by LPMNC cultures reported to be reduced in both UC and CD (236,253), but with elevated tissue levels of IL-4 mRNA in UC, but not CD (235). However, a recent study reported increased tissue levels of IL-4 mRNA in early post-surgical recurrences of CD (254).

12.3.3 Growth factors

Transforming growth factors (TGF) α and β are important mediators of intestinal epithelial restitution and defence, and levels of TGFβ, but not of TGFα, are increased in active CD and UC lesions, whereas in quiescent IBD the reverse is found (255). This has led to the hypothesis that enhanced TGFβ may promote healing, whilst increased TGFα production may cause epithelial hyperproliferation and contribute to the increased risk of intestinal malignancy in IBD.

12.4 Abnormalities of eicosanoids

There is evidence documenting increased levels of prostaglandins in IBD that fall with successful treatment (256,257), and other arachadonic acid derivatives such as thromboxanes, prostacyclins and leukotriene B_4 are all also elevated in IBD (258,259).

12.5 Abnormalities of complement

Unsurprisingly, there is evidence of increased complement activation in IBD, which is likely to mediate tissue destruction and chemoattraction of inflammatory cells (260).

12.6 Animal models of IBD induced by immune dysregulation

There are now many animal models of IBD induced by immune dysregulation, which illustrate that chronic intestinal inflammation can be the result of a primary immunoregulatory defect, with the more recent models demonstrating the central role of T-cells and their immunoregulatory cytokines. One of the first studies demonstrated gut inflammation by transfer of $CD45RB^{high}$, CD4 T-cells (a functionally distinct subset of T helper cells) into mice with severe combined immunodeficiency, and the resulting colitis was characterised by high levels of IFN-γ and TNFα (261).

A feature of several models is the importance of microbial antigens in the pathogenesis of gut inflammation, and this supports indirect clinical evidence of a similar effect in CD (167). In HLA-B27 transgenic rats, inflammation is seen in many organs, but inflammation in the intestine is spared when the rats are bred in a germ-free environment (262). Similar observations were made in IL-2 (244) and IL-10 (263) gene knockout models of IBD. Furthermore, when the microbial intestinal environment is restored, particularly with *Bacteroides* species, to germfree HLA-B27 transgenic mice, gut inflammation recurs (264).

The central role of T-cells in the pathogenesis of experimental IBD is demonstrated by experiments in which IL-2-deficient mice were crossed with either B cell-deficient mice or B cell- and T-cell-deficient mice, when colitis was prevented only when T cell function was restored, with no improvement in the colitis on re-introduction of B cells

(265). Abnormalities in T-cell function may not have to be primary, congenital abnormalities to affect the mucosal immune system, as demonstrated in a study where appendicectomy at one month prevented the subsequent development of the colitis that is usually seen in T-cell receptor α-mutant mice (266), which is in keeping with the observations regarding the protective effect of appendicectomy against the onset of UC in man (267).

Although there are many animal models in which interference with the immune system by gene knock-out results in intestinal inflammation, there are also other genetically-altered animal models of colitis, such as mice with 'dominant negative N-cadherin' genes, which develop IBD because of increased intestinal permeability associated with reduced levels of cadherin-complexes that mediate cell polarity and formation of junctional complexes (268). This model supports the hypothesis of altered gut permeability as a primary abnormality in IBD, with inflammation developing as a secondary immune response to translocated luminal antigens.

12.7 Conclusions from studies of the immunological abnormalities in Crohn's disease

As with most organs, the range of reactions of the bowel to injury is limited. In the bowel, this limited reaction to injury is compounded by a stereotyped reaction to luminal antigens once the integrity of the epithelial barrier is breached. Thus, there is a 'final common pathway' of intestinal inflammation, and it is difficult to distinguish observations on immunological responses that may be of *primary* importance in the pathophysiology of CD from this complex final common pathway of inflammation.

However, described in a simplistic manner, the evidence presented above *suggests* a primary state of T-cell activation with a predominantly Th-1 pattern of cytokine activation, with a bystander effect of injury to the epithelium, rather than a primary autoimmune abnormality directed against the epithelium. Macrophages appear to be important in the response to luminal antigens and tissue damage is effected by recruited PMN's. Whether this primary state of T-cell activation is a purely genetically-determined effect, or whether, more likely, environmental factors act on a background of genetic susceptibility, is unclear.

Part C: Introduction to the results chapters

The original aim of this thesis was to determine the site within the bowel wall of early inflammatory events in CD by studying the site of activation of NFκB within macroscopically and microscopically unaffected CD bowel. The central, early role of NFκB in co-ordinating gene expression of numerous inflammatory mediators in response to many pathological stimuli would be utilised to determine the site of early events of CD and the cell type involved.

At the start of the studies contained in this thesis, no method existed to study *in situ* activation of NFκB, and so in Chapter 2, a method using ISH is explored. These experiments led to important observations on methodological problems in using oligonucleotide ISH in sections of bowel, and in Chapters 3 and 4, the mechanisms of these problems are determined. In Chapter 5, an antibody that recognises only the activated form of NFκB, which became available during the course of these studies, is used successfully to study the activation of NFκB in normal bowel, and in both uninflamed and inflamed CD bowel. In Chapter 6, the same antibody is used to develop a method of measuring activation of NFκB in cultured cells using flow cytometry.

Chapter 2

Measurement of activation of NFκB in sections of human bowel by *in situ* hybridisation for IκBα mRNA.

1. Introduction

1.1 Aim

The aim of the work presented in this chapter was to develop a method of detecting *in situ* activation of NFκB within cells in sections of tissue, and to use this method to study the activation of NFκB in normal and diseased bowel, as further discussed in Aims of Thesis.

1.2 Established methods to detect activation of NFκB

NFκB is a pre-formed complex that is present in an inactive state in the cytosol of many different cell types. Study of its activation requires a method of distinguishing the inactive, cytosolic complex from the activated, nuclear-translocated form.

There are established methods that measure activation of NFκB in *homogenised* tissue, such as electrophoretic mobility shift assay (EMSA) and Western blotting, and distinguish active from inactive forms by separation of nuclear and cytosolic fractions. An additional method for detecting only the activated form of NFκB is provided by the detection method used in EMSA, which is a radiolabelled oligonucleotide whose

sequence is complementary to the NFκB consensus binding sequence. Thus, the radiolabelled oligonucleotide binds only to activated NFκB.

However, when investigations were started, there was no method to detect activated NFκB *in situ*. Antibodies that bind to the p65 and p50 subunits of NFκB were commercially available, but when used for immunocytochemistry, these bind to both inactive and activated NFκB, and no antibody that recognised only the activated form of NFκB had then been developed.

1.3 Basis of a new method to detect activated NFκB *in situ*

When cells are stimulated with agents that activate NFκB, the inactive, dormant, cytoplasmic p50-p65-IκBα complex is activated by proteolytic degradation of the IκBα protein, allowing nuclear translocation of the p50-p65 (together termed NFκB) complex, which is subsequently deactivated, and transported back to the cytoplasm, by synthesis of new IκBα protein. IκBα mRNA transcription is initiated by binding of the active p50-p65 heterodimer to κB consensus sequences in the promoter of the IκBα gene, thus completing a feedback loop. Thus, IκBα is degraded and requires re-synthesis, whereas p50 and p65 are recycled by deactivation by newly-synthesised IκBα and subsequent transportation back into the cytoplasm.

Separate studies have demonstrated rises of mRNA for p50 and p65 (269) and of mRNA for IκBα (37) when NFκB is activated by stimulation of tumour cell lines, such as U937 and Jurkat T cells, with agents known to activate NFκB (TNFα and PMA), but there is no published study directly comparing their concurrent appearance. When comparing these two studies, mRNA for IκBα appears sooner (at twenty minutes) after stimulation than mRNA for p50 and p65, but methodological differences between

the studies prevent conclusions about the magnitude of the responses. However, the postulated mechanism of activation of NFκB would suggest a larger rise in IκBα mRNA, to allow physiological repletion of degraded IκBα protein, in contrast to the conserved p50 and p65 proteins.

Thus, presence of IκBα mRNA in a cell implies activation of NFκB in that cell, as all stimuli that initiate IκBα transcription do so by activating NFκB (270), and development an *in situ* hybridisation (ISH) method for detecting IκBα mRNA as an *in situ* marker of activation of NFκB was proposed.

1.4 *In situ* hybridisation

ISH is used for detecting specific sequences of nucleic acid, most commonly messenger RNA (mRNA), in intact cells or tissue sections using complementary nucleic acid probes. It has several advantages over other techniques for localising gene expression. First, the half-life of mRNA is short, usually ranging from one to sixty minutes (271) and thus detection suggests recent transcription of a gene, in contrast to immunocytochemistry that cannot usually distinguish between newly-produced and stored protein. Second, combination of different visualisation systems allows simultaneous identification of several mRNA species within the same tissue section. Finally, ISH may also be combined with immunocytochemistry to identify cells currently containing both a particular nucleic acid sequence and the corresponding transcribed protein.

Different types of probe can be used to hybridise to and detect mRNA:

1. complementary, single-stranded RNA probes (riboprobes) derived from transcription vector plasmids, typically 0.1-1.0 kbases in length (272);

2. complementary single-stranded deoxyribonucleic acid (cDNA) probes prepared by polymerase chain reaction (PCR) (273);

3. double-stranded DNA probes, prepared by nick translation, random priming or PCR, that are less sensitive than single stranded probes since the two strands can re-anneal in the hybridisation solution, thus reducing the concentration of probe available to the target (274), and

4. synthetic complementary oligodeoxyribonucleotides (oligonucleotide) probes, typically 20-35 bases long (275).

Riboprobes are most often used for detection of mRNA (276,277), although synthetic oligonucleotide probes are also widely used and offer advantages of rapid and inexpensive synthesis of sequences selected from published DNA databases, effective penetration of fixed and unfixed tissue sections (278) and resistance to ubiquitous ribonucleases (RNases), since they are DNA strands. Thus, oligonucleotide ISH was chosen as the method.

2. Methods

All solutions were made using RNase-free 'Q' water (one litre of deionised water with 1 ml of diethylpyrocarbonate (DEPC) (Sigma Chemical Company), left overnight and then autoclaved).

2.1 Biopsy specimens

Gastrointestinal biopsy specimens were obtained from macroscopically inflamed areas from patients with inflammatory bowel disease undergoing routine colonoscopy and specimens of normal control large bowel from patients undergoing colonoscopy for follow-up of colonic polyps. Normal control small bowel biopsy specimens (distal duodenum) were obtained from patients undergoing oesophagogastroduodenoscopy for investigation of dyspepsia or anaemia, and nasal polyp was obtained from a patient undergoing polypectomy for allergic rhinitis. Specimens were orientated using watchmaker forceps (Raymond A Lamb Ltd., London, UK) a dissecting microscope (Zeiss, Zurich, Switzerland) and frozen in Optimum Cutting Temperature (OCT) compound (BDH, Poole, UK) over thawing isopentane (BDH) and stored in liquid nitrogen (British Oxygen Company, Guildford, UK).

2.2 Preparation of microscope slides

Microscope slides (Sigma Chemical Company) were washed twice in 'Q' water and then dried at 60 °C in an oven. Slides were then immersed in a 10 % (v/v) solution of poly-L-lysine (Sigma Chemical Company) for ten minutes, air-dried and stored at –70 °C for up to two weeks.

2.3 Sectioning of biopsy specimens

Biopsy specimens were transported from the liquid nitrogen storage cylinder (BDH) to the cryotome (Cryotome 620M, Anglia Scientific Instruments, Cambridge, UK) in a portable liquid nitrogen container (BDH). Biopsy specimens were orientated and then fixed to a 1 x 1 cm cork square (BDH) with OCT compound, which was then frozen within the cryotome. The cork square was then fixed to the mounting plate of the cryotome with frozen water. Sections of 8 μm thickness were cut onto poly-L-lysine-coated slides, air-dried for ten minutes, then fixed in a 4 % (w/v) solution of paraformaldehyde (Sigma Chemical Company) in phosphate buffered saline (PBS), pH 7.3 (Oxoid, Unipath Ltd., Basingstoke, UK) for fifteen minutes followed by immersion in a 15 % (w/v) solution of sucrose (Sigma Chemical Company) for fifteen minutes, twice, and then stored at –70 °C.

2.4 Probes and radioactive labelling

2.4.1 Probes

Sequences for the three different exon-specific oligonucleotide (30-mers) probes (Table 1) for the mRNA for IκBα, the inhibitory protein of the transcription factor NFκB, were chosen by Dr. Steve Jones (Retinitis Pigmentosa Research Unit, The Rayne Institute, St. Thomas' Hospital) using the published sequences of the gene for IκBα (16). Sequences were analysed using the Genetics Computer Group (Wisconsin, USA) Version 7 Program, made available through the Human Genome Mapping Project Resource Centre (Hinxton, UK) and a PC, to ensure there was no significant likelihood (defined as > 60 % matching of bases) of cross-hybridising with other

known sequences. For closely related genes, a direct homology search was performed using the DNAsis program (Hitachi Europe Ltd., Maidenhead, UK) and a PC. Sequences were chosen that provided a near even mix of A/T and G/C base pairs and also minimal self-complimentarity, to prevent hairpin formation by internal base-pairing, using the DNAsis secondary structure analysis program. The three oligonucleotides for IκBα mRNA, together with three previously documented (279) oligonucleotide probes for TNFα mRNA (Table 1), were manufactured according to the chosen sequences (Pharmacia Biotech UK Ltd., St. Albans, UK). A poly-deoxyribothymidine (poly-d(T)) probe (Pharmacia Biotech UK Ltd.), which hybridises to the poly-riboadenosine tail present on all mRNA (280), and equimolar cocktails of three oligonucleotide probes for each of the mRNAs for insulin, IL-4 and IL-10 (R & D Systems, Abingdon, UK) were also used (see section 3, for rationale for use of these additional probes). All probes were thirty bases long.

Table 1. Sequences of oligonucleotide probes for IκBα mRNA and TNFα mRNA.

Protein	Probe	Sequence (5′ → 3′)
IκBα	antisense 1	TCC TTG ACC ATC TGC TCG TAC TCC TCG TCT
IκBα	antisense 2	CCC CTT TGC ACT CAT AAC GTC AGA CGC TGG
IκBα	antisense 3	ACA AAG GTG AGG TTT AAA AGA AGT TTT CTC
IκBα	sense	AGA CGA GGA GTA CGA GCA GAT GGT CAA GGA
TNFα	antisense 1	GCT GGG CTC CGT GTC TCA AGG AAG TCT GGA
TNFα	antisense 2	CGG GGT TCG AGA AGA TGA TCT GAC TGC CTG
TNFα	antisense 3	AGT AGG CCG ATT ACA GAC ACA ACT CCC TGG

Oligonucleotide antisense probe cocktails for insulin, IL-4 and IL-10 were obtained from commercial sources (sequences not released).

2.4.2 Radioactive labelling

For each mRNA target, three antisense probes, in an equimolar cocktail, were labelled at the 3' termini with deoxyadenosine 5' S^{35}-thiotriphosphate (^{35}S-dATP) (Pharmacia Biotech UK Ltd.), catalysed by overnight incubation with terminal deoxynucleotidyl transferase solution (Promega, Southampton, UK) (15-30 units μl^{-1} in 50 nM potassium phosphate pH 7.4, 1 mM mercaptoethanol and 50 % (v/v) glycerol, where 1 unit is the amount of enzyme required to catalyse transfer of 1 nmol deoxyadenosine triphosphate to poly-$d(T)_{50}$ in 60 minutes at 37°C). To 4 pmol of probe (3 µl of a 1.6 ng ml^{-1} solution) was added 3.2 µl of a 370 MBq ml^{-1} (10 mCi ml^{-1}) solution of S^{35}-dATP, 2.5 µl of terminal deoxynucleotidyl transferase solution and 8 µl of terminal deoxynucleotidyl transferase buffer (Promega) (500 mM cacodylate buffer, pH 6.8, 5 mM cobalt chloride, 0.5 mM dithiothrietol, 500 µg ml^{-1} bovine serum albumin), and made up to 40 µl with 'Q' water and incubated at 37 °C overnight.

2.4.3 Purification of labelled probes

NICK spin columns (Pharmacia Biotech UK Ltd.) (containing Sephadex G-50 fine, DNA grade) were prepared according to the manufacturer's instructions. First, the gel was resuspended by inverting the columns and then excess fluid allowed to drain. Second, to each column was added 1 ml elution buffer (0.1 M Tris (Sigma Chemical Company), 50 mM EDTA (BDH), pH 7.5), which was allowed to drain, and finally, 2 ml elution buffer was added to each column which were then centrifuged at 500 x g at room temperature for four minutes in an IEC 6000B centrifuge (International Equipment Company, Dunstable, UK). The labelled oligonucleotide solutions, with 40 µl of elution buffer added to each sample, were pipetted carefully onto the prepared

columns and centrifuged at 500 x g at room temperature for four minutes, and the elute collected in microcentrifuge tubes. The specific activity of each purified, labelled probe was then measured in triplicate by pipetting 1 µl aliquots of the recovered probe into three scintillation vials, followed by addition of 3 ml Betaplate Scint scintillation buffer (Fisons Chemicals, Loughborough, UK) to each vial and the β-emission in one minute measured using a scintillation counter (Wallac 140g liquid scintillation counter, Wallac, Turku, Finland). The specific activity of the labelled, purified probes was greater than 1 x 10^8 counts per minute μg^{-1}.

2.5 *In situ* hybridisation

ISH was performed according to the method of Hamid *et al* (281) including standard steps to reduce non-specific binding, namely:

- acetylation
- 'pre-hybridisation' with hybridisation solution containing Denhardt's solution and excluding probe
- incorporation of non-complementary DNA sequences in the hybridisation solution to compete with probe for non-specific binding sites.

In general, microscope slides were removed from storage at –70°C and were allowed to come to room temperature whilst still within their protective covering of aluminium foil (BDH) within sealed polythene storage bags (BDH), to minimise condensation of water onto the sections. Sections were air-dried and then permeabilised in a 0.3 % (v/v) solution of Triton X-100 (Sigma Chemical Company) in PBS for 10 minutes followed by a solution of proteinase K (1 $\mu g\ ml^{-1}$) (Sigma Chemical Company) in 0.1M Trizma base (Sigma Chemical Company), pH 7.4, containing 50 mM

ethylenediaminetetraacetic acid (EDTA) (Sigma Chemical Company) at 37 °C for thirty minutes. In some experiments as a negative control (see Results), slides were then treated with 100 μg ml^{-1} deoxyribonuclease-free RNase (Pharmacia Biotech UK Ltd.) for thirty minutes to remove target mRNA. Sections were post-fixed in a 0.4 % (w/v) solution of paraformaldehyde in PBS for ten minutes, acetylated in a freshly prepared 0.25 % (v/v) solution of acetic anhydride (Sigma Chemical Company) in 0.1M triethanolamine (Sigma Chemical Company) for ten minutes, and then pre-hybridised in a solution containing 50 % (v/v) formamide (Sigma Chemical Company), 1 x Denhardt's solution (Sigma Chemical Company) (0.02 % (w/v) bovine serum albumin, 0.02 % (w/v) Ficoll, 0.02 % (w/v) polyvinylpyrollidone) and 2 x standard saline citrate (SSC) (Sigma Chemical Company) (0.15 M sodium chloride, 0.015 M sodium citrate), for thirty minutes at 37 ^{0}C.

Overnight hybridisation was performed at 39 ^{0}C with 50 μl of a solution containing 0.12 μg ml^{-1} probe (6 ng of probe), 2 x SSC, 50 % (v/v) formamide, 0.4 mg ml^{-1} denatured, sheared (by immersion of vial in boiling water for three minutes) salmon sperm DNA (Sigma Chemical Company) and 10 % (w/v) dextran sulphate (Sigma Chemical Company). Three consecutive post-hybridisation washes were performed for thirty minutes each at 39 ^{0}C in solutions of 2 x SSC, 1 x SSC plus 50 % (v/v) formamide and 0.1 x SSC. In later experiments (see results), the effect of graded reductions in stringency of washes was investigated.

Sections were then dehydrated in a 95 % (v/v) solution of absolute alcohol (BDH) in DEPC-treated water, followed by a 99 % solution, for 30 seconds each, and then dried at room temperature for 30 minutes.

For autoradiography, sections were dipped in nuclear track emulsion, namely Ilford K5 photographic gel emulsion (Ilford Scientific Products (Ceiba-Geigy), London) diluted 1:1 with distilled water at 43 °C, dried in a darkroom for two hours, and then incubated at 4 °C in a light-proof container containing silica gel (Sigma Chemical Company) for five days. Slides were developed in a 4.4 % (w/v) solution of Dektol (Kodak, via Sigma Chemical Company) for two minutes, washed briefly in distilled water and fixed in a 30 % (w/v) solution of sodium thiosulphate (Sigma Chemical Company) at 4 °C for five minutes, and then washed in running water for five minutes and counterstained with filtered Mayer's haematoxylin (Sigma Chemical Company) for three minutes, followed by 'blue-ing' in tap water for one minute. Sections were dehydrated in serial, graded alcohols (70, 90 and 99 % (v/v) solutions of alcohol in distilled water for 30 seconds each) and then immersed in xylene (BDH) for 30 seconds, twice, air-dried for 15 minutes and then mounted in Ralmount (BDH) and covered with a cover-slip (Sigma Chemical Company).

In addition, ISH experiments with single probes were performed with each of the three antisense probes and the sense probe for IκBα mRNA, when quantitation of positive cells containing hybridised oligonucleotide probe was undertaken. Positive cells were arbitrarily defined as cells with at least 25 overlying positive granules, and positive cells in the lamina propria were counted in ten high-powered (× 400) microscope fields avoiding the epithelium, by an observer who was blinded to the identity of the slide, and quantitation expressed as number of positive cells per microscope field.

Variations in the above protocol were made, as indicated in Results, during attempts to optimise specific staining.

2.6 Photography

Photomicrographs were taken using an Axioscop microscope (Zeiss, Zurich, Switzerland) fitted with an HE photofilter (Nikon, Tokyo, Japan) and a Canon AV-1 camera (Canon UK, London, UK), using Ektachrome 64 tungsten photographic film (Kodak via Sigma Chemical Company)

2.7 Statistical analysis

In the experiments with individual probes, the number of positive cells per microscope field were compared for different probes using a Student t-test with a Bonferroni correction for multiple comparisons (Tables 2 and 3).

3. Results

3.1 ISH on sections of bowel using probes for mRNA for IκBα, TNFα and insulin, and poly-d(T) probe

ISH using oligonucleotide probe cocktails for both TNFα and IκBα mRNA targets showed apparently positive cells within the lamina propria of sections of both normal large (n = 8) and small (n =5) bowel from control patients (Figure 1). Findings were similar for patients with inflammatory bowel disease (n = 7 for large bowel, n = 3 for small bowel), but with a greater number of positive cells (Figure 2). The positive control probe, poly-d(T) (Figure 3), showed a pattern of positive cells similar to that seen with both probe cocktails for TNFα and IκBα mRNA, and not, as was expected, a positive signal over all cells. Staining with probe cocktails for TNFα and IκBα mRNA and with poly-d(T) probe was only partially abolished by pre-treatment of sections with RNase (Figure 4), and a similar pattern was observed with a probe cocktail for insulin mRNA (Figure 5) that should not be present in bowel. Furthermore, a similar pattern, but with fewer positive cells (see section 3.9) was also observed using a sense probe for IκBα mRNA as a negative control (Figure 6).

All experiments were repeated at least three times using sections from different patients with the same findings on each occasion, and together suggested probes were not hybridised to target mRNA but were bound non-specifically to scattered cells within the lamina propria (see section 4.1 for detailed explanation of this deduction) with bilobed nuclei and granular cytoplasm, that were provisionally identified by these morphological criteria (282) as eosinophils (Figure 7).

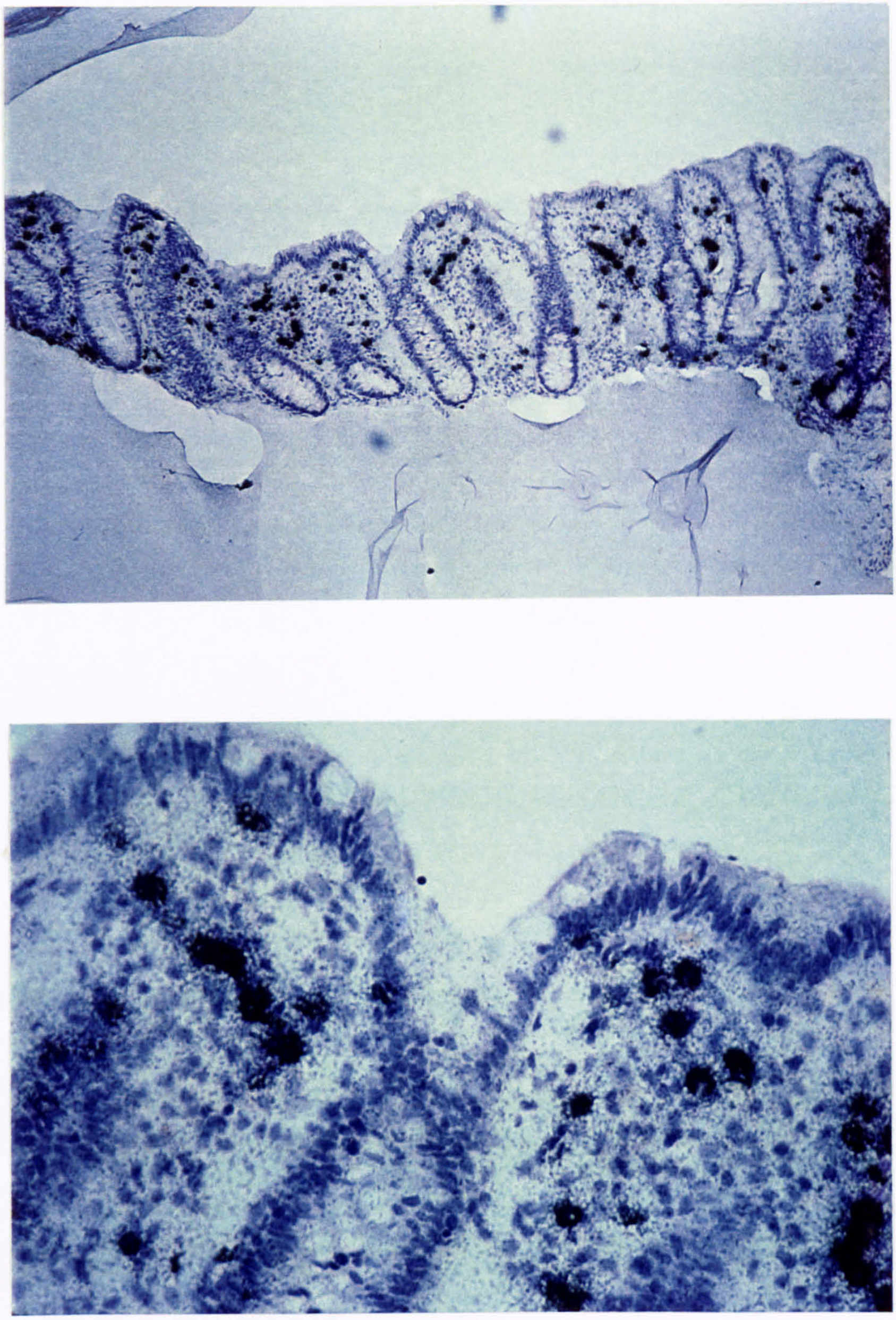

Figure 1. Photomicrographs (above × 100, below × 400) of a frozen section of normal large bowel from a patient with carcinoma, with ISH using an oligonucleotide probe cocktail for mRNA for IκBα, showing positive cells within the lamina propria (appearances similar with probe cocktail for mRNA for TNFα).

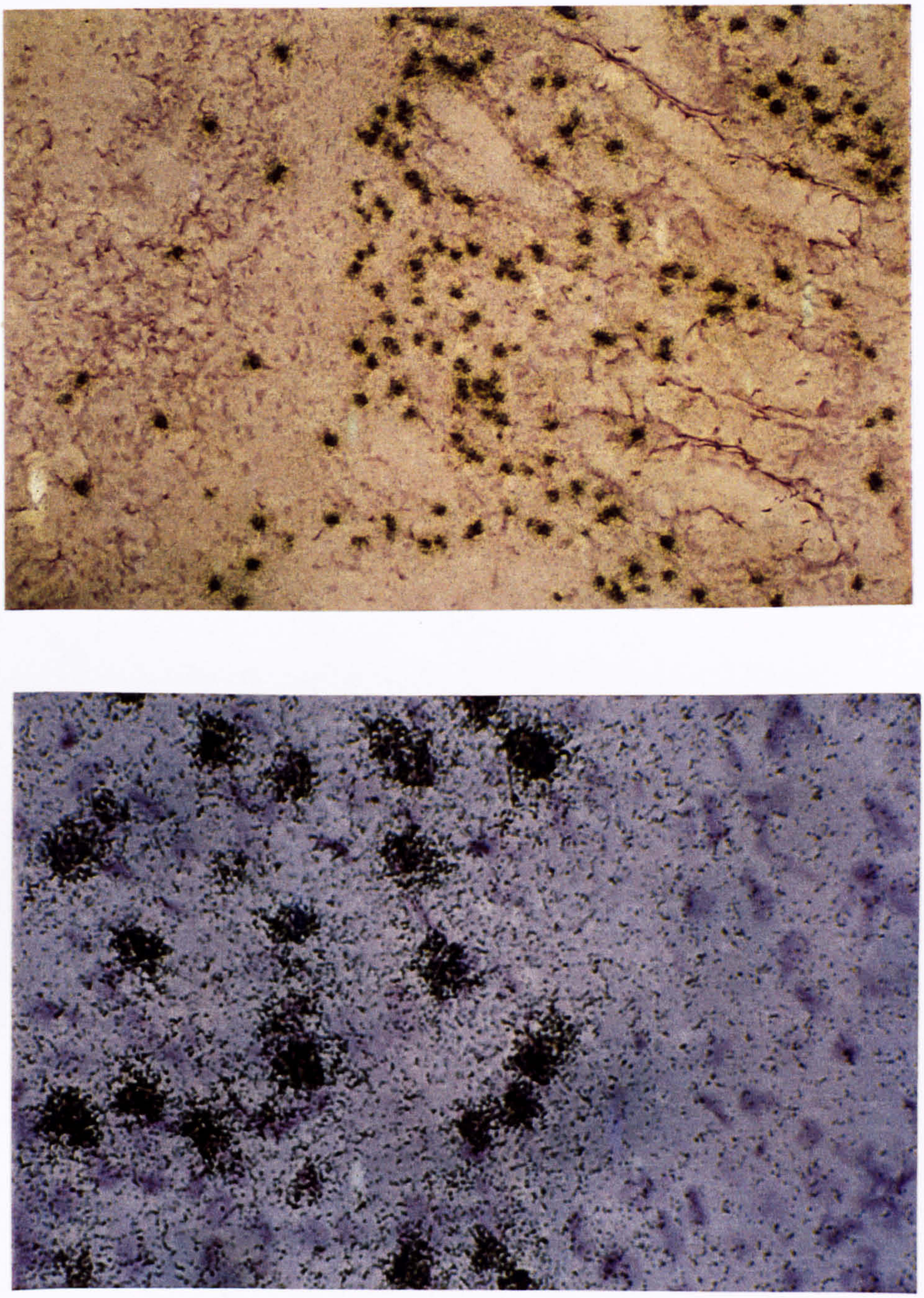

Figure 2. Photomicrographs (above × 100, below × 400) of a frozen section of inflamed large bowel from a patient with inflammatory bowel disease (ulcerative colitis), with ISH using an oligonucleotide antisense probe cocktail for mRNA for IκBα, showing a greater number of positive cells than seen in normal bowel (Figure 1) within the lamina propria (appearances similar with probe cocktails for mRNA for TNFα, IL-4 and IL-10).

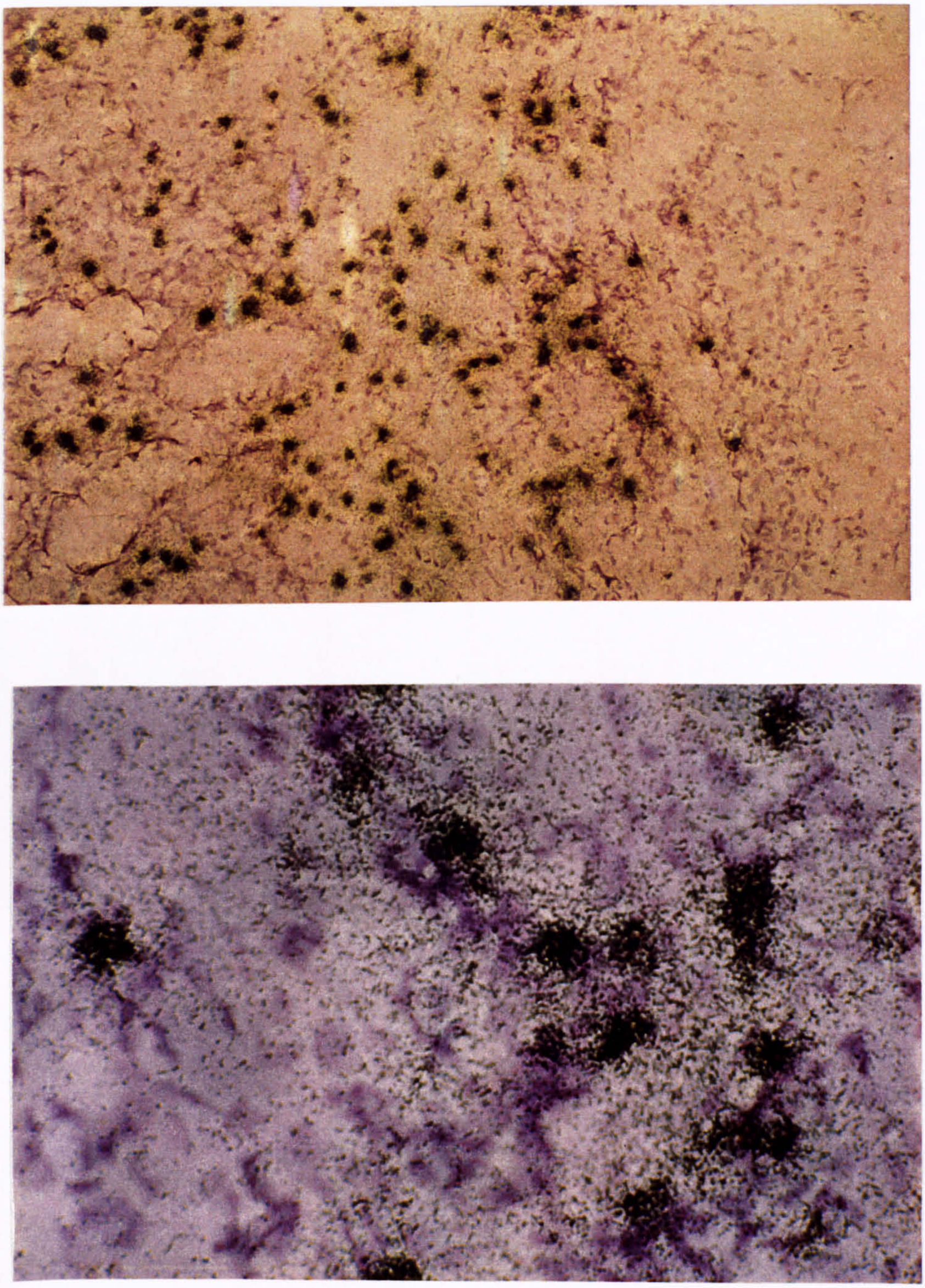

Figure 3. Photomicrographs (above × 100, below × 400) of a frozen section of inflamed large bowel from a patient with inflammatory bowel disease (ulcerative colitis) with ISH using poly-d(T) probe showing a pattern within the lamina propria similar to that seen with probes for cytokine mRNAs (Figure 2), and not positivity of all cells, as is expected if poly-d(T) probe remains hybridised to the poly-riboadenosine tail present on all mRNA.

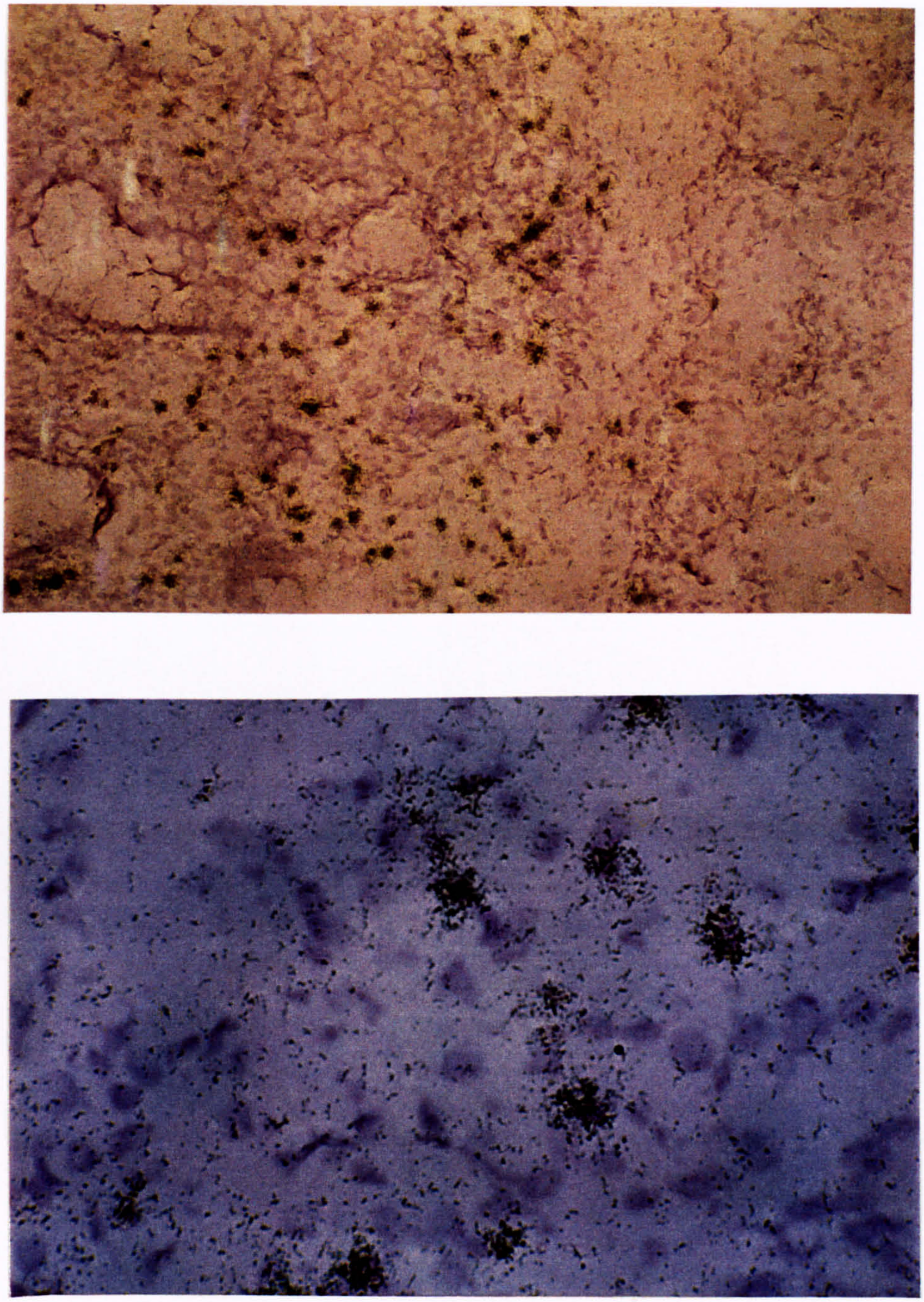

Figure 4. Photomicrographs (above × 100, below × 400) of a frozen section of inflamed large bowel from a patient with inflammatory bowel disease (ulcerative colitis), pre-treated with RNase, with ISH using an oligonucleotide antisense probe cocktail for mRNA for IκBα, showing a similar pattern of positive cells, at reduced levels to that seen without pre-treatment with RNase (Figure 2) (appearances similar with probe cocktails for mRNA for TNFα and poly-d(T) probe).

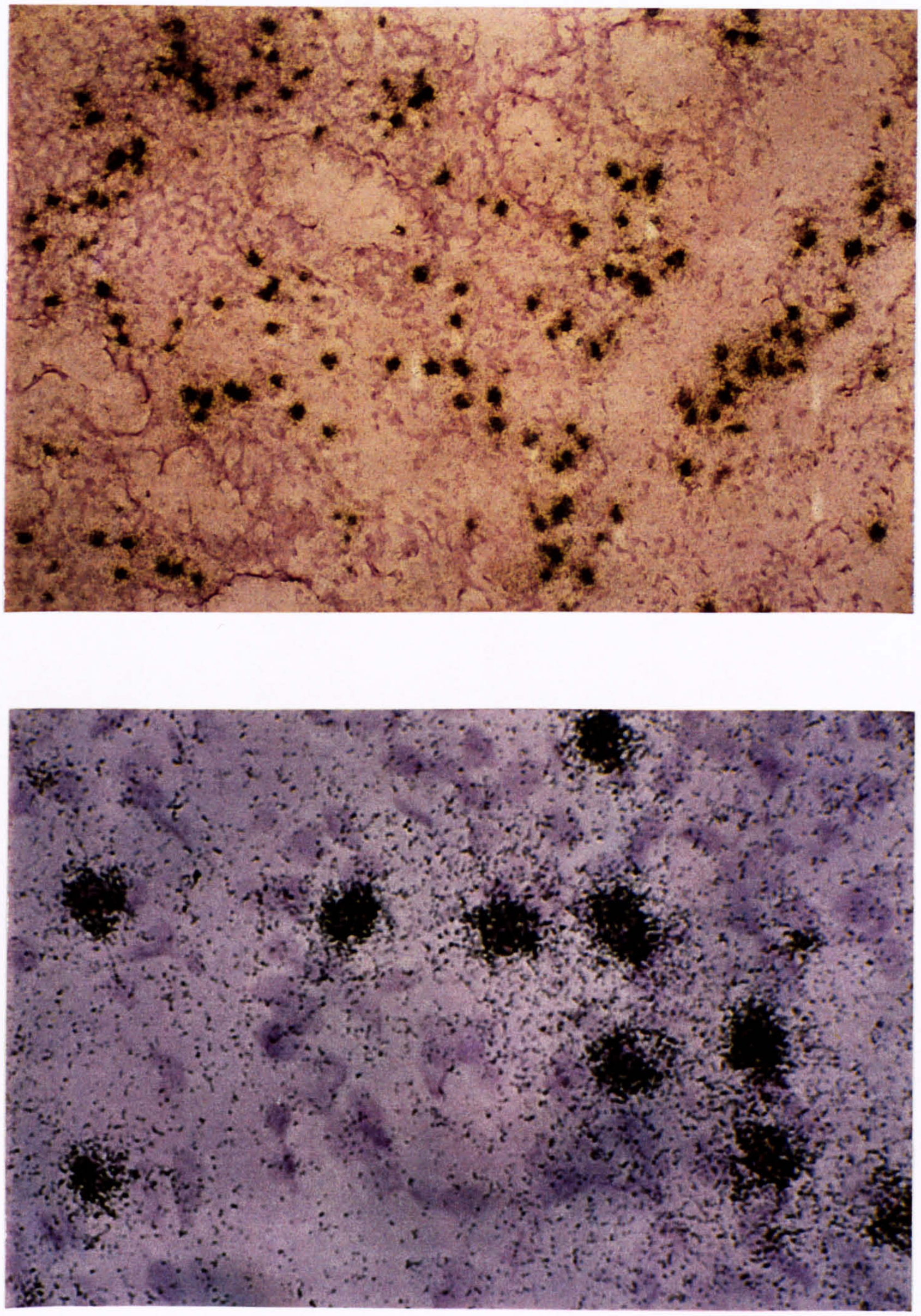

Figure 5. Photomicrographs (above × 100, below × 400) of a frozen section of inflamed large bowel from a patient with inflammatory bowel disease (ulcerative colitis), with ISH using an oligonucleotide antisense probe cocktail for mRNA for insulin, showing a pattern of positive cells similar to that seen with all other probes; insulin mRNA should not be present in bowel, and therefore the pattern suggests binding of probes to another element.

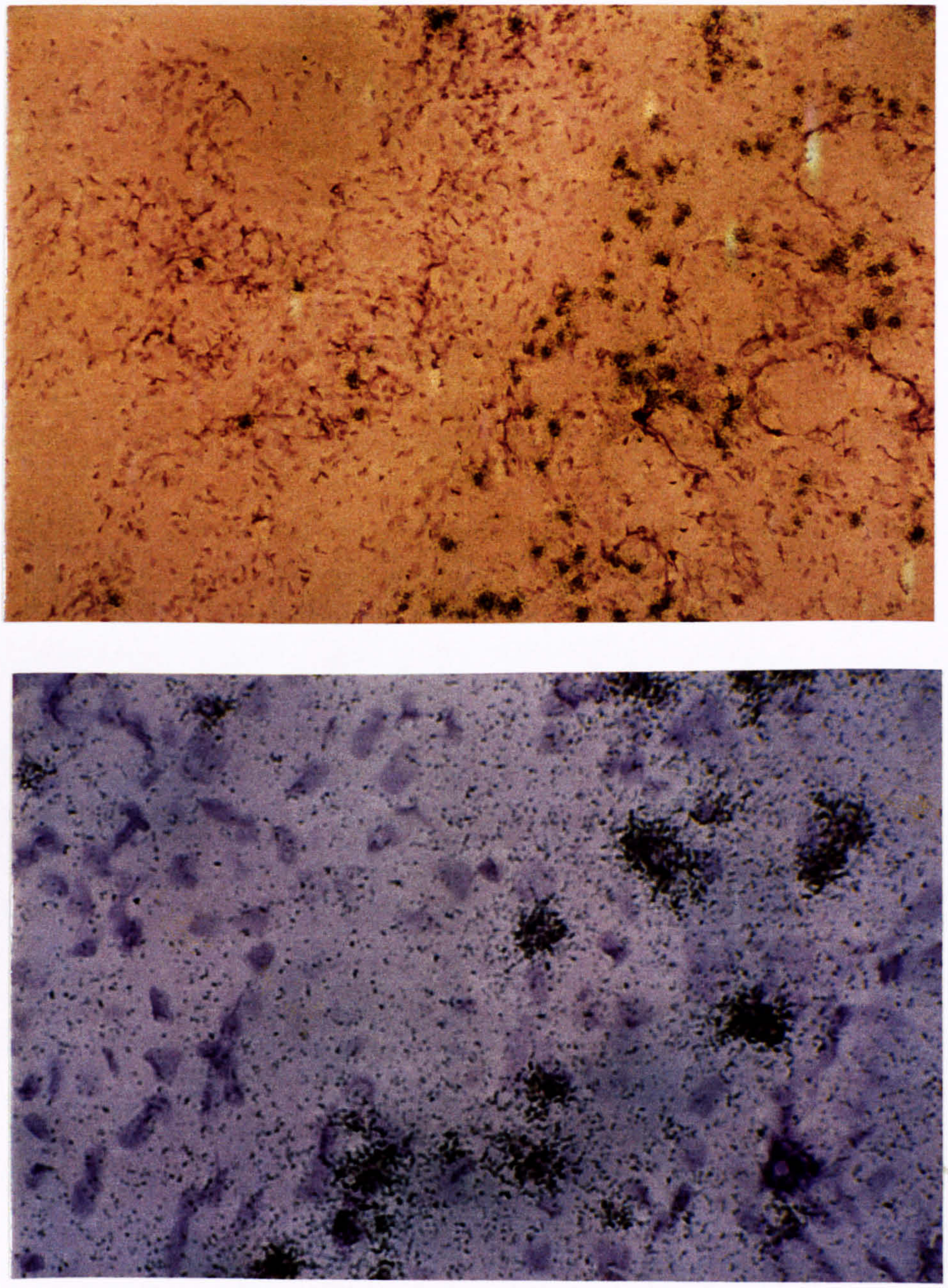

Figure 6. Photomicrographs (above × 100, below × 400) of a frozen section of inflamed large bowel from a patient with inflammatory bowel disease (ulcerative colitis), with ISH using an oligonucleotide *sense* probe for mRNA for IκBα, showing a pattern of positive cells within the lamina propria similar to that seen with the antisense cocktail (Figure 2), but with fewer positive cells and each positive cell with fewer overlying granules. The concentrations of probe in the sense and antisense hybridisation solutions were equal.

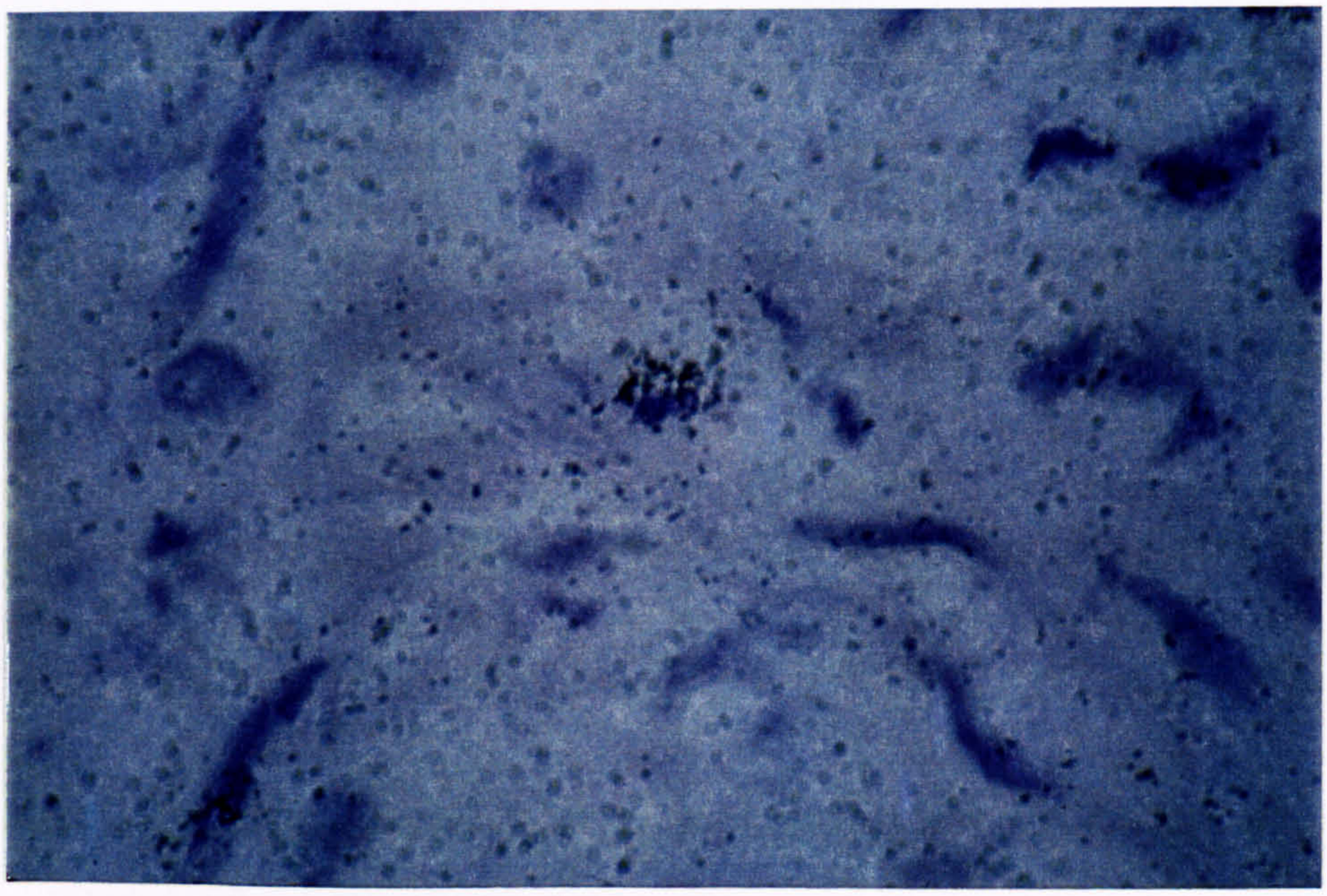

Figure 7. Photomicrograph (x 1000) of a frozen section of inflamed large bowel from a patient with inflammatory bowel disease (ulcerative colitis) with ISH using an oligonucleotide antisense probe cocktail for mRNA for IκBα. The cell with overlying positive granules has a bilobed nucleus and granular cytoplasm, suggesting it to be an eosinophil. Many similar cells had denser overlying positive granules, but this cell was chosen for photography as the underlying cell morphology was easily seen.

3.2 Identification of cells binding oligonucleotide probes

3.2.1 Staining with eosin

The identity of cells binding probes during ISH was confirmed as eosinophils by pre-staining the sections before ISH with a 1 % (w/v) solution of alcoholic eosin (Sigma Chemical Company) in a 95 % (v/v) solution of alcohol in DEPC-treated water. Eosin stains eosinophils bright orange, but also stains other polymorphonuclear neutrophils (PMNs) to a lesser extent (283) and is therefore not specific.

The strength of the eosin stain was considerably reduced by subsequent ISH, and to prevent this, the following modifications to the method were made:

1. it was noted that the hybridisation solution covering sections pre-stained with eosin turned orange and was therefore leaching eosin from the section, so to prevent this, the strength of the 'post-fixation step' of ISH, immediately prior to covering the section with hybridisation solution, was increased to 4 % (w/v) paraformaldehyde to fix the eosin stain;
2. repeating the eosin stain after hybridisation, but, as eosin stains the emulsion yellow, prior to coating with photographic emulsion.

However, neither of these modifications increased the intensity of the stain, and although the reduction of the eosin stain by ISH reduced visualisation for photography, it resulted in a more specific staining of eosinophils than occurs with stronger eosin stains, with only cells that appeared morphologically to be eosinophils staining orange, with no discernible staining of PMNs.

Thus, all cells that bound oligonucleotide probes during ISH were confirmed as eosinophils by staining with eosin (Figure 8). However, some cells that stained with eosin after ISH, and had morphological appearances of eosinophils, did not bind oligonucleotide probes, suggesting that not all eosinophils bound probes, or did not bind them sufficiently strongly to prevent their removal during post-hybridisation washes.

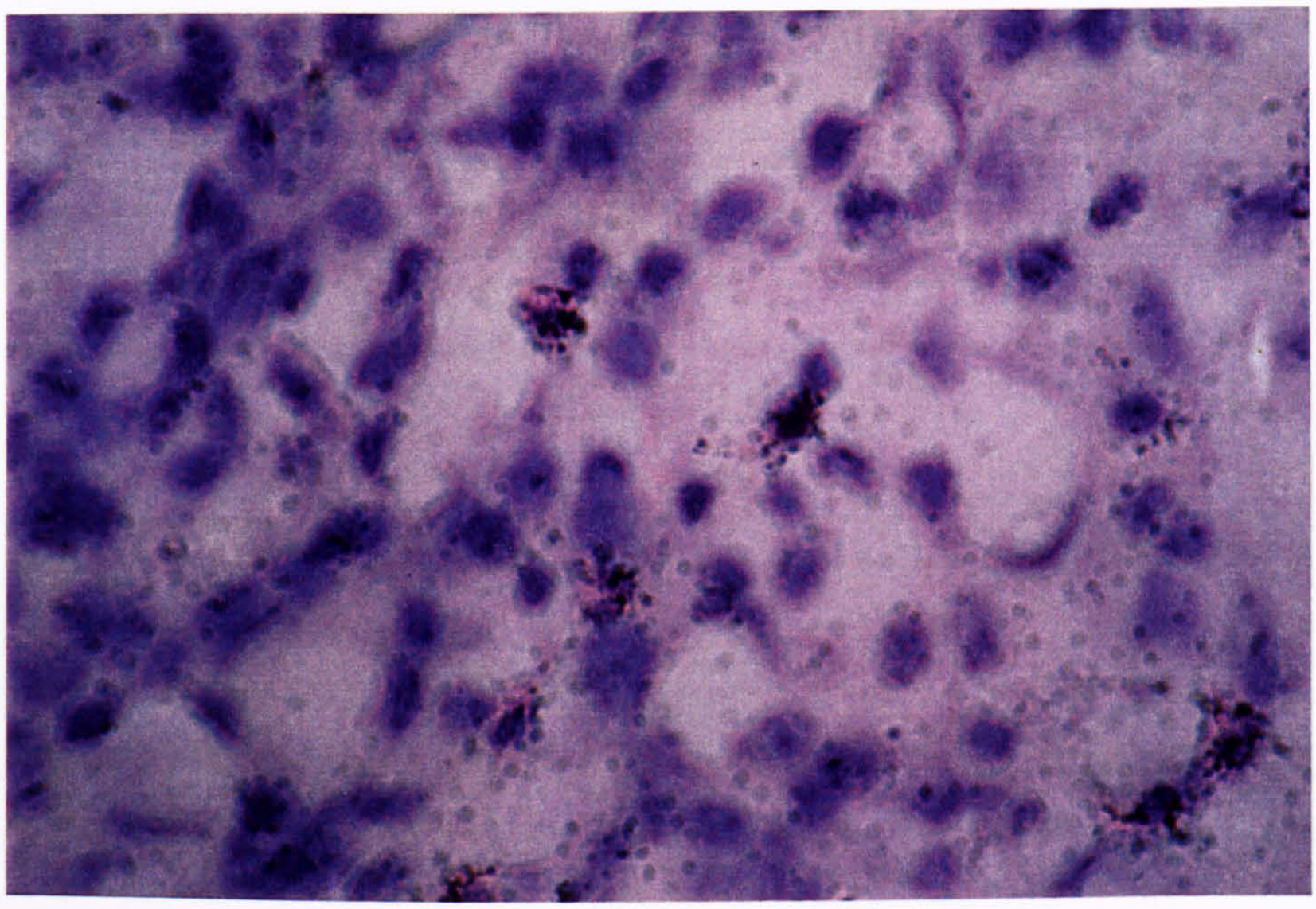

Figure 8. Photomicrograph (x 1000) of a frozen section of inflamed large bowel from a patient with inflammatory bowel disease (ulcerative colitis) pre-stained with eosin, with subsequent ISH using an oligonucleotide antisense probe cocktail for mRNA for IκBα; all cells with overlying positive granules, indicating binding of probes during ISH, also stained with eosin, suggesting them to be eosinophils (appearances similar with probe cocktails for mRNA for TNFα, IL-4, IL-10 and insulin, and with poly-d(T) probe).

3.2.2 Carbol chromotrope

Chromotrope 2R is a specific bright red stain for eosinophils. The method described by Lendrum in 1944 (284) uses carbol chromotrope, a 0.5 % (w/v) solution of chromotrope 2R in a 1 % (w/v) solution of phenol (Sigma Chemical Company) in distilled water, applied to formalin-fixed intestinal sections for 30 minutes and washed off with tap water. To optimise this staining method for identification of eosinophils in paraformaldehyde-fixed frozen sections of bowel, a range from 0.5 to 15 % carbol chromotrope (Sigma Chemical Company) concentrations were applied for a range from 15 to 60 minutes. Optimum staining of eosinophils with minimum background staining in sections of normal and inflamed large bowel, that had not undergone ISH, was achieved with 15 % carbol chromotrope for 30 minutes (Figure 9), and this was therefore used in subsequent attempts to stain eosinophils during ISH.

Because carbol chromotrope pre-staining has been used in a previous study to block binding of long DNA probes to eosinophils in bone marrow smears (285) (see section 3.6 for application of the blocking properties of carbol chromotrope to the present study), to *identify* eosinophils in ISH sections in the present study, carbol chromotrope was applied after hybridisation and prior to coating slides with photographic emulsion. This method did not result in a clear staining of eosinophils, presumably because the process of ISH had reduced the capacity of eosinophils to stain with carbol chromotrope.

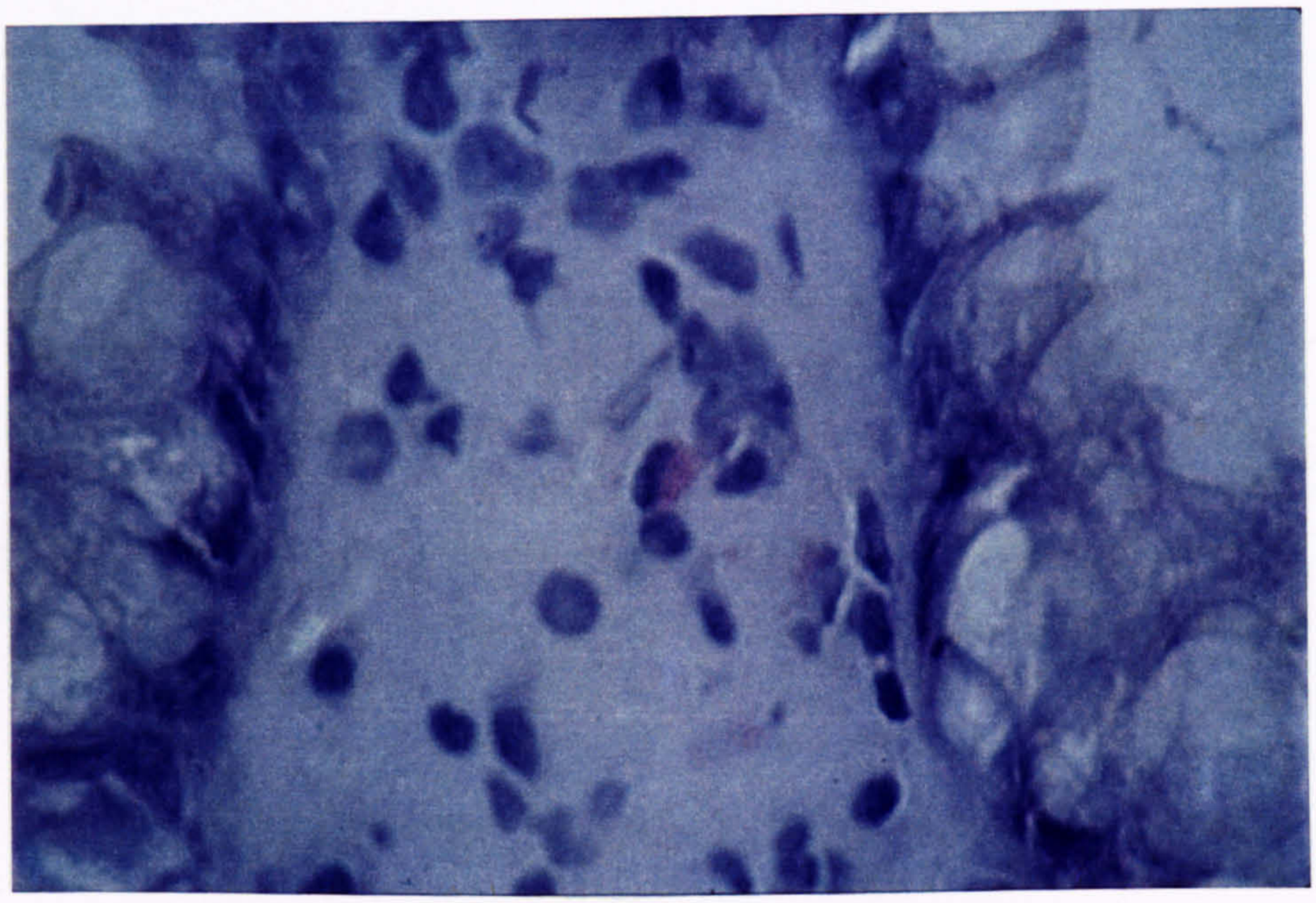

Figure 9. Photomicrograph (x 1000) of a frozen section of inflamed large bowel from a patient with inflammatory bowel disease (ulcerative colitis) stained with 15 % carbol chromotrope for 30 minutes; only the granular cytoplasm of eosinophils stains red.

3.3 Other tissues

3.3.1 Small bowel

To determine whether binding of oligonucleotides to eosinophils in the gastrointestinal tract occurred in areas other than the colon, ISH experiments were repeated on sections of distal duodenal biopsy specimens, when an oligonucleotide probe cocktail for IκBα mRNA and poly-d(T) probe bound in a pattern similar to that seen in the colon.

3.3.2 Nasal polyp

To confirm binding of oligonucleotide probes to eosinophils, and to investigate whether this is an effect isolated to bowel, oligonucleotide ISH was performed on paraformaldehyde-fixed, frozen sections of nasal polyp taken from a patient with allergic rhinitis, that are known to contain large numbers of eosinophils. Findings were identical to those in bowel, with cells identified as eosinophils by staining with eosin, binding all probes tested, namely probe cocktails for IκBα mRNA, TNFα mRNA and insulin mRNA, and poly-d(T) probe (Figure 10).

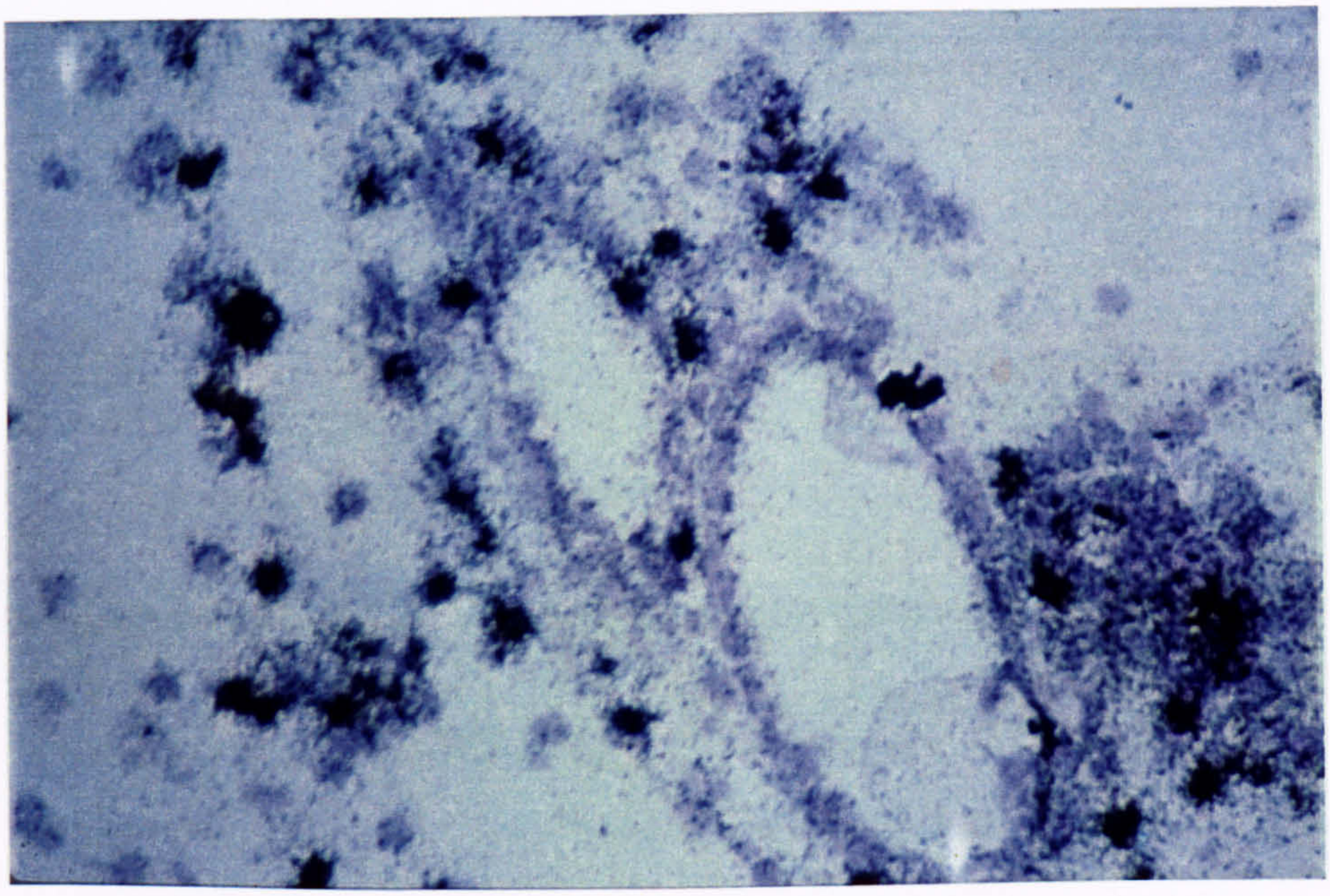

Figure 10. Photomicrograph (x 400) of a frozen section of nasal polyp from a patient with allergic rhinitis, with ISH using an oligonucleotide probe cocktail for mRNA for IκBα, showing numerous positive cells within the lamina propria (appearances similar with probe cocktail for mRNA for TNFα and insulin, and with poly-d(T) probe).

3.3.3 Rat cerebral cortex

Rat cerebral cortex was used as a control tissue as it contains no eosinophils. In addition, NFκB is constitutively activated in neurones of rat cerebral cortex (81), and, according to studies in tumour cell lines (see section 1.2 and Chapter 1), is therefore likely to be accompanied by an increase in IκBα mRNA. The cerebral cortices of Sprague-Dawley rats, that had been freshly killed for harvesting of hearts for use in isolated perfusion experiments in another laboratory, were dissected, set in OCT compound, frozen in liquid nitrogen and processed in the same manner as specimens of bowel. No positive cells were seen in ISH experiments performed with all probes (Figure 11), which is consistent with the hypothesis that positive cells in previous experiments using sections of bowel were due to non-specific binding of probes to eosinophils, which are absent in cerebral cortex, and not due to hybridisation to specific mRNA, confirmed, in this case, by the absence of cells expected to be positive for IκBα mRNA.

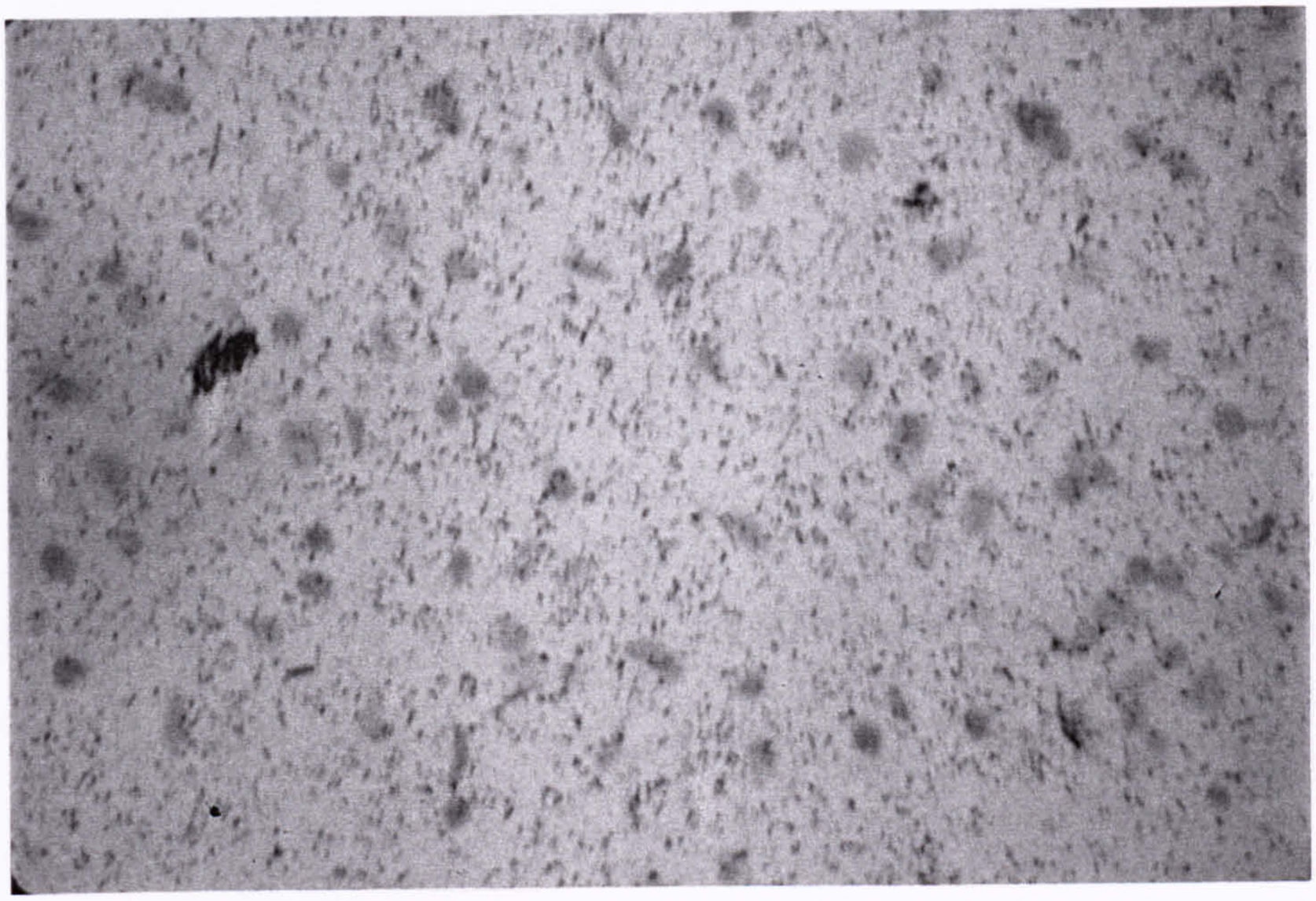

Figure 11. Photomicrograph (x 400) of a frozen section of rat cerebral cortex, with ISH using an oligonucleotide antisense probe cocktail for mRNA for IκBα, showing no positive cells (appearances similar with probe cocktails for mRNA for TNFα and insulin, and with poly-d(T) probe).

3.4 Reproduction of findings by other investigators

To ensure that the observed binding of oligonucleotide probes to eosinophils was not a phenomenon confined solely to my ISH experimental technique and skills, sections of colonic biopsy specimens from patients with inflammatory bowel disease were given to an independent investigator within The Rayne Institute who was conducting similar oligonucleotide ISH experiments based on the same protocol, except using different probe cocktails, namely for mRNA for IL-10 and IL-4, and a fixation technique that differed slightly from that used in this project with sections being initially fixed in acetone for 30 seconds, before storage at -70°C, and finally, as in the protocol used in this project, fixed in a 4 % (w/v) solution of paraformaldehyde in PBS immediately prior to ISH. A similar pattern of staining was observed, with binding of probes only to cells staining with eosin, confirming their identity as eosinophils. Thus, this phenomenon is not due to my experimental ISH technique or skills, and also does not appear to be dependent on fixation technique, as is also demonstrated by similar findings in formaldehyde-fixed, paraffin-embedded specimens (see section 3.5).

Similarly, to ensure that the observations were not due to mistakes in collection and sectioning of specimens, ISH was performed on sections prepared by another investigator, when findings were identical.

3.5 Formaldehyde-fixed, paraffin-embedded specimens

ISH experiments were also conducted on formaldehyde-fixed, paraffin-embedded specimens from small bowel resection specimens from patients with Crohn's disease stored in the Histopathology Department at St. Thomas' Hospital. Sections of seven μm thickness were cut into 'Q' water, and then dried onto microscope slides. Paraffin was removed from the sections in a standard manner by immersion in xylene for two minutes, twice, 100 % alcohol for one minute, twice, and then successive solutions of reducing concentrations of alcohol for one minute each (95 %, 70 % and 50 % (v/v) solutions of alcohol in 'Q' water), and finally washed in 0.5 x SSC for one minute. All solutions used for removing paraffin contained 1 % DEPC to destroy RNases. ISH was then conducted using the same protocol as for frozen sections. However, a range of concentrations from 0 - 40 $\mu g\ ml^{-1}$ of proteinase K were used to establish the ideal pre-digestion of sections, as is recommended for ISH on paraffin-embedded sections (272). Probes for mRNA for IκBα and insulin, and poly-d(T) probe were tested and all bound to eosinophils in a manner similar to that observed with frozen sections, with most binding seen with no pre-digestion with proteinase K (Figure 12). Thus binding of oligonucleotide probes to eosinophils occurred in paraffin-embedded sections as well as in frozen sections of bowel.

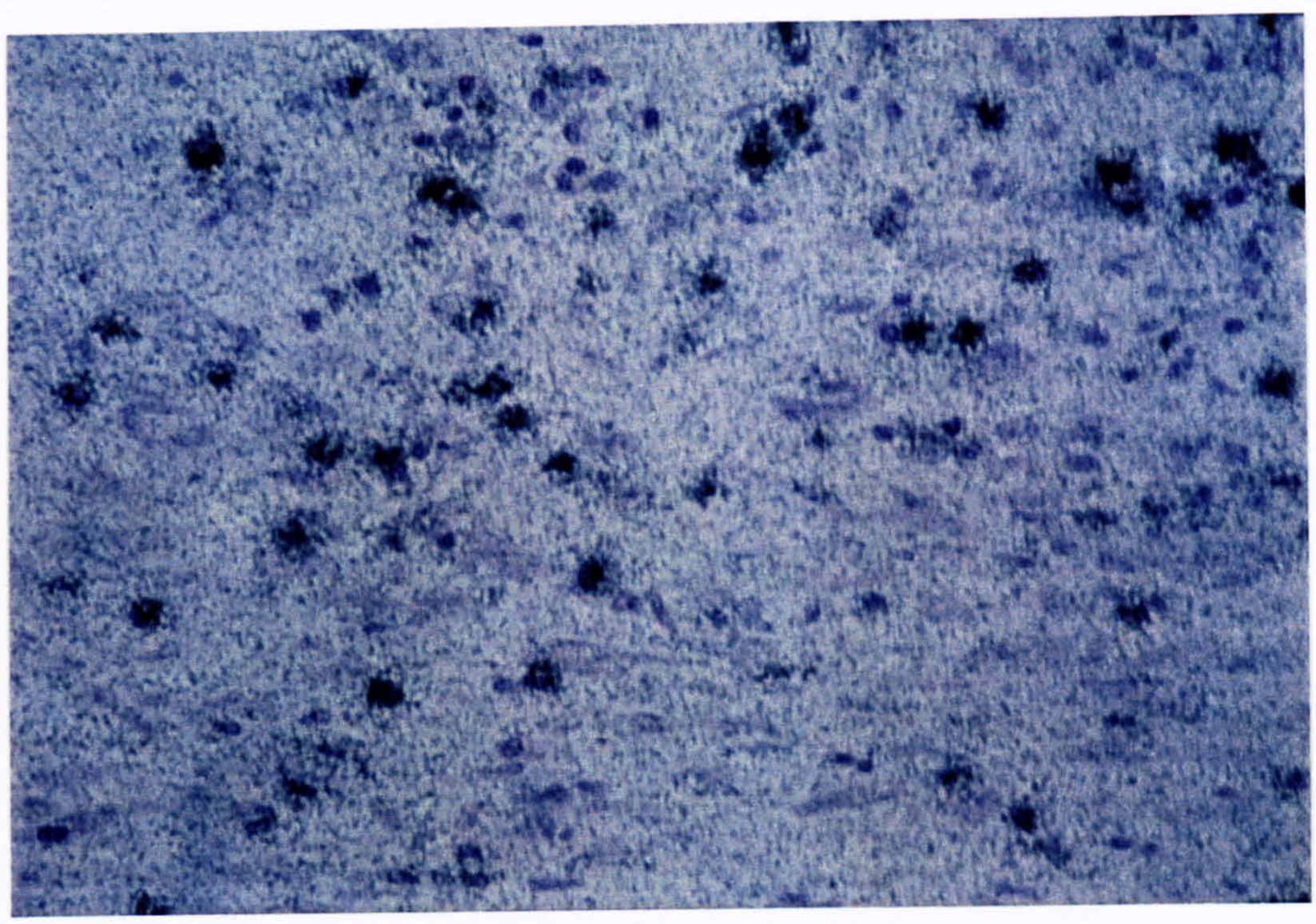

Figure 12. Photomicrograph (x 400) of a section of paraffin-embedded, inflamed large bowel from a patient with inflammatory bowel disease (Crohn's disease), with ISH using an oligonucleotide antisense probe cocktail for mRNA for IκBα, showing a pattern of positive cells within the lamina propria similar to that seen in frozen sections (appearances similar with probe cocktails for mRNA for TNFα and insulin, and with poly-d(T) probe).

3.6 Blocking of non-specific binding of oligonucleotide probes to eosinophils

Thus far, it has been demonstrated that when using standard conditions for oligonucleotide ISH, probes bound non-specifically to eosinophils but did not appear to hybridise to specific target mRNA.

I hypothesised that the stringency of washes used in this protocol was set at a level that removed probe hybridised to target mRNA but allowed persistence of probe bound non-specifically to eosinophils. To test this hypothesis, the ability of blocking manoeuvres to prevent non-specific binding of probe to eosinophils, together with differing stringencies of washes to allow persistence of probe hybridised to specific mRNA, was then investigated.

3.6.1 Blocking of non-specific binding of oligonucleotide probes to eosinophils using carbol chromotrope

In a previous report by others, binding of longer DNA probes (200-mers) to eosinophils in bone marrow smears was completely blocked by pre-staining with carbol chromotrope (a 1.25 % (w/v) solution of chromotrope 2R in a 1 % (w/v) solution of phenol in 'Q' water) prior to ISH (285).

Thus, in the present study, pre-staining was investigated with a range of concentrations of carbol chromotrope from 1.25 to 15 % (w/v), in combination with a range of incubation times from 30 to 120 minutes, and, in contrast to the previous report by others, only a reduction, but not elimination, of non-specific binding of probe to eosinophils was achieved, with maximal blocking achieved by 15 % for 30 minutes, with no additional benefit from longer incubation periods.

3.6.2 Competitive inhibition of non-specific binding of oligonucleotide probes to eosinophils

To determine if non-specific binding sites within eosinophils could be saturated with excess unlabelled oligonucleotide, thus preventing non-specific binding of labelled oligonucleotide probe, an unlabelled, irrelevant probe (a 30-mer oligonucleotide for mRNA for IL-6) was added at excess concentration (800 times the concentration of labelled probe) to the hybridisation solution to competitively inhibit non-specific binding to eosinophils. Reduction, but not elimination, of non-specific binding to eosinophils was achieved

Pre-treatment with carbol chromotrope and competitive inhibition by an unlabelled, irrelevant probe were combined, and led to a further reduction, but not complete elimination of non-specific binding to eosinophils.

3.6.3 Blocking of non-specific binding of oligonucleotide probes to eosinophils by pre-treatment with dithiothreitol and iodoacetamide

Pre-treatment of sections with 0.2M dithiothreitol (DTT) (Sigma Chemical Company) for twenty minutes to maintain thiols in the reduced state and to reduce disulphide groups, followed by a solution of 0.1M iodoacetamide (Sigma Chemical Company) in 0.1M triethanolamine at pH 8.2, for thirty minutes has been previously used to block non-specific binding of *riboprobes* to eosinophils in sections of bowel (286), and was therefore explored with oligonucleotide ISH: it resulted in a complete loss of positive cells in different experiments with all probes (Figure 13), confirming that all positive cells were eosinophils.

Furthermore, as successful blocking of non-specific binding to eosinophils resulted in no positive cells, the hypothesis that probe hybridised to target mRNA was not persisting after washes was confirmed, or, alternatively, hybridisation was not occurring because, for instance, of prior destruction of target mRNA by contamination with RNases.

Excessively stringent post-hybridisation washes were hypothesised to be the most likely explanation for the absence of hybridised probe, and experiments to test this hypothesis are described below. The stringencies of washes were taken from previous publications that developed the methodology (281,287-291), and were, in retrospect, excessively stringent because binding to eosinophils may have been mistaken for true hybridisation.

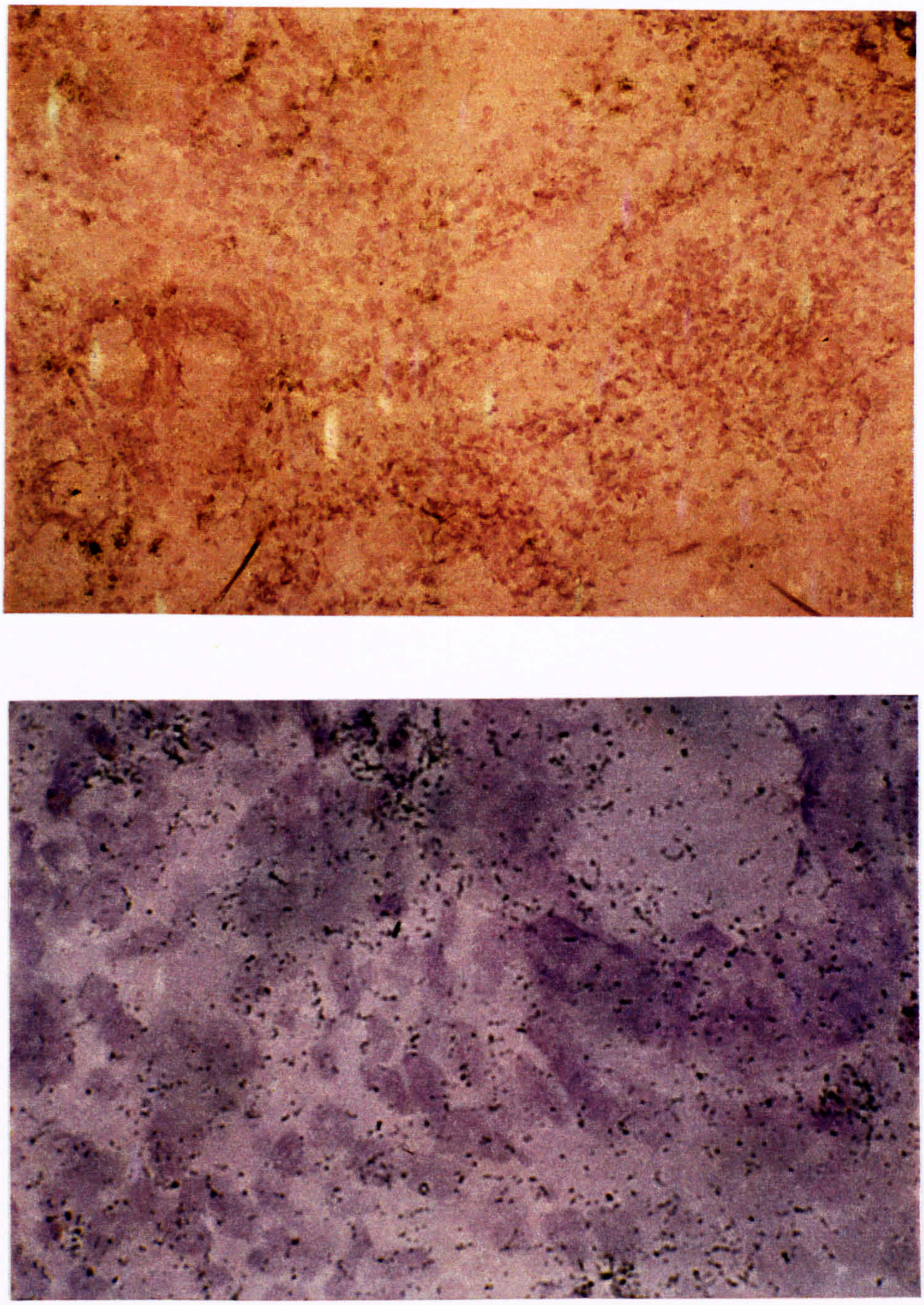

Figure 13. Photomicrographs (above × 100, below × 400) of a frozen section of inflamed large bowel from a patient with inflammatory bowel disease (ulcerative colitis) pre-treated with dithiothreitol and iodoacetamide, with ISH using poly-d(T) probe, showing no positive cells, indicating successful blocking of non-specific binding of probe to eosinophils (appearances similar with probe cocktails for mRNA for TNFα and insulin, and with poly-d(T) probe).

3.7 Reducing wash stringency to retain hybridised probe

To prove this hypothesis and to determine the ideal stringency of post-hybridisation washes to allow retention of hybridised probe, further experiments were performed with washes of reduced stringency, after binding sites within eosinophils had been blocked by pre-treatment of sections with DTT and iodoacetamide. Poly-d(T) probe was used in these experiments, to allow easy distinction between successful retention of probe hybridised to mRNA, which, with poly-d(T) probe, would result in a positive signal over all cells, and recurrence of binding to eosinophils in bowel and nasal polyp, which would result in a positive signal over only scattered cells in the lamina propria. For the same reasons, probe cocktails for specific mRNA (e.g. IκBα or TNFα mRNA) were *not* used as successful retention of hybridised probe might then have resulted in a pattern of scattered positive cells within the lamina propria that would be difficult to distinguish from the similar pattern, which would result if binding to eosinophils in bowel and nasal polyp recurred.

Thus, ISH experiments were performed on sections of normal human bowel, rat cerebral cortex and human nasal polyp. Sections were pre-treated with DTT and iodoacetamide, to prevent binding to eosinophils, and ISH with poly-d(T) probe was then followed by reduced stringency washes at 5 x SSC, thrice. Positive signal was observed over all cells indicating successful retention of hybridised probe to mRNA in all cells (Figure 14).

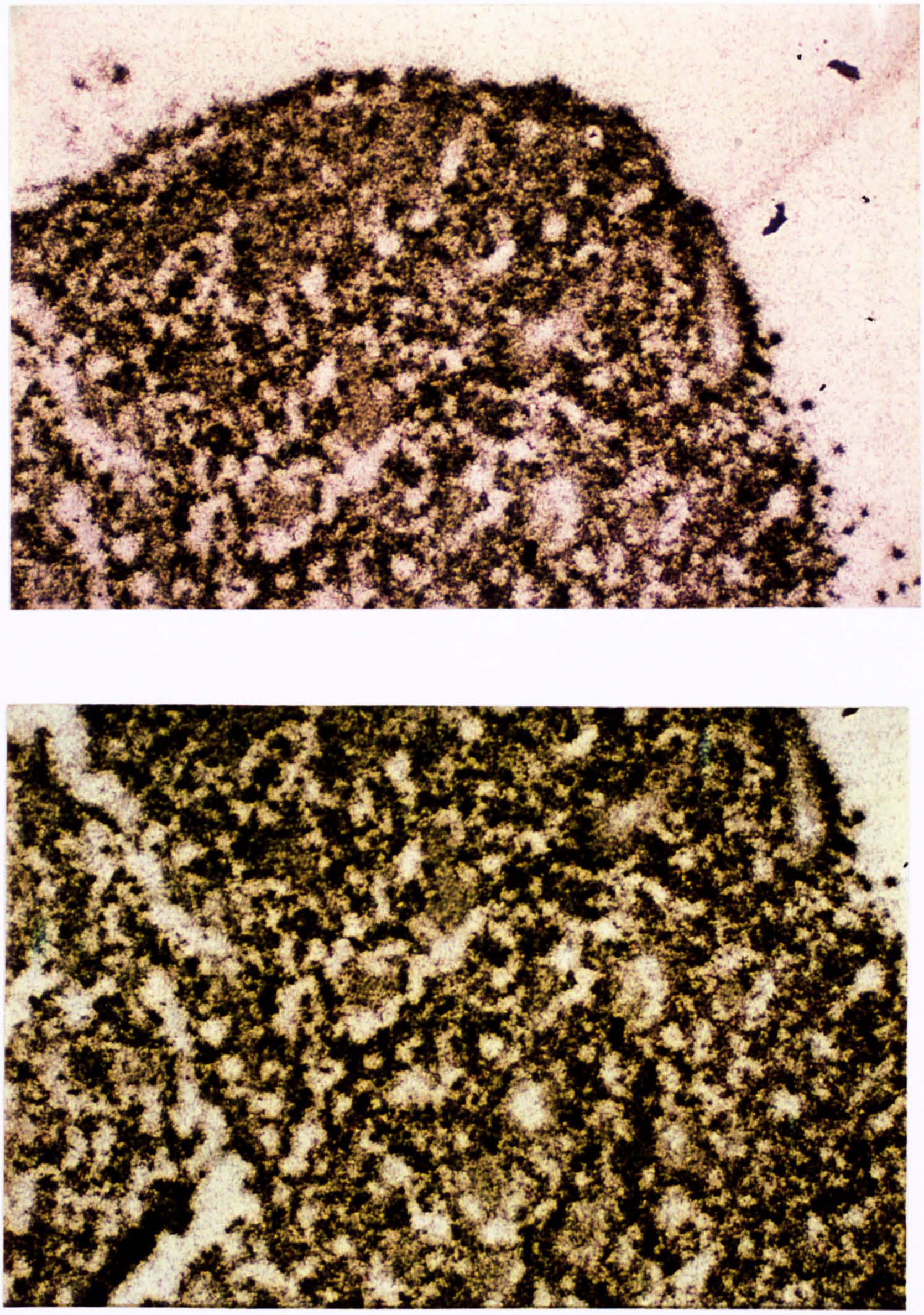

Figure 14. Photomicrographs (above × 100, below × 400) of a frozen section of inflamed large bowel from a patient with inflammatory bowel disease (ulcerative colitis) pre-treated with dithiothreitol and iodoacetamide, with ISH using poly-d(T) probe, followed by reduced stringency washes (5 x SSC), showing positive signal overlying all cells, indicating retention of poly-d(T) probe hybridised to the poly-riboadenosine tail on all mRNA.

To ensure that *some* of the observed many positive cells in the above ISH experiments with reduced stringency washes using poly-d(T) probe on sections of bowel and nasal polyp were not due to recurrence of binding of probes to eosinophils, despite the blocking measures with DTT and iodoacetamide used to prevent this, some sections were first treated with RNase (see section 2.5) to remove target mRNA and prevent hybridisation. Thus, if any positive cells occurred in this experiment, they would be due to recurrence of non-specific binding of probes to eosinophils.

Unfortunately, despite blocking measures, re-appearance of non-specific binding of probes to eosinophils was demonstrated (Figure 15). It was therefore postulated that the previous success in removing non-specific binding of probes to eosinophils was due to a combination of the blocking effects of DTT and iodoacetamide *and* the subsequent high stringency washes, and that when wash stringency was reduced to a strength that allowed retention of probe hybridised to target mRNA, non-specific binding of probes to eosinophils recurred, despite pre-treatment with DTT and iodoacetamide.

3.8 Further attempts to eliminate eosinophil binding at low stringency washes

In an attempt to eliminate the recurrence of non-specific binding of probes to eosinophils when low stringency washes were used, pre-treatment of sections with carbol chromotrope and with DTT and iodoacetamide were combined, but proved to be unsuccessful.

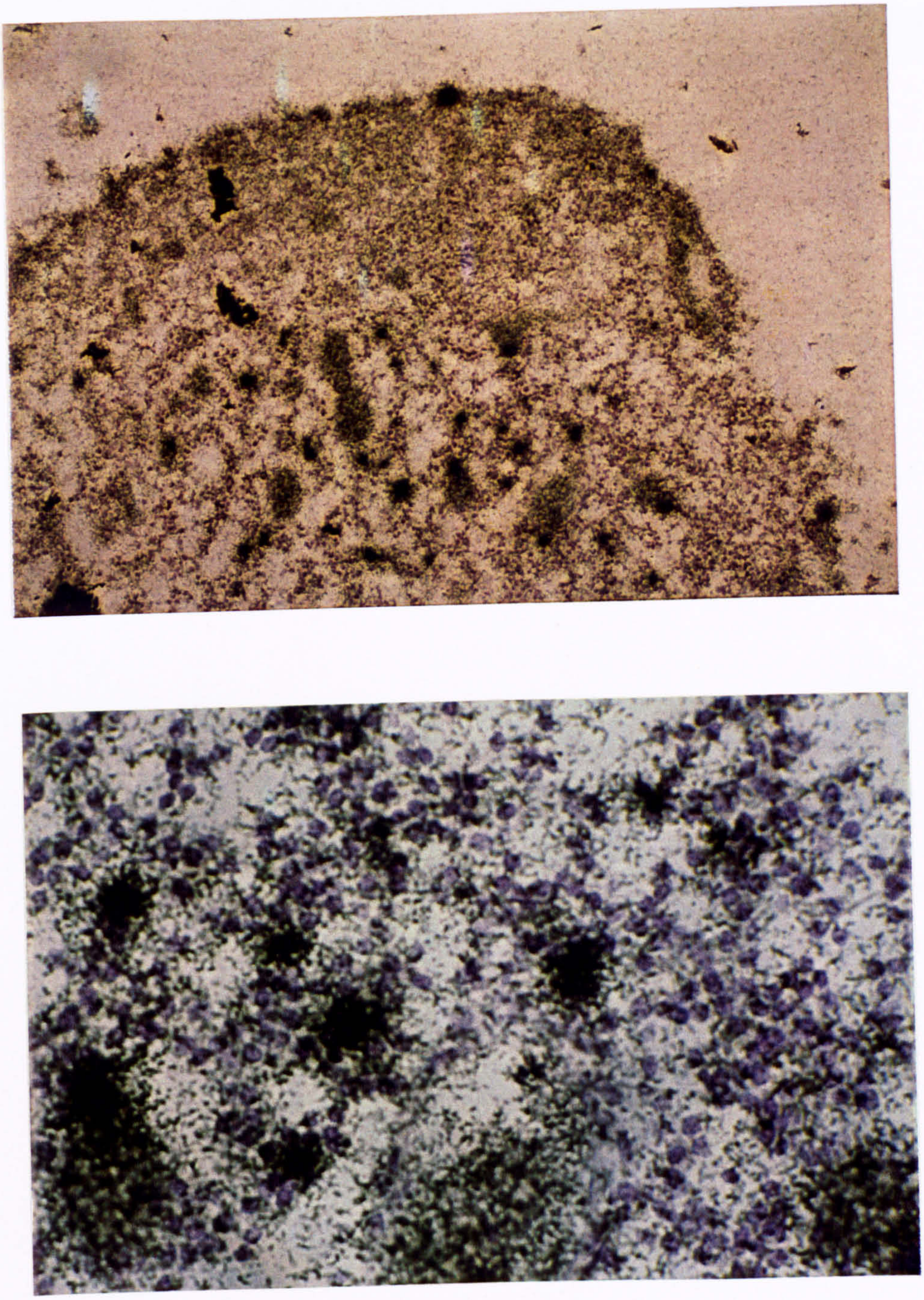

Figure 15. Photomicrographs (above × 100, below × 400) of a frozen section of inflamed large bowel from a patient with inflammatory bowel disease (ulcerative colitis) pre-treated with RNase, thus removing all mRNA, and then pre-treated with dithiothreitol and iodoacetamide, with ISH using poly-d(T) probe, followed by reduced stringency washes (5 x SSC), showing recurrence of non-specific binding of probe to eosinophils.

3.9 Quantitation of binding of single oligonucleotide probes for IκBα mRNA to eosinophils

At the start of the investigations, fewer 'positive cells' (later identified as non-specific binding to eosinophils) were noted with use of a cocktail of antisense probes for IκBα mRNA than with use of a single sense probe (see section 3.1), used at an equivalent concentration as a negative control. Furthermore, each 'positive cell' had fewer overlying black granules of photographic emulsion with the sense than with the cocktail of antisense probes. This observation, with the sense negative control being 'less positive' than the antisense cocktail, might have falsely suggested successful hybridisation of the antisense probe cocktail to target mRNA, rather than the correct observation of non-specific binding of probes to eosinophils. To explore further this finding of differential non-specific binding of probes to eosinophils, ISH experiments were performed with each single individual probe for IκBα mRNA (three antisense probes, one sense probe) at identical concentrations, rather than with the cocktail of antisense probes, when the number of positive cells for all three individual antisense probes was significantly greater than for the sense probe (Tables 2 and 3), and when Bonferroni corrections for multiple comparisons were made, these differences remained significant. Thus, differential binding of probes to eosinophils was confirmed, and possible explanations for this phenomenon are explored in the Discussion.

Table 2. Number of positive cells in the lamina propria of a section of inflamed bowel in an ISH experiment with individual oligonucleotide probes for IκBα mRNA.

Probe	Mean number of positive cells per microscope field	Standard deviation
Antisense 1	27.3	10.6
Antisense 2	28.6	12.3
Antisense 3	36.7	8.2
Sense	16.2	6.3

Table 3. Comparison of number of positive cells in the lamina propria of a section of inflamed bowel in an ISH experiment with individual oligonucleotide probes.

comparison	difference between means of numbers of positive cells per microscope field	95 % confidence intervals of the difference*	p-value#	adjusted p-value*
antisense 1 vs sense	11.1	(2.9, 19.3)	0.011	0.032
antisense 2 vs sense	12.4	(3.2, 21.6)	0.011	0.033
antisense 3 vs sense	20.5	(13.6, 27.4)	<0.001	<0.001

values compared to values for sense using an unpaired Student's t-test
* p-values adjusted using Bonferroni corrections for multiple comparisons

4. Discussion

4.1 Non-specific binding of probes to eosinophils

I have shown that oligonucleotide probes bind to eosinophils in the lamina propria of sections of bowel, a conclusion based on the following observations:

1. all tested probes (probes for IκBα, TNFα, insulin, IL-10 and IL-4, and poly-d(T) probe) bound to scattered cells within the lamina propria of large bowel;

2. the cells that bound these probes have morphological appearances of eosinophils;

3. probes for insulin mRNA, which should not be present in bowel, bound in a similar pattern;

4. poly-d(T) probe bound in a similar pattern and not to all cells, as would be expected if hybridisation to the poly-riboadenosine tail present on all mRNA had occurred;

5. the sense probe for IκBα, a negative control, bound in a similar pattern, albeit at a slightly reduced level;

6. binding was not prevented by pre-treatment of sections with RNase to destroy target mRNA;

7. cells binding probes stained with eosin;

8. binding of all probes to the putative eosinophils, which had not been prevented by standard methods of reducing non-specific binding included in the protocol, namely acetylation, pre-hybridisation with Denhardt's solution and addition of non-complementary DNA sequences (salmon sperm DNA) to the hybridisation solution, was reduced by pre-treatment of sections with carbol chromotrope, and by competitive inhibition by addition of a high concentration of unlabelled, irrelevant probe to the hybridisation solution;

9. binding of all probes to the putative eosinophils was completely blocked by pre-treatment of sections with DTT and iodoacetamide.

Findings were similar in sections of small bowel and sections of nasal polyp, which is rich in eosinophils, but no binding was observed in sections of rat cerebral cortex, which contains no eosinophils.

Non-specific binding to eosinophils was not due to personal experimental technique, as findings were similar when experiments were performed by a different investigator in another laboratory where the technique was in use. Furthermore, non-specific binding to eosinophils was not isolated to sections fixed only in paraformaldehyde, and was seen when sections were initially fixed in acetone followed by paraformaldehyde, and in sections fixed in formaldehyde and then embedded in paraffin wax.

Non-specific binding of oligonucleotide probes to eosinophils in bowel and nasal polyp was only partially inhibited by pre-staining with carbol chromotrope, unlike in a previous report, when non-specific binding of longer DNA probes to eosinophils in bone marrow smears was completely blocked by the same measure (285), and this difference may be due to the additional effect of higher stringency washes allowed by use in the previous report of longer probes, as high stringency of washes may have an additive effect to pre-hybridisation manoeuvres in blocking non-specific binding (see below).

Complete inhibition of non-specific binding of probes to eosinophils was achieved by pre-treatment with dithiothreitol followed by iodoacetamide, a method used previously to block non-specific binding of riboprobes to eosinophils in sections of bowel (286), and when the stringency of post-hybridisation washes was reduced, hybridisation of

poly-d(T) probe to mRNA in all cells was observed. This suggests a stronger interaction between probes and eosinophils than between poly-d(T) probe and mRNA. When the stringency of washes was reduced so that poly-d(T) probe hybridised to mRNA was no longer removed, non-specific binding to eosinophils returned, and could not be prevented despite combining carbol chromotrope with DTT and iodoacetamide pre-treatments.

4.2 Melting temperature of nucleic acid hybrids in hybridisation solutions and post-hybridisation washes

Specific binding of oligonucleotide probes to target mRNA in sections involves formation of RNA-DNA hybrids and is termed hybridisation. The strength of hybridisation is reflected by the stability of the RNA-DNA hybrid. The stability of nucleic acid hybrids is determined by several factors including the temperature of the solution in which the hybrids form. The melting temperature (T_m) of identical hybrids in a solution is defined as the temperature of the solution at which half the hybrids would dissociate if left to equilibrate, and is influenced by:

1. the nature of the hybrid: RNA-RNA hybrids are more stable than RNA-DNA hybrids, which in turn are more stable than DNA-DNA hybrids;

2. the length of the probe: longer nucleotides form more stable hybrids;

3. the base composition of the probe: increasing GC content of the nucleotide results in more stable hybrids, and

4. the composition of the hybridisation solution: higher concentrations of monovalent cations, such as sodium, increase the stability of hybrids, while increasing concentrations of formamide reduce stability.

A formula for RNA-DNA hybrids has been derived to calculate the T_m of hybrids in hybridisation solutions and post-hybridisation washes (272):

$$T_m = 81.5 + 16.6 \log (\text{molarity of monovalent cations}) + 0.41 (\% \text{ GC content}) - 500/\text{length of probe in bases} - 0.5 (\% \text{ (v/v) formamide})$$

Using this formula, the following values for T_m of hybrids in the hybridisation solution and the post-hybridisation washes are calculated using mean % GC content (0.47) of all oligodeoxynucleotide probes for specific mRNA used (for IκBα and TNFα, but not for insulin, IL-4 or IL-10, as base composition was not released by manufacturers), excluding poly-d(T) probe (see section 4.2), and the appropriateness of the actual temperatures used in ISH experiments is discussed.

Calculated melting temperatures for hybrids in the hybridisation solution in ISH experiments using probes for specific target mRNA

The calculated Tm of hybrids in the hybridisation solution is 52.3 °C. The optimum temperature for hybridisation to occur maximally at 5-6 hours is 25 °C below the T_m of hybrids in the hybridisation solution. However, if hybridisation is performed overnight, as in the protocol described above, more stringent conditions can be used (276), and thus the hybridisation temperature of 39 °C used in the protocol described above was appropriate.

Calculated melting temperatures for hybrids in the post-hybridisation washes in ISH experiments using probes for specific target mRNA

The calculated T_ms of hybrids in the post-hybridisation washes are:

- first post-hybridisation wash (2 × SSC): 77.3 °C
- second post-hybridisation wash (1 × SSC, 50 % formamide): 47.3 °C
- third post-hybridisation wash (0.1 × SSC): 55.7 °C

Thus, as is commonly practised, the second wash was the most stringent, with the final wash being of reduced stringency and containing no formamide with the aim of simply washing formamide from the tissue section. The ideal temperature for the most stringent post-hybridisation wash is several degrees Centigrade below the calculated Tm of hybrids in the wash solution (272), and so 39 °C was not theoretically over-stringent, although the results of ISH experiments described above suggest it, in fact, to be over-stringent, as there was complete removal of hybridised probe. The alternative hypothesis, that hybridisation had not initially occurred, is unlikely, as the temperature of the hybridisation solution was appropriate to the calculated T_m of hybrids in the hybridisation solution, and results of later experiments with poly-d(T) probe and reduced stringency washes indicated that hybridisation was occurring, at least to the poly-riboadenosine tail on all mRNA, and must therefore have been removed by the more stringent washes used in early experiments (see below).

Experiments using specific oligonucleotide probe cocktails, for instance for IκBα mRNA, as opposed to poly-d(T) probe, with reduced stringency washes were not performed. This was because it would be difficult to distinguish the recurrence of binding of probe to eosinophils, that was shown to occur with reduced stringency

washes, from true, persisting hybridisation of probe to IκBα mRNA, which both would result in scattered positive cells in the lamina propria. Indeed, a few cells containing probe hybridised to specific target mRNA may have been present amongst the numerous eosinophils that bound probe in the early experiments with stringent washes. However, this is unlikely because only eosinophils, as identified by pre-staining with eosin, displayed overlying positive signal and it is unlikely that only eosinophils would contain mRNA for IκBα and TNFα.

Calculated melting temperatures for hybrids in post-hybridisation washes in experiments using poly-d(T) probe

As indicated in the formula to calculate T_m, G-C bonds are stronger than A-T bonds, and thus poly-d(T) probe forms hybrids with a lower T_m than mixed-base oligonucleotide probes, such as the probes within the cocktails for specific mRNA (IκBα, TNFα). Would calculated T_ms for hybrids in the initial high stringency and subsequent lower stringency washes explain the experimental findings and fit with the hypothesis that the initial high stringency washes removed hybridised poly-d(T) probe, leaving only probe bound non-specifically to eosinophils, and the subsequent lower stringency washes did not remove poly-d(T) probe hybridised to mRNA in all cells?

Early ISH experiments with stringent post-hybridisation washes

The T_m for poly-d(T) probe in the most stringent post-hybridisation wash used in early experiments (1 × SSC, 50 % formamide) is 28 °C, and so a wash temperature of 39 °C would remove hybridised poly-d(T) probe, as was concluded from the results of the experiments. Indeed, this apparent error in the initial methodology taken from previous

reports was fortuitous, as it resulted in removal of poly-d(T) probe hybridised to mRNA in all cells and left only probe bound non-specifically to eosinophils, and this surprising result, of only scattered cells with overlying positive signal within the lamina propria in experiments with poly-d(T) probe, contributed to the realisation that probes were, in fact, binding non-specifically to eosinophils.

Later ISH experiments with less stringent post-hybridisation washes

The T_m of hybrids in the less stringent post-hybridisation washes (5 × SSC) used in later experiments with poly-d(T) probe is 64.7 °C, indicating very low stringency of the wash at 39 °C, appropriate to the aim of ensuring that hybridised poly-d(T) would not be removed during washing. This aim was achieved when the predicted result of positive signal over all cells was observed.

In conclusion, the ISH methods used previously by others (281,287-291), and modified in this project, do not allow successful blocking of non-specific binding of oligonucleotide probes to eosinophils as well as successful hybridisation of probe to target mRNA, and the technique of ISH using oligonucleotide probes cannot be used to investigate gene expression in the lamina propria of bowel unless other blocking manoeuvres are developed, as non-specific binding of probe to eosinophils appears identical to probe genuinely hybridised to target mRNA. Furthermore, this phenomenon occurred in sections of nasal polyp that is rich in eosinophils, and therefore probably occurs in other eosinophil-containing tissues, such as lung and liver.

Investigation of the epithelium with ISH using oligonucleotide probes may still be possible as few eosinophils are present.

Interestingly, there was greater non-specific binding of the *antisense* probe cocktail for IκBα to eosinophils than of an equivalent concentration of a single *sense* probe. This might have been due to different probes occupying different binding sites within eosinophils, but later experiments with *individual* IκBα probes still showed significantly less non-specific binding of sense than antisense probes to eosinophils. This effect, of greater non-specific binding of antisense than sense probes to eosinophils, might lead to a false conclusion of successful hybridisation to target mRNA, and emphasises the importance of strict observation of negative controls, i.e. the sense probe should be entirely negative and not only 'less positive'. The explanation for the difference in non-specific binding of probes to eosinophils is unclear and is further explored in Chapter 3.

4.3 Review of previous literature

ISH using oligonucleotide probes has previously been extensively used in bowel using a similar protocol, particularly to identify cells containing cytokine mRNA, without recognition of binding of probes to eosinophils (221,287-292). Results in these studies have shown 'positive' cells within the lamina propria with no staining within other expected areas, such as the epithelium. Hence, it may be possible that these apparently 'positive' cells were, in fact, due to probes binding to eosinophils. Furthermore, increased numbers of eosinophils in sections of inflamed specimens result in increased numbers of cells binding probes, which, when mistaken for hybridisation to target

mRNA, appears consistent with hypotheses of increased numbers of cells expressing cytokine mRNAs in inflamed specimens. Other reports, using similar methods in the gastrointestinal tract, may also have been subject to this effect (293-296).

Binding of oligonucleotide probes to eosinophils was also observed in nasal polyp, and is therefore likely to occur in other eosinophil-containing tissues such as lung, liver and skin, and previous studies using oligonucleotide ISH with these tissues (297-299) may have been unknowingly subject to this effect.

Furthermore, there are studies that suggest that non-specific binding to eosinophils may occur with probes other than oligonucleotide probes. A study of expression of transforming growth factor-β in nasal polyp using a 640 base-pair cDNA probe, demonstrated a positive signal over eosinophils only, and none over fibroblasts, macrophages and endothelial cells as was expected from *in vitro* studies (300). In another study, riboprobes bound to eosinophils in bowel despite higher stringency washes allowed by long probes and the stronger interaction between DNA-RNA compared to DNA-DNA hybrids, and despite post-hybridisation treatment with RNase to destroy non-hybridised probe (286); this suggests RNase is ineffective in hydrolysing RNA bound non-specifically to eosinophil granules. Thus, non-specific binding to eosinophils may occur with all types of probe, and so these findings are relevant for all types of ISH in eosinophil-containing tissues.

Furthermore, non-specific binding of nucleotide probes to eosinophils may explain the apparently contradictory literature on expression of interleukin-5 (IL-5) mRNA in Crohn's disease; a study using ISH with riboprobes demonstrated increased expression of IL-5 mRNA in the lamina propria of inflamed bowel from patients with Crohn's

disease (254), but no increase was found when IL-5 mRNA was assessed by quantitative reverse transcriptase polymerase chain reaction performed on homogenates of mucosal biopsy specimens (235). In addition, it has previously been suggested that eosinophil granules may contain RNA based on localisation of labelled nucleic acids to eosinophil granules (301), but this observation may be explained by non-specific binding of nucleic acids to eosinophils.

Another study has identified potential problems when using oligonucleotide probes for ISH in the gastrointestinal tract of the rat. An unusually strong signal was noted overlying immune cells of the lamina propria using ^{35}S-dATP-labelled probes, which was thought to represent an amplification of a specific hybridisation signal due to crosslinking of thiosulphate groups on ^{35}S-labelled probes, co-ordinated by cobalt ions in the hybridisation buffer (302). Specific hybridisation was thought to have occurred because experiments with sense probes were negative, and because use of riboprobes for the same mRNA produced a similar pattern of positive cells within the lamina propria. However, as described above, there may be differential non-specific binding of antisense and sense probes to eosinophils, and binding of riboprobes may also occur, which may explain these findings.

Paneth cells in rat stomach and small intestine have also been shown to non-specifically bind nucleic acid probes, providing a further potential hazard when using ISH in the gastrointestinal tract (303).

5. Conclusion

Eosinophils within sections of bowel and nasal polyp non-specifically bind oligonucleotide probes. Non-specific binding to eosinophils was prevented by a combination of pre-treatment of sections with dithiothreitol and iodoacetamide and stringent post-hybridisation washes, but the stringency of these washes resulted in loss of hybridised probe. When wash stringency was reduced to a level that allowed retention of hybridised probe, non-specific binding to eosinophils returned, despite pre-treatment of sections with dithiothreitol and iodoacetamide. It is concluded that these methods do not allow successful blocking of non-specific binding to eosinophils as well as successful hybridisation, and that the technique of ISH using oligonucleotide probes should be used with caution to investigate gene expression in the lamina propria of bowel, and probably in other eosinophil-containing tissues, unless other blocking manoeuvres are developed.

Differential non-specific binding of individual oligonucleotide probes to eosinophils was observed, which may lead to misinterpretation of non-specific binding to eosinophils as successful hybridisation to target mRNA, and the causes of this phenomenon are explored in Chapter 3.

Chapter 3

Oligonucleotide probes bind to eosinophilic cationic protein

1. Introduction

In Chapter 2, non-specific binding of oligonucleotide probes to eosinophils in sections of bowel during ISH was demonstrated and methods of blocking this interaction were investigated. Furthermore, greater non-specific binding of antisense than of sense oligonucleotide probes to eosinophils was observed.

1.1 Aim

The aim of the present chapter was to investigate the nature of this binding further using *in vitro* techniques, and to identify the element(s) within eosinophils that binds oligonucleotide probes. Eosinophilic cationic protein (ECP), contained within eosinophil granules, was hypothesised to be this element for the reasons explained below.

1.2 Eosinophils

Eosinophils are often considered a subset of PMNs because of similar structure with multi-lobed nuclei and prominent cytoplasmic granules, but they have different functions and are derived from different progenitor cells. Eosinophils are mainly concerned with allergic reactions, parasitic infections and chronic inflammatory

responses and are found predominantly in tissues, whereas neutrophils are primarily involved in acute bacterial infections, ischaemic lesions and reactions to damaged cells and tissues, and defend predominantly intravascular sites. Neutrophils phagocytose material whereas eosinophils secrete their granules. Eosinophil granules contain large quantities of major basic protein (8.6 μg per 10^6 cells) that is thought to be an important mediator of eosinophil-dependent damage to parasites and host tissues, and also of ECP (25 μg per 10^6 eosinophils) within cytoplasmic granules (304).

1.3 Biochemistry of ECP

ECP is a single-chain, highly cationic glycoprotein that contains 2.5 moles of zinc per mole of protein (283). It exists in three molecular weight forms of 18.5, 20 and 22 kDa and has an isoelectric point (pI) of over 11 (305). It is secreted from eosinophils by degranulation and has ribonuclease activity, histamine-releasing properties and neurotoxic effects.

The pI of a protein describes the pH of a solution of that protein at which the protein carries no net charge. The unusually high pI of ECP results in ECP bearing a strongly cationic charge at physiological pHs, and it was therefore hypothesised that oligonucleotide probes, known to be mildly anionic at physiological pHs, were binding to ECP within eosinophils. Biomolecular interaction analysis, which is a method that records and characterises the real-time interaction between two biomolecules, was used as an *in vitro* method to demonstrate this proposed interaction.

2. Description of real-time biomolecular interaction analysis using a biosensor approach

2.1 Background

A biosensor is defined as an instrument that combines a biological recognition mechanism with a sensing device or transducer, and is used to monitor interactions between biomolecules. Early biosensor methods, such as enzyme-linked immunosorbent assay and affinity chromatography, give information about the conditions and specificity of such interactions but only provide a snap-shot and are unable to continuously monitor the interaction. Spectrophotometric methods are rapid and can be used to follow interactions, but require the molecules to contain a suitable absorbent or fluorescent group. Alternatively, one of the molecules can be labelled, but this may interfere with the interaction and requires the interactants to be purified in relatively large quantities.

A recently developed biosensor method, termed real-time biomolecular interaction analysis, continuously monitors the interaction of unlabelled molecules using the optical phenomenon of surface plasmon resonance, which is the sharp reduction in intensity of reflected light that occurs at a specific incident angle of a light beam that is totally internally reflected at a thinly metal-coated surface.

2.2 Surface plasmon resonance

At an interface between two transparent media of different refractive indices, light from the side of higher refractive index is partly reflected and partly refracted. Below a certain critical angle of incidence, no light is refracted across the interface and total internal reflection occurs. Although the incident light is totally reflected, an

electromagnetic field component, the evanescent wave, penetrates a short distance into the medium of lower refractive index (Figure 1). If the interface between the two media is coated with a thin layer of metal, the evanescent wave interacts with delocalised surface electrons (plasmons) in the metal, resulting in collective resonant oscillation of the electrons, termed surface plasmon resonance (SPR). An amplification of electromagnetic field strength occurs with SPR and causes a reduction in intensity of reflected light, and the angle of reflection at which this reduction occurs is termed the SPR angle and is measured by the BiacoreX™ instrument as an SPR signal in resonance units (RU) and plotted as a graph against time, the sensorgram (Fig. 2).

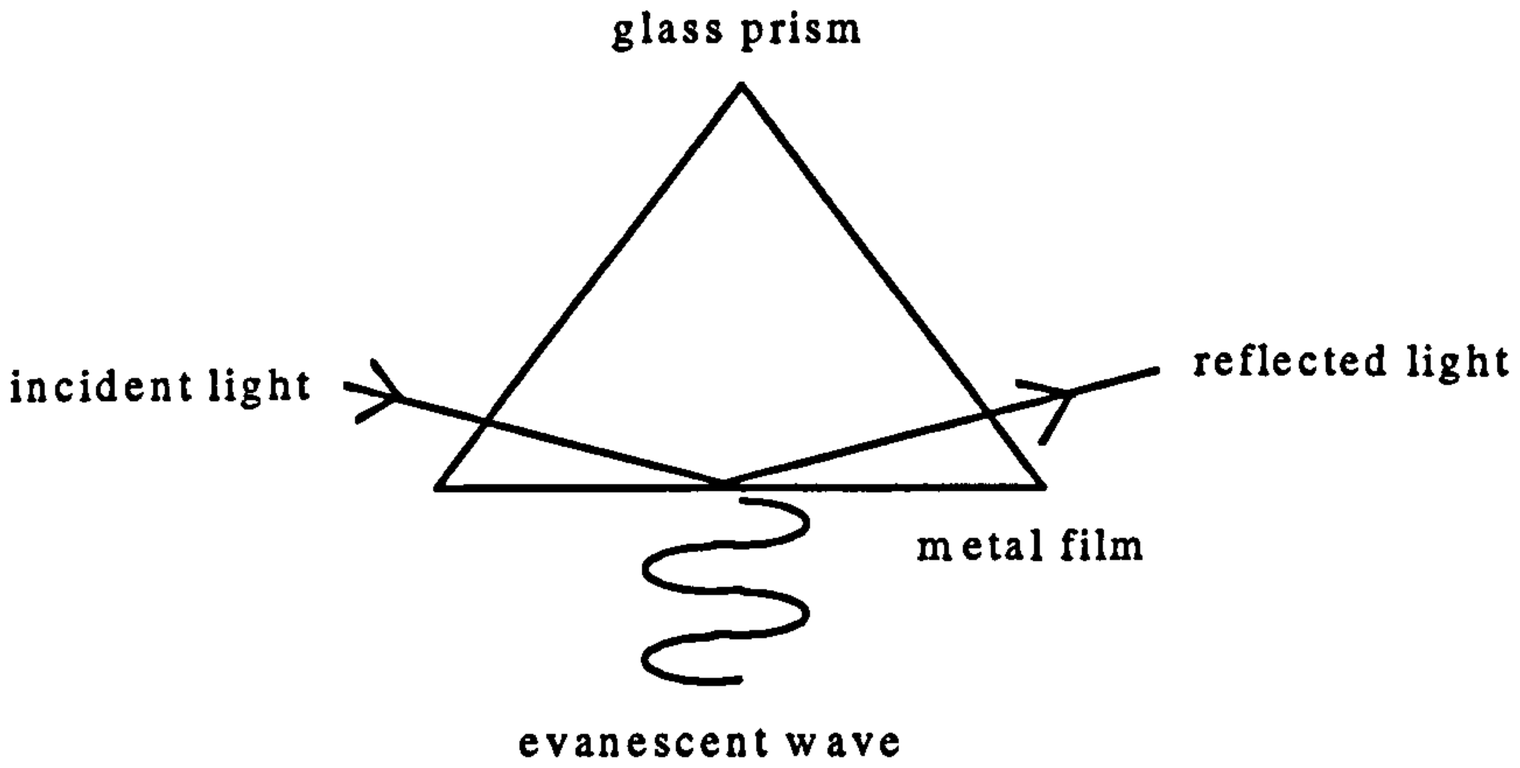

Figure 1. Principle of total internal reflection. Total internal reflection at the interface between two media of different refractive indices causes an evanescent wave in the medium of lower refractive index on the non-illuminated side (adapted from BIA technology handbook, Pharmacia Biosensor, Uppsala, Sweden).

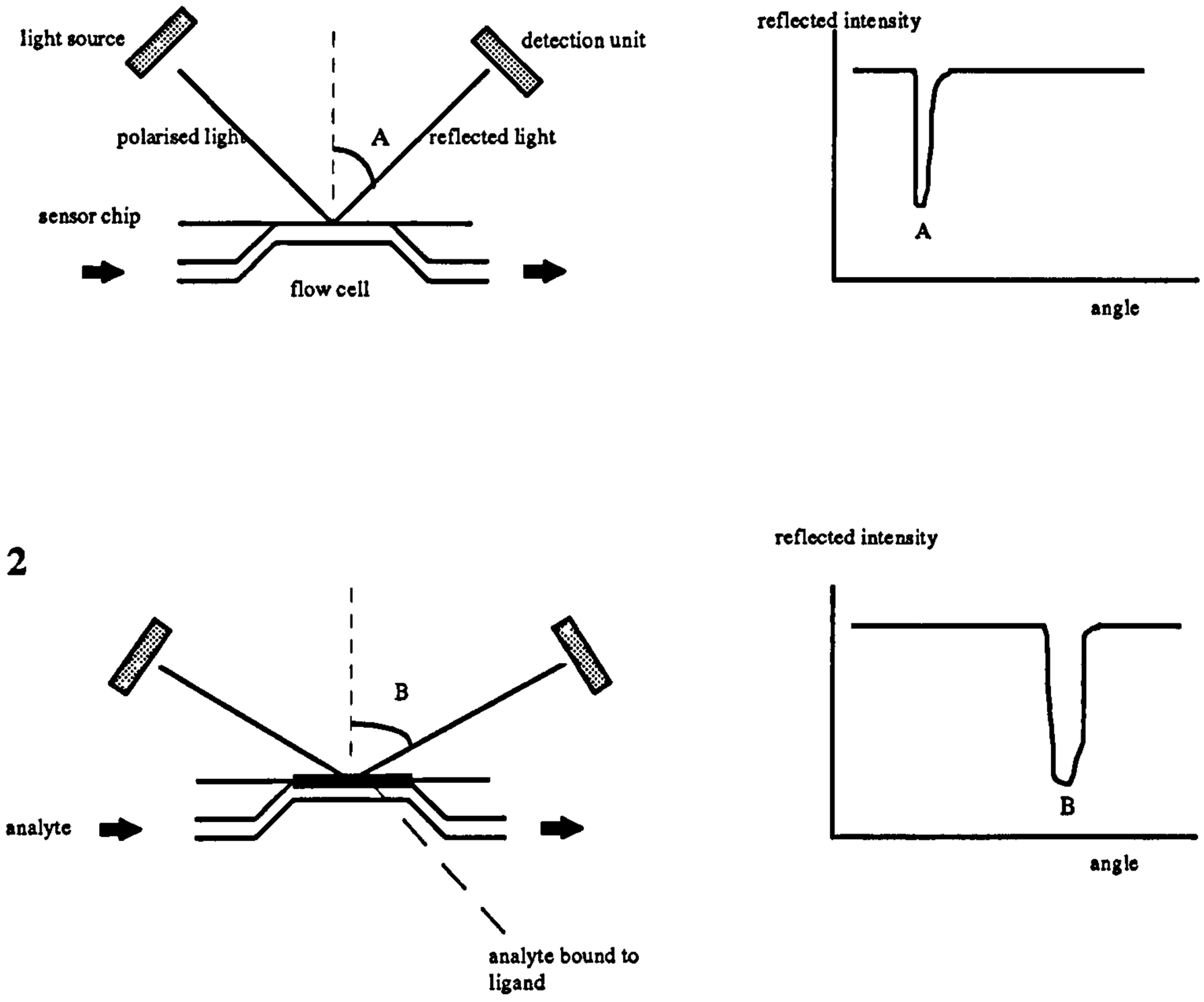

Figure 2. Principles of biomolecular interaction analysis using a BiacoreX™ instrument.

1. SPR at the sensor chip surface results in a sharp reduction in the intensity of reflected light at a specific angle of reflection (A).

2. When analyte binds to ligand on the sensor chip surface, the angle of the reduction in the intensity of reflected light changes from A to B.

3. The angles A and B are recorded as changes in 'resonance signal' in RU and plotted against time as a 'sensorgram' (adapted from BIA technology handbook, Pharmacia Biosensor).

The SPR angle is determined by three parameters:

1. the properties (thickness, optical constants etc.) of the metal film

2. the wavelength of the incident light, and

3. the refractive indices of the media on either side of the metal film.

In the BiacoreX™ instrument, 1 and 2 are constant and therefore the SPR angle is determined solely by the refractive indices of the media. The denser medium on the illuminated side of the interface is glass with a constant refractive index. The less dense medium on the non-illuminated side, into which the evanescent wave penetrates, is a carboxymethylated dextran matrix on which one of the molecules under investigation, the ligand, is immobilised. The refractive index of this medium is altered by binding of the other molecule under investigation, the analyte, to the ligand, and by the ionic strength of the overlying aqueous solution (running buffer), which affects the hydration of the dextran matrix. Providing that the running buffer is constant, then the sole variable determining SPR is binding of analyte to ligand.

2.3 Components of BiacoreX™

A. Light source and sensor. The light source is a high efficiency light-emitting diode that produces light nearly in the infrared range. The light is focused on the glass-gold interface of the 'sensor chip' in a wedge-shaped beam, giving a range of simultaneous incident angles. Reflected light is monitored by a two-dimensional diode array that determines the SPR angle to a resolution corresponding to 0.1 RU.

B. Sensor chip. The sensor chip forms the interface at which total internal reflection and SPR occur. It consists of a glass slide coated with a thin layer of gold, chosen for its combination of chemical inertness and good SPR response, that is linked to a

surface matrix of carboxy-methylated dextran. The dextran matrix allows covalent immobilisation of the ligand using well-characterised chemistry and provides a hydrophilic environment for the interaction between ligand and analyte with a very low degree of non-specific binding to the matrix. The dextran matrix is swollen to approximately 100 nm in aqueous media, and higher pH and lower ionic strength increase the depth of the matrix, and so change the baseline SPR response, by increasing electrostatic repulsion between negatively-charged carboxyl groups within dextran (306). However, running conditions of high ionic strength (physiological salt concentrations of 0.15M or higher) are preferred, so that electrostatic interactions between immobilised ligand and carboxyl groups of the dextran matrix are minimised.

The analyte is passed over the dextran-ligand surface in free solution and as the interaction proceeds, the concentration of analyte binding to ligand in the surface layer changes, producing a change in SPR angle that is continuously measured. The dextran-ligand surface is then regenerated by stripping off the analyte with a regeneration solution.

3. Flow cells. Analyte is passed through two flow cells, with the dextran surface of the sensor chip forming one wall of the cells, while the gold film is illuminated through the glass from outside the cell (Figure 2). The two cells are used in parallel, allowing simultaneous binding of analyte to two ligands, one a control that is subtracted from the index ligand. Temperature is closely controlled because of its effect on refractive index and reaction kinetics.

2.4 Immobilisation of ligand

ECP and control proteins, rather than the oligonucleotide probes, were immobilised on the dextran matrix because first, only a single immobilisation of each was required, producing a fixed concentration of immobilised ligand over which different analytes (oligonucleotide probes) could be repeatedly passed, and second, immobilisation of the larger molecules was less likely to interfere with the active site(s) responsible for the proposed interaction between ECP (and control proteins if this occurred) and oligonucleotide probes.

The following methods can be used to immobilise ligand to the dextran matrix:

- amine coupling using reactive esters
- coupling by thiol-disulphide exchange
- binding biotinylated ligands to immobilised streptavidin
- aldehyde coupling to a hydrazine-activated surface

Amine coupling is the most generally applicable immobilisation method (307) and is particularly recommended for neutral and basic proteins, such as ECP and the control proteins myoglobin and lysozyme.

Amine coupling comprises the following steps:

1. activation of the chip surface by injection of 0.05M N-hydroxysuccinimide and 0.2M N-ethyl-N'-dimethylaminopropylcarbodiimide, which modifies about 40 % of the carboxymethyl groups in the dextran matrix;
2. injection of ligand in a solution at a pH below the pI of the ligand, resulting in its protonation and thus increasing electrostatic attraction to the negatively-charged

carboxyl groups of the dextran matrix, a process termed 'pre-concentration'. However, the pH should not be so low that the carboxyl groups of the dextran matrix are no longer negatively charged. Electrostatic attraction is further favoured by a ligand solution of low ionic strength, and

3. deactivation of excess reactive groups in the dextran matrix with 1M ethanolamine hydrochloride at pH 8.5. In addition, the high ionic strength of this solution removes non-covalently bound ligand from the dextran matrix.

The amount of ligand immobilised is determined by the duration of injection of the dextran matrix activator, the concentration of the ligand and the pH and ionic strength of its buffer.

2.5 Regeneration of the dextran-ligand surface

After each binding study, the surface must be regenerated by removal of the non-covalently bound analyte, leaving only the ligand covalently bound to the dextran matrix. Ideal regeneration conditions vary with the nature of the ligand-analyte interaction and weak interactions simply require return to the running buffer, and so the choice of running buffer may be relevant to regeneration. However, for stronger interactions, a regeneration solution with a pH different to that of the running buffer is usually required, when the temporary change in pH strips the analyte from the ligand.

3. Methods

3.1 Preparation of dextran matrix

Hydration of dextran matrix

The sensor chip CM5 (Pharmacia Biosensor) was docked in the BiacoreX™ instrument (Pharmacia Biosensor) and the dextran matrix hydrated by injecting HEPES-EDTA-buffered saline (HBS) running buffer (Pharmacia Biosensor) (10 mM N-2-hydroxyethylpiperazine-N-2-ethanesulphonic acid (HEPES), 150 mM NaCl and 3 mM EDTA, pH 7.4, in a 0.005 % (v/v) solution of polysorbate 20 surfactant in distilled water) at 5 µl min^{-1} for forty minutes until the baseline sensorgram had stabilised. The running buffer was then passed continually at 5 µl min^{-1} over the dextran matrix, and between all subsequent injections.

Activation of dextran matrix

The dextran matrix was then activated by injecting 35 µl of 0.05M N-hydroxysuccinimide (Biosensor Pharmacia) and 0.2M N-ethyl-N'-dimethylaminopropylcarbodiimide (NHS/EDC solution, Biosensor Pharmacia) at 5 µl min^{-1}, followed by return to HBS running buffer.

3.2 Immobilisation of ligands

3.2.1 Ligands

Two proteins were used as controls for ECP (MW 18.5 kDa, pI >11), namely myoglobin, which has similar MW (18 kDa) and different pI (6.9-7.4), and lysozyme, which has similar MW (14.3 kDa) and similar pI (>10) (308). These proteins were chosen to define the nature of the proposed interaction between ECP and oligonucleotide probes.

Myoglobin and lysozyme were obtained from commercial sources and ECP was kindly donated by Professor Per Venge, University of Uppsala, Uppsala, Sweden, after isolation from human eosinophils (305).

Two different chips were prepared, the first, chip A, containing ECP and myoglobin, and the second, chip B, containing ECP and lysozyme. Thus, in each chip, simultaneous binding of oligonucleotide probes to ECP and a control protein were compared, and the two resulting sensorgrams were subtracted (see Figures 3 and 4) to remove background changes in the sensorgrams and hence determine true binding to ECP.

3.2.2 Preparation of two chips

Chip A: ECP was immobilised (net immobilisation 3482 RU, 0.188 pmol mm^{-2}) in one cell and the control protein, myoglobin from horse heart (Sigma Chemical Company), in the other (net immobilisation 3477 RU, 0.193 pmol mm^{-2}).

Chip B: ECP was again immobilised in one cell (net immobilisation 3755 RU, 0.203 pmol mm^{-2}) and in the other the control protein, lysozyme from chicken egg white (Sigma Chemical Company) (net immobilisation 981 RU, 0.069 pmol mm^{-2}).

3.2.3 Immobilisation conditions

a) Myoglobin

Myoglobin was immobilised in one of the two flow cells of chip A by injecting 10 µl of a 500 µg ml^{-1} solution of myoglobin in 10 mM sodium acetate buffer (BDH) pH 3.0 at 5 µl min^{-1}, followed by return to HBS running buffer.

b) ECP

ECP was immobilised in one of the two flow cells of both chips A and B by injecting 10 µl of a 500 µg ml^{-1} solution of ECP in 200 mM sodium acetate buffer pH 5.5 at 5 µl min^{-1}, followed by return to HBS running buffer.

c) Lysozyme

Lysozyme was immobilised in one of the two flow cells of chip B by injecting 10 µl of a 500 µg ml^{-1} solution of lysozyme in 200 mM sodium acetate buffer pH 5.5 at 5 µl min^{-1}, followed by return to HBS running buffer. To achieve an immobilisation level for

lysozyme of equivalent order of magnitude to that achieved for myoglobin and for ECP, a further 20 µl followed by 40 µl of a 500 µg ml^{-1} solution of lysozyme, and then finally 35 µl of a 1000 µg ml^{-1} solution were injected.

3.3 Deactivation of dextran matrix

Excess reactive groups were then deactivated by injection of 50 µl of ethanolamine hydrochloride 1M, pH 8.5 (Sigma) at 5 µl min^{-1} followed by return to HBS running buffer.

3.4 Protocol for binding of analytes

The binding of four oligonucleotide probes to ECP was examined, namely antisense 1, antisense 2, antisense 3 and sense probes for IκBα mRNA (see Chapter 2, Table 1 for sequences). These probes were chosen as individual *in situ* binding of these probes to eosinophils had been quantitated in Chapter 2, hence allowing comparison of *in situ* binding to eosinophils with *in vitro* binding to ECP.

All oligonucleotides were at a concentration of 100 µg ml^{-1}, which was 833 times greater than the concentration of probe in the hybridisation solution (0.12 µg ml^{-1}) used during ISH. This concentration was chosen arbitrarily, as the concentration of immobilised ECP could not be equated to the concentration of ECP in eosinophil granules, which is unknown (although it is known that 10^6 eosinophils contain 26 µg ECP (304)). Oligonucleotide probes were injected over the dextran-ligand surface at 20 µl min^{-1}. The net binding of probe was measured in RU as the difference in the sensorgram from immediately pre-injection to a fixed interval (80 seconds) after the end of injection of the oligonucleotide probe.

3.5 Solutions tested to regenerate the dextran-ligand surfaces

The following regeneration solutions were tested to obtain optimal conditions (see section 4.1 for results of testing):

solution A. Pierce antibody/antigen buffer (Pierce & Warriner (UK) Ltd., Chester, UK) - a regeneration solution widely used to disrupt many interactions (formula not released by manufacturer);

solution B. Pierce antibody/antigen buffer diluted 1 in 10 in the appropriate running buffer, and

solution C. 0.15M KCl (BDH) adjusted to pH 12 with KOH (BDH) - a strong alkali to deprotonate ligands, including those with high pI (ECP and lysozyme), resulting in a net negative charge on the ligand and thus aiding dissociation of the negatively-charged oligonucleotide analytes. To reprotonate the ligand, 10 µl of 200 mM sodium acetate with 50 mM NaCl (BDH), adjusted to pH 5.5 with NaOH (BDH), was injected, followed by a return to HBS running buffer, pH 7.4, thus returning the ligand to its physiological state.

3.6 Method of analysis of sensorgrams to obtain data for kinetics of binding

The proposed interaction between ECP and oligonucleotide probes was assumed to be of 1:1 stoichiometry, and therefore described by the formula:

$$A + B \underset{k_d}{\overset{k_a}{\rightleftharpoons}} AB$$

where the association rate, k_a in $M^{-1}\ s^{-1}$, is defined in the formula:

$$d[AB] / dt = k_a [A][B]$$

and the dissociation rate, k_d in s^{-1}, is defined in the formula:

$$- d[AB] / dt = k_d [A][B]$$

The dissociation constants at equilibrium (K_D in M), which describe the balance between complexes and free components at equilibrium and are therefore indices of affinity, were calculated using calculated values for k_a and k_d and the formula:

$$K_D = k_d / k_a.$$

To examine the kinetics of the association between ECP and oligonucleotide probes, standard analysis of the data in sensorgrams was performed using a computer program, BIA evaluation (Pharmacia Biosensor), specifically designed for analysis of data collected with a BiacoreX™ instrument, and a PC. Using this package, the sensorgrams of the simultaneous injection of one probe into both flow cells of a chip, one containing ECP, and the other myoglobin or lysozyme, in chips A and B respectively, were

precisely superimposed to allow subtraction of the sensorgram for the control protein from that for ECP, thus removing bulk refractive effects of solutions and fluctuations due to, for example, opening and closing of the valves controlling injection.

3.6.1 Chip A containing ECP and myoglobin

A representative example of sensorgrams for one of the five injections of antisense 1 probe into chip A, thus injected simultaneously over ECP and myoglobin, is displayed in Figure 3. The large negative deflection of both sensorgrams that occurs at the start of injection represents a combination of the bulk refractive effect and any binding of oligonucleotide probe to ECP or the control protein, myoglobin. A smaller negative deflection of the ECP sensorgram than the control protein sensorgram is observed, due to the expected binding of oligonucleotide probe to ECP, but not to the control protein.

In chip A at the start of injection (Figure 3), there are small delays in the negative deflection of the ECP sensorgram in comparison to the myoglobin sensorgram, and, similarly, in the return to baseline at the end of injection. These are not due to a mismatch in the timings of the injections, which occur simultaneously (with recording of sensorgrams to within 0.1 s), as the bulk refractive shift effect of the injection of the probe solution occurs on both sensorgrams at precisely the same moment.

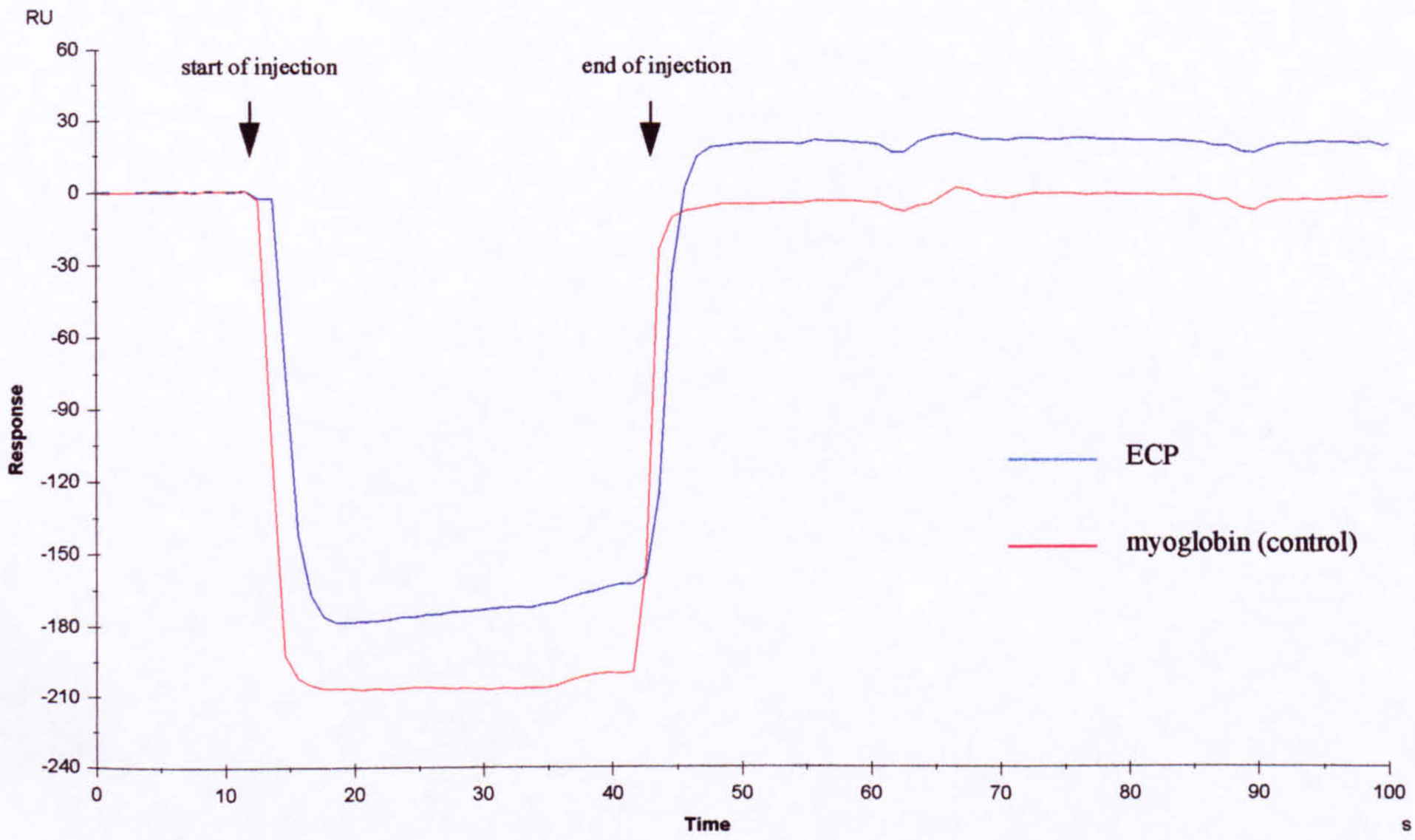

Figure 3. A representative example of one of five injections of antisense 1 probe over ECP and myoglobin in chip A, displayed as overlaid sensorgrams. Similar sensorgrams were plotted for the three other oligonucleotide probes. The large negative deflection of both sensorgrams that occurs at the start of injection represents a combination of the bulk refractive effect and any binding of oligonucleotide probe to ECP or the control protein, myoglobin. A smaller negative deflection of the ECP sensorgram than the control protein sensorgram is observed, due to the expected binding of oligonucleotide probe to ECP, but not to the control protein. The sensorgrams are precisely superimposed but a slower, as well as smaller, negative deflection of the ECP sensorgram is observed (see section 3.6.2 for explanation).

Thus, when the myoglobin sensorgrams are subtracted from the simultaneous ECP sensorgrams for each probe, the sensorgrams in Figure 4 result, with an initial large peak and subsequent large trough in the subtracted sensorgrams. Figure 5 demonstrates the reproducibility these *subtracted* sensorgrams (ECP–myoglobin) for five successive bindings of antisense 1 to ECP and myoglobin in chip A.

Association rate constants were calculated from the straight line data between the start and end of injection in the graphs in Figure 4, during the period when the probes were passed over the dextran-ECP surface. Dissociation rate constants were calculated from the data after the end of injection.

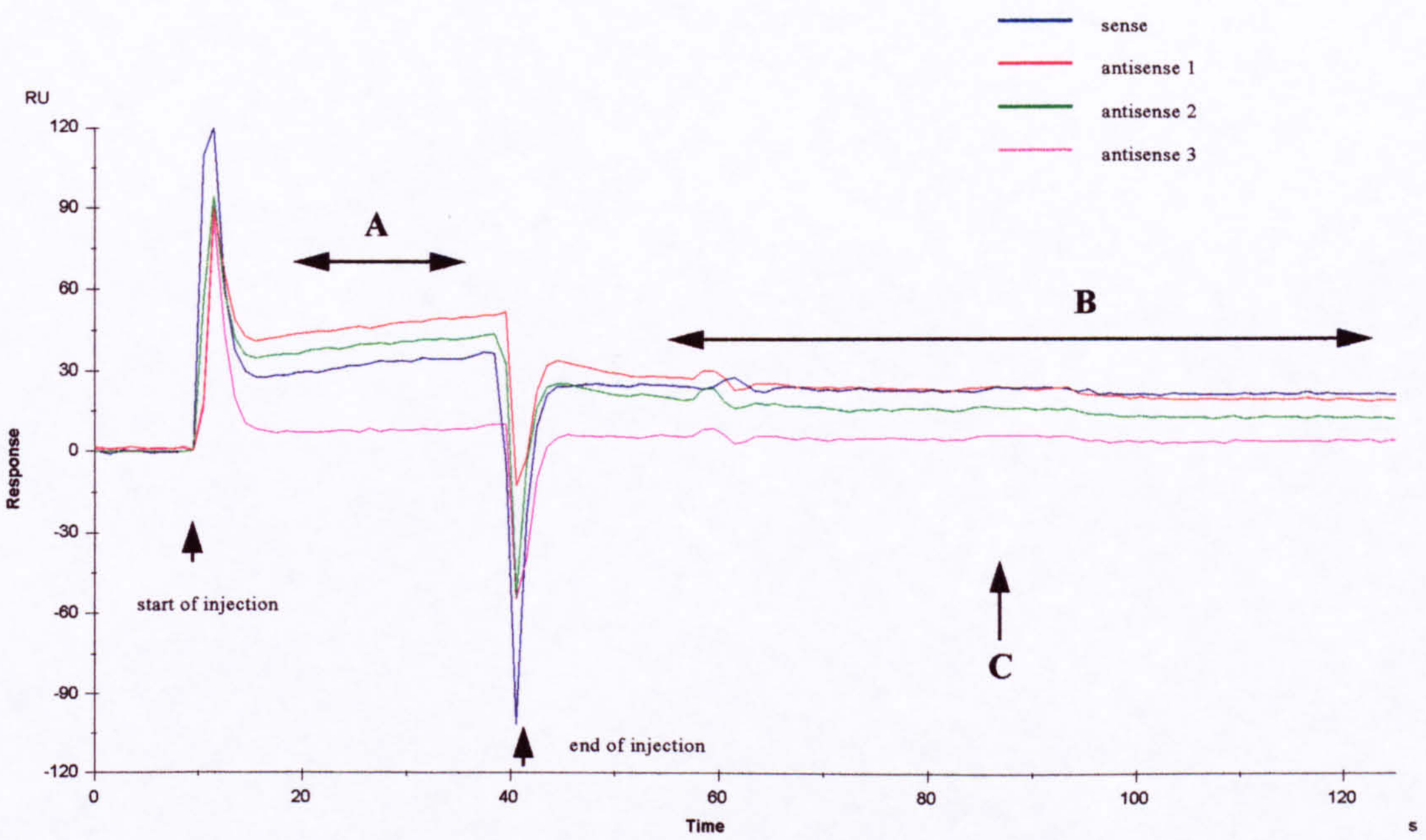

Figure 4. Subtracted sensorgrams (ECP–myoglobin) representing net binding to ECP in chip A for all four oligonucleotide probes. The sensorgrams are representative examples of one of five cycles of injections of probes. They were created by subtraction of the sensorgrams for injection over myoglobin from the sensorgrams for simultaneous injection over ECP for each probe, and represent on-off curves for the interaction between ECP and oligonucleotide probes. The association and dissociation rate constants were calculated using the data contained in the areas of the graphs marked 'A' and 'B' respectively, while the magnitude of binding was measured at an arbitrary point, 80 seconds after the start of injection, marked 'C'. The genesis of the initial large peak at the start of injection and the subsequent large trough at the end of injection is explained in the legend to Figure 3, and their meaning discussed in section 3.6.

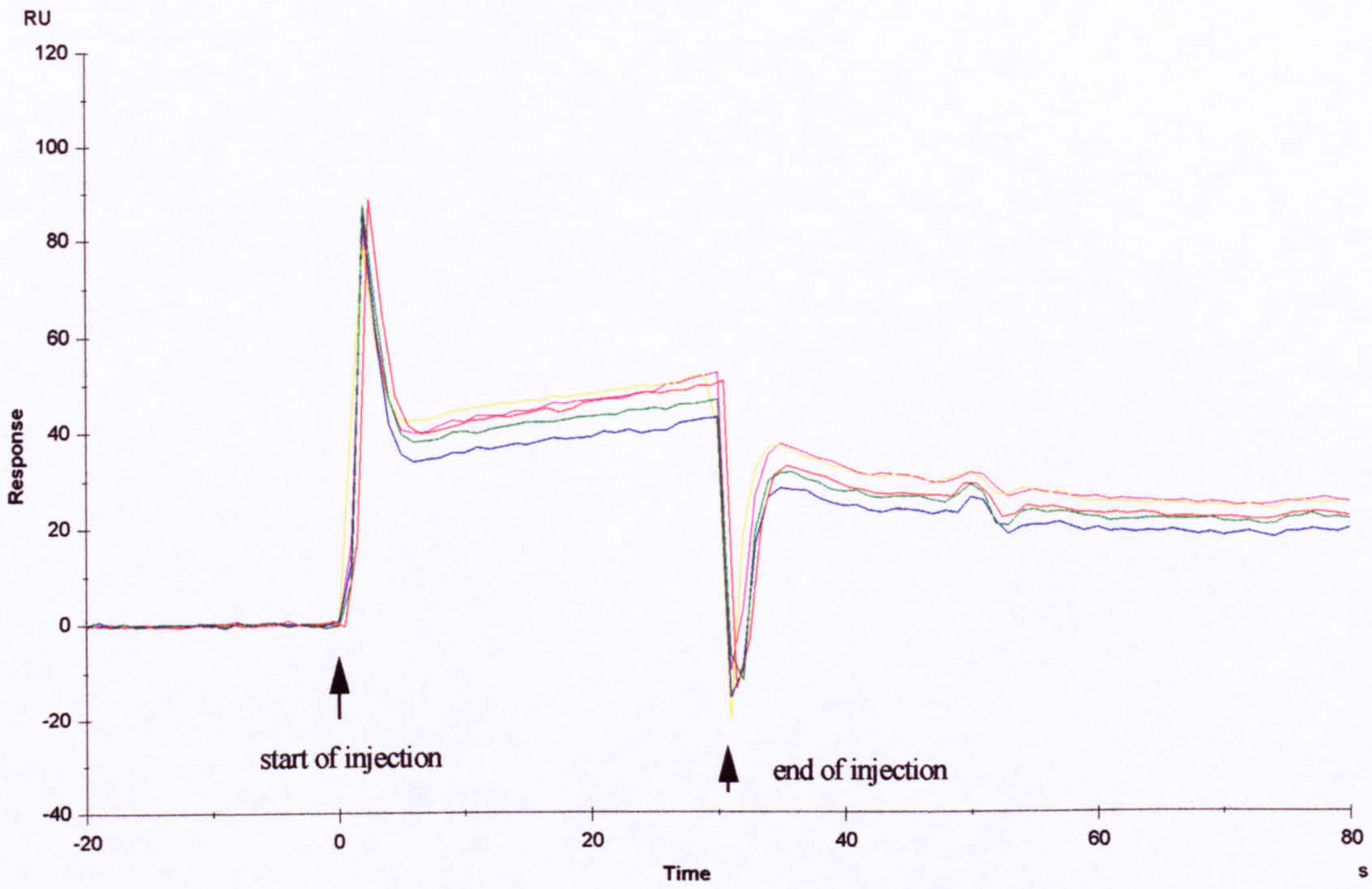

Figure 5. Reproducibility of subtracted sensorgrams (ECP–myoglobin) representing five successive bindings of antisense 1 to ECP in chip A. Sensorgrams were created by subtraction of the sensorgrams for injection of probes over the control protein, myoglobin, from the sensorgrams for simultaneous injections over ECP. The graphs demonstrate that the data were highly reproducible, and that the initial large peak at the start of injection and large trough at the end of injection were conserved between injections.

3.6.2 Chip B containing ECP and lysozyme

In chip B, there was no mismatch in the simultaneous sensorgrams of injection of antisense 1 over ECP and lysozyme (Figure 6), and hence the subtraction of the sensorgrams results in a sensorgram with a smooth on-off curve representing binding to ECP (Figure 7, red curve), with no peak and trough at the beginning and end of injection, as occurred in chip A with ECP and myoglobin. Similar smooth on-off curves were obtained in chip B for antisense 2, antisense 3 and sense probes. The mismatch in chip A may be due to the difference in pI of ECP and myoglobin that may have caused a charge-related artefact, that was not seen in chip B because of the similarity in the pI of ECP and lysozyme.

3.7 Statistical analysis

Statistical analysis was performed using STATA (Stata statistical software, Release 5.0, Stata Corporation, College Station, Texas, USA) and a PC, and was performed by Dr. Roger Newson, Lecturer in Medical Statistics, Imperial College Medical School, London.

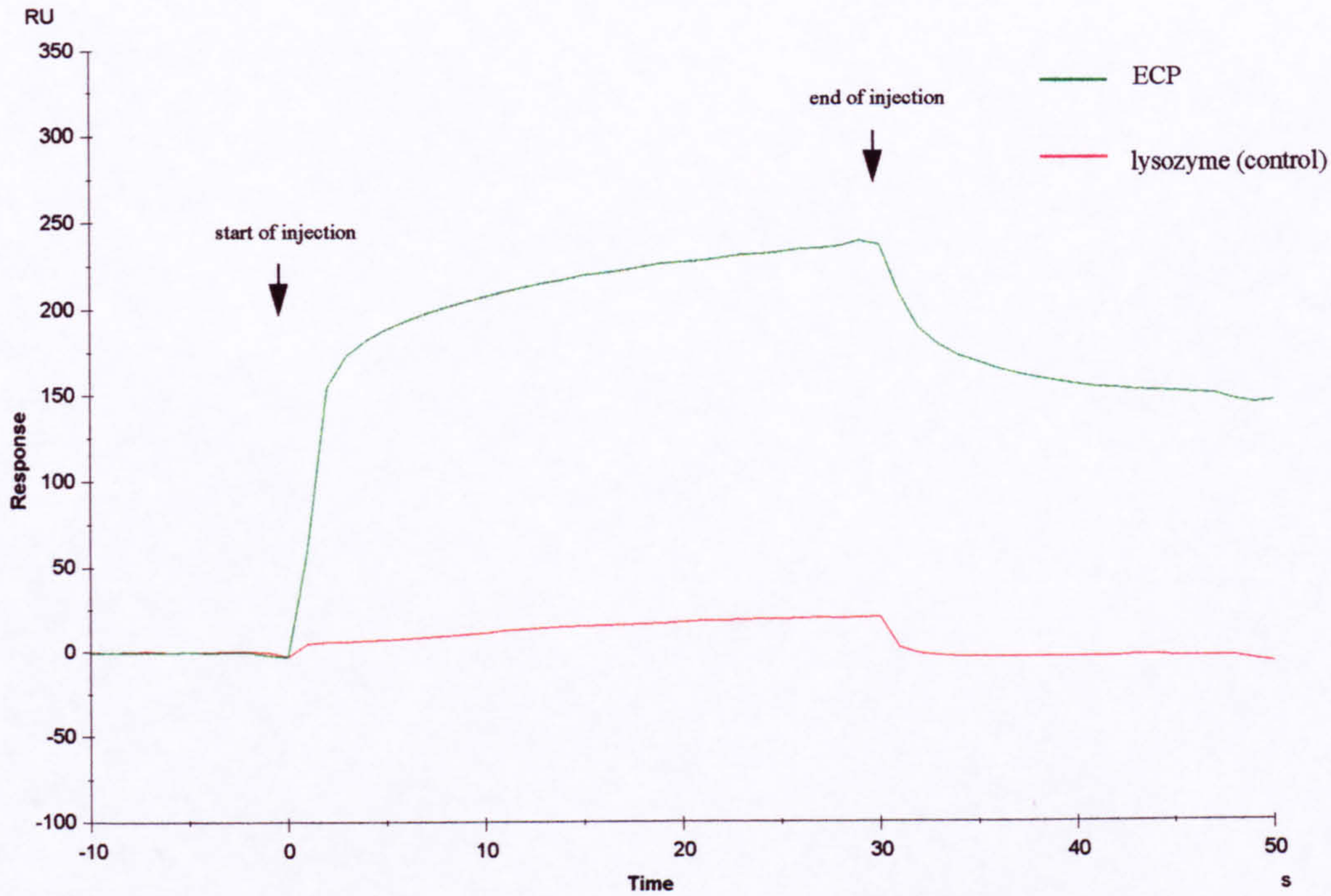

Figure 6. A representative example of one of four injections of antisense 1 probe over ECP and lysozyme in chip B, displayed as overlaid sensorgrams. In contrast to Figure 5, there is no delay in the deflection of the two sensorgrams at the start and end of injection, and in this chip, the bulk refractive effect of the injection solution is negligible.

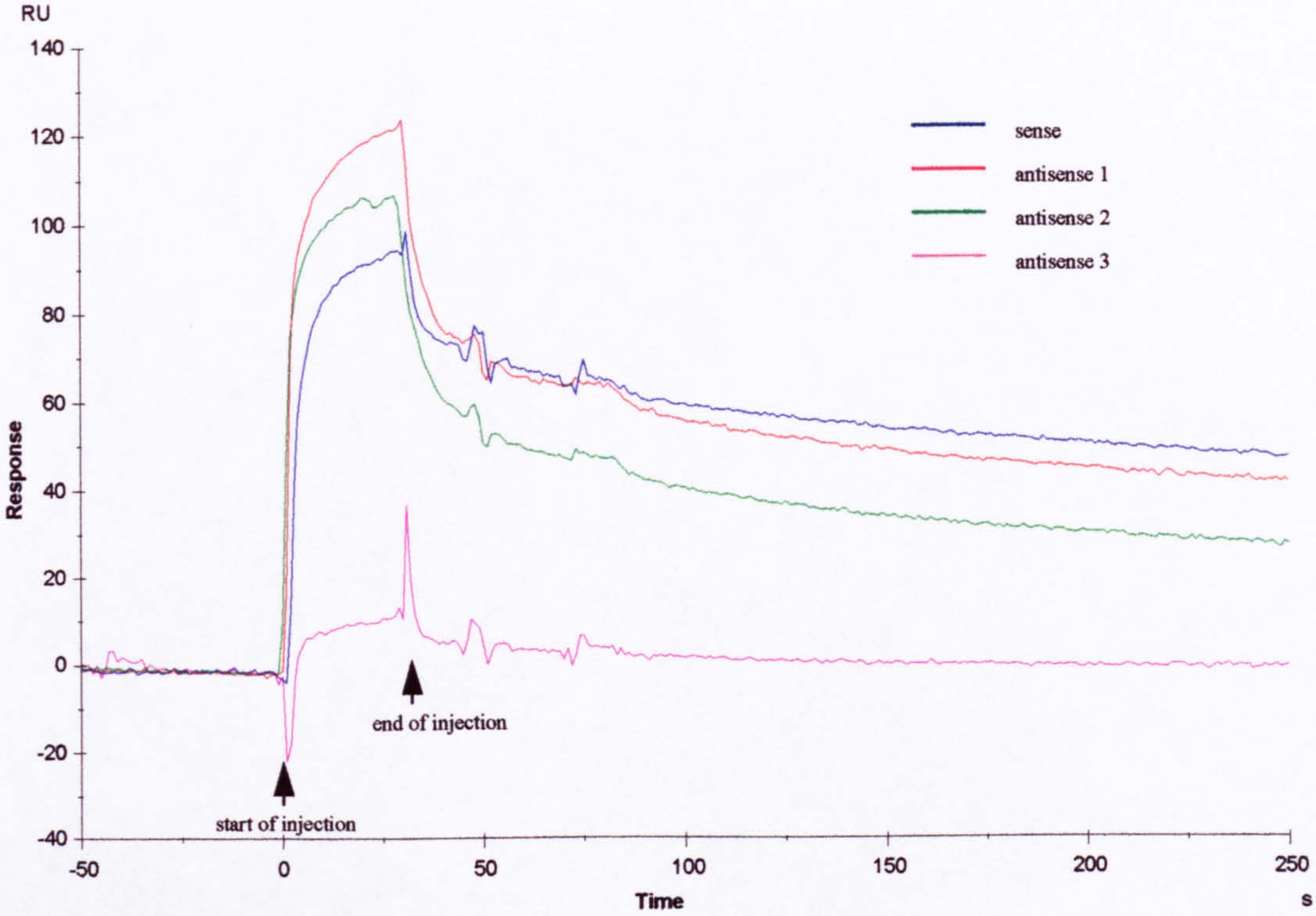

Figure 7. Subtracted sensorgrams (ECP–lysozyme) representing net bindings to ECP in chip B of all four oligonucleotide probes to ECP. Sensorgrams were created by subtraction of the sensorgrams for injection over the control protein, lysozyme, from the sensorgrams for simultaneous injections over ECP, for each probe. The curves represent *smooth* on-off curves for the interaction between ECP and the four tested oligonucleotide probes, and are the only complete cycle of injections of all four probes in chip B.

4. Results

4.1 Establishment of conditions for regeneration of dextran-ligand surface

Ideal regeneration of the dextran-ligand surfaces results in reproducible bindings of analyte to the ligands (ECP and control protein). For this to be achieved, the sensorgram should return after each regeneration injection to the level prior to binding of analyte, suggesting complete removal of the analyte from the dextran-ligand surface without stripping of any ligand from the dextran. Experiments to establish ideal regeneration conditions are described in Appendix I and, based on these findings, 2 µl of solution C was chosen as the regeneration injection and HBS was used as the running buffer.

4.2 Binding of different oligonucleotide probes to ECP and to myoglobin in chip A

Oligonucleotide probes were injected simultaneously over the two ligands in chip A, ECP and myoglobin, and the dextran-ligand surfaces regenerated between bindings. The four oligonucleotide probes were injected in succession and the sequence of successive injections was changed in each cycle. The changes in the baselines from before injection to after regeneration were satisfactory for all four probes and are displayed in Table 1 in relation to the mean binding for each probe.

Table 1. Regeneration of dextran-ligand surface in chip A. Regeneration was assessed by change, in RU, in baseline sensorgram from before injection of oligonucleotide probe to after regeneration in five successive cycles of simultaneous injections of oligonucleotide probes over ECP and myoglobin in chip A.

	antisense 1		antisense 2		antisense3		sense	
	ECP	**MG**	**ECP**	**MG**	**ECP**	**MG**	**ECP**	**MG**
mean binding of probe (RU)	18.4	0.0	12.2	-0.4	2.9	0.0	23.4	0.3
mean Δ baseline sensorgram (RU)	3.2	-0.5	0.6	-1.8	-1.8	-1.2	-2.1	-1.6
SD Δ baseline sensorgram (RU)	1.1	2.0	1.7	0.9	2.1	2.1	1.0	0.8

Where Δ = change, MG = myoglobin, ECP = eosinophil cationic protein.

binding = RU of sensorgram 80 seconds after injection – RU immediately before injection of oligonucleotide probe

4.2.1 Assessment of data for drift between cycles of injections of oligonucleotide probes in chip A

Binding data are displayed in Table 2 and Figure 8 and were first analysed using Kendal's tau-a test to test for a significant drift between cycles in the magnitudes of bindings of oligonucleotide probes to ECP and myoglobin, and in the differences between them (ECP – myoglobin). There was a significant drift between cycles of bindings to myoglobin only (Table 2), with a significant drift from a small net fall (negative 'binding') to a small net rise (positive 'binding') in the sensorgram with each successive cycle of injections of probes (mean difference in 'binding' to myoglobin between successive cycles = 0.44 RU (95 % confidence intervals (CI) 0.14 to 0.73), p = 0.005, derived from data in Table 2). The cause of this significant upward drift for myoglobin, but not for ECP, is unclear, but may relate, in some manner, to the small, but progressive, fall in the baseline myoglobin sensorgram between successive cycles (mean (SD) change in baseline myoglobin sensorgram between cycles = .-4.5 (3.7), in comparison to ECP sensorgram = 0.8 (2.0))

To allow for the drift in 'binding' to myoglobin, data from Table 2 were then analysed by regression with robust variance clustered by cycle in section 4.2.2.

4.2.2 Comparison of binding of oligonucleotide probes to ECP with 'binding' to the control protein, myoglobin, in chip A

There were significant differences for all oligonucleotide probes between binding to ECP and 'binding' to the control protein, myoglobin (Table 3), indicating binding to ECP but not to myoglobin.

4.2.3 Comparison of sense with antisense oligonucleotide 'net' binding to ECP in chip A

In Chapter 2, a significant difference in *in situ* binding to eosinophils between sense and antisense oligonucleotide probes was demonstrated. Thus the data for *in vitro* binding to ECP in the present chapter were *a priori* analysed for this comparison. The mean difference between ECP and myoglobin binding, termed mean net binding to ECP, for the sense probe was significantly greater than for the three antisense probes (mean difference between antisense and sense probes in net binding to ECP = 12.3 RU (CI 10.5 to 14.1), $p < 0.001$, by regression with robust variance clustered by cycle, derived from data in Table 2). Thus, significantly greater *in vitro* binding of sense than antisense probes to ECP was observed, the converse of the *in situ* observations.

Comparison of net binding to ECP between different *antisense* probes was not made, as this was not the original intention of the *in vitro* experiments and, if performed, would therefore have compromised the statistical analysis because of multiple retrospective comparisons.

Table 2. Magnitudes of bindings of different oligonucleotide probes to ECP and to myoglobin in chip A (data displayed in graphic form in Figure 8). In each cycle, each probe was injected once, and the order of injections was changed between cycles. Means and standard deviations of magnitudes of bindings of each oligonucleotide probe are displayed in RU.

	bindings of antisense 1 (RU)		bindings of antisense 2 (RU)		bindings of antisense 3 (RU)		bindings of sense (RU)	
cycle	**ECP**	**MG**	**ECP**	**MG**	**ECP**	**MG**	**ECP**	**MG**
1	20.0	-1.2	15.3	-1.0	2.5	-1.1	23.4	-2.0
2	20.0	-2.4	10.0	-1.2	2.4	-0.5	25.6	0.5
3	18.4	0.8	11.9	-0.1	3.1	0.2	22.0	0.5
4	17.5	0.5	13.1	0.3	3.2	0.0	23.6	0.5
5	16.4	2.3	10.7	-0.1	3.5	1.5	22.4	-0.8
mean	18.4	0.0	12.2	-0.4	2.9	0.0	23.4	0.3
SD	1.6	1.8	2.1	0.7	0.5	1.0	1.4	1.1

MG = myoglobin, ECP = eosinophil cationic protein

binding = RU of sensorgram 80 seconds after injection – RU immediately before injection of oligonucleotide probe

Figure 8. Graph displaying means and standard deviations of magnitudes of bindings of different oligonucleotide probes to ECP (×) and to myoglobin (•) in chip A in RU (data displayed in tabulated form in Table 2).

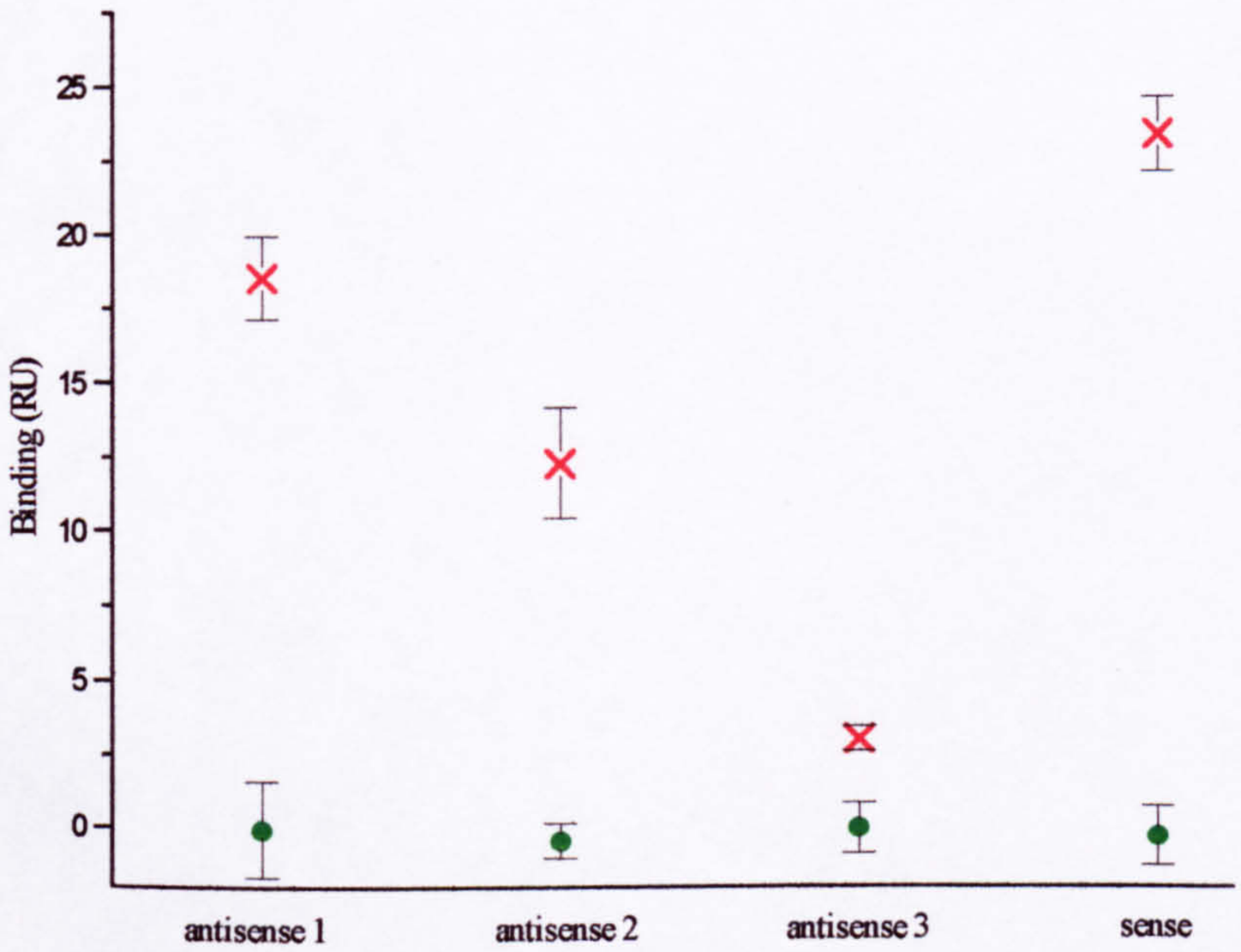

Table 3. Differences in magnitude of binding of oligonucleotide probes to ECP and the control protein myoglobin (termed net bindings to ECP in text) in chip A.

probe	mean difference between binding to ECP and binding to myoglobin (RU)	95 % confidence intervals of the difference (RU) *	p value*
antisense 1	18.5	(15.3, 21.6)	< 0.001
antisense 2	12.6	(10.5, 14.7)	< 0.001
antisense 3	2.9	(2.4, 3.5)	< 0.001
sense	23.7	(22.1, 25.2)	<0.001

* analysis by regression with robust variance clustered by cycle

4.3 Binding of different oligonucleotide probes to ECP and to lysozyme in chip B

The magnitudes of binding of antisense 1 and sense probes to ECP and lysozyme in chip B are displayed in Table 4. The two other probes were tested only once.

Table 4. Magnitudes of bindings of antisense 1 and sense oligonucleotide probes to ECP and to lysozyme in Chip B. Four injections of antisense 1 were followed by four injections of sense probe, and means and standard deviations of magnitudes of bindings for each oligonucleotide probe are displayed in RU.

	magnitudes of bindings of antisense 1 (RU)		**magnitudes of bindings of sense (RU)**	
	ECP	**LYS**	**ECP**	**LYS**
	129.7	2.4	14.3	-0.9
	75.1	3.5	12.2	2.8
	55.6	2.5	10.9	0.5
	42.7	2.1	8.4	2.1
mean	75.7	2.6	11.5	1.1
SD	38.3	0.6	2.5	1.7

ECP = eosinophil cationic protein, LYS = lysozyme

Interestingly, in chip B, there appeared to be more binding of antisense 1 to ECP than of sense to ECP, a reverse of the findings in chip A. However, the reproducibility of bindings to ECP in chip B was less well established than in chip A, with a marked decay in binding with each successive injection of the same probe. A similar exponential decay in early bindings had been noted in chip A when conditions of regeneration were being established, but quantitation of oligonucleotide binding was not performed with this chip until the rate of decay of binding had fallen to an insignificant level, because of the series of experiments to establish regeneration conditions. However, in chip B, quantitation of oligonucleotide binding was performed, regrettably, without a similar 'run-in' period and, furthermore, a series of four sense probe bindings were performed after a series of four antisense 1 probe bindings, rather than in rotation as in chip A, and this probably accounts for the apparent reversal in the magnitudes of antisense 1 and sense bindings to ECP between the two chips.

Thus, because of the marked decay in bindings between successive injections, the data from chip B cannot be used to compare bindings of the two probes, antisense 1 and sense, but can be used to compare paired bindings of individual oligonucleotide probe injections to ECP and lysozyme, which occur *simultaneously* within the two cells of the chip. In this manner, a significant difference is demonstrated between binding to ECP and lysozyme for both oligonucleotide probes by a paired t test (mean difference in binding of antisense 1 probe to ECP and lysozyme (net binding to ECP) = 73.2 RU (CI 7.4 to 139.0), p = 0.038; mean difference in binding of sense probe to ECP and lysozyme (net binding to ECP) = 10.3 RU (CI 4.0 to 16.7), p = 0.014).

The absolute level of 'binding' of probes to lysozyme (mean (SD) for antisense 1 = 2.6 (0.6) RU, and for sense = 1.1 (1.7)) were small, indicating negligible 'binding' to lysozyme.

4.4 Kinetics of binding

The values calculated using BIA evaluation software (see section 3.6 for method) for association rate constants (k_a), dissociation rate constants (k_d) and dissociation constants at equilibrium (K_D) for the interaction between ECP and oligonucleotide probes in chip A are displayed in Table 5.

Data for the sense oligonucleotide probe were *a priori* compared by regression by robust variance clustered by cycle with mean data for antisense oligonucleotide probes, when a significant difference was found only for k_d, with mean k_d for the sense probe significantly less than the mean k_d for antisense probes (Table 6), and no significant differences for k_a and K_D.

Smaller k_d implies slower dissociation of oligonucleotide probes from ECP, and therefore implies that the interaction between ECP and sense probe is stronger than the interaction between ECP and antisense probes. The potential relevance of this finding to the *in situ* observations made in Chapter 2 is explored in the Discussion (section 5).

Table 5. Rate and equilibrium constants for the interaction between oligonucleotide probes and ECP in chip A

(k_a in M^{-1} s^{-1}, k_d in s^{-1} and K_D in M).

	Antisense 1			Antisense 2			Antisense 3			Sense		
Cycle	k_a $\times 10^3$	k_d $\times 10^{-3}$	K_D $\times 10^{-6}$	k_a $\times 10^3$	k_d $\times 10^{-3}$	K_D $\times 10^{-6}$	k_a $\times 10^3$	k_d $\times 10^{-3}$	K_D $\times 10^{-6}$	k_a $\times 10^3$	k_d $\times 10^{-3}$	K_D $\times 10^{-6}$
1	1.8	6.7	3.7	1.8	8.8	4.9	*	4.0	*	3.1	2.1	0.7
2	0.7	6.2	8.9	1.8	6.8	3.8	*	4.1	*	10.0	2.7	0.3
3	5.2	2.9	0.6	4.4	2.5	0.6	*	2.0	*	2.2	1.2	0.5
4	4.6	3.5	0.8	7.3	4.1	0.6	19.7	1.5	0.1	3.4	1.4	0.4
5	1.4	4.4	3.3	4.5	6.6	1.5	*	3.4	*	1.5	1.9	1.2
mean	2.7	4.7	3.4	4.0	5.7	2.2	-	3.0	-	4.0	1.8	0.6
SD	2.0	1.7	3.4	2.3	2.5	2.0	-	1.2	-	3.4	0.6	0.4

* indicates the value was less than 0, and therefore meaningless, and was omitted from calculations.

- indicates the value could not be calculated, because magnitude of binding of antisense 3 probe to ECP was generally small (see Table 2), hence exaggerating the effect of background noise in the data when calculating kinetic constants, to a degree that the computer program was unable to determine rate constants.

Table 6. Rate and equilibrium constants for the interaction between oligonucleotide probes and ECP in chip A. Comparison of sense and antisense oligonucleotide probes (k_a in $M^{-1} s^{-1}$, k_d in s^{-1} and K_D in M).

	mean difference between mean of sense and mean of antisenses	confidence intervals of the difference*	p-value*
k_a	0.7×10^3	(–5.3, 6.6)	0.771
k_d	-3.4×10^{-3}	(–5.3, –1.5)	0.008
K_D	-2.2×10^{-6}	(–5.4, 1.0)	0.134

* analysis by regression with robust variance clustered by cycle

5. Discussion

A method was established for measuring the *in vitro* interaction between probes and ECP or control proteins using biomolecular interaction analysis with a BiacoreX™ instrument. For the results to be reliable, it was necessary to regenerate the dextran-ligand surface to the pre-binding baseline allowing accurate reproduction of successive bindings of the same probe.

The data in sections 4.2. and 4.3 demonstrate binding of oligonucleotide probes to ECP but not to the control proteins myoglobin and lysozyme.

The absence of oligonucleotide probe binding to lysozyme, which has a similar pI to ECP, suggests that binding to ECP is unlikely to be a charge-related effect due to its unusually high pI. The biological explanation for why ECP binds oligonucleotides is unknown, but ECP is known to have ribonuclease activity (283) and therefore may possess a binding site(s) for nucleic acids.

The dissociation constant at equilibrium (K_D) indicates the affinity of an interaction and in section 4.4 values of the order of 10^{-6} M were obtained for the interaction between ECP and probes. This can be compared, for instance, with a very similar value of 6.5×10^{-6} M for the interaction between major histocompatibility complex-protein conjugates with T-cell receptors (309), which is considered a relatively strong and specific biological interaction between ligand and receptor. Thus the interaction between ECP and probes is affinous, and likely to be of high capacity because of the abundance of ECP.

The concentration of probe in the ISH solution was 833 times less than the concentration used during biomolecular interaction analysis (0.12 vs 100 μg ml^{-1} respectively), but the density of ECP on the Biosensor chip surface (0.18-0.20 pmol mm^{-2}) cannot be equated to the concentration of ECP in eosinophil granules, as although it is known that 10^6 eosinophils contain 26 μg of ECP (305), the concentration of ECP within granules is unknown. However, this uncertainty does not invalidate the *in vitro* demonstration of binding of oligonucleotide probes to ECP, or comparison of binding of sense and antisense probes.

In Chapter 2, significantly less *in situ* binding to eosinophils of the sense than of the antisense oligonucleotide probes was demonstrated (see Chapter 2, Table 2 displaying

quantitation of individual probe binding to eosinophils during ISH). Thus in section 4.2.3, the data for *in vitro* magnitude of binding to ECP were *a priori* analysed for this comparison, and the mean net binding of the sense probe to ECP was significantly greater than the mean net binding of the three antisense probes, the converse of the *in situ* findings. Thus, differences in magnitude of binding of oligonucleotide probes to ECP *in vitro*, used as a marker for the strength of the probe-ECP interaction, do not account for differential *in situ* binding.

When similar comparisons for calculated rate and equilibrium constants were made in section 4.4, the only significant difference was for k_d, with the mean for the sense probe significantly less than the mean for antisense probes. Smaller k_d implies slower dissociation of oligonucleotide probes from ECP, and therefore this finding, like the finding for magnitude of binding, does not account for differential *in situ* binding.

However, it is possible that one or more of the properties of ECP-probe interactions may combine with another factor during ISH to produce the observed binding to eosinophils. It is hypothesised that this other factor be tissue penetration of probes, which is determined by their physical characteristics, particularly hydrophobicity, and in Chapter 4, reverse-phase ion-pair liquid chromatography is used to measure their hydrophobicity.

6. Conclusion

Using a biosensor approach with biomolecular interaction analysis, *in vitro* binding to ECP, but not to control proteins, of all tested oligonucleotide probes was demonstrated, which explains binding of oligonucleotide probes to eosinophils observed during ISH in Chapter 2. The interaction is not due to the unusually high pI of ECP, as no *in vitro* binding to the control protein lysozyme, which has a similar pI, was demonstrated.

The magnitude of binding to ECP of the sense probe for IκBα mRNA was significantly greater than the mean of the magnitudes of bindings of the three antisense probes, which is the reverse of observed binding to eosinophils during ISH. Thus, another factor, namely tissue penetration of probes, is hypothesised to influence the degree of oligonucleotide probe binding to ECP in eosinophils in tissue sections, and thus produce the observed differential binding of antisense and sense probes during ISH.

Chapter 4

Measurement of hydrophobicity of oligonucleotide probes by ion-pair reverse-phase high performance liquid chromatography

1. Introduction

In Chapter 2, different levels of binding of different oligonucleotide probes to eosinophils in sections of bowel were observed during ISH, and when binding of individual probes for IκBα was quantitated, significantly less binding occurred with sense than the three antisense probes. In Chapter 3, binding of the same probes to ECP *in vitro* was quantitated when mean binding of sense probe was significantly greater than mean binding of antisense probes. Thus, the differential *in vitro* binding did not explain the differential *in situ* binding, and neither did the measurements of rate and equilibrium constants for the *in vitro* interaction between ECP and oligonucleotide probes. Thus, another factor must be involved, which is hypothesised to be tissue penetration. Tissue penetration by probes is determined by probe length, but in this instance this is the same for all probes and therefore not the factor responsible for differential binding *in situ*, and also by probe hydrophobicity/hydrophilicity.

Hydrophobicity/hydrophilicity of oligonucleotides of the same length can be accurately measured by retention times in ion-pair reverse-phase high performance liquid chromatography (IP-RP HPLC) columns (310) and this technique was therefore employed. The work was kindly performed by Dr. Paul Taylor of Transgenomics Incorporated, Santa Clara, California, USA.

2. Methods

IP-RP HPLC was used to measure the hydrophobicity/hydrophilicity of individual probes in a system where greater hydrophobicity results in longer retention. The IP-RP HPLC system comprised a Waters Action Analyser (Waters Co., Milford, MA, USA), a column heater (Model 105, Interaction Chromatography, San Jose, CA, USA), a biocompatible injection valve (Model K-1760, Rheodyne, Cotati, CA, USA), a 20 µl titanium loop (Superflex, SGE Austin, TX, USA) and a 5 µl syringe (Superflex) for sample introduction. To improve thermal equilibration of the mobile phase and the sample, the injection valve was mounted on the column heater with the sample loop inside the heater. A Waters 484 UV variable ultraviolet light monitor (Waters Co.) was used for detection.

Mobile phases were prepared using a 1M stock solution of HPLC-grade triethylammonium acetate (Transgenomic Inc., San Jose, CA, USA), pH 7.0, and distilled water (Wheaton Autostill, Millville, NJ, USA), with probe concentration of 0.15 mg l^{-1}. The eluent was 25 % (v/v) acetonitrile (EM Science, San Jose, CA, USA) in 0.1 M triethylammonium acetate, and the gradient used to separate the oligonucleotides was from 10 to 60 % acetonitrile in fifteen minutes, then from 60 to 100 % in one minute and back to 10 % in one minute.

3. Results

Retention times for individual IκBα oligonucleotide probes on the IP-RP HPLC columns are displayed in the Table. As in Chapter 3, data were *a priori* analysed for a difference between antisense and sense probes, and mean hydrophobicity of the antisense oligonucleotides was found to be significantly greater than for the sense probe (difference of means = 0.65 (95 % CI 0.63 to 0.67), $p < 0.00001$ using a Student's t-test).

Table. Retention times of individual IκBα oligonucleotide probes in IP-RP HPLC columns.

run	oligonucleotide probe			
	antisense 1	antisense 2	antisense 3	sense
1	8.83	8.10	8.58	7.84
2	8.84	8.09	8.55	7.83
3	8.83	8.08	8.57	7.85
4	-	8.09	-	-
mean	8.83	8.09	8.57	7.84
standard deviation	0.006	0.008	0.02	0.01

4. Discussion

IP-RP HPLC was successfully used to measure probe hydrophobicity and provided data with small standard deviations and consequently highly significant differences between antisense and sense probes. The relationship between probe hydrophobicity, *in vitro* probe-ECP binding and *in situ* binding of probes to eosinophils is explored in Chapter 7.

Chapter 5

An immunohistochemical study of the activation of NFκB in inflammatory bowel disease

1. Introduction and aim

In Chapter 2, attempts to develop an ISH method to study activation of NFκB via expression of IκB mRNA in tissue sections were unsuccessful because of non-specific binding of oligonucleotide probes to eosinophils. Whilst these ISH studies were being conducted, an antibody, developed by Professor P.A. Baeuerle's group in Germany, that recognised only the activated, nuclear-translocated form of NFκB, was commercially manufactured by Boehringer Mannheim and became available in October 1995 (311). The antibody recognises an epitope overlapping the nuclear location signal (NLS) of the p65 subunit of NFκB, which is revealed when IκB is proteolytically degraded during activation of NFκB, and so it selectively binds to the activated form (312).

After the development of this antibody, there remained little advantage in an ISH method over an immunohistochemical method to study activation of NFκB, and, indeed, the proposed ISH method used IκBα mRNA expression is only a marker of activation of NFκB, whereas the recently developed antibody directly detected activated NFκB. Thus, the new antibody was used to study the location and degree of activation of NFκB in inflammatory bowel disease, and findings are presented in this chapter.

2. Methods

2.1 Collection and preparation of tissues for immunostaining

2.1.1 Tissues for validating the antibody

To validate the specificity of the antibody for activated NFκB, experiments were performed using two unrelated tissues as positive controls, namely HeLa cells that express activated NFκB upon stimulation with phorbol 12-myristate 13-acetate (PMA) (Sigma Chemical Company) (2), and mouse cerebral cortex containing neurones that constitutively express activated NFκB (81).

Unsectioned cultured cells

HeLa Ohio cells (gift of The Imperial Cancer Research Fund, Lincoln's Inn Field, London, UK) were grown to confluency in 25 ml sterile culture flasks (BDH) in sterile tissue culture medium (TCM), consisting of Eagle's minimum essential medium with Hank's balanced salt solution (Life Technologies, Paisley, Scotland, UK) supplemented with 10 % fetal calf serum (Life Technologies), 2 mM L-glutamine (Life Technologies), 100 units ml^{-1} penicillin (Sigma Chemical Company), 100 $\mu g ml^{-1}$ streptomycin (Sigma Chemical Company) and 50 μg ml^{-1} gentamicin (Sigma Chemical Company). Flasks were incubated in a carbon dioxide incubator (IRE93, J Bio Co., San Jose, CA, USA) with a continuous supply of 5 % carbon dioxide, 95 % air at 37°C. All work with cell cultures was performed in a 'Class 2' laminar flow cabinet (Intermed Microflow, Microflow Pathfinder Ltd., Fleet, Hampshire, UK). Cells were harvested using 2 ml of a solution containing 0.025 % (w/v) beef pancreas

trypsin (Sigma Chemical Company) and 0.02 % (w/v) EDTA (Sigma Chemical Company) in serum-free TCM (prepared as described above with the omission of fetal calf serum), and then a 0.25 ml sample of the cell culture was stained with 0.25 ml trypan blue (Sigma Chemical Company) and counted using a haemocytometer (BDH) to allow subsequent dilution to the required concentrations and to ensure non-viable cells were below 5 % of the total cells. Cells were then seeded on to individual glass coverslips (Sigma Chemical Company) in each of the wells of six-well culture plates (Sigma Chemical Company), by pipetting 2 ml of cells suspended at 2×10^4 cells ml^{-1} in TCM, and cultured as before for 24 hours. The medium was then removed and replaced with 2 ml of either TCM alone or TCM containing 50 ng ml^{-1} phorbol 12-myristate 13-acetate (PMA) (Sigma Chemical Company). Cells were incubated for one hour, the medium then removed, and cells fixed by filling wells with an excess of absolute ethanol (BDH) for two minutes followed by an excess of a solution of 3.7 % (v/v) formaldehyde (Sigma Chemical Company) in PBS for five minutes (311), and finally washed in PBS before immunostaining for activated NFκB as described below.

The following modifications to this protocol were tested to optimise stimulation and immunostaining of cells:

(i) different stimulants - cells were stimulated with both recombinant TNFα alone (R&D Systems), at 200 units ml^{-1} TCM for one hour, or a combination of PMA and TNFα for one hour, which are known synergistically to stimulate NFκB (83). The duration of stimulation was varied over a range of 20 minutes (the shortest time required for marked activation NFκB (11)) to two hours;

(ii) different fixatives - both 100 % methanol (BDH) at –20 °C for five minutes, and a 4 % (w/v) solution of paraformaldehyde (Sigma Chemical Company) in PBS, for five

minutes, were tested as alternatives to the ethanol/formaldehyde fixation method as described above;

(iii) permeabilisation - after fixation with each of the three fixatives, half the cell cultures were permeabilised with a 0.2 % (v/v) solution of Triton X-100 (Sigma Chemical Company) in PBS for five minutes, and then 0.1 % (v/v) Triton X-100 was added to all immunostaining solutions;

(iv) tumour cell type - as an alternative to HeLa Ohio cells grown in sheets onto coverslips, HeLa S3 cells (European Collection of Cell Cultures, Salisbury, UK) were grown in suspension to a concentration of 3–9 x 10^5 cells ml^{-1} in TCM. The proportion of non-viable cells was determined by trypan blue exclusion and kept below 5 % by passaging cell cultures every 2-3 days. Before stimulation, cells contained in one 25 ml culture flask were washed twice in serum-free TCM by centrifuging cells into a pellet at 400g at 20° C for five minutes using a Centra-3 centrifuge (International Equipment Company, Dunstable, UK), and then resuspending cells in serum-free TCM. The cells were spun into a pellet again, and then finally resuspended at 2×10^4 cells ml^{-1} in TCM either with or without stimulant. After stimulation for one hour, cells were spun onto poly-L-lysine-coated microscope slides (Sigma Chemical Company) at 500 rpm for five minutes at room temperature using a Cytospin 2 centrifuge (Shandon, Runcorn, Cheshire, UK), using 0.5 ml of cell suspension for each slide. Cell preparations were then fixed, as described above, using the three different protocols.

Frozen sections of mouse cerebral cortex

Samples (0.25 cm cubed) of cerebral cortex from the brains of freshly killed BALB/c mice were rapidly dissected out and embedded in OCT compound (Sigma Chemical Company). Eight μm frozen sections were cut with a cryotome (Cryotome 620M, Anglia Scientific Instruments, Cambridge, UK) on to poly-L-lysine coated slides, air-dried for 30 minutes, fixed by immersion in methanol at –20 ^{0}C for five minutes, air dried again for ten minutes, and then stored until processed at –70 ^{0}C within individual packages of aluminium foil and three air-tight plastic bags.

Paraffin-embedded sections of cells and mouse cerebral cortex

For both unstimulated and stimulated cells, the contents of one 25 ml culture flask of HeLa S3 cells were spun into a pellet as described above, then fixed by resuspending in an excess (10 ml) of 10 % (v/v) formaldehyde in PBS for five minutes, and then centrifuged into gelatine (Sigma Chemical Company) and embedded in paraffin by the Histopathology Department, St. Thomas' Hospital.

Samples (0.25 cm cubed) of mouse cerebral cortex were fixed overnight in a 10 % (v/v) solution of formaldehyde, and embedded in paraffin.

The Histopathology Department performed sectioning of all paraffin-embedded tissue. Seven μm sections were floated onto water and then air-dried overnight onto poly-L-lysine-coated microscope slides. Paraffin was removed from sections in a standard manner by immersion in successive baths of xylene for two minutes, twice, 100 % alcohol for one minute, twice, and then successive solutions of reducing concentrations of alcohol for one minute each (95, 70 and 50 % (v/v) solutions of

alcohol in distilled water). Endogenous peroxidase was blocked as for frozen sections (section 2.3.1), except hydrogen peroxide solution was diluted in methanol (313).

Some paraffin-embedded sections were pre-treated to expose antigen that may have been hidden by the highly cross-linking fixative, formaldehyde, by either:

(i) trypsinisation (314) - sections were incubated at 37°C in a solution of 0.1 % (w/v) beef pancreas trypsin and 0.1 % (w/v) calcium chloride in distilled water at pH 7.8 for ten minutes and then washed in PBS at room temperature, or

(ii) microwaving (315) - sections were placed in a covered, boiling solution of 0.1 M tri-sodium citrate pH 6.0 (adjusted with 0.1 M acetic acid) and microwaved at 700 Watts for ten minutes, and then rinsed once by immersion in PBS.

2.1.2 Full thickness frozen sections of bowel from CD and control patients

Full thickness samples of small or large bowel were taken from thirteen patients with active CD undergoing intestinal resection at St. Thomas' Hospital and St. Mark's Hospital (mean age 37 years, range 15 to 48, four male). The diagnosis of CD was made using conventional clinical, histological and endoscopic and/or radiographic criteria. Eight CD patients were receiving corticosteroid therapy (range 0-60 mg prednisolone per day), one azathioprine (2 mg kg^{-1}) and nine aminosalicylates (Table 1). Pairs of samples, one from a macroscopically diseased and the other from a macroscopically non-involved area at least five centimetres distant from the macroscopically inflamed area, were taken from each patient, nine pairs from the ileum and four from the colon.

Samples of bowel were also taken from two patients with ulcerative colitis undergoing proctectomy after previous sub-total colectomy, one patient with diverticulitis and one endoscopic biopsy from a patient with Wegener's granulomatosis with colonic vasculitis (Table 1).

Full thickness samples of bowel were also taken from eleven patients undergoing intestinal resection for carcinoma of the colon to act as controls with normal bowel (mean age 72 years, range 38 to 84, eight male) (Table 2). Samples, at least five centimetres from the margins of the carcinoma, were taken from the small bowel in four patients and from the large bowel in seven. Control patients were taking no corticosteroids, 5-ASA compounds or aspirin, but received a single dose of intravenous metronidazole and a cephalosporin antibiotic at induction for anaesthesia.

The protocol for the study was approved by The Research Ethics Committee of St. Thomas' Hospital and The Research Ethics Committee of Northwick Park and St. Mark's Hospitals National Health Service Trust.

Biopsy specimens of bowel were frozen in OCT compound and sectioned and fixed in methanol as described for mouse cerebral cortex (see section 2.1.1).

2.1.3 Formaldehyde-fixed, paraffin-embedded full thickness biopsy specimens of bowel from CD patients

To test use of the antibody on formaldehyde-fixed, paraffin-embedded sections, samples from small bowel resection specimens from five patients with CD were obtained from the library of paraffin-embedded specimens in the Histopathology Department, St. Thomas' Hospital.

Table 1. Clinical details of patients from whom operative resection specimens were collected for immunostaining of frozen sections.

Patient	Diagnosis	Age (years)	Sex	ESR	CRP (mg dl^{-1}) (NR<7)	Corticosteroid dose (mg day^{-1})	ASA	Azathioprine	Location
1	CD	55	F	35	15	0	+	+	ileum
2	CD	58	F	40	38	0	+	–	ileum
3	CD	26	M	40	65	5	–	–	ileum
4	CD	32	F	10	<7	25	+	–	ileum
5	CD	28	F	21	35	60	+	–	ileum
6	CD	39	M	35	20	0	–	–	ileum
7	CD	32	F	40	16	0	–	–	caecum
8	CD	41	F	15	–	15	+	–	colon
9	CD	28	F	15	<7	20	–	–	ileum
10	CD	31	M	-	18	15	+	–	colon
11	CD	35	F	44	53	15	+	–	ileum
12	CD	48	F	18	28	30	+	–	ileum
13	CD	30	F	25	10	0	+	–	rectum
14	UC	28	M	–	–	0	+	–	rectum
15	UC	70	M	46	–	40	+	–	rectum
16	Wegener's granulomatosis	42	M	32	38	0	–	–	colon
17	Diverticulitis	80	F	–	–	–	–	–	sigmoid colon

ESR = erythrocyte sedimentation rate (mm in first hour); CRP = C-reactive protein; ASA = aminosalicylate therapy; F = female; M = male; NR = normal range.

Table 2. Clinical details of control patients from whom operative resection specimens were collected for immunostaining of frozen sections.

Control patient	Diagnosis	Age	Sex	Location
1	carcinoma	80	F	colon
2	carcinoma	75	M	terminal ileum
3	carcinoma	38	M	colon
4	carcinoma	84	F	colon
5	carcinoma	78	M	terminal ileum
6	carcinoma	79	M	colon
7	carcinoma	78	F	colon
8	carcinoma	67	M	colon
9	carcinoma	73	F	terminal ileum
10	carcinoma	69	F	terminal ileum
11	carcinoma	68	M	colon

2.2 Histological grading of inflammation

Four different sections of the same biopsy specimens immunostained for activated NFκB, from patients with CD, were stained with haematoxylin and eosin (see Appendix II) and assessed by an histopathologist (Dr John Goodlad, Senior Registrar in Histopathology, St. Thomas' Hospital) who was blind to the patient status. Inflammation was graded using a previously validated scoring system according to the cellularity of the mucosa and the severity of changes in the enterocytes and crypts (316) (Table 3). In this system, grade 0 represents no inflammation, termed 'non-inflamed', and grades 1 to 3 represent increasing degrees of inflammation, together termed 'inflamed' (Table 4). Any samples from macroscopically non-involved areas that showed evidence of microscopic inflammation were excluded from analysis.

Table 3. Scanning system for histological assessment of biopsy specimens. An inflammatory score was calculated by adding the scores from four categories, namely enterocytes, mononuclear cells, crypts and neutrophils. Four sections from each biopsy specimen were examined and scored, and the mean of these scores allocated as the final inflammatory score for the specimen.

EPITHELIUM		**LAMINA PROPRIA**	
Enterocytes		**Mononuclear cells**	
Normal	0	Normal	0
Loss of single cells	1	Slight increase	1
Loss of groups of cells	2	Moderate increase	2
Frank ulceration	3	Marked increase	3
Crypts		**Neutrophils**	
Normal	0	Normal	0
Single inflammatory cells	1	Slight increase	1
Cryptitis	2	Moderate increase	2
Crypt abscesses	3	Marked increase	3

Table 4. Conversion of histological scores to grades, and categorisation into inflamed and non-inflamed specimens.

	Grade	**Total score**
Non-inflamed	0	0
Inflamed	1	1-4
	2	5-8
	3	9-12

2.3 Immunostaining

2.3.1 Immunostaining of frozen sections of mouse cerebral cortex

Stored slides and coverslips were brought to room temperature and pre-treated by immersion into a 0.18 % (v/v) solution of hydrogen peroxide (Sigma Chemical Company) in PBS for five minutes to block endogenous peroxidase by providing an excess of substrate. Sections and cells were then covered with a 5 % (v/v) solution of rabbit serum in phosphate-buffered saline (PBS) (Oxoid, Unipath Ltd., Basingstoke, UK) and incubated for ten minutes to block non-specific binding sites for the secondary antibody (serum from the species in which the secondary antibody is raised, maximally blocks non-specific binding of the secondary antibody). The excess of the solution of rabbit serum was then carefully removed from the sections with a pipette, and the sections then completely covered with 50 µl of a 1 in 200 dilution of mouse anti-p65 primary antibody (Boehringer Mannheim, Lewes, East Sussex, UK) and incubated for one hour in a moist chamber followed by two, five minute washes in PBS. A 50µl aliquot of a 1 in 300 dilution of the secondary, biotinylated, rabbit anti-mouse IgG antibody (Dako Ltd., High Wycombe, Hertfordshire, UK) was applied and the slides incubated for 35 minutes, followed by two washes by immersion in a bath of PBS containing a magnetic stirrer. All antibodies were diluted in a 1 % (w/v) solution of blocking agent in PBS (constituents not released by Boehringer Mannheim) and incubations performed at room temperature.

A 50 µl aliquot of a 1 in 500 dilution of streptavidin-peroxidase conjugate (Dako Ltd.) was applied as a tertiary layer, the slides incubated at room temperature for 45 minutes and washed twice in PBS. The sections were covered with an excess of the chromogen, imidazole-enhanced diaminobenzidine (317) (a 1 M solution of imidazole

(Sigma Chemical Company) in 0.1 M Tris buffer (Sigma Chemical Company) at pH 7.6, was diluted 1:100 with a solution of 0.5 mg ml^{-1} diaminobenzidine (Grade 2, Sigma Chemical Company) in 0.1 M Tris buffer at pH 7.6 with 0.03 % (v/v) hydrogen peroxide). After incubation at room temperature for ten minutes, slides were washed for ten minutes, twice, in PBS. Sections were counterstained with Mayer's haematoxylin (Sigma Chemical Company) for two minutes, washed in tap water, and then dehydrated in serial, graded alcohols (successive solutions of 90, 95 and 99 % (v/v) alcohol in distilled water), air-dried for fifteen minutes, mounted in Ralmount (BDH) and finally covered with a coverslip. As negative-staining controls, sections of the same specimens prepared in an identical manner were processed by the same method except with PBS substituted for the primary antibody.

The above protocol was finally determined after several experiments to determine the ideal experimental conditions for frozen sections of mouse cerebral cortex:

- different fixatives, namely acetone at -20°C, which resulted in poorer quality immunostaining than with use of methanol at -20°C in the above protocol;
- use of varying dilutions of blocking rabbit serum from 0 to 100 % at different points in the immunohistochemistry protocol, namely, before application of the primary antibody, before application of the secondary antibody, or both, and with and without a PBS wash before application of the subsequent antibody. Least background staining was obtained when a 5 % solution was applied only before application of the primary antibody, and not followed by a PBS wash and this was thus used in the above protocol;

- without dilution of antibodies in blocking solution, which increased background staining, and therefore blocking solution was included in the above protocol;

- two 'chequer-boards' of ranges of dilutions of primary (from 1 in 50 to 1 in 400) and secondary antibodies (from 1 in 100 to 1 in 600) were immunostained, one chequer-board with a tertiary layer dilution of 1 in 100 and the other with 1 in 300, to choose the combination of dilutions of antibodies that resulted in the best signal and least background staining. Results from this experiment demonstrated the optimal dilutions to be 1 in 200, 1 in 300 and 1 in 500 for the primary, secondary and tertiary layers respectively, which were therefore used in the above protocol.

2.3.2 Modifications in immunostaining protocol for unsectioned cultured cells and frozen sections of bowel

Immunostaining was performed for all tissues as described above (section 2.3.1) for mouse cerebral cortex except:

(i) immunostaining of cultured cells

Blocking of endogenous peroxidase was omitted, as none is present in cultured HeLa cells.

(ii) frozen sections of bowel

When a peroxidase-based detection system was used on sections of bowel, despite steps in the protocol to block endogenous peroxidase, numerous positive cells were seen that were recognised to be due to non-specific staining because the negative control, namely when PBS was substituted for the primary antibody, showed similar staining. Furthermore, when PBS was substituted for the primary, secondary and tertiary layers and only the chromogen-peroxidase solution added, a similar pattern of

staining was seen, thus strongly suggesting endogenous peroxidase activity, and the appearances of dark brown, granular staining were characteristic (1061).

Further methods to block endogenous peroxidase activity, such as increasing the pre-treatment concentration of hydrogen peroxide to 0.3 % (v/v), and pre-treatment with 6 % (v/v) hydrogen peroxide followed by 2.5 % (v/v) periodic acid and finally 0.02 % sodium borohydride (1061), were unsuccessful.

Therefore, an alkaline phosphatase-based detection system was used instead of a peroxidase-based system. Thus, a tertiary layer of a 1 in 200 dilution of streptavidin-alkaline phosphatase conjugate (Dako Ltd.) was applied for one hour, followed by two, five minute washes in PBS. The substrate, VectorRed alkaline phophatase substrate (VectorLabs, Peterborough, UK), prepared as recommended by the manufacturer with the addition of one drop of levamisole solution (VectorLabs) to block non-intestinal, endogenous alkaline phosphatase activity, was applied to sections and incubated for a further twelve minutes before two final washes in PBS. Brush border intestinal alkaline phosphatase, which is not blocked by this concentration of levamisole (higher concentrations will block intestinal enzyme, but also block the chromogen reaction and are therefore not used), was clearly seen as a continuous red line on the luminal surface of the epithelium, and was disregarded.

2.4 Photography

Microscopy and photography was performed with the apparatus described in Chapter 2, section 2.6.

2.5 Quantitation of cells immunostaining positive for activated NFκB and statistical analysis

Each section of bowel wall was subdivided into muscle, submucosa and mucosal layers. Each level was assessed separately for cells staining positive for activated NFκB and quantitation undertaken using a point counting technique as used by others for quantitating cells staining positive for cytokines in IBD (318). Briefly, ten high-powered fields (× 400) were chosen at random and the positive cells that lay under a Lennox graticule (Graticules Ltd, Tonbridge, UK) point counted (319), and counts of any endogenously-positive cells in the matched negative control slides (see Appendix III) subtracted. Cell counts were converted to tissue-densities, expressed as number of positive cells per mm^2 of tissue section, by multiplication by a factor (26.5) provided by the manufacturer of the graticule. As assessed by others, reproducibility of counts was evaluated by repeating counts on sections to which the assessor was blinded (318). The difference was always less than ten percent of the mean of the scores (mean difference 6.7 %, standard deviation 1.6 %) (see Appendix IV).

Data were analysed using the Mann-Whitney U-test and Spearman's method of correlation, and 95 % confidence intervals of the ratio of medians of unpaired samples were calculated in the conventional manner with replacement of a value of zero with a value of one, to avoid ratios of infinity. This method of calculating confidence intervals is equivalent to confidence intervals of the logged difference of medians, and was performed because the distributions were log-normal.

3. Results

3.1 Validation of the antibody using frozen sections of mouse cerebral cortex and unsectioned HeLa cells

Stimulated HeLa cells, fixed in ethanol/formaldehyde, showed densely staining nuclei, representing activated, nuclear-translocated NFκB, in contrast to unstimulated cells (Figure 1). However, only small numbers of cells stained positive for activated NFκB and were seen only in some areas of the stimulated culture, and so quantitation of the difference in numbers of positive cells between unstimulated and stimulated cultures was not possible. Modifications to methods (see section 2.1.1.1) of stimulation, permeabilisation, and tumour cell type had no effect on the results.

Mouse cerebral cortex showed staining related to the nuclei of most neurones (Figure 3), as expected from previous studies (81). The nuclear localisation of the antibody confirmed its specificity for activated, nuclear-translocated NFκB.

The negative controls, with PBS substituted for the primary antibody, showed no positive cells in either stimulated HeLa cells (Figure 2) or mouse cerebral cortex (Figure 3), confirming that non-specific binding was not occurring .

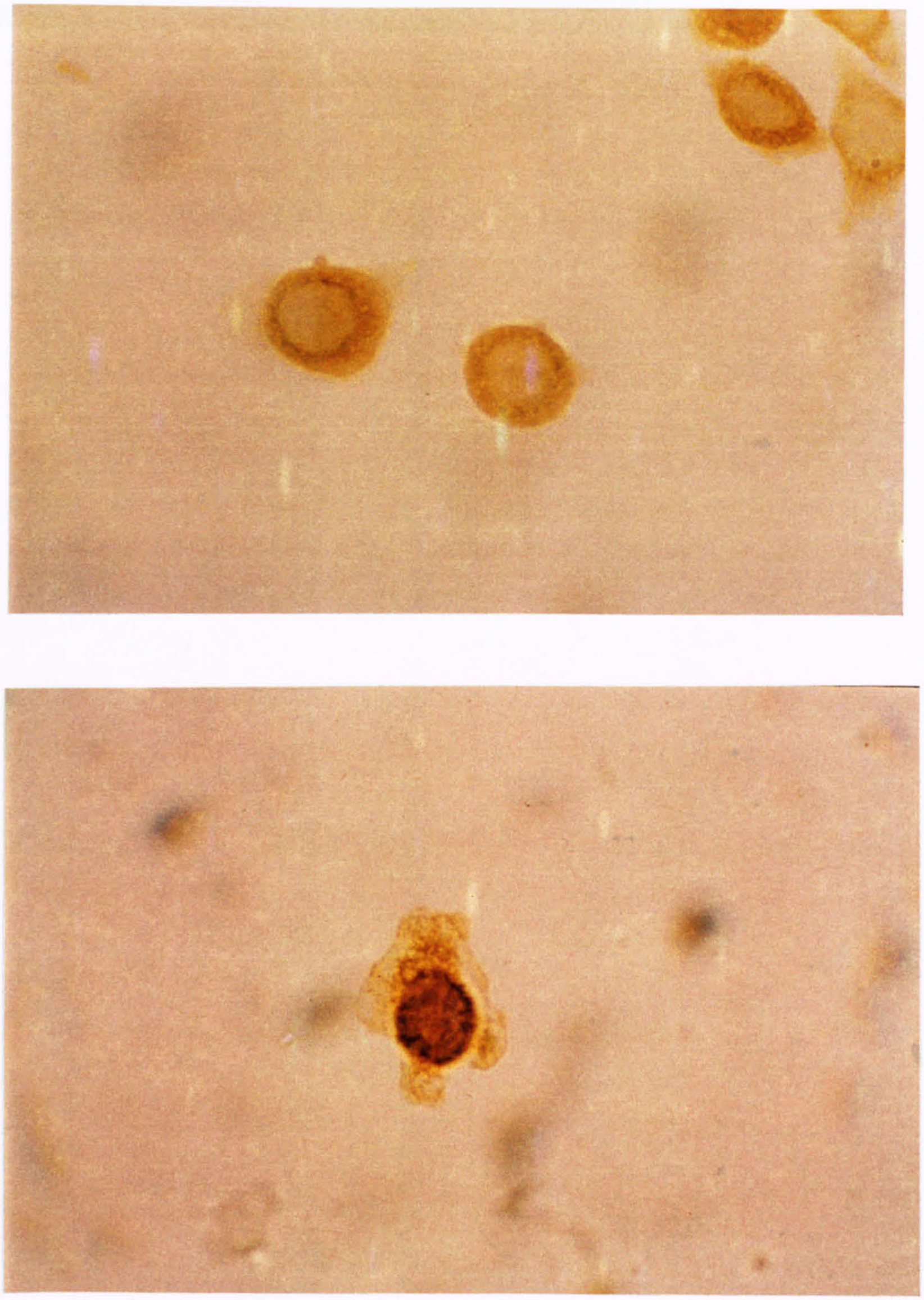

Figure 1. Photomicrographs (magnification × 1000) of unstimulated (above) and stimulated (below) HeLa Ohio cells grown onto cover slips and immunostained for activated NFκB. Cells were stimulated with TNFα and PMA and fixed in ethanol/formaldehyde. The stimulated cell shows dense nuclear staining (brown, peroxidase-based detection system). The results show, together with results displayed in Figures 2 and 3, that the antibody binds to the nuclei of stimulated cells, which is consistent with its proposed specificity for activated NFκB.

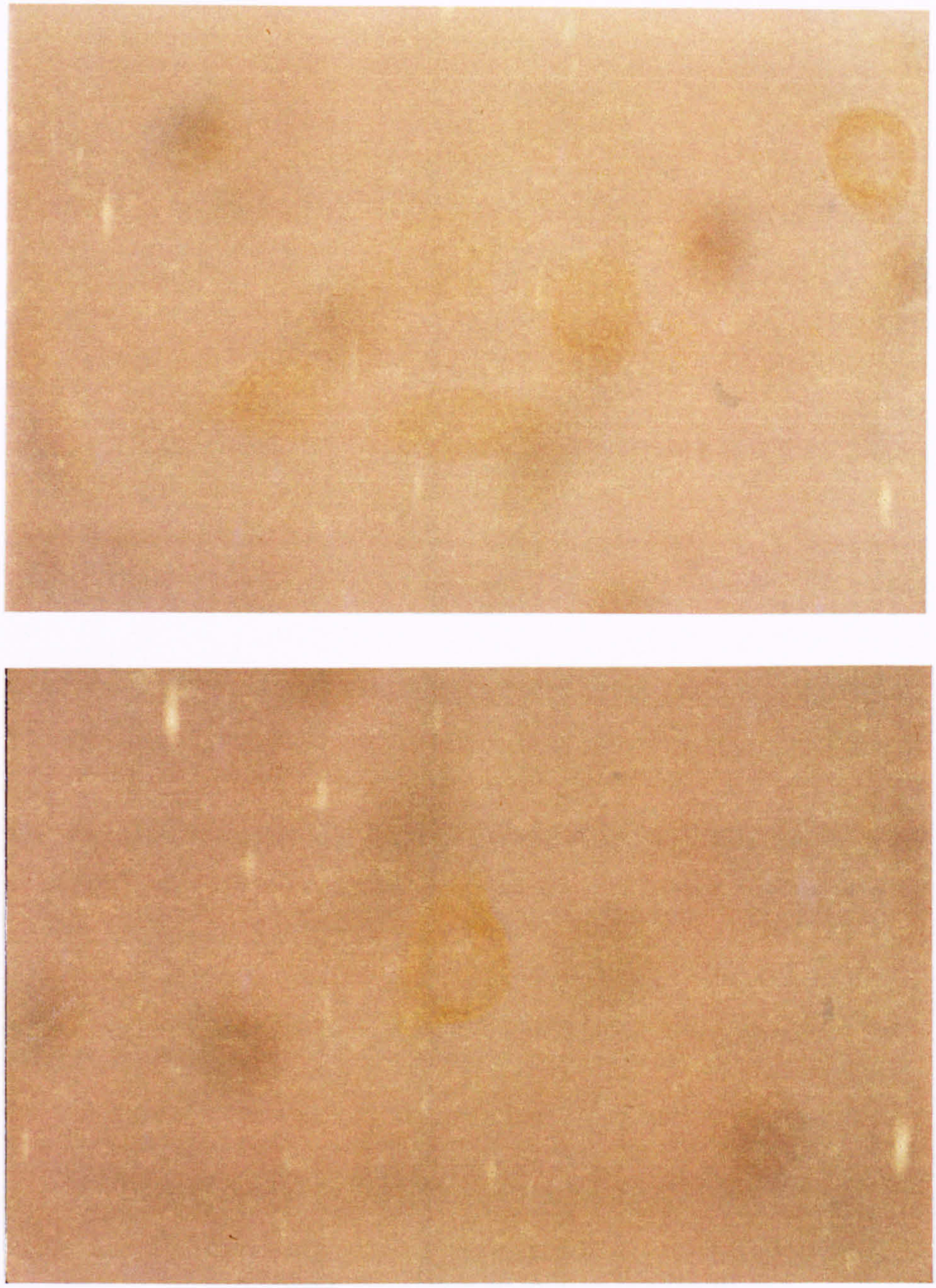

Figure 2. Photomicrographs (magnification × 1000) of negative controls of unstimulated (above) and stimulated (below) HeLa Ohio cells grown onto cover slips and immunostained with substitution of PBS for the primary (anti-p65 NFκB) antibody (brown, peroxidase-based detection system). Cells were stimulated with TNFα and PMA and fixed in ethanol/formaldehyde. The absence of staining confirms that the staining in Figure 1, with use of the primary antibody, is not due to non-specific binding of secondary or tertiary layers of immunostaining, or due to endogenous peroxidase activity.

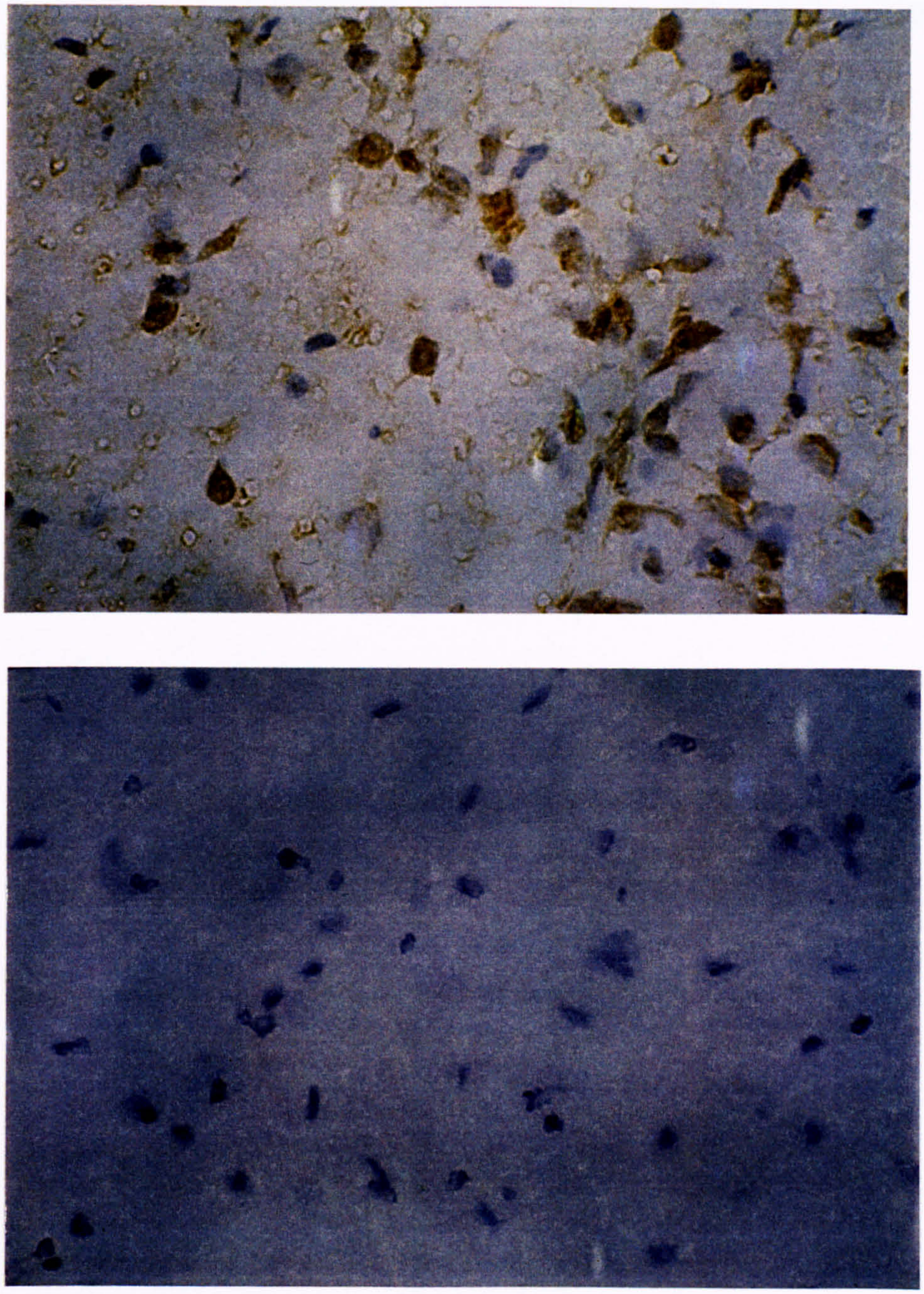

Figure 3. Photomicrographs (magnification × 400) of a frozen section of mouse cerebral cortex immunostained for activated NFκB (above) showing nuclear staining, and negative control (below) immunostained in the same manner with PBS substituted for the primary antibody (brown, peroxidase-based detection system) and counterstained with Mayer's haematoxylin. Neurones in mouse cerebral cortex are known to constitutively express activated NFκB, and so the results are consistent with the proposed specificity of the primary antibody.

3.2 Frozen sections of bowel from Crohn's disease and control patients

Positive staining of cells for nuclear, activated NFκB, similar to that seen with the stimulated HeLa cells, was seen in sections of bowel from CD patients (Figures 4, 5 and 6). Some cells showed a peri-nuclear ring of staining, particularly in the muscle layer, which may possibly represent cytoplasmic, activated NFκB. Negative staining controls, with PBS substituted for the primary antibody, gave no positively stained cells, but minimal areas of background staining (Figure 7), which was quantitated and subtracted from the positive cell count (see Appendix III), as performed by others (318). Cells positive for activated NFκB were predominantly large, mononuclear, macrophage-like cells, although a few small, mononuclear, lymphocyte-like cells, were also observed in the mucosa.

In all CD patients, and the majority of control patients (Figure 8), at least some cells staining positive for activated NFκB were observed in all layers, namely the mucosa, submucosa and muscle, although the number of positive cells was lower in control patients. There were, however, no cells positive for activated NFκB in the epithelium or endothelium of CD or control patients.

In all three layers, the tissue-density of positively-stained cells was significantly ($p = 0.001$) greater in inflamed areas of CD, compared to normal bowel from controls (Figure 9) (95 % confidence intervals of the ratio of medians of inflamed CD to controls: mucosa 2.6-23.5; submucosa 3.0-41.5; muscle 10.7-95.8).

In non-inflamed areas of CD, only in the submucosa was there a significantly ($p = 0.009$) greater tissue-density of activated NFκB positive cells compared to normal bowel from controls (95 % confidence intervals of the ratio of the medians of non-inflamed areas to controls: 1.36-39.7). There was no such difference in the mucosa or muscle layer.

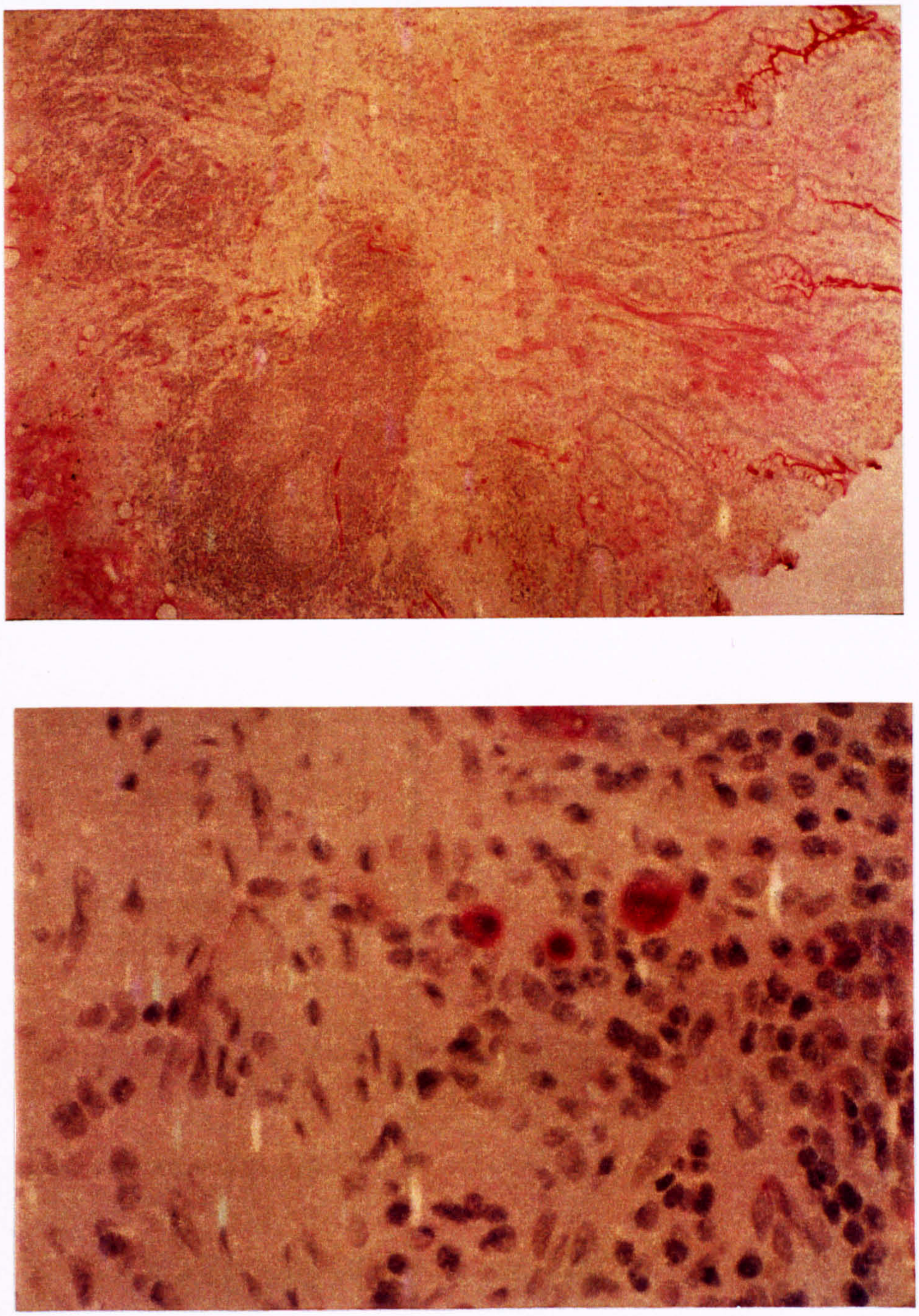

Figure 4. Photomicrographs of the *mucosa* of a frozen section (above, magnification × 100; below, magnification × 400) of inflamed CD bowel (patient 10) immunostained for activated NFκB and counterstained with Mayer's haematoxylin, showing scattered cells positive for activated NFκB (red, alkaline phosphatase-based detection system).

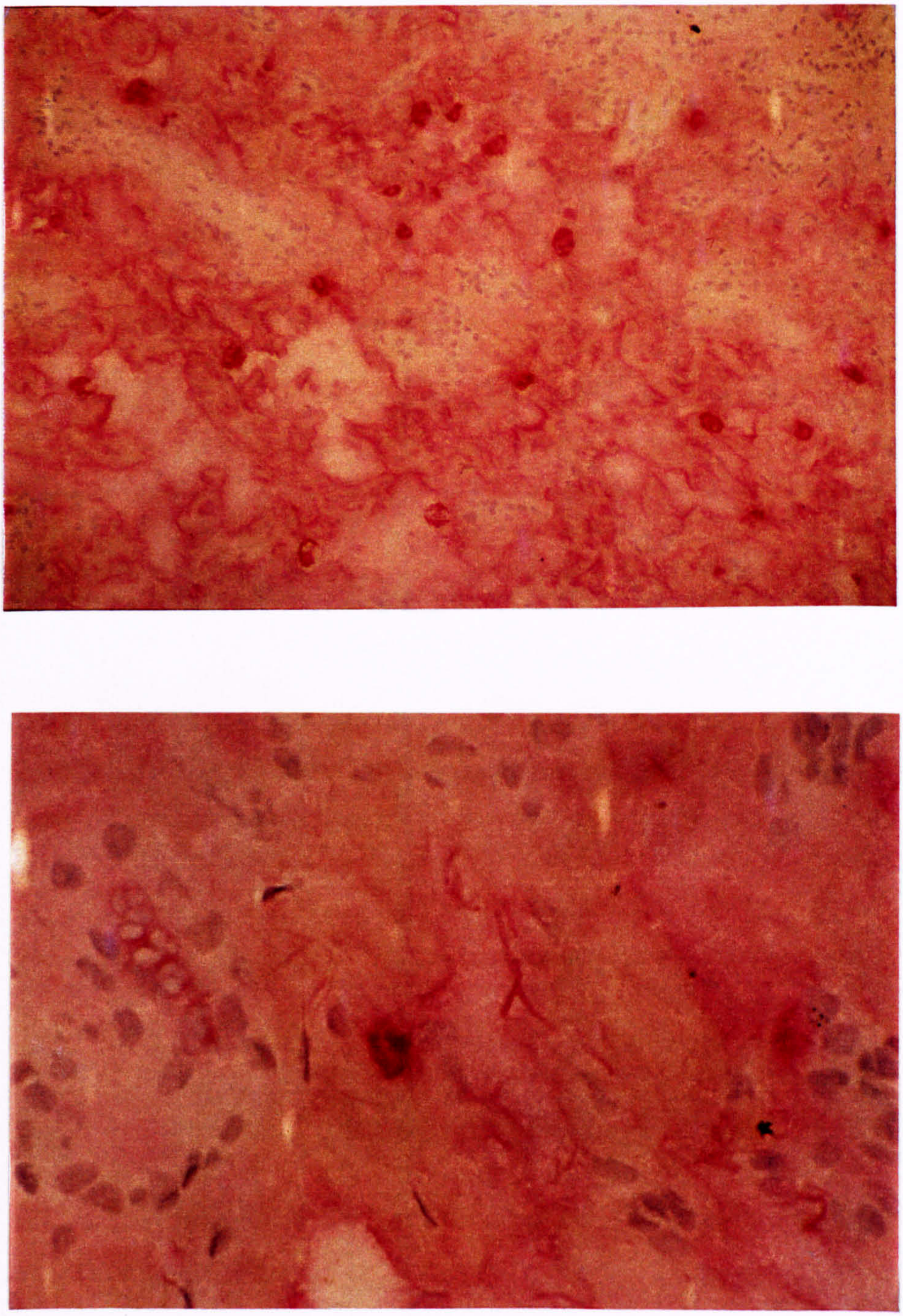

Figure 5. Photomicrographs of the *submucosa* of a frozen section (above, magnification × 100; below, magnification × 400) of inflamed bowel from a patient with CD (patient 10) immunostained for activated NFκB and counterstained with Mayer's haematoxylin, showing scattered cells positive for activated NFκB (red, alkaline phosphatase-based detection system).

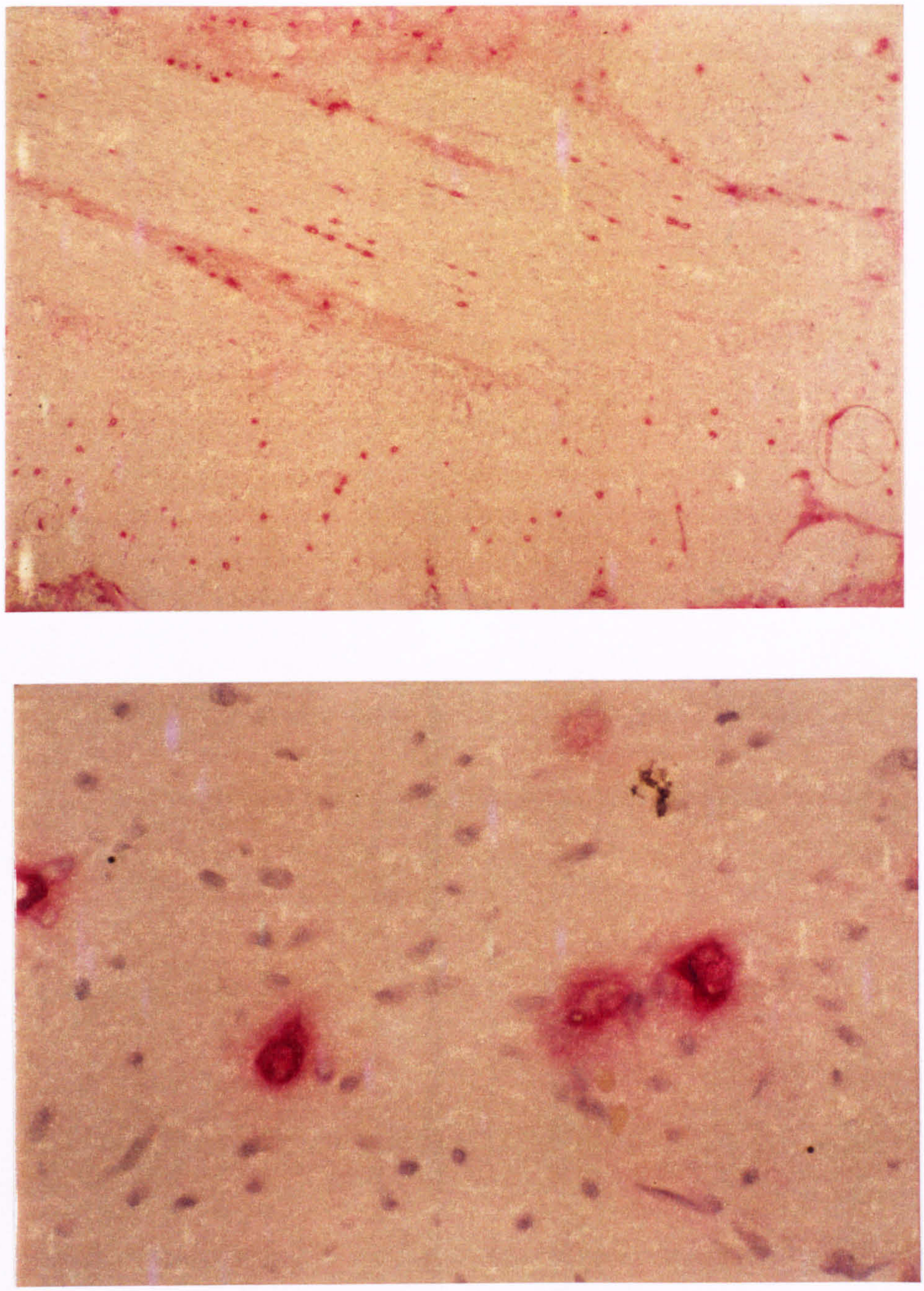

Figure 6. Photomicrographs of the *muscle* layer of a frozen section (above, magnification × 100; below, magnification × 400) of inflamed bowel from a patient with CD (patient 10) immunostained for activated NFκB and counterstained with Mayer's haematoxylin, showing scattered cells positive for activated NFκB (red, alkaline phosphatase-based detection system).

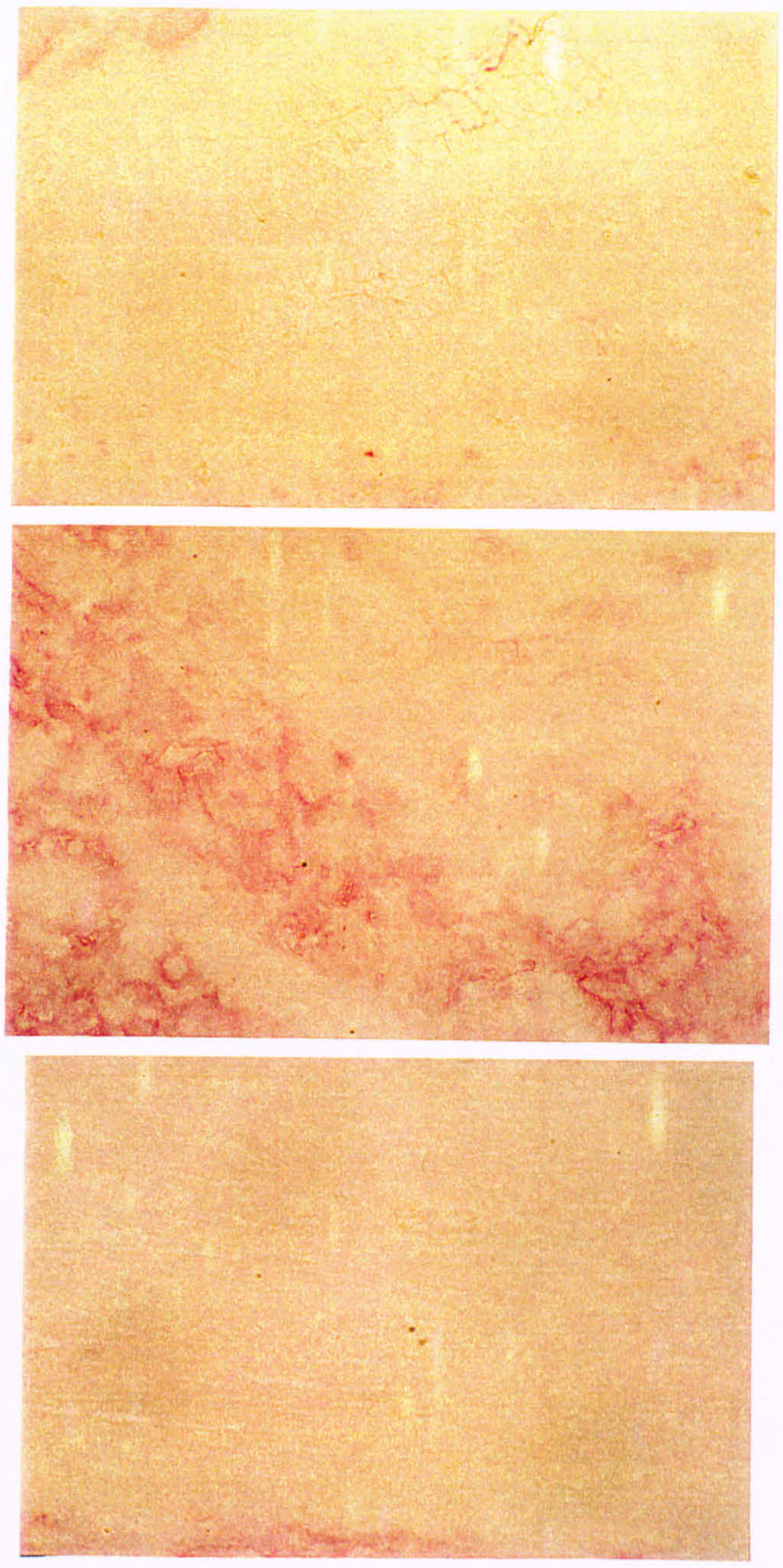

Figure 7. Photomicrographs (magnification × 200) of a frozen section (above, mucosa; middle, submucosa; below, muscle) of inflamed bowel from a patient with CD (patient 10) immunostained for activated NFκB with PBS substituted for the primary antibody as a negative control. The sections were not counterstained with Mayer's haematoxylin to ensure background staining was not obscured. No positive cells and minimal background staining is observed (red, alkaline phosphatase-based detection system). The results demonstrate that the positive cells in Figures 4, 5 and 6 were not due to non-specific binding of the secondary or tertiary layers of immunostaining, or due to endogenous alkaline phosphatase activity.

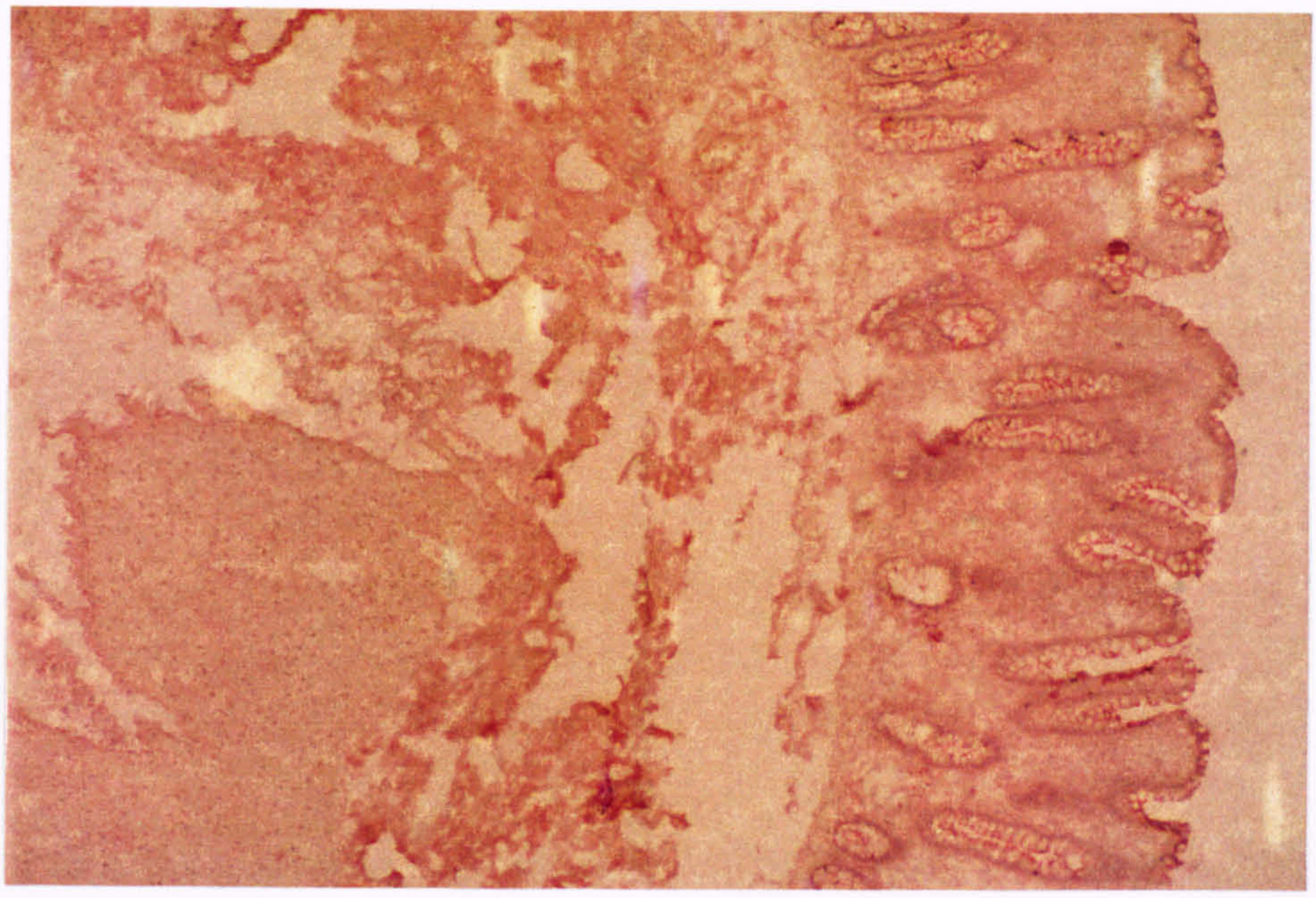

Figure 8. Photomicrograph of a frozen section (magnification × 100) of normal bowel from a control patient (control 6) immunostained for activated NFκB and counterstained with Mayer's haematoxylin, showing few cells positive for activated NFκB (red, alkaline phosphatase-based detection system).

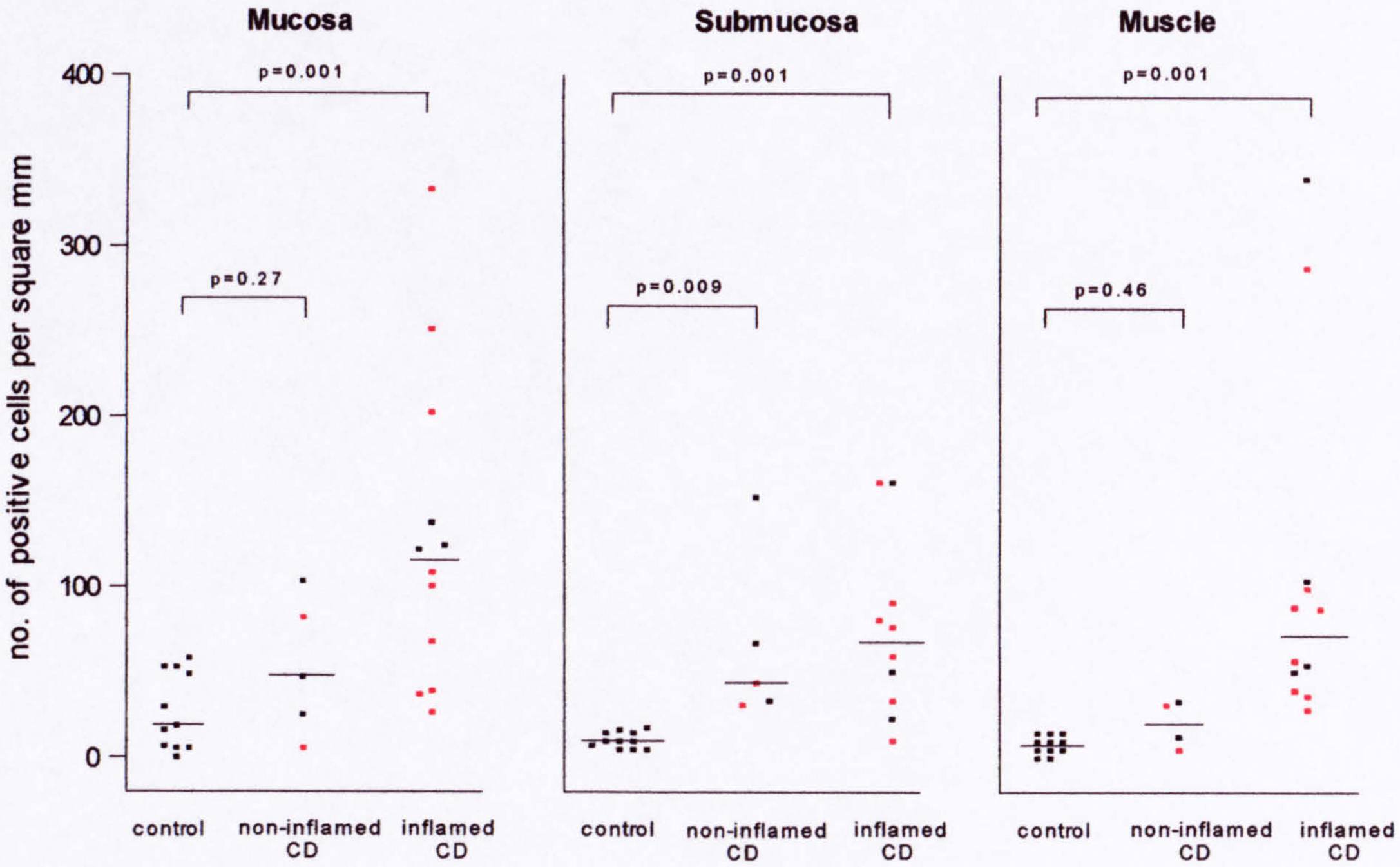

Figure 9. Number of cells positive for activated NFκB per mm^2 in the three layers of normal bowel from control patients, non-inflamed CD bowel and inflamed CD bowel. The levels of significance of comparisons between groups using the Mann-Whitney test are displayed. Horizontal bars indicate median values. Red data points represent patients receiving corticosteroid therapy. The data on which these graphs are based are displayed in Appendix III. The results demonstrate significantly increased tissue-densities of positive cells in all layers of inflamed CD bowel in comparison to normal bowel from controls. In only the submucosa of non-inflamed CD bowel was there a significantly increased tissue-density of positive cells in comparison to normal bowel from controls.

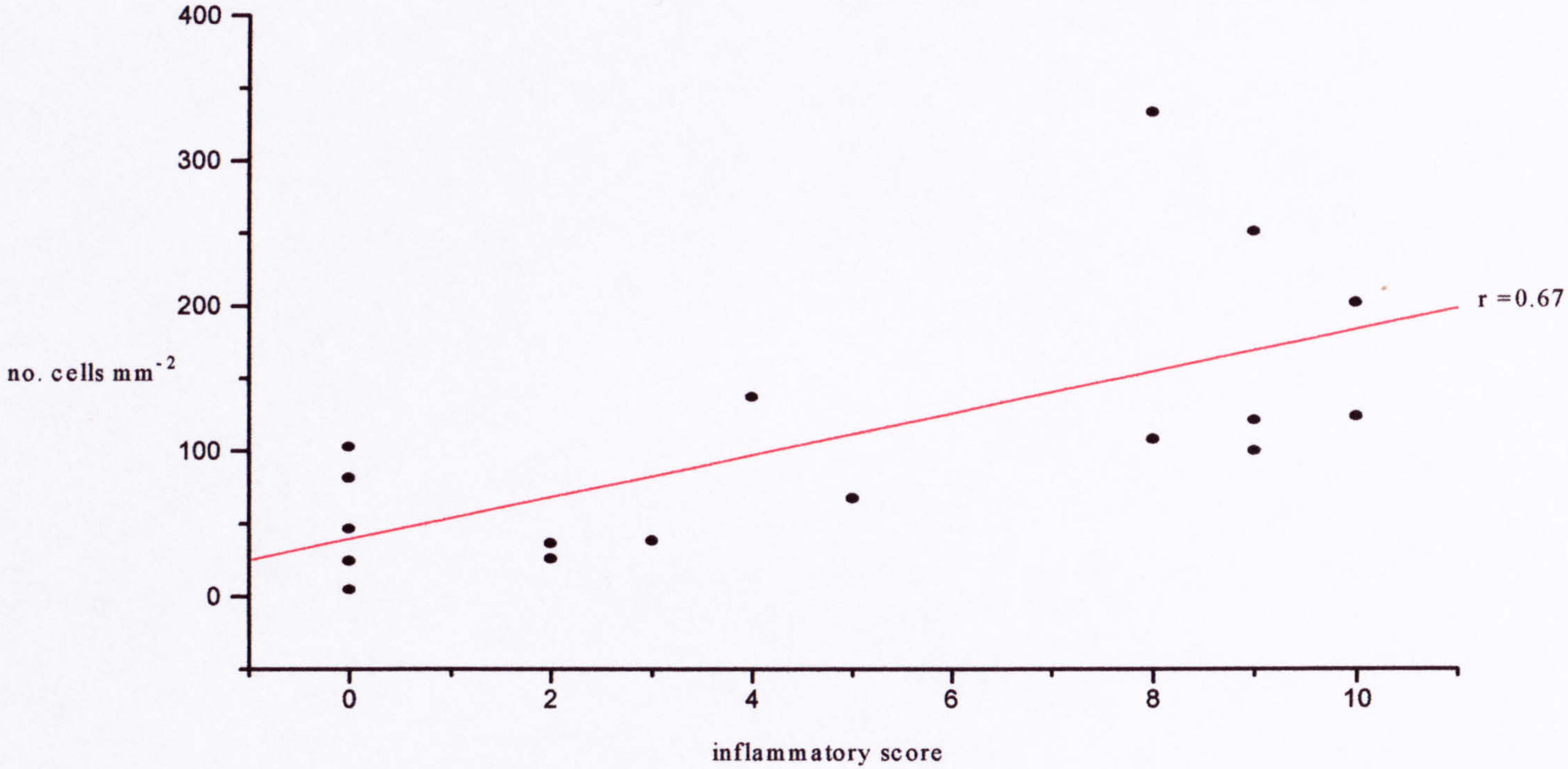

Figure 10. Graph of number of cells positive for NFκB per mm^2 in the *mucosa* of CD patients against the inflammatory score of sections taken from the same biopsy specimen. Specimens taken simultaneously from non-inflamed areas of five patients were included (allocated an inflammatory score of 0) and hence in five patients there are two specimens within this graph. A regression line is fitted and the Spearman's rank correlation coefficient displayed.

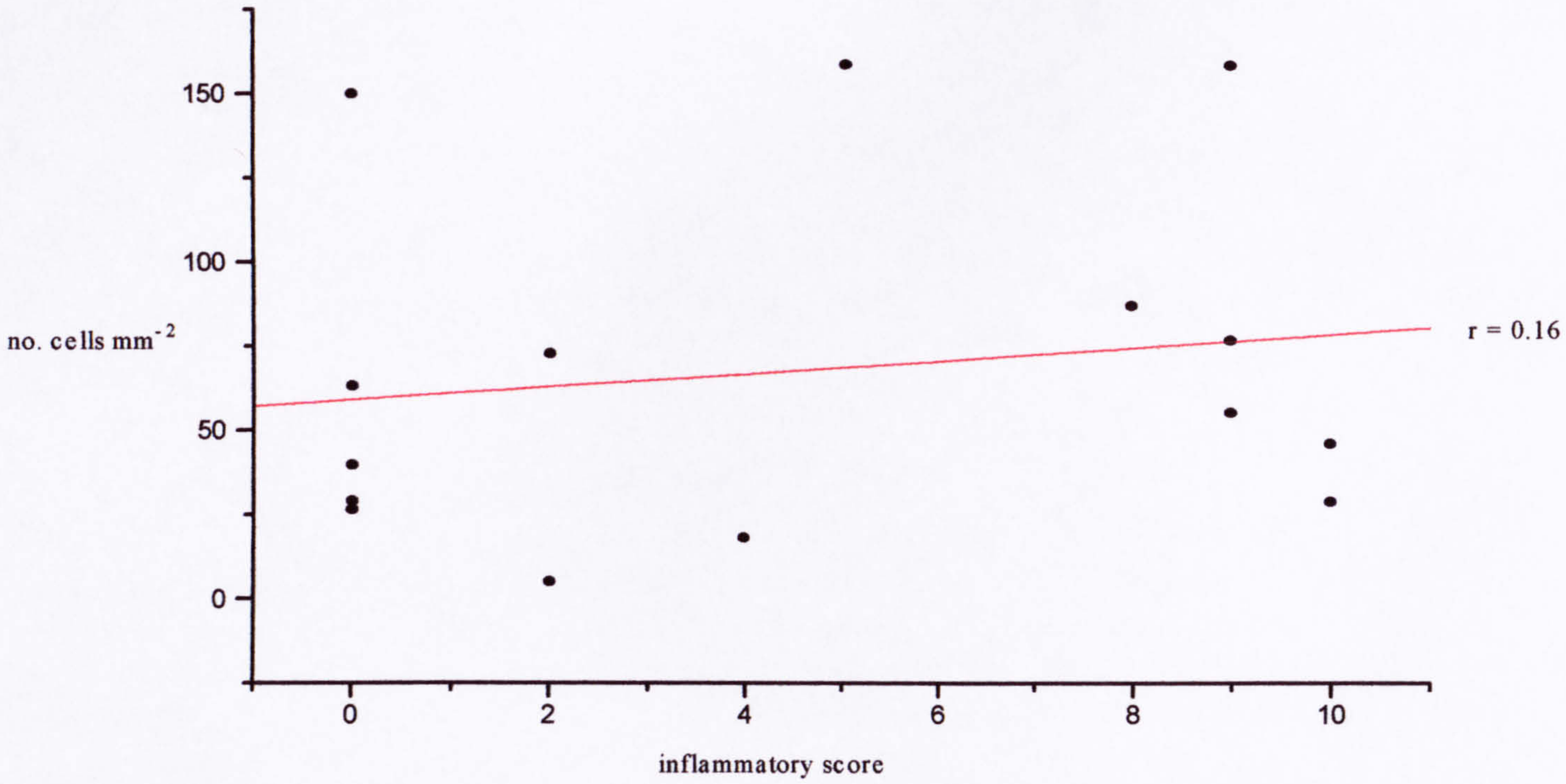

Figure 11. Graph of number of cells positive for NFκB per mm^2 in the *submucosa* of CD patients against the inflammatory score of sections taken from the same biopsy specimen. Specimens taken simultaneously from non-inflamed areas of five patients were included (allocated an inflammatory score of 0) and hence in five patients there are two specimens within this graph. A regression line is fitted and the Spearman's rank correlation coefficient displayed.

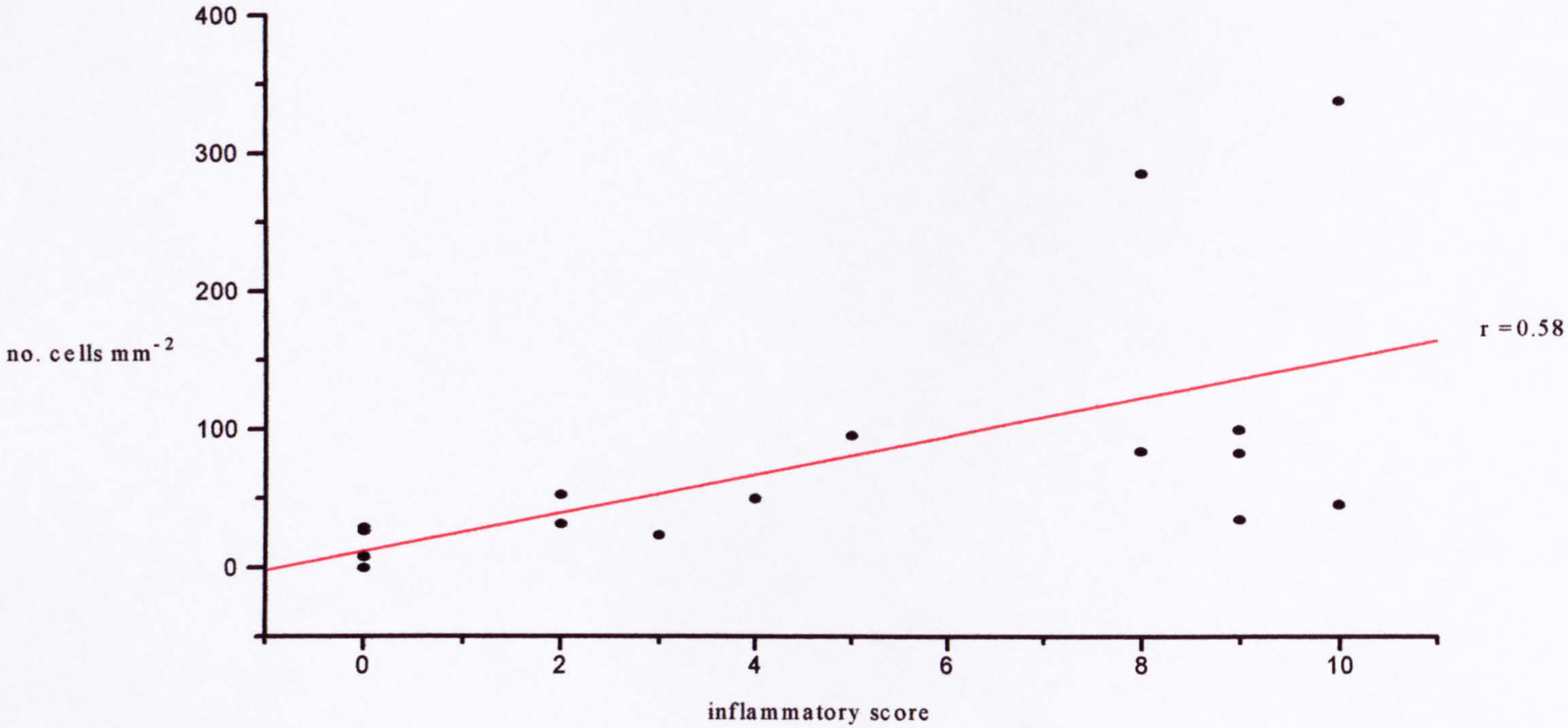

Figure 12. Graph of number of cells positive for NFκB per mm^2 in the *muscle* layer of CD patients against the inflammatory score of sections taken from the same biopsy specimen. Specimens taken simultaneously from non-inflamed areas of four patients were included (allocated an inflammatory score of 0) and hence in four patients there are two specimens within this graph. A regression line is fitted and the Spearman's rank correlation coefficient displayed.

3.3 Correlation of activation of NFκB with inflammatory scores

Moderately significant correlations between inflammatory score and tissue-density of cells positive for activated NFκB were seen in the mucosa ($r = 0.67$, $p = 0.003$ (Figure 10)) and muscle ($r = 0.58$, $p = 0.018$ (Figure 12)), but not in the submucosa ($r = 0.16$, $p = 0.57$ (Figure 11)).

3.4 Effect of corticosteroids on activation of NFκB

Although corticosteroids inhibit activation of NFκB *in vitro,* in no layer of sections from inflamed bowel was there a correlation between tissue-density of positive cells and corticosteroid dose ($r = -0.36$, 0.06 and 0.32, for mucosa, submucosa and muscle respectively). The degree of inflammation is a possible confounding factor on this correlation, and so tissue-density of positive cells was divided by inflammatory score, hence giving a figure representing amount of activated NFκB corrected for degree of inflammation, but still no correlation with dose of steroid was found ($r = -0.28$, -0.27 and -0.25 for mucosa, submucosa and muscle respectively)

3.5 Ulcerative colitis and inflammatory controls

There were increased numbers of cells staining for activated NFκB in sections from both patients with ulcerative colitis and from two inflammatory controls, although numbers were insufficient to perform significance testing (see Appendix III).

3.6 Paraffin-embedded sections

No staining was seen when formaldehyde-fixed, paraffin-embedded sections of mouse cerebral cortex, HeLa cells and CD bowel received either no pre-treatment or were pre-treated with trypsin. However, with microwave pre-treatment, the following staining was observed:

1. cytoplasmic staining of neurones in mouse cerebral cortex, and in some areas clear nuclear staining (Figure 13);

2. in HeLa cells, possible nuclear staining in one experiment, but this is likely to represent artefact, because of the irregular contour of the nuclear staining and difficulty in reproducing these appearances (Figure 14), and

3. in sections from patients with CD, cytoplasmic staining of large mononuclear cells, possibly plasma cells, but no nuclear staining (Figure 15).

Thus, no unequivocal nuclear staining was observed in paraffin-embedded sections and therefore it was concluded that, with this protocol, the antibody could not be used on paraffin-embedded sections.

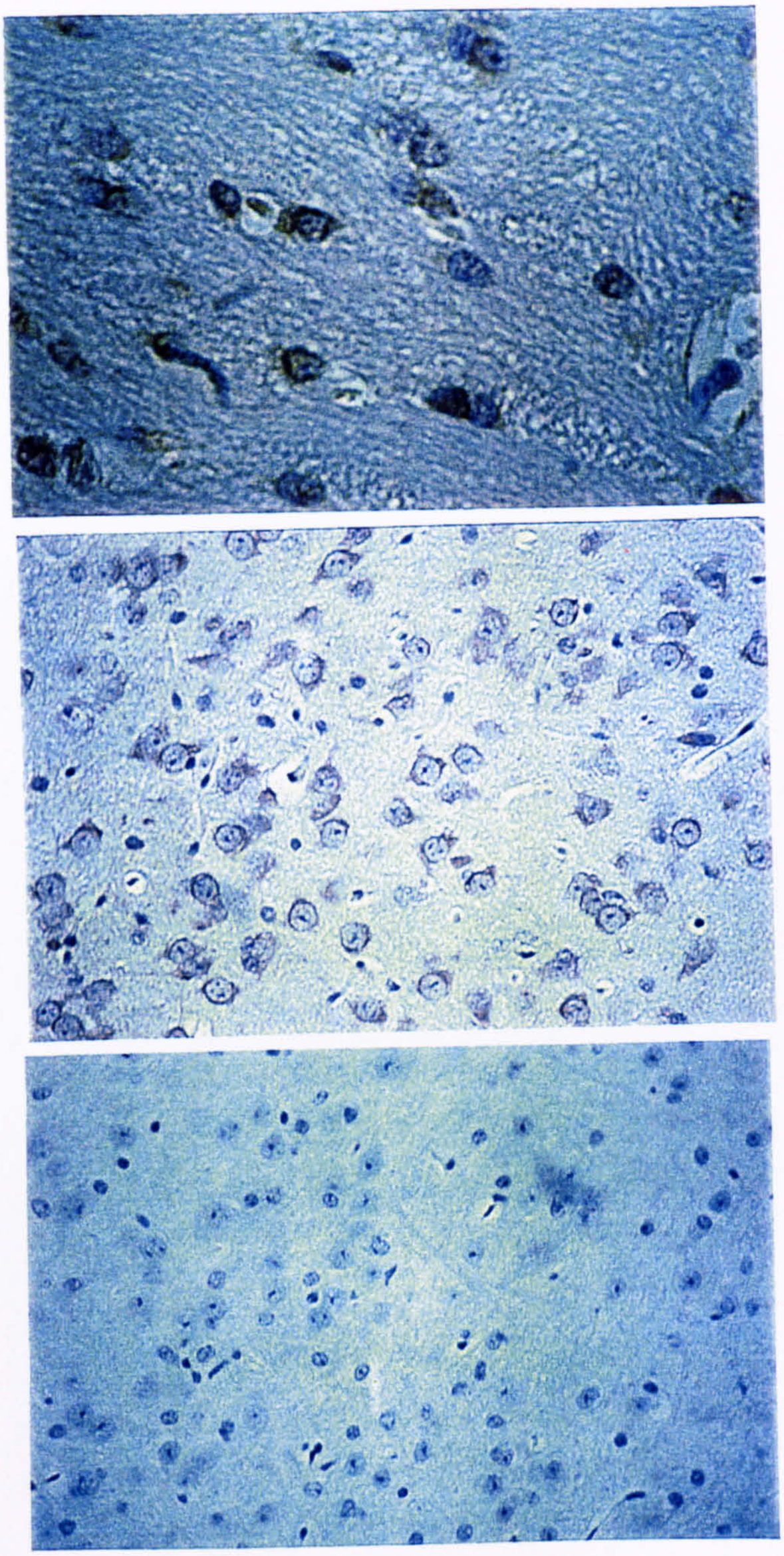

Figure 13. Photomicrographs of formaldehyde-fixed, paraffin-embedded sections of mouse cerebral cortex pre-treated by microwaving, and then immunostained for activated NFκB (above and middle), showing cytoplasmic staining of neurones within an area of the section (above, magnification × 400), and nuclear staining in another area of the section (middle, magnification × 200), (brown, peroxidase-based detection system). Negative control section (below, magnification × 200) immunostained in the same manner with PBS substituted for the primary antibody showing no positive cells. Sections were counterstained with Mayer's haematoxylin. Results are difficult to interpret, but suggest that when used in microwave pre-treated, paraffin-embedded tissue, the primary antibody is not specific for activated NFκB. Alternatively, the microwave pre-treatment may have altered cytoplasmic stores of NFκB, such that the antibody then binds to them.

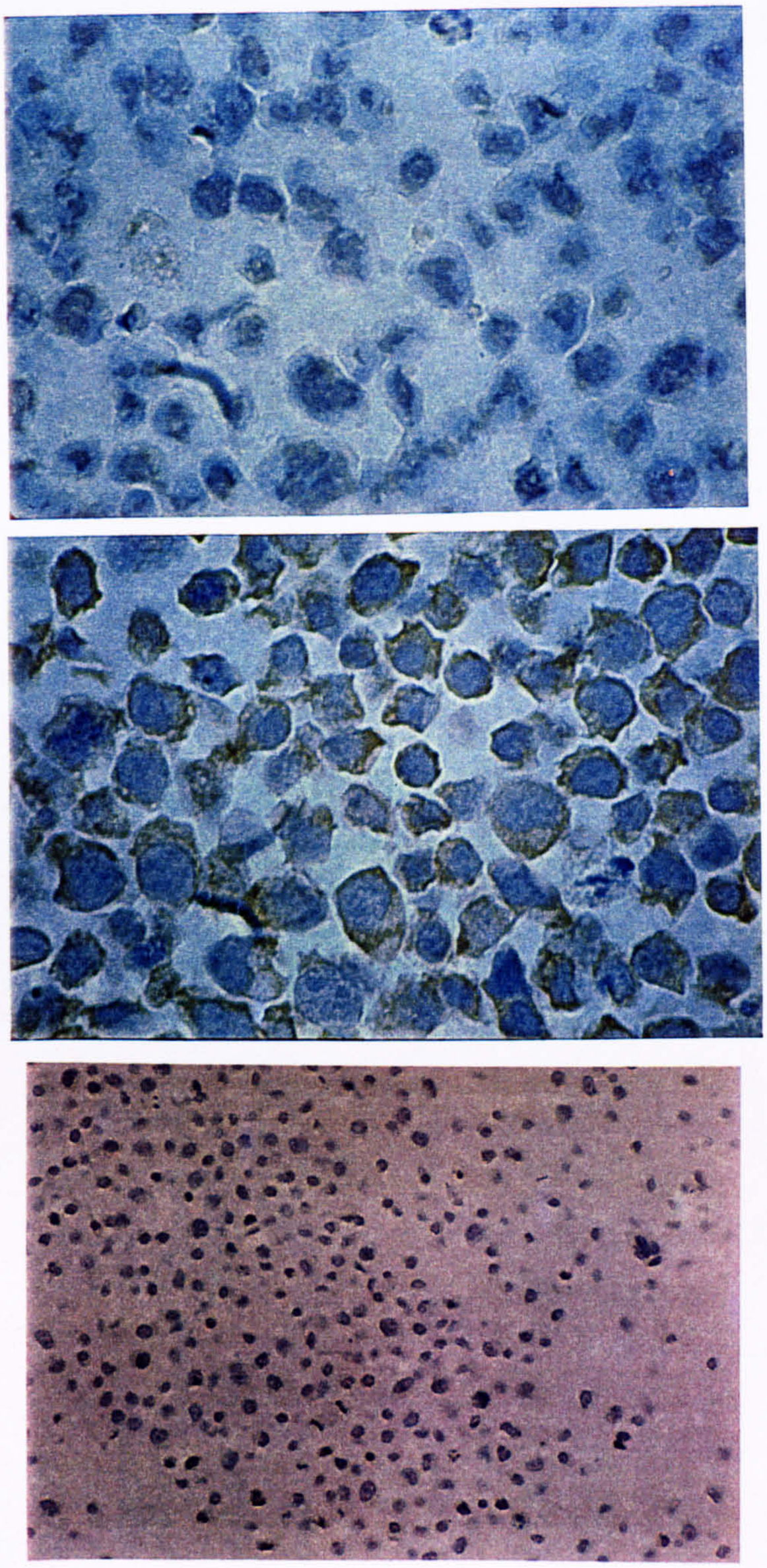

Figure 14. Photomicrographs (magnification × 400) of formaldehyde-fixed, paraffin-embedded sections of HeLa S3 cells pre-treated by microwaving, and then immunostained for activated NFκB (brown, peroxidase-based detection system). Cells treated with PMA to activate NFκB (above) show nuclear staining most likely to represent artefact, as suggested by the irregular contour of the nuclear staining and difficulty in reproducing these appearances. Unstimulated cells (middle) show cytoplasmic staining, but no nuclear staining. Negative control section (below) of stimulated cells immunostained in the same manner, but with PBS substituted for the primary antibody, showing no staining. Sections were counterstained with Mayer's haematoxylin.

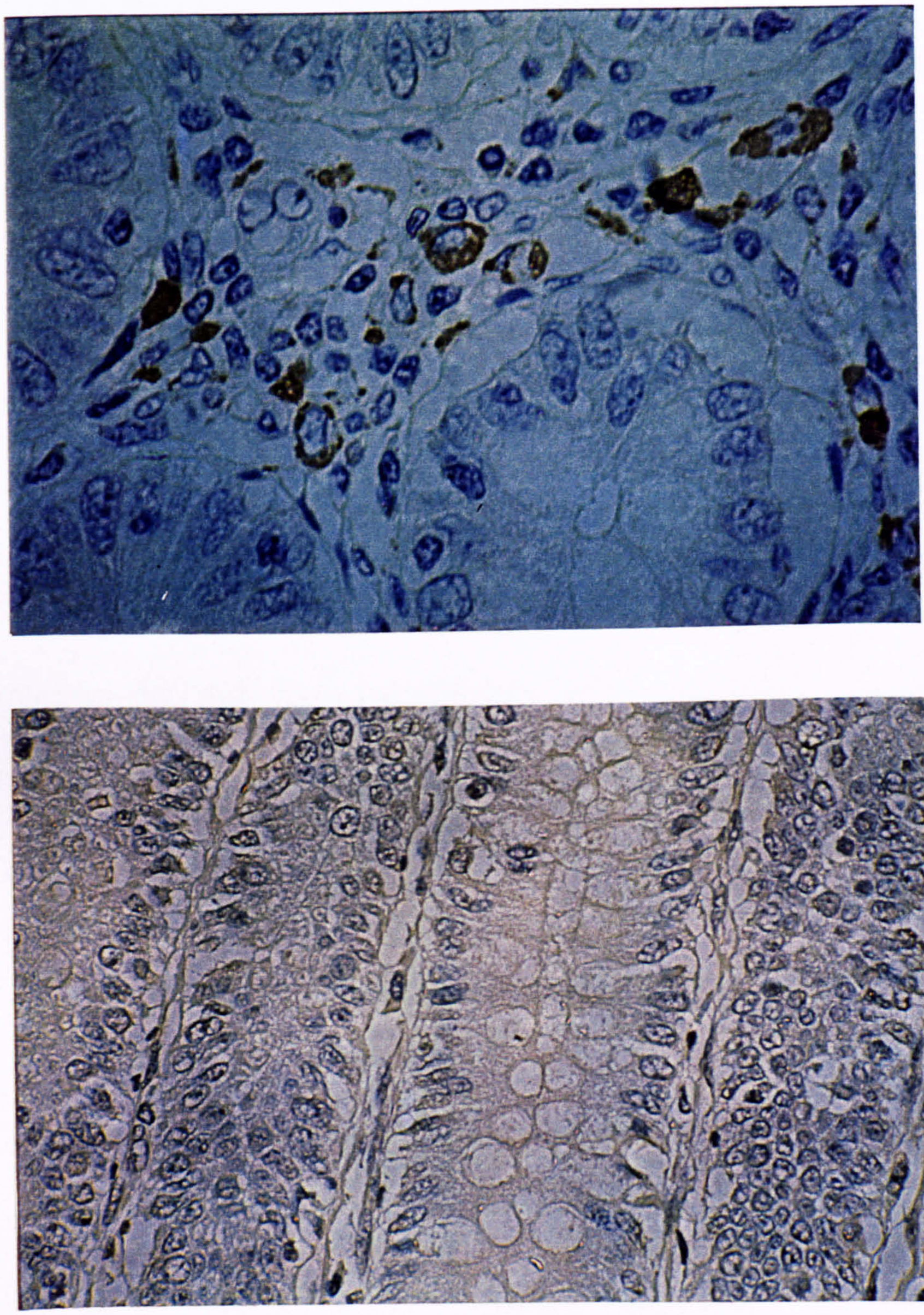

Figure 15. Photomicrographs (magnification × 400) of formaldehyde-fixed, paraffin-embedded sections of inflamed small bowel from a patient with CD, pre-treated by microwaving and then immunostained for activated NFκB (above), showing cytoplasmic staining of large mononuclear cells, but no nuclear staining (brown, peroxidase-based detection system). Exclusive cytoplasmic staining suggests that in sections of bowel prepared in this way, staining of cells containing nuclear-translocated, activated NFκB did not occur. Negative control section (below) immunostained in the same manner with PBS substituted for the primary antibody showing no positive cells. Sections were counterstained with Mayer's haematoxylin.

4. Discussion

4.1 Paraffin-embedded sections

Paraffin-embedded sections offer considerable advantages of good morphology, easy handling and access to historical specimens in libraries. There have been no previous publications using anti-p65 NFκB antibody manufactured by Boehringer Mannheim on paraffin-embedded tissue sections.

In the present chapter, the staining in paraffin-embedded sections of bowel, pre-treated by microwaving, was exclusively cytoplasmic. This was difficult to interpret given the specificity of the antibody for activated NFκB and the known nuclear localisation of the activated form, and occurred in mononuclear cells of one type, probably plasma cells. Some activated NFκB may be present within the cytoplasm (3), but in paraffin-embedded sections of bowel, *exclusive* cytoplasmic, with no nuclear, staining was seen. It is possible that in cytoplasmic pools of inactive, IκB-bound NFκB, the process of microwaving may have revealed the epitope to which the antibody binds, thus falsely resulting in staining, but a greater number of positive cells, and of different morphologies, might have been expected if this had occurred, as many different cell types contain the p65 subunit of NFκB (see section 4.2).

In paraffin-embedded sections of mouse cerebral cortex, pre-treated with microwaving, cytoplasmic staining was seen in some areas, but definite nuclear staining in others. In paraffin-embedded sections of stimulated HeLa cells, no convincing staining was seen. Thus, the findings in paraffin-embedded sections were difficult to interpret and work therefore concentrated on frozen sections and unsectioned cultured cells grown on to cover-slips.

4.2 Frozen sections and unsectioned cultured cells

The nuclear staining seen in positive controls of activated HeLa cells and mouse cerebral cortex is consistent with the specificity of the antibody and the rapid translocation of activated NFκB to the nucleus. Similar staining was seen in sections of bowel, but cytoplasmic, peri-nuclear staining was seen in some cells in all layers, but particularly in the muscle layer, which may represent activated, cytoplasmic NFκB (3). Previous studies have shown that in HeLa cells stimulated for thirty minutes, all activated, nuclear-translocated NFκB is inactivated by newly synthesised IκB within eight hours of the original stimulus (320), which suggests that the activation of NFκB in the present study in bowel reflects recent events.

Immunohistochemical staining revealed a significantly greater tissue-density of cells expressing activated NFκB in the inflamed bowel in CD compared to normal bowel from controls, and expression was highest in the mucosa and muscle layers.

In all three layers of the bowel wall, expression of activated NFκB in CD patients was mainly restricted to large mononuclear cells, morphologically suggestive of macrophages, suggesting these are a major cell-type involved in propagating inflammation in CD.

This is comparable to findings from two previous studies using the same antibody in rheumatoid arthritis (RA) and osteoarthritis (106) and in atherosclerosis (105). In the study in arthritis, patients with chronic joint disease had increased activation of NFκB within the synovial lining, specifically in cells of a macrophage lineage, the type A synoviocytes. As in the present study, there was a low level of activation of NFκB in normal control subjects. Interestingly, in arthritis patients with acute disease, but not

those with chronic disease, there was increased activation of NFκB in endothelial cells, an event not found in the present study, possibly due to the chronic nature of CD in the patients studied.

In the study in atherosclerosis, activation of NFκB was found in macrophages, fibroblasts and endothelial cells in the active atherosclerotic lesion.

In another study, increased activation of NFκB was demonstrated by electrophoretic mobility shift assay in macrophage-enriched mucosa mononuclear cells from mice with 2,4,6,-trinitrobenzene sulfonic acid (TNBS)-induced granulomatous colitis, and the active form of NFκB contained both p50 and p65 subunits (321). Using Western blotting, this study demonstrated a significant increase in p65 levels in nuclear extracts from macrophage-enriched mucosa mononuclear cells from patients with CD as compared to controls. These findings were confirmed in another study using both Western blotting and EMSA of nuclear extracts of endoscopic biopsy specimens from inflamed CD bowel (322), and are consistent with the findings in this chapter. In the second study (322), reduction in levels of activated NFκB were demonstrated from before, to after, treatment of patients with corticosteroids. In the present Chapter, no correlation between corticosteroid dose and activation of NFκB was found.

Activated NFκB controls transcription of the gene for the cytokine TNFα, and TNFα activates NFκB; hence NFκB plays an essential role in the regulation of TNFα and could form a positive feedback mechanism (3). Studies using immunohistochemistry (318) and *in situ* hybridisation (221) have found that expression of TNFα in CD is restricted to a small number of macrophages and some lymphocytes, mainly in the lamina propria, with no expression in the epithelium, and fewer positive cells in

normal bowel from control patients. This is similar to the pattern of NFκB activation seen in the present study. It is thus possible that there is a direct relationship between TNFα expression and activation of NFκB in the bowel. However, co-staining studies are required to determine whether expression of TNFα and activated NFκB occurs within the same macrophages.

NFκB is expressed in a wide variety of cell types *in vitro* including T cells, B cells, monocytes/macrophages, neurones, colonic epithelial cells, endothelial cells and connective tissue cells, and its most important role is in cells of the immune system (3). Unexpectedly, in the present study, activation in many different cell types in inflamed tissue was not seen, with only mononuclear cells staining positive for activated NFκB. As has been suggested to explain similar results in the joint, this may be because other cell types may use alternative forms of the NFκB heterodimer (e.g. p50-p50 heterodimer) that do not contain the p65 (Rel A) subunit, which is the epitope for the antibody used in the present study, such as the p50-Rel-B heterodimer (106).

The greater tissue-density of cells expressing activated NFκB in inflamed CD could simply reflect the increase of a particular cell type in inflamed areas. However, in view of the central role that NFκB plays in many inflammatory events, a functional increase in its activation is more likely. Furthermore, as stated above, in RA it is clear that increased activation, rather than changes in cell number, causes the observed increase in expression of activated NFκB during inflammation. The few cells positive for activated NFκB found in normal bowel from controls may represent normal immunological activity in the mucosa, for instance, the continual process of antigen sampling and consequent immunological reaction.

There was a significantly greater tissue-density of cells expressing activated NFκB in the submucosa, but not in the mucosa or muscle layers, of macroscopically and microscopically non-inflamed CD bowel compared to normal bowel from controls. The absence of a significant difference between non-inflamed areas and control specimens in the mucosa and muscle layers may be a correct finding or may be due to a type II sampling error, particularly as only small numbers of non-inflamed specimens were collected (microscopically normal areas of resection specimens were difficult to accumulate and several specimens from macroscopically normal areas showed microscopic evidence of inflammation, and were not included in either group since they were not completely non-inflamed and specimens from macroscopically (and microscopically) inflamed areas from these patients were already included in the inflamed group). However, the difference observed in the submucosa strongly suggests that the apparently non-inflamed bowel in CD is more immunologically active than completely normal bowel from controls.

A moderately significant correlation between inflammatory score and number of cells staining for activated NFκB was seen in the mucosa and muscle layer, but not in the submucosa. This supports an hypothesis that the increased levels of activation of NFκB in the submucosa do not simply reflect inflammation and, together with the observation of increased expression of activated NFκB in the submucosa of non-inflamed specimens, suggests that a process independent of inflammation may occur there. However, it could be hypothesised that the absence of a correlation in the submucosa may simply reflect inclusion of data from specimens scored as non-inflamed, but which contained increased numbers of cells positive for activated NFκB in the submucosa (for whatever reason) and which, in the submucosa, diluted a

significant correlation that existed in inflamed specimens. When the non-inflamed specimens are removed from the analysis of correlation, there is still no significant correlation in the submucosa ($r = 0.17$, $p = 0.62$), but a weak correlation just persists at significant levels in the mucosa ($r = 0.62$, $p = 0.03$), but not in the muscle layer ($r = 0.45$, $p = 0.13$). However, the small numbers of patients may miss real correlations due to type II sampling errors.

Other studies have demonstrated subtle abnormalities in CD bowel that is normal by macroscopic and microscopic criteria, namely changes in: immunohistochemically demonstrated plasma cells (323); immunohistochemically demonstrated nerve fibres (324) and axonal necrosis of nerves by electron microscopy (325); vasoactive intestinal polypeptide containing nerves (326,327); nerves positive for major histocompatibility complex class II antigen (328); T cells and macrophages (329), and in intercellular adhesion molecule-1 (330). Such changes in non-inflamed areas in CD may predate overt inflammation and further study of these areas, rather than those that are already inflamed and possess a compromised mucosal barrier, may reveal more about the early events that generate inflammation in CD.

Comparisons were not made between non-inflamed and inflamed areas as this was not the original aim of the study, and because of advice from the statistician, that such multiple significance testing would require a Bonferroni correction that would reduce the power of the data.

Although corticosteroids inhibit activation of NFκB *in vitro,* which explains their diverse anti-inflammatory effects *in vivo* (127,128), in the present study *ex vivo*, there was no correlation between the current dose of corticosteroid and activation of NFκB, despite correcting for the degree of inflammation as a confounding factor. This might

be explained by the use of resection tissue from patients who, by definition, were unresponsive to corticosteroids and hence required surgery, i.e. these patients may have possessed corticosteroid resistance. Alternatively, the severity of the underlying disease may have overridden the inhibitory effects of corticosteroids on NFκB activation.

It was not possible to collect many full-thickness operative specimens from patients with ulcerative colitis, as most operations are unplanned, and are becoming less common with improvements in medical therapy. Endoscopic biopsy specimens are more easily obtained and were collected, but good quality staining with low background staining was difficult to obtain, as indicated by the high background count obtained in the only endoscopic biopsy included for analysis, from a patient with Wegener's granulomatosis (see Appendix III). Furthermore, endoscopic biopsy specimens contain only mucosa and occasionally submucosa, but no muscle layer. In the two patients with UC from whom full thickness specimens were collected, cells positive for NFκB were plentiful, particularly in the mucosa and submucosa, consistent with the pathology of UC as a disease affecting predominantly the mucosa, extending into the deeper layers only in more active disease.

In inflammatory controls with diverticulitis and vasculitis, many cells positive for activated NFκB were also seen, and so increased activation of NFκB in bowel is not confined to CD.

A large increase in activation of NFκB in inflamed areas of CD bowel was demonstrated. NFκB is activated by diverse stimuli and it is unclear whether this increase in activation is in response to a causal agent e.g. viruses, to reactive oxygen species, or to increased immunological signalling. Recently, antagonists of NFκB

activation that specifically inhibit the proteasome that degrades IκB have been shown to be effective in treating chronic granulomatous colitis in rats (124) and local administration of antisense oligonucleotides improves both TNBS-induced granulomatous colitis in mice and colitis in IL-10 deficient mice (321). This suggests that activation of NFκB, and hence the cells expressing it, are fundamental to the process of inflammation in the bowel. NFκB thus represents a potent target for new anti-inflammatory agents in CD.

5. Conclusion

In this chapter, an immunohistochemical method to study activation of NFκB in frozen sections of bowel was established. Increased tissue-density of cells positive for activated NFκB was demonstrated in sections of bowel from patients with CD in all layers of inflamed areas in comparison to sections of bowel from control patients. Activation was restricted mainly to large mononuclear cells, morphologically suggestive of macrophages, suggesting that these are a major cell type involved in propagating inflammation in CD.

A greater tissue density of cells expressing activated NFκB was found in the submucosa, but not in the mucosa or muscle layers, of macroscopically and microscopically non-inflamed CD bowel compared to normal bowel from controls, which suggests that the apparently non-inflamed bowel in CD may be more immunologically active than completely normal bowel from controls, consistent with other studies that have demonstrated subtle abnormalities in these areas. The first molecular inflammatory events of CD may therefore occur in the submucosa.

Chapter 6

Activation of NFκB in cell cultures measured by flow cytometry

1. Introduction

1.1 Aim

In Chapter 4, immunohistochemistry was used to investigate the activation of NFκB in sections of bowel using an antibody that was specific for the activated form of NFκB. The antibody was validated using sections of mouse cerebral cortex and cultured HeLa cells grown on to coverslips, immunostained with a peroxidase-based system.

In the present chapter, a method to measure activation of NFκB by flow cytometry, which has not previously been published, is developed. The reasons for developing a method were:

- immunocytochemistry allows *in situ* identification and quantitation of cells staining positive for NFκB, but definitive identification of the cell-type(s) staining positive requires double staining, which is technically difficult and often unsuccessful, whereas
- flow cytometry allows rapid measurement of antibody staining of large numbers of cells, and allows sorting of cells into different populations. Once a method was established, these characteristics would be used in two ways:

1. to measure activation of NFκB in isolated lamina propria cells from patients with inflammatory bowel disease and controls, and to identify sub-populations of cells containing activated NFκB, and

2. it is known that NFκB plays an essential role in silica-induced inflammatory mediator production in macrophages (331,332), and flow cytometry would be used to measure activation of NFκB in cultured cells stimulated with solutions of inorganic sub-micron particles with bioactive bacterial products adsorbed onto their surface, thus linking with other work within The Gastrointestinal Laboratory examining the potency, and mechanism of action, of these particles in inducing inflammatory responses, and their possible role in the aetiology of Crohn's disease.

1.2 Description of flow cytometry

Flow cytometry measures the properties of individual cells or particles as they move, or flow, in liquid suspension. Measurements are made separately on each particle within the suspension in turn and not simply as a total value for the whole population.

A laser emits an intense beam of monochromatic light that falls on individual cells, or particles, moving singly through the viewing field at rates of up to several thousand cells per second. Light is scattered by particles in cells and is measured by highly sensitive light detectors, called photomultiplier tubes, which are located both opposite and to one side of the laser and measure forward and side light scatter, respectively.

Forward light scatter provides information on the relative size of individual cells, whereas side light scatter provides information on the relative granularity of individual cells. Additional photomultiplier tubes measure light emitted at a different wavelength by fluorescent labels in, or on, cells, with incident light removed by filters.

Since all measurements are made on each cell simultaneously, one or two measurements, usually forward and side scatter, can be used to select a subset of cells for study using another measurement, usually light from a fluorophore.

1.3 Proposed methods

In previous studies of flow cytometric measurement of other nuclear antigens, numerous techniques for fixation and permeabilisation of cell suspensions have been used, and when using a new antibody, it is difficult to predict which will result in optimal results, and so a range of methods need to be tested (333). Alcohol fixation has previously been extensively used in flow cytometry and it both fixes and permeabilises cells by dissolving lipids in the cell membrane, which allows penetration of antibodies. Other techniques use cross-linking fixatives such as paraformaldehyde, which preserve structure well, but may reduce permeability, and are hence often combined with permeabilising agents such as Triton X-100.

Camplejohn (333) has categorised four basic methods, namely: 70 % ethanol at 4°C; absolute methanol at –20°C; paraformaldehyde fixation followed by permeabilisation, and detergent enucleation followed by alcohol fixation. In this chapter, five fixation methods, that were previously tested by Landberg *et al* (334) for analysis by flow cytometry of a nuclear antigen, proliferating cell nuclear antigen, were used plus a further commercially available method, Ortho Permeafix, (composition withheld by the manufacturer).

One of these methods, detergent enucleation, involves removal of the cytoplasm of cells with a solution of detergent, and was therefore of particular interest as it would prevent any possibility of staining of inactive, cytoplasmic NFκB. For this reason, an

antibody that is not specific for the activated form of NFκB, namely an anti-p65 NFκB antibody manufactured by Santa Cruz (335), could also be tested to measure only activated, nuclear-translocated NFκB. It was desirable to test more than one antibody, because it is known that antibodies that are successfully used for immunohistochemistry, as the Boehringer antibody was in Chapter 5, are not always successfully applied to flow cytometry (333).

Immunostaining techniques can be single-layer methods, where the fluorophore is directly attached to the primary antibody, or, as used here, two or three layer techniques, where the fluorophore is attached to the final layer, which increase sensitivity.

Thus, a range of fixation techniques were combined with a range of immunostaining protocols and two primary antibodies, to optimise results.

To allow identification of flow cytometry protocols that succeeded in accurately measuring activation of NFκB from the results of mean levels of activation of NFκB within cell suspensions, tumour cell lines in four different states of stimulation were tested, namely:

1. untreated cell suspensions that were termed 'unstimulated' and should contain only a minority of cells containing activated NFκB;
2. cell suspensions stimulated with a combination of PMA and TNFα, which are known to synergistically activate NFκB (83), termed 'stimulated';
3. cell suspensions incubated with an agent that inhibits activation of NFκB, termed 'inhibited'. Pyrrolidine dithiocarbamate (PDTC) is such an agent, which inhibits

activation of NFκB because of antioxidant properties that inhibit the ROI-induced activation of NFκB (34) (see Chapter 1, section 3.6);

4. cell suspensions incubated with PDTC to inhibit activation of NFκB, and then stimulated with TNFα and PMA, termed 'inhibited, then stimulated'. This group was included to demonstrate that any increased levels of activated NFκB measured in the 'stimulated' suspension, returned to baseline levels (similar to the level of activation in the 'inhibited' suspensions) when activation of NFκB was inhibited prior to stimulation. Thus, alternative hypotheses for increased levels of activated NFκB in the stimulated suspensions, such as increased non-specific binding to proteins other than activated NFκB because of increased total cellular protein content in stimulated cells, could be excluded.

2. Methods

2.1 Cell culture

HeLa S3 cells were grown in suspension as described in Chapter 4. Jurkat T cells (gift of Dr. G. A. Limb, Department of Immunology, The Rayne Institute, St. Thomas' Hospital) were cultured in a similar manner except with replacement of Eagle's minimum essential medium containing Hank's balanced salt solution with Roswell Park Memorial Institute 1640 culture medium (Life Technologies, Paisley, Scotland, UK).

2.2 Stimulation of cells

As in Chapter 4, cells were washed twice in serum-free tissue culture medium (TCM), stained with trypan blue and then counted to ensure non-viable cells were below 5 %. Cells were then resuspended in TCM at 2 x 10^6 cells ml^{-1} and, as described in section 1.3, divided into four suspensions in separate culture flasks:

1. to be left unstimulated for 2 hours (termed 'unstimulated');

2. to be left for one hour and then stimulated with a combination of TNFα and PMA (200 units ml^{-1} and 50 ng ml^{-1} respectively) for one hour (termed 'stimulated');

3. to be left for one hour and then cultured for one hour with 100 μM PDTC (Sigma Chemical Company) (termed 'inhibited'), and

4. to be cultured with PDTC for one hour and then TNFα and PMA added for one hour (termed 'inhibited, then stimulated').

Aliquots of 1.5 x10^6 cells were pipetted into flow cytometry tubes (Sigma Chemical Co. Ltd.) and then washed once in serum-free TCM, as described in Chapter 5, and once in PBS, and fixed and immunostained using the following methods.

2.3 Fixation

In the following methods, whole cells were centrifuged at 400g for five minutes and nuclei at 640g for ten minutes.

Method A. Stimulation, enucleation and fixation in 100 % methanol.

1. Cells were centrifuged at 4 °C and the supernatant decanted, and then resuspended in the residual volume by shaking the tube.

2. To each tube, 500 µl of enucleating/lysing solution (0.5 % (v/v) Triton X-100, 0.2 µg ml^{-1} EDTA in PBS) was added, mixed gently and then incubated on ice for fifteen minutes.

3. To each tube, 3 mls of 100 % methanol at – 20 °C was slowly added while agitating vigorously by hand.

4. Cells were vortexed and stored at – 20 °C.

Method B. Stimulation and fixation of whole cells in 70 % ethanol.

1. Cells were centrifuged at 4 °C and the supernatant decanted, and then resuspended in 200µl of PBS.

2. To each tube, 2.8 mls of a 70 % (v/v) solution of ethanol in distilled water at 4°C was added while agitating vigorously by hand, and then stored at 4°C.

Method C. Fixation of whole cells in 100 % methanol.

1. Cells were centrifuged at 4 °C and the supernatant decanted, and then resuspended in 200µl of PBS.

2. 2.8 mls of 100 % methanol at - 20°C was added while agitating vigorously by hand.

3. Cells were cooled to -20°C for five minutes, and 1 ml of distilled water added to each tube. Cells were then mixed and stored at 4°C.

Method D. Fixation of whole cells in paraformaldehyde/Triton X-100.

1. Cells were centrifuged at 4 °C and the supernatant decanted, and then resuspended in 200µl of PBS.

2. To each tube, 1 ml of a 1 % (w/v) solution of paraformaldehyde in PBS was added and incubated at room temperature for fifteen minutes.

3. To each tube, 1 ml of a 0.2 % (v/v) solution of Triton X-100 in PBS was added to the paraformaldehyde/cell mixture. Cells were then mixed and stored at 4 °C.

Method E. Fixation of whole cells in Triton X-100/ paraformaldehyde.

1. Cells were centrifuged and the supernatant decanted, and then resuspended in the residual volume.

2. To each tube, 1 ml of a 0.1 % (v/v) solution of Triton X-100 in PBS was added and incubated at room temperature for fifteen minutes.

3. To each tube, 1 ml of a 2 % (w/v) solution of paraformaldehyde in PBS at 4 °C was added, and then cells stored at 4 °C.

Method F. Stimulation and fixation of whole cells in Ortho Permeafix (Ortho Diagnostic Systems, Raritan, New Jersey, USA) (as per manufacturer's instructions).

1. Cells were centrifuged at 4 °C and the supernatant decanted, and then resuspended in 2 ml of Ortho Permeafix and incubated at room temperature for forty minutes.

3. Cells were then centrifuged, the supernatant decanted, and then resuspended in the residual volume.

4. To each tube, 2 ml of wash buffer (5 % (v/v) fetal calf serum, 1.5 % (v/v) bovine serum albumin (BSA) (Sigma Chemical Company) and 0.005 % (w/v) EDTA in PBS) was added, and then incubated at room temperature for ten minutes.

5. Cells were centrifuged at 4 °C, the supernatant decanted, and then resuspended in the residual volume and immediately immunostained with a two layer technique (see section 2.4.3).

2.4 Immunostaining

2.4.1 Immunostaining of nuclei using a three layer technique.

1. Clumped nuclei were separated by passing forcefully through a 16 gauge needle (Sigma Chemical Company) with a 1 ml syringe (Sigma Chemical Company).

2. Nuclei were washed twice, by centrifuging at 4 °C, decanting the supernatant, and then adding 2 ml of enucleating/lysing solution. The supernatant was then again decanted and the nuclei resuspended in the residual volume, and one of two tested primary antibody layers (A and B below) added and incubated at room temperature for one hour. In all experiments, as a negative control, to a second tube prepared in an identical manner, was added an isotype control antibody (C below) in place of the primary antibody.

A: 100µl of a solution of Boehringer Mannheim anti-p65 NFκB antibody diluted 1 in 50 in enucleating/lysing solution.

B: 100µl of a solution of Santa Cruz anti-p65 NFκB antibody (335) (Santa Cruz Biotechnology, Inc., Autogen Bioclear, Devizes, Wiltshire, UK) diluted 1 in 20 in enucleating/lysing solution.

C: 100µl of a solution of mouse IgG3κ isotype control antibody (Sigma Chemical Company) diluted 1 in 100 in enucleating/lysing solution.

3. Nuclei were washed twice with enucleating/lysing solution, as before. The supernatant was then decanted and the nuclei resuspended in the residual volume.

4. The secondary antibody appropriate to the primary antibody was then added, mixed gently and incubated at room temperature for one hour as follows:

For primary antibody A and C: 100µl of a solution of biotinylated, rabbit anti-mouse antibody (Dako Ltd.) diluted 1 in 100 in enucleating/lysing solution.

For primary antibody B: 100µl of a solution of biotinylated, goat anti-rabbit antibody (Sigma Chemical Company) diluted 1 in 100 in enucleating/lysing solution.

5. Nuclei were washed twice with enucleating/lysing solution as before, and the tertiary layer, 100 µl of a solution of Extravidin™-FITC (Sigma Chemical Company) diluted 1 in 200 in enucleating/lysing solution, added and incubated at room temperature for one hour.

6. Nuclei were washed twice with antibody diluent. The supernatant was then decanted and the nuclei resuspended in the residual volume.

7. For identification, nuclei were stained with 200 µl propidium iodide (PI) solution, which stains PI (336) (10 µg ml^{-1} PI (Sigma Chemical Company), 1.8 Kunitz units ml^{-1} RNase, 0.5 % (v/v) Nonidet P-40 (Sigma Chemical Company) in PBS), then

resuspended by passing forcefully through a 16 gauge needle prior to analysis by flow cytometry.

2.4.2 Immunostaining of nuclei using a two layer technique

1. Steps 1 and 2 of method 1 were performed using only Boehringer Mannheim anti-p65 NFκB and isotype control antibody.

2. Nuclei were washed twice with enucleating/lysing solution as before. The supernatant was then decanted and the nuclei resuspended in the residual volume.

3. A solution of secondary antibody, FITC-labelled rabbit anti-mouse antibody (Dako Ltd.) diluted 1 in 10 in enucleating/lysing solution was applied and incubated at room temperature for 45 minutes.

4. Nuclei were washed twice with antibody diluent as before. The supernatant was then decanted and the nuclei resuspended in the residual volume.

5. Nuclei were stained with 200 µl PI solution, then resuspended by passing forcefully through a 16 gauge needle prior to analysis by flow cytometry.

2.4.3 Immunostaining of whole cells using a two layer technique.

1. Cells were washed once, as before, with wash buffer (5 % (v/v) fetal calf serum, 1.5 % (v/v) BSA and 0.005 % (w/v) EDTA in PBS).

2. The supernatant was decanted, and the cells then resuspended in the residual volume and the primary antibody applied (100µl of a solution of Boehringer Mannheim anti- p65 NFκB antibody diluted 1 in 50 in enucleating/lysing solution, or 100µl of a solution of isotype control antibody diluted 1 in 100 in enucleating/lysing

solution). Cells were then mixed gently by hand and incubated at room temperature for one hour.

3. Cells were washed twice with wash buffer, as before, and the supernatant decanted and the cells then resuspended in the residual volume.

4. The secondary antibody, 100µl of a solution of FITC-labelled rabbit anti-mouse antibody diluted 1 in 10 in wash buffer, was then added and incubated at room temperature for 45 minutes.

5. Cells were washed twice with wash buffer as before, and finally resuspended in 200 µl of wash buffer prior to analysis by flow cytometry.

2.5 Flow cytometry analysis

Fixed and immunostained suspensions of cells and nuclei were analysed by flow cytometry using a Becton Dickinson FACScan (Becton Dickinson, Mountain View, California, USA) and LYSIS II software package (Becton Dickinson), simultaneously measuring forward scatter, side scatter, FITC fluorescence (detected by fluorochrome 1 photomultiplier tube), and for suspensions of nuclei, PI fluorescence (detected by fluorochrome 2 photomultiplier tube). Data were then analysed using a Personal Computer (PC) and Windows multiple document interface software package, version 2.7 (Microsoft Corporation, Redmond, WA, USA), that is specifically designed for analysis of flow cytometry data.

When suspensions of nuclei were stained with two fluorophores, analysis was adjusted for spectral overlap of FITC and PI immunofluorescence by electronic spectral overlap correction. Furthermore, control samples of nuclei labelled only with

FITC, were analysed in the PI spectrum, and *vice versa*, to confirm that no significant spectral overlap occurred.

2.5.1 Selection of populations of cells

Whole cells within cell suspensions were defined by forward- and side-scatter characteristics: a 'dot-plot' of forward versus side-scatter was created, and an area selected, termed a 'gate' (R1, Figure 1), such that particles at the extremes of forward- or side- scatter, that might represent fragments or small clumps of cells respectively, were excluded from subsequent recording of fluorescence. The same gate was used within individual experiments, to allow direct comparison of stimulated and unstimulated states, but varied slightly between experiments, because different cell cultures had slightly differing forward- and side-scatter characteristics.

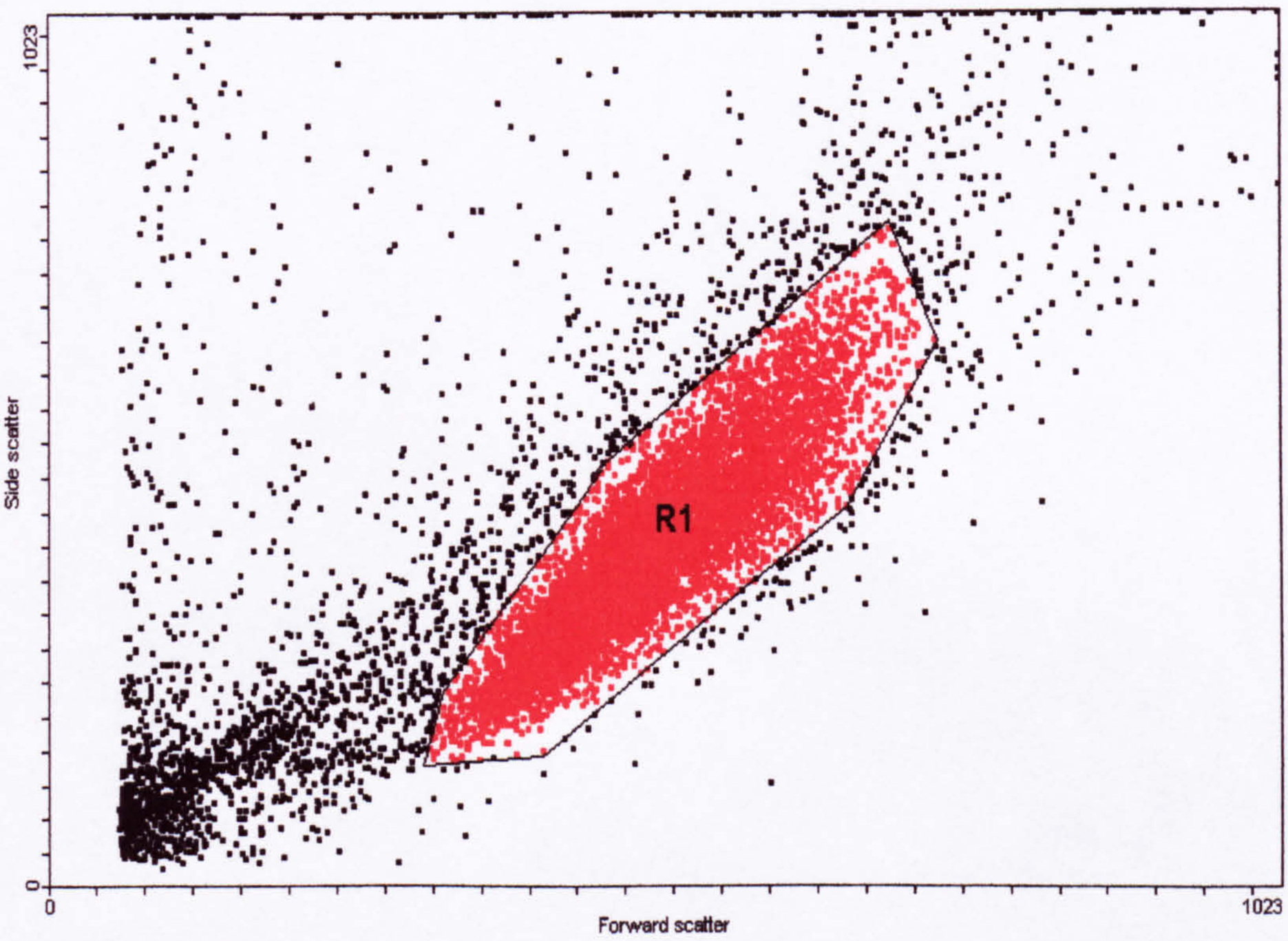

Figure 1. An example of a dotplot of forward scatter versus side scatter characteristics of HeLa cells, showing a gated area, R1, that is designated as representing whole cells. Similar dotplots were obtained for Jurkat T cells.

2.5.2 Selection of populations of nuclei

To create a gate for selection of a population of single nuclei, a DNA histogram (Figure 2) was created by plotting number of nuclei against log PI fluorescence. The DNA histogram represents a range of quantity of DNA within different nuclei, with the first peak (A) representing nuclei from cells in the G_1 phase of the cell cycle when division is first triggered, and the second peak (B) representing nuclei from cells in the G_2 phase, when the DNA content is doubled immediately prior to mitosis (336). The population of single nuclei to be analysed was defined by a gate (M1) applied to the DNA histogram, so excluding, for instance, clumped nuclei that have a combined DNA content higher than single nuclei from cells in the G_2 phase and small fragments of nuclei or cytoplasm.

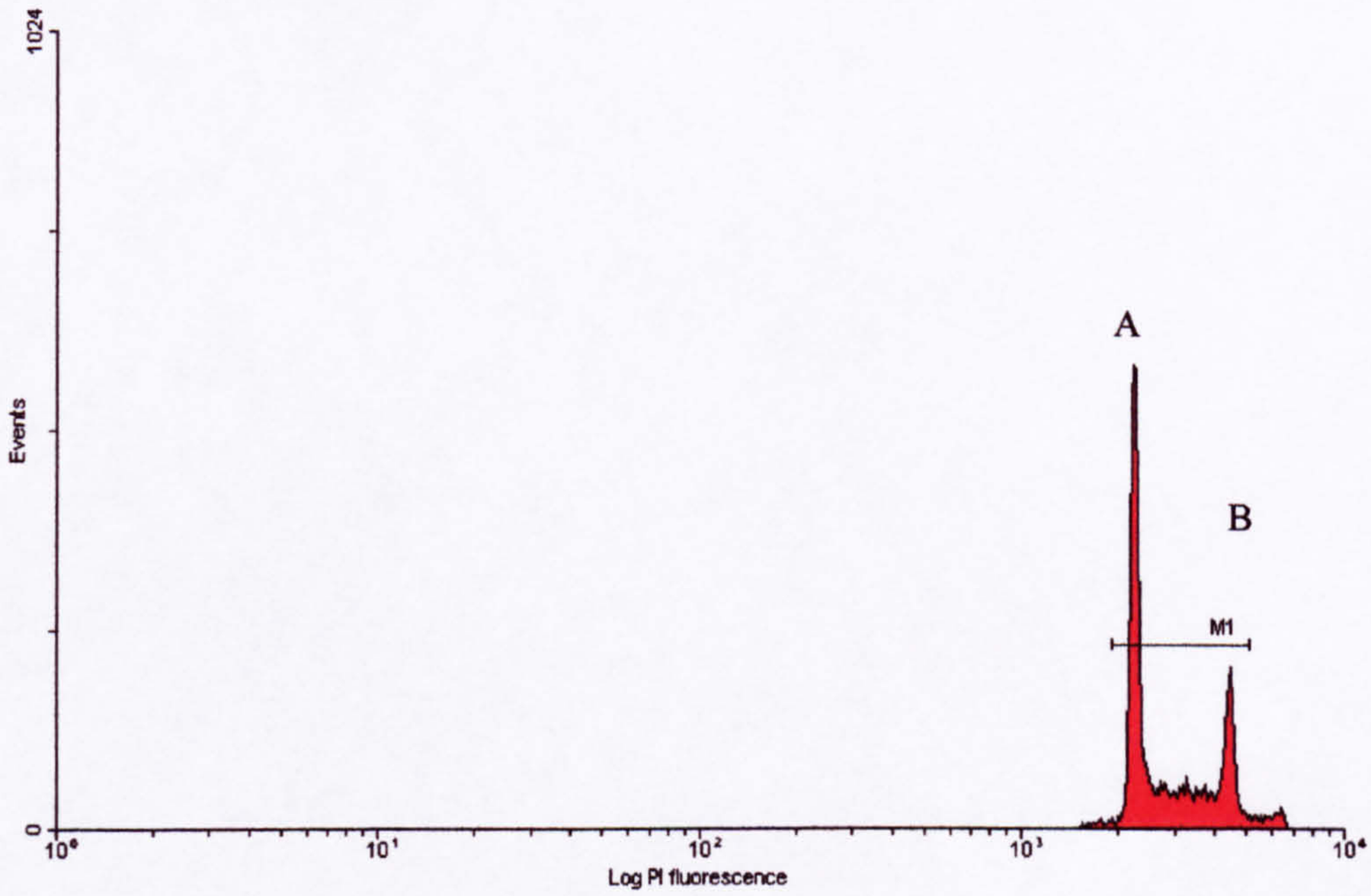

Figure 2. An example of a DNA histogram. A plot of number of nuclei versus PI fluorescence for a suspension of HeLa cell nuclei. A region, M1, is gated and used for subsequent analysis. Similar histograms were obtained for Jurkat T cell nuclei.

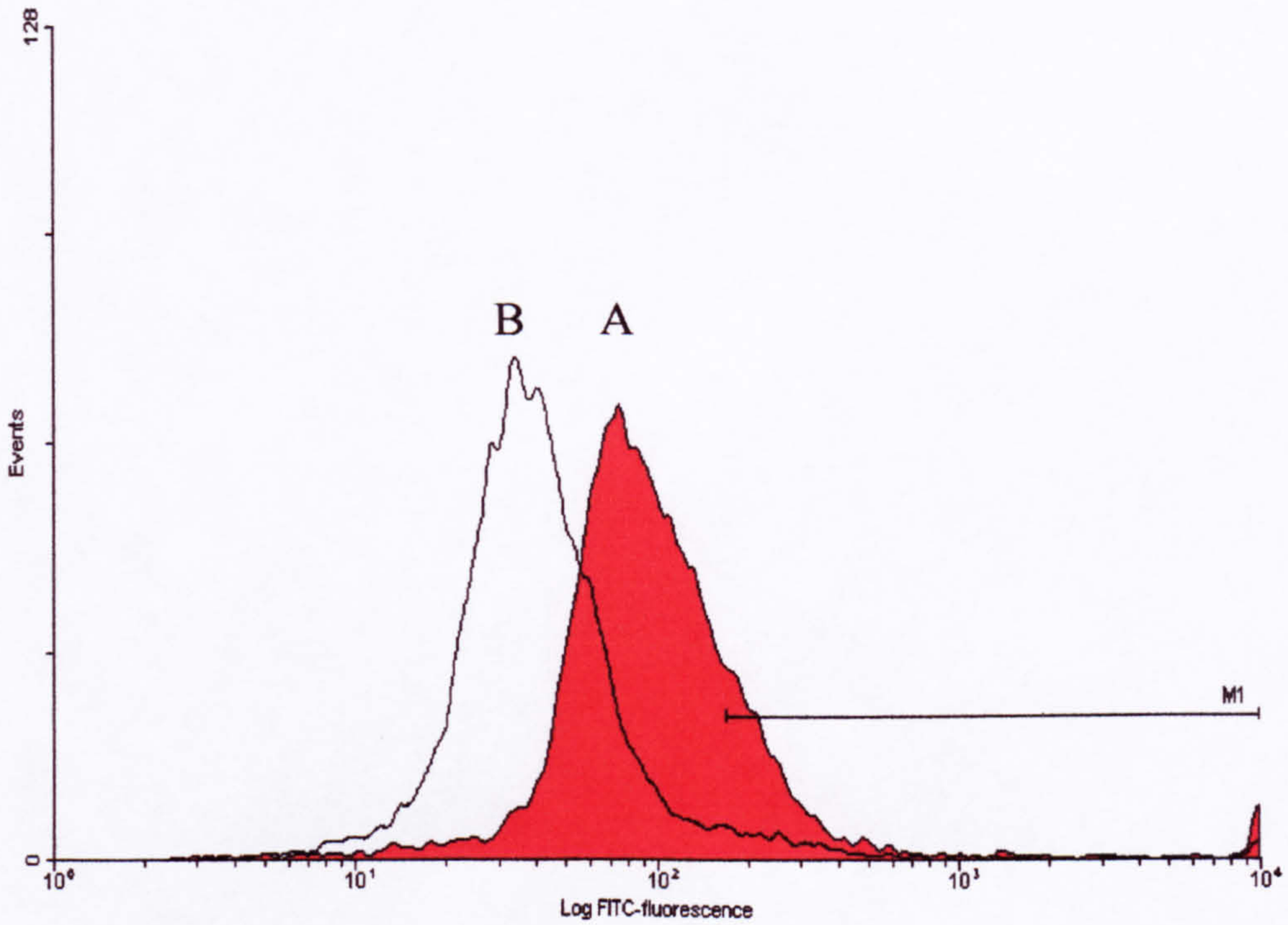

Figure 3. An example of a histogram of number of HeLa cells versus log FITC-fluorescence. Population A is stained with anti-p65 NFκB antibody (Boehringer Mannheim) and population B with isotype control antibody. The region M1 represents fluorescence intensity above the 95th centile of fluorescence intensity of the isotype control antibody-stained population. Similar histograms were obtained for whole Jurkat T cells and suspensions of nuclei of both cell types.

2.5.3 Assessment of data

Once the population of cells or nuclei to be analysed had been defined, staining of the population with anti-p65 NFκB antibody was measured by plotting a histogram of number of cells against fluorescence of the FITC label (Figure 3). The FITC-fluorescence of an identical cell population stained with isotype control antibody was overlaid on this histogram to allow derivation of the following data:

1. mean fluorescence intensity (MFI) of cells or nuclei immunostained with anti-p65 NFκB antibody (termed 'NFκB' in the Results tables);

2. MFI of cells or nuclei immunostained with isotype control antibody (termed 'isotype' in the Results tables);

3. 1 minus 2, to control for non-specific binding of antibody to nuclei or cells (termed 'NFκB - isotype' in the Results tables);

4. a ratio of 1 divided by 2, as used by others (334) as a further measure to control for non-specific factors influencing the intensity of staining (termed 'NFκB / isotype' in the Results tables);

5. MFI of the population of cells or nuclei stained with anti-p65 NFκB antibody that fluoresced with greater intensity than the fluorescence of the 95th centile of the isotype control antibody-stained population (termed 'NFκB > 95 %' in the Results tables). This analysis was chosen to determine the MFI of cells or nuclei that had 'significantly' stained with anti-p65 NFκB antibody, and

6. percentage of the population of cells or nuclei stained with anti-p65 NFκB antibody that fluoresced with greater intensity than the fluorescence of the 95th centile of the isotype control antibody-stained population (termed '% positive cells' in the Results

tables). This analysis was chosen to determine a percentage of cells or nuclei that had 'significantly' stained with anti-p65 NFκB antibody.

The data for each of the experimental protocols, manipulated in the ways described above (1-6), were assessed for biological plausibility of the results, to identify a protocol that succeeded in staining cells containing activated NFκB. Thus, the expected order of ranking of magnitude of data was:

stimulated > unstimulated > inhibited then stimulated ≥ inhibited.

4. Results

The results of each experiment are displayed below in tables.

	Cell treatment			
Type of analysis	**Unstimulated**	**Stimulated**	**Inhibited**	**Inhibited then stimulated**
NFκB	115	99	113	94
Isotype	46	44	46	42
NFκB-isotype	69	55	67	52
NFκB /isotype	2.5	2.3	2.2	2.4
NFκB > 95% isotype	148	111	107	123
% positive cells	65	84	88	80

Table 1. Results of experiment where whole *HeLa* cells were fixed in 70 % ethanol (fixation method B) and then immunostained with anti-p65 NFκB antibody (Boehringer Mannheim) and isotype control antibody (immunostaining method 3, two-layer technique). MFIs are displayed. None of the different types of analysis of the data (far left column) produced the expected order of ranking of magnitude for different cell treatments, and it was therefore concluded that the protocol had not resulted in successful staining of activated NFκB.

	Cell treatment			
Type of analysis	**Unstimulated**	**Stimulated**	**Inhibited**	**Inhibited then stimulated**
NFκB	105	109	122	67
Isotype	49	57	45	59
NFκB-isotype	56	52	77	8
NFκB /isotype	2.1	1.9	2.7	1.1
NFκB > 95% isotype	210	227	166	1088
% positive cells	44	31	63	2

Table 2. Results of experiment where whole *Jurkat T* cells were fixed in 100 % methanol (fixation method C) and then immunostained with anti-p65 NFκB antibody (Boehringer Mannheim) and isotype control antibody (immunostaining method 3, two-layer technique). MFIs are displayed. None of the different types of analysis of the data (far left column) resulted in the expected order of ranking of magnitude for different cell treatments, and it was therefore concluded that the protocol had not resulted in successful staining of activated NFκB.

	Cell treatment			
Type of analysis	**Unstimulated**	**Stimulated**	**Inhibited**	**Inhibited then stimulated**
NFκB	88	86	91	67
Isotype	36	53	62	37
NFκB-isotype	52	33	29	30
NFκB /isotype	2.4	1.6	1.5	1.8
NFκB > 95% isotype	115	150	320	148
% positive cells	59	30	10	18

Table 3. Results of experiment where whole *HeLa* cells were fixed in 100 % methanol (fixation method C) and then immunostained with anti-p65 NFκB antibody (Boehringer Mannheim) and isotype control antibody (immunostaining method 3, two-layer technique). MFIs are displayed. None of the different types of analysis of the data (far left column) resulted in the expected order of ranking of magnitude for different cell treatments, and it was therefore concluded that the protocol had not resulted in successful staining of activated NFκB.

	Cell treatment			
Type of analysis	**Unstimulated**	**Stimulated**	**Inhibited**	**Inhibited then stimulated**
NFκB	199	210	107	181
Isotype	115	143	155	131
NFκB-isotype	84	67	-48	50
NFκB /isotype	1.7	1.5	0.7	1.4
NFκB > 95% isotype	666	784	507	1388
% positive cells	19	14	1	16

Table 4. Results of experiment where whole *HeLa* cells were fixed in PFA/Triton-X (fixation method D) and then immunostained with anti-p65 NFκB antibody (Boehringer Mannheim) and isotype control antibody (immunostaining method 2). MFIs are displayed. None of the different types of analysis of the data (far left column) resulted in the expected order of ranking of magnitude for different cell treatments, and it was therefore concluded that the protocol had not resulted in successful staining of activated NFκB.

	Cell treatment			
Type of analysis	**Unstimulated**	**Stimulated**	**Inhibited**	**Inhibited then stimulated**
NFκB	33	25	31	24
Isotype	40	49	33	45
NFκB-isotype	-7	-24	-2	-21
NFκB /isotype	0.8	0.5	0.9	0.5
NFκB > 95% isotype	386	640	260	873
% positive cells	4.0	2.7	7.3	1.4

Table 5. Results of experiment where whole *Jurkat T* cells were fixed in Triton-X/PFA (fixation method E) and then immunostained with anti-p65 NFκB antibody (Boehringer Mannheim) and isotype control antibody (immunostaining method 3, two-layer technique). MFIs are displayed. None of the different types of analysis of the data (far left column) resulted in the expected order of ranking of magnitude for different cell treatments, and it was therefore concluded that the protocol had not resulted in successful staining of activated NFκB.

	Cell treatment			
Type of analysis	**Unstimulated**	**Stimulated**	**Inhibited**	**Inhibited then stimulated**
NFκB	594	612	602	611
Isotype	669	623	-57	689
NFκB-isotype	-75	-11	-57	-129
NFκB /isotype	0.9	1.0	0.9	0.8
NFκB > 95% isotype	2107	1875	2038	2189
% positive cells	4.3	4.6	3.9	2.9

Table 6. Results of experiment where whole *HeLa* cells were fixed in Ortho Permeafix (fixation method F) and then immunostained with anti-p65 NFκB antibody (Boehringer Mannheim) and isotype control antibody (immunostaining method 3, two-layer technique). MFIs are displayed. None of the different types of analysis of the data (far left column) resulted in the expected order of ranking of magnitude for different cell treatments, and it was therefore concluded that the protocol had not resulted in successful staining of activated NFκB.

	Cell treatment			
Type of analysis	**Unstimulated**	**Stimulated**	**Inhibited**	**Inhibited then stimulated**
NFκB	665	543	727	697
Isotype	640	738	619	826
NFκB-isotype	25	-195	108	-129
NFκB /isotype	1.0	0.7	1.2	0.8
NFκB > 95% isotype	4239	5088	4333	8908
% positive cells	4.6	3.2	8.5	3.0

Table 7. Results of experiment where whole *Jurkat T* cells were fixed in Ortho Permeafix (fixation method F) and then immunostained with anti-p65 NFκB antibody (Boehringer Mannheim) and isotype control antibody (immunostaining method 3, two-layer technique). MFIs are displayed. None of the different types of analysis of the data (far left column) resulted in the expected order of ranking of magnitude for different cell treatments, and it was therefore concluded that the protocol had not resulted in successful staining of activated NFκB.

	Cell treatment							
Type of analysis	**Unstimulated**		**Stimulated**		**Inhibited**		**Inhibited then stimulated**	
	A	**B**	**A**	**B**	**A**	**B**	**A**	**B**
NFκB	457	471	549	517	-	532	472	254
Isotype	208	254	213	193	-	217	158	244
NFκB-isotype	249	213	336	324	-	315	314	10
NFκB /isotype	2.2	1.9	2.6	2.7	-	2.5	3.0	1.0
NFκB > 95% isotype	564	663	745	624	-	623	508	551
% positive cells	58	57	64	80	-	78	88	5

A and B= repeated experiments ·

Table 8. Results of experiments where *HeLa* cells were fixed and enucleated in 100 % methanol (fixation method A) and then immunostained with anti-p65 NFκB antibody (Boehringer Mannheim) and isotype control antibody (immunostaining method 1, three-layer technique). MFIs are displayed. All the analyses (far left column) of the data from experiment A, except the '% positive cells' analysis, are consistent with the expected order of ranking of magnitude for different cell treatments. However, when the experiment was repeated in B, the order was no longer as expected, with the largest MFI being the 'inhibited' cell population (see section 3.2).

Type of analysis	Cell treatment															
	Unstimulated				Stimulated				Inhibited				Inhibited then stimulated			
	A	B	C	D	A	B	C	D	A	B	C	D	A	B	C	D
NFκB	322	394	584	491	513	398	459	390	470	259	585	530	446	327	509	450
Isotype	196	185	236	172	157	170	210	196	274	207	179	226	211	221	207	152
NFκB - isotype	126	209	348	319	353	228	249	194	196	52	406	304	235	108	302	298
NFκB /isotype	1.6	2.1	2.5	2.9	3.3	2.3	2.2	2.0	1.7	1.3	3.3	2.3	2.1	1.5	2.5	3.0
NFκB > 95% isotype	486	521	751	593	591	530	737	618	679	488	652	689	575	497	622	545
% positive cells	35	57	67	72	83	64	37	38	61	42	90	61	61	16	70	72

A, B, C and D = repeated experiments

Table 9. Results of experiments where *Jurkat T* cells were fixed and enucleated in 100 % methanol (fixation method A) and then immunostained with anti-p65 NFκB antibody (Boehringer Mannheim) and isotype control antibody (immunostaining method 1, three-layer technique). MFIs are displayed. The experiment was repeated four times (A, B, C and D), but none of the different types of analysis of the data (far left column) consistently resulted in the expected order of magnitude for different cell treatments, and it was therefore concluded that the protocol had not resulted in successful staining of activated NFκB.

	Cell treatment		
Type of analysis	**Unstimulated**	**Stimulated**	**Inhibited then stimulated**
NFκB	691	702	584
Isotype	208	213	158
NFκB - isotype	483	489	426
NFκB /isotype	3.3	3.3	3.7
NFκB > 95% isotype	724	731	601
% positive cells	92	94	98

Table 10. Results of experiment where *HeLa* cells were fixed and enucleated in 100 % methanol (fixation method A) and then immunostained with anti-p65 NFκB antibody (Santa Cruz) and isotype control antibody (immunostaining method 1, three-layer technique). MFIs are displayed. None of the different types of analysis of the data (far left column) resulted in the expected order of ranking of magnitude for different cell treatments, and it was therefore concluded that the protocol had not resulted in successful staining of activated NFκB.

5. Discussion

None of the experiments gave a clear, unequivocal result suggesting a successful method for measurement of activated NFκB by flow cytometry. The most promising results were those displayed in Table 8, in a repeated experiment where enucleated HeLa cells were fixed in 100 % methanol and stained with the Boehringer Mannheim antibody using a three layer technique. In the first of these experiments (Table 8, experiment A), all the analyses of the data, except the '% positive cells' analysis, are consistent with the expected order of ranking of magnitude for different cell treatments.

In this experiment, the data analysis termed 'NFκB' (Table 8, experiment A) for unstimulated and stimulated states is displayed in Figure 4 in overlaid histograms of number of cells versus FITC-fluorescence intensity. The difference between these histograms for stimulated and unstimulated nuclei is accentuated by integrating the percentage of the total population of analysed nuclei and plotting this against FITC-fluorescence intensity of anti-p65 NFκB antibody staining (Figure 5). Subtraction of the resulting two curves produces the curve in Figure 6, which may represent a method of detecting activation of NFκB within suspensions of nuclei by flow cytometry.

However, in the repeat of the experiment (Table 8, experiment B), although the findings for stimulated and unstimulated nuclei were similar to those in the first experiment (Table 8, experiment A), for all data analyses (far left column), the MFI for the 'inhibited ' nuclei is larger than for the 'stimulated' nuclei.

Furthermore, in Table 9, the same methods were employed using Jurkat T cells and although, in experiments A and B in this table, MFI of the stimulated nuclei is larger than that with other cell treatments, this is not repeated in experiments C and D. Thus considerable doubt exists as to whether this is a reliable method of measuring activation of NFκB by flow cytometry.

Finally, staining of suspensions of nuclei with the Santa Cruz anti-p65 NFκB antibody (Table 10) did not result in the expected order of ranking of magnitude for different cell treatments, and is therefore unlikely to represent successful staining of activated NFκB.

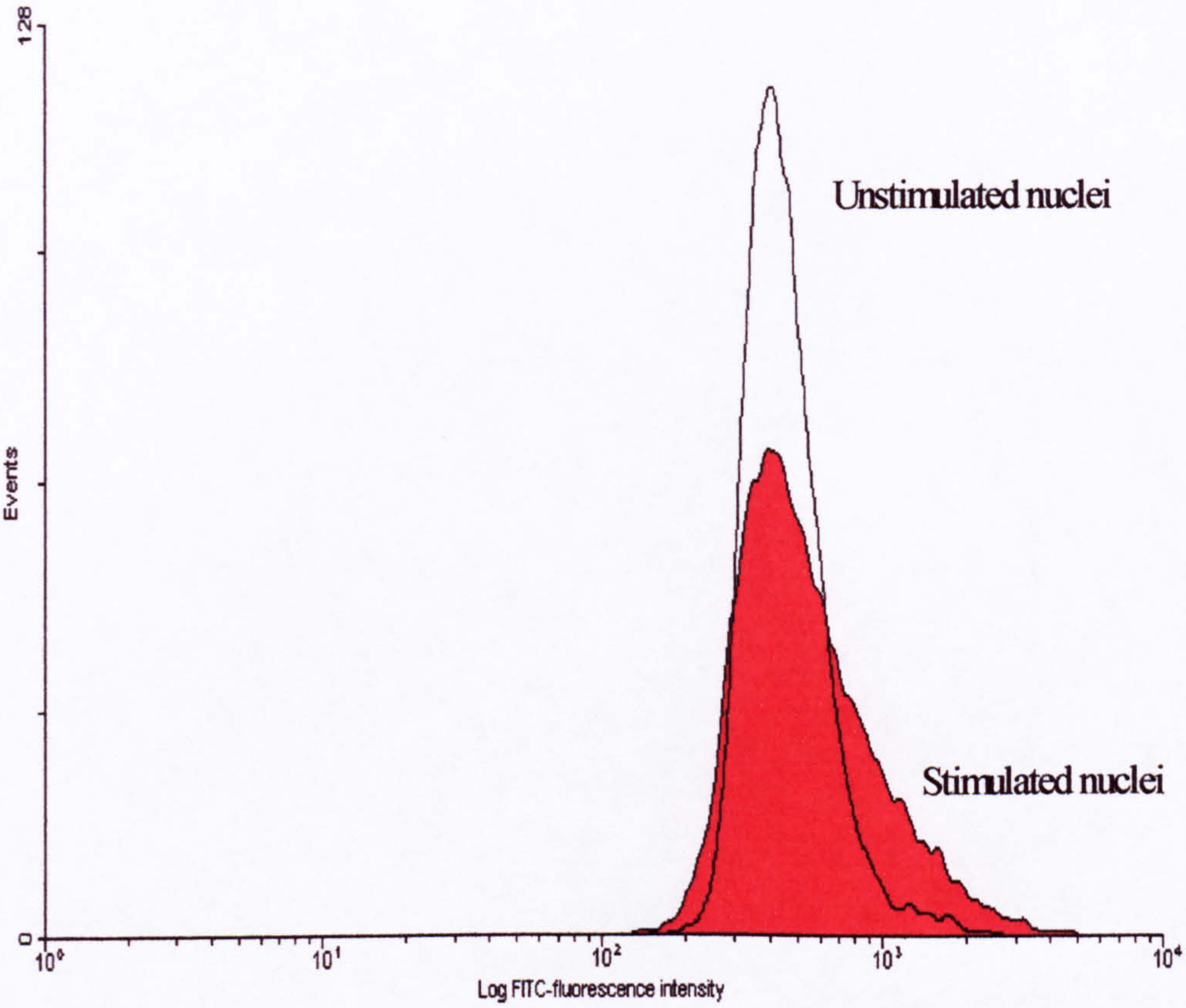

Figure 4. Overlaid histograms of number of cells versus FITC-fluorescence intensity for Boehringer Mannheim anti-p65 NFκB antibody staining of stimulated and unstimulated suspensions of nuclei from HeLa cells prepared and fixed by fixation method A and stained by immunostaining method 1.

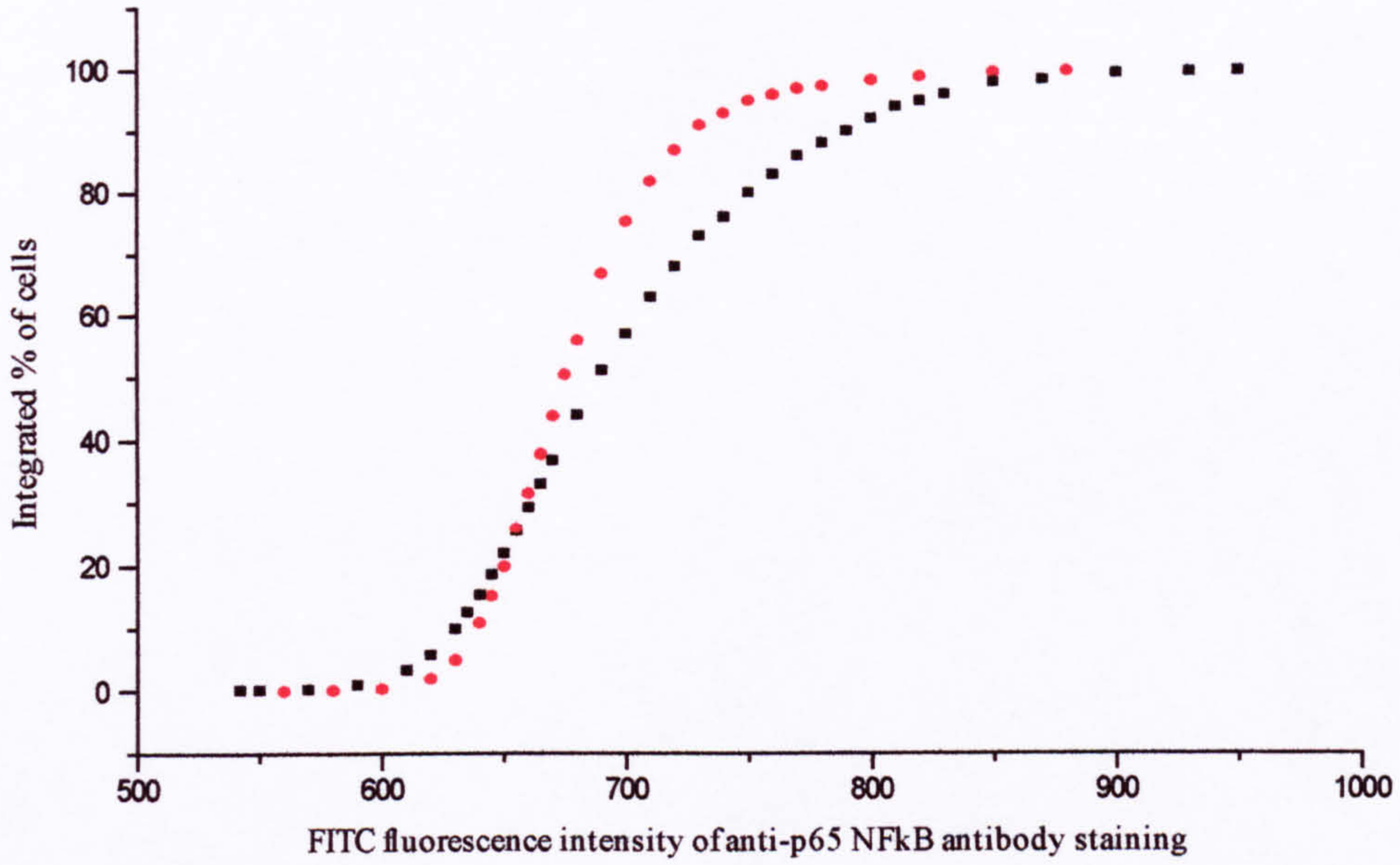

Figure 5. Graph displaying integrated percentage of the total analysed population of stimulated and unstimulated suspensions of nuclei from HeLa cells, prepared and fixed by fixation method A, and stained by immunostaining method 1, versus the FITC-fluorescence intensity of anti-p65 NFκB antibody staining. Subtraction of these curves results in the graph displayed in Figure 6.

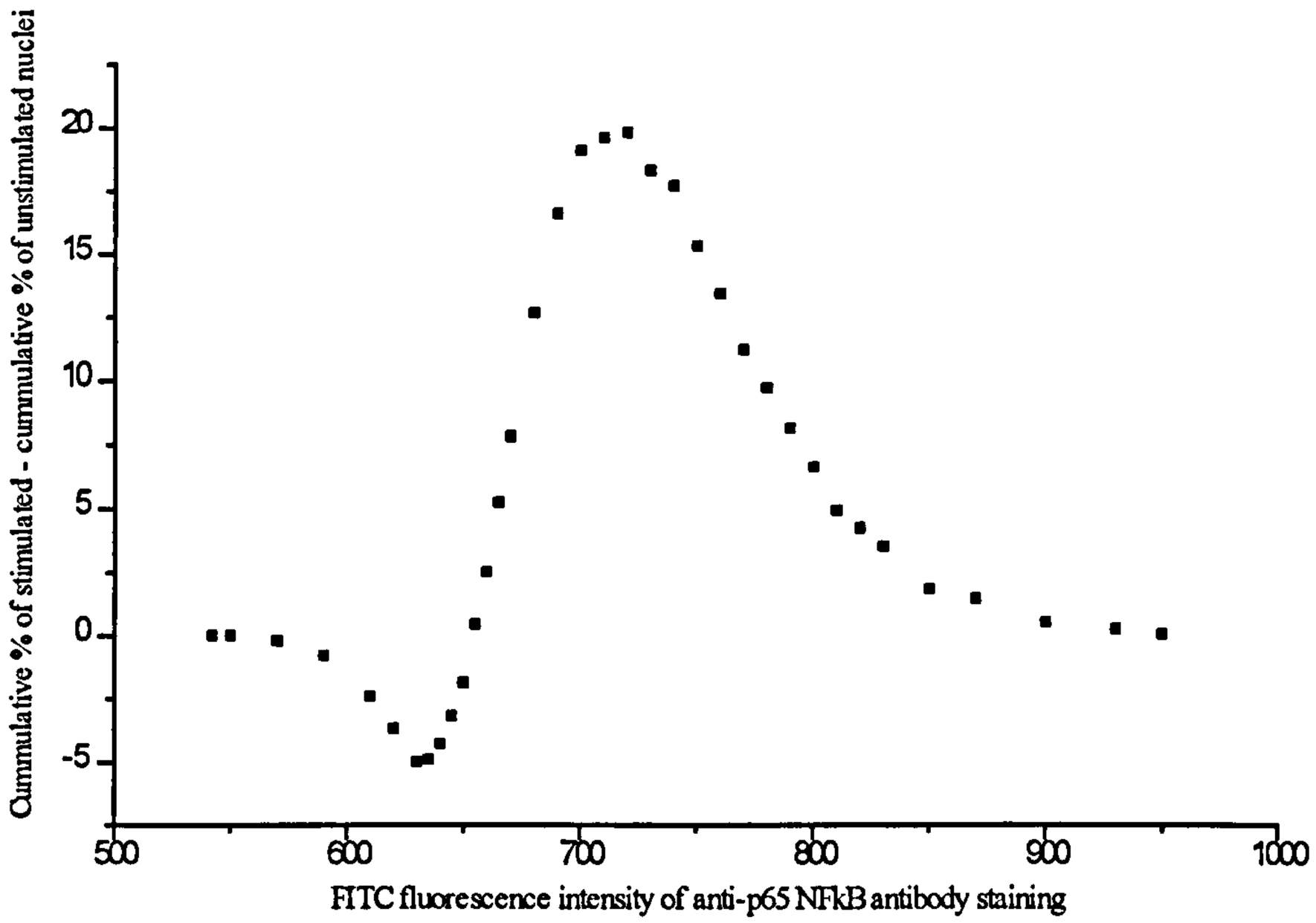

Figure 6. Graph displaying the result of subtraction of the curve for unstimulated nuclei from the curve for stimulated nuclei in Figure 5. Thus, difference in cumulative percentage of nuclei is plotted against FITC-fluorescence intensity of anti-p65 NFκB antibody staining. The curve may represent measurement of activation of NFκB (see section 4.2).

6. Conclusion

A standard range of fixation methods of suspensions of cells and nuclei, different staining protocols and two different antibodies were tested to develop a method of measuring activation of NFκB by flow cytometry. No method was conclusively successful, but the best results were obtained by enucleation of HeLa cells, followed by fixation in 100 % methanol, with immunostaining with the Boehringer Mannheim anti-p65 NFκB antibody using a triple layer technique. The technique was not sufficiently reliable to apply to the investigations outlined in the section 1.1, and further experiments are required to investigate the method further before it can be used. Nevertheless, the experiments show that it should be possible to develop such a method, and this would allow measurement of NFκB activation in subpopulations of suspensions of large numbers of cells.

Chapter 7. Discussion and future work

In Chapter 2, while developing an ISH method to study *in situ* activation of NFκB, non-specific binding of oligonucleotide probes to eosinophils in sections of bowel was demonstrated. On review of the literature, a similar effect was observed between longer (400-mer) DNA probes and eosinophils in bone marrow (285) smears, and between riboprobes and eosinophils in sections of bowel (286). However, there were no similar reports of this effect occurring during oligonucleotide ISH, including studies using it in bowel.

Non-specific binding of probes was successfully prevented by pre-treatment of sections with dithiothreitol and iodoacetamide followed by high stringency washes. Hybridisation of poly-d(T) probe to the polyriboadenosine tail on all mRNA within cells was demonstrated when low stringency post-hybridisation washes were used, but non-specific binding to eosinophils returned when low stringency washes were used, despite pre-treatment of sections with DTT and iodoacetamide. It is therefore concluded that oligonucleotide probes cannot be used to investigate gene expression in the lamina propria of bowel, unless other blocking manoeuvres are developed, as non-specific binding of probe to eosinophils appears identical to the appearances of probe genuinely hybridised to target mRNA. Furthermore, this phenomenon occurred in sections of nasal polyp that are rich in eosinophils, and therefore probably occurs in other eosinophil-containing tissues, such as lung.

In addition, there was greater non-specific binding of the *antisense* probe cocktail for IκBα to eosinophils than of an equivalent concentration of a single *sense* probe.

Experiments with *individual* IκBα probes confirmed significantly less non-specific binding of sense than all antisense probes to eosinophils. This effect, of differential binding of different oligonucleotide probes, may explain why non-specific binding to eosinophils has not been reported in previous publications using oligonucleotide ISH in bowel, as it was presumably mistaken for genuine hybridisation to target mRNA.

In Chapter 3, the mechanism of non-specific binding of oligonucleotide probes to eosinophils was explored. Using biomolecular interaction analysis with a BiacoreX™ instrument, a method was established for measuring the *in vitro* interaction between probes and eosinophilic cationic protein, which was hypothesised to be the agent within eosinophils binding oligonucleotide probes, or control proteins. Binding of all oligonucleotide probes to ECP, but not to the control proteins, myoglobin and lysozyme, was demonstrated. The absence of binding to lysozyme, which has a similar pI to ECP, suggests that binding to ECP is unlikely to be a charge-related effect due to its unusually high pI. The reason that ECP binds oligonucleotide probes is unclear, but it possesses ribonuclease activity (283) and may therefore contain a binding site(s) for nucleic acids.

The dissociation constant at equilibrium indicates the affinity of an interaction and values obtained for the interaction between probes and ECP were of the order of 10^{-6} M, indicating moderate affinity, although the interaction is likely to be of high capacity because of the abundance of ECP.

In vitro binding of antisense and sense oligonucleotide probes for IκBα mRNA were compared using four parameters, namely magnitude of total binding, association rate constant (k_a), dissociation rate constant (k_d) and dissociation constant at equilibrium

(K_D). Significant differences between values for sense and antisense oligonucleotides were found for magnitude of binding and k_d, with the differences in both parameters consistent with more binding of sense than antisense oligonucleotides, the converse of the *in situ* observations. Thus, these *in vitro* differences do not alone explain the observation of less non-specific binding of sense than antisense oligonucleotide probes to eosinophils during ISH. It is possible that an undetected, real difference in k_a and K_D, which might explain the differential *in situ* binding, may have been missed due to a type II statistical error. However, it is probable that the property of the *in vitro* probe-ECP interaction that is most relevant to the *in situ* binding of probes to eosinophils *is* the dissociation constant, k_d, as although equilibrium between association and dissociation will probably be reached during overnight incubation of the sections of bowel with the hybridisation solution containing the probes, during subsequent washes, which determine the amount of probe left on the sections, only dissociation of probes from eosinophils into the wash solution will occur, with virtually no association.

Therefore, another factor must be the major determinant of the observed differential *in situ* binding of oligonucleotide probes, and this was hypothesised to be differential tissue penetration of probes, determined by their physical characteristics, particularly hydrophobicity. In Chapter 4, reverse-phase ion-pair liquid chromatography was used to measure hydrophobicity of oligonucleotide probes, when the antisense probes for IκBα mRNA were found to be significantly more hydrophobic than the sense probe. Hydrophobic probes will penetrate tissue sections more easily, and so the findings for oligonucleotide probe hydrophobicity are consistent with the observed greater *in situ* non-specific binding to eosinophils by antisense than by sense probes, and suggests

the amount of individual probe binding non-specifically to eosinophils *in situ* is determined predominantly by probe hydrophobicity, which limits tissue penetration and so limits the amount of probe available to bind to ECP in eosinophils.

In early experiments, oligonucleotide probe bound non-specifically to eosinophils was retained after washes that removed poly-d(T) probe hybridised to the polyriboadenosine tail on all mRNA, which suggests that hybridisation of poly-d(T) probe to the polyriboadenosine tail on all mRNA is weaker than the interaction between oligonucleotide probes and ECP. As stated above, the amount of probe bound to ECP within eosinophils was determined predominantly by probe hydrophobicity, and it is likely that hybridisation of oligonucleotide probes to mRNA is affected by probe hydrophobicity to a similar or, more likely (because the interaction is weaker), a greater degree. There has been no previous investigation of this effect, which may be vitally important in establishing the validity of sense negative controls, which are widely used and rely on differential binding to target mRNA between sense and antisense probes.

Hence, it may be important to match hydrophobicity of sense and antisense probes when choosing gene sequences for design of oligonucleotide probes. This effect is less likely to be important for longer probes, such as riboprobes or long cDNA probes, because long antisense and sense probes are statistically more likely to possess similar hydrophobicities.

Previous studies using IP-RP-HPLC to determine the contribution of individual bases to the total hydrophobicity of oligonucleotides have established the order of hydrophobicity of individual bases as C < G < A < T for the bulk of the

oligonucleotide, and C < G < T < A for the 3' terminal base (310). Approximate matching of probe hydrophobicity may be achieved without resorting to measurement by IP-RP-HPLC by calculating a proposed 'hydrophobicity score', where one point is allocated for an A at the 3' terminal and one point for each T in the rest of the oligonucleotide. In the present study, there was a strong correlation (r = 0.97 by Pearson's method of correlation, see Figure) between the measured hydrophobicity of the four probes and their respective calculated hydrophobicity scores.

Figure. Measured hydrophobicity (retention time in RP-IP HPLC columns in minutes) versus calculated hydrophobicity score of the four oligonucleotide probes for IκBα. Correlation coefficient (r) calculated by Pearson's method.

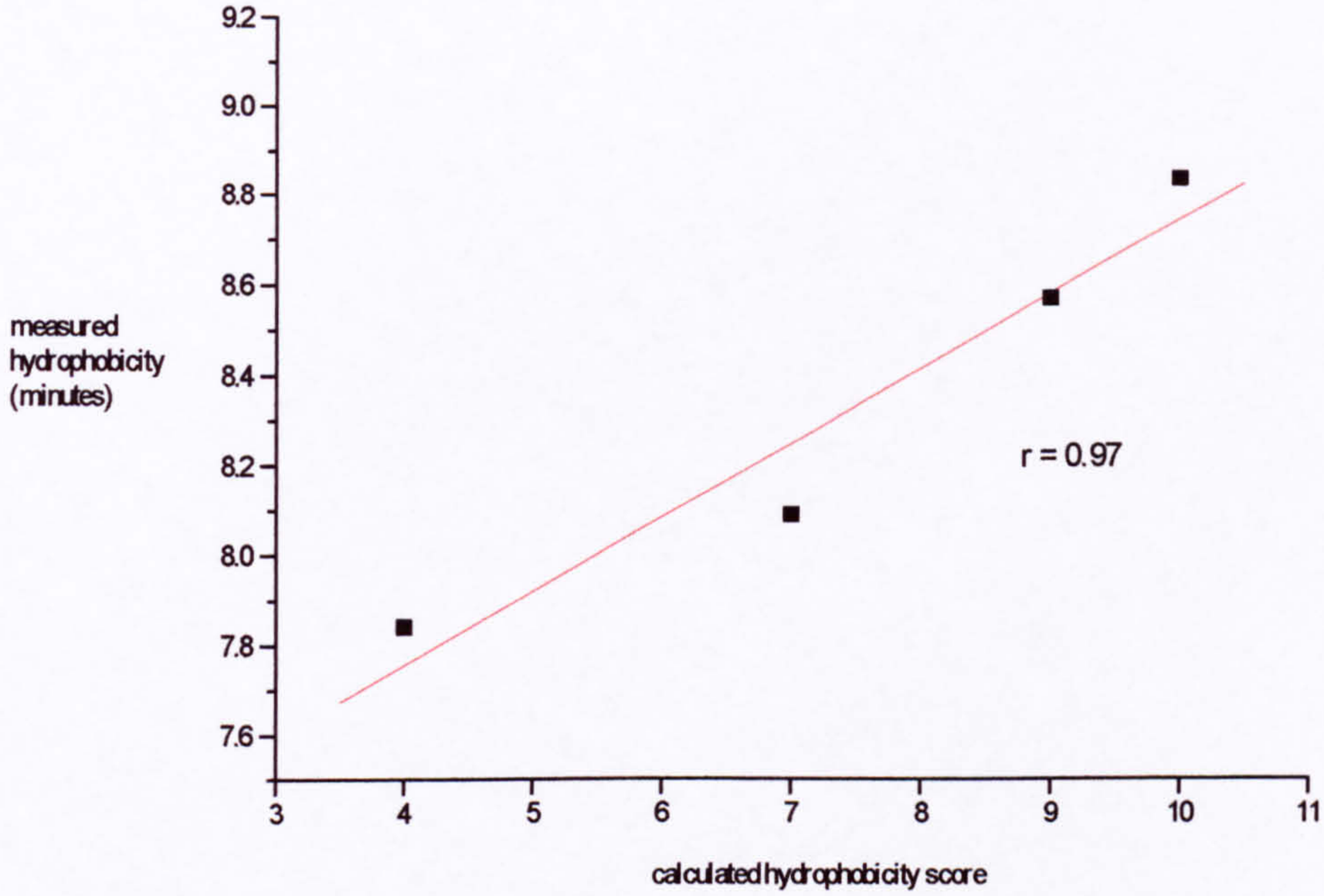

As stated above, IκBα antisense probes were more hydrophobic than the sense probe, and therefore penetrated sections better and bound in greater quantities to eosinophils than the sense probe. Was it by chance that the sequence chosen for the IκBα mRNA sense probe was less hydrophobic than the antisense probes? This question is important, because the use of sense probes in ISH is based on the premise that the chosen sequence renders them statistically unlikely to hybridise to mRNA within cells. Thus, if, as proposed above, matching of hydrophobicity *is* important for parity in tissue penetration and subsequent opportunity to *hybridise* to target mRNA, or not hybridise in the case of sense probes, then a systematic bias in the sequences chosen for antisense vs sense probes that resulted in greater hydrophobicity of antisense than

sense probes would be of enormous significance, as it would bias the opportunity for hybridisation towards antisense probes.

To help determine whether a systematic bias exists, hydrophobicity scores from the published sequences chosen for oligonucleotide antisense and sense probes in previous studies using oligonucleotide ISH were therefore calculated (Appendix V). In these studies, the mean (SD) calculated hydrophibicity score for antisense probes (9.1 (3.0)) was significantly greater ($p = 0.047$, compared using a paired t-test) than the mean for sense probes (6.4 (2.9)).

Calculated hydrophobicity scores are predominantly dependent on the number of thymidine bases within the probe and, based on the calculated hydrophobicity scores of probes used in the literature, a systematic bias for selection of thymidine bases in antisense probes may exist. Potential explanations for this bias include:

- a systematic bias in the method of selection of oligonucleotide probe antisense sequences towards choice of thymidine bases, thus concomitantly biasing towards fewer thymidine bases in the mirror-image sense probes. The principles and method of sequence selection are described in Chapter 2, section 2.4.1. No potential explanation for a systematic bias in this process could be suggested by an expert in the method (Dr. Steve Jones, Retinitis Pigmentosa Laboratory, The Rayne Institute, St. Thomas' Hospital), and

- a relative excess of thymidine bases in the human genome. Relative nucleotide content of genomes varies between species, but in humans is approximately 30 %

A, 30% T, 20 % G and 20 % C. The relative nucleotide content of DNA in the genome of human liver, sperm and thymus is displayed in Appendix 6. Antisense oligonucleotide probes, which hybridise in ISH experiments to target mRNA, are of identical sequence to DNA coding for mRNA, and will therefore contain a mean of 30 % thymidine bases. However, because there is also an equal percentage of adenosine bases in DNA (and antisense probes), which are transcribed to thymidine bases in sense probes, the percentage of thymidine bases in sense probes will be similar to that in antisense probes. Therefore, the mean base constitution of the human genome will not result in a systematic bias in the hydrophobicity of probes.

Thus, the explanation for the apparent difference in mean hydrophobicities of antisense and sense probes remains unclear. It may be that the difference in hydrophobicities of antisense and sense probes in this thesis occurred by chance, and that the difference observed in the published literature is due to a type I sampling error of the literature.

Thus, attempts to develop an ISH method to detect activation of NFκB in sections of bowel were unsuccessful, but lead to important observations on the technique of oligonucleotide ISH.

Whilst performing this work, an antibody that is specific for the activated form of NFκB became commercially available and, in Chapter 5, this antibody was used to demonstrate a greater tissue-density of cells expressing activated NFκB in all layers of inflamed bowel from patients with CD compared to normal bowel from controls. Activation was restricted mainly to large mononuclear cells, morphologically

suggestive of macrophages, suggesting that these are a major cell involved in propagating inflammation in CD. Interestingly, a greater tissue-density of cells expressing activated NFκB was found in the submucosa, but not in the lamina propria or muscle layers, of macroscopically and microscopically non-inflamed CD bowel compared to normal bowel from controls, which suggests that the apparently non-inflamed bowel in CD may be more immunologically active than completely normal bowel from controls, consistent with other studies that have demonstrated subtle abnormalities in these areas. Such changes in non-inflamed areas in CD may predate overt inflammation and further study of these areas, rather than those that are already inflamed and possess a compromised mucosal barrier, may reveal more about the early events that generate inflammation in CD.

In Chapter 6, a method to study the activation of NFκB with flow cytometry was proposed and investigated. A range of methods were tested, but only a method using enucleation of cells and subsequent fixation in 100 % methanol, followed by immunostaining with a three-layer technique, produced promising results. Unfortunately, results were not reliably reproduced in the time available for this project, and further work is required before this method can be utilised. Such a method would be a powerful tool that could be applied to many experiments. For instance, activation of NFκB in large numbers of cultured cells could be rapidly quantitated, and while this can already be assessed by existing methods such as EMSA, activation in subsets of cells, for instance subsets of isolated LPMNCs and PBMNCs, could also be quantitated. Such information might provide important insights into activation of subsets of cells of the immune system in IBD.

Future work

1. To develop additional manoeuvres that more effectively block binding of oligonucleotide probes to eosinophils during ISH. These manoeuvres could be developed *in vitro* using biomolecular interaction analysis with ECP and oligonucleotide probes, and then applied to ISH.

2. To investigate further the relationship between oligonucleotide probe hydrophobicity, tissue penetration and non-specific binding to eosinophils in sections of bowel with further experiments using new oligonucleotide probes of different base composition.

3. To confirm the hypothesis that probe hydrophobicity is relevant to *hybridisation* of oligonucleotide probes to target mRNA, by performing ISH experiments using a range of different oligonucleotide probes, with differing base sequences, for the same target mRNA (using non-eosinophil-containing tissue, such as brain, as the problem of successful hybridisation without concomitant non-specific binding to eosinophils in sections of bowel is, as yet, unsolved).

4. To confirm increased activation of NFκB in the submucosa of macroscopically and microscopically non-inflamed specimens of resected bowel from a larger group of patients. If the possibility of a type II sampling error could be more definitely excluded, then this important finding would concentrate future work on the submucosa of non-inflamed areas as the site of early changes in CD. Furthermore,

it would be interesting to correlate the activation of NFκB with other previously documented subtle changes in these areas, such as neural changes (324,325), and to investigate the activation of other early response genes such as c-fos and c-jun.

5. To perform immunohistochemical co-staining to confirm the identity of the cell type(s) expressing activated NFκB in CD.

6. To develop further the initial promising results using flow cytometry to measure activation of NFκB, and to apply this technique to measure and quantitate activation of NFκB in isolated lamina propria mononuclear cells from patients with inflammatory bowel disease and controls, and to identify sub-populations of cells containing activated NFκB. Furthermore, this method could be used to measure activation of NFκB in cultured cells stimulated with solutions of inorganic sub-micron particles with bioactive bacterial products adsorbed onto their surface, thus linking with work within The Gastrointestinal Laboratory examining the potency, and mechanism of action, of these particles in inducing inflammatory responses, and their possible role in the aetiology of Crohn's disease (337,338).

Appendix I

Establishment of conditions for regeneration of dextran-ligand surfaces in the Biocore X™ chip

Ideal regeneration of the dextran-ligand surfaces of the chips in the Biocore X™ in Chapter 3 results in reproducible bindings of analyte to the ligands (ECP and control proteins). For this to be achieved, the sensorgram should return after each regeneration injection to the level prior to binding of analyte, resulting in a small change in the baseline sensorgram, and suggesting complete removal of the analyte from the dextran-ligand surface without stripping of any ligand from the dextran. In addition, there should be reproducible magnitudes of binding of the probe analytes. The results in the Table and Figure represent a step-wise evolution of the constitution of the regeneration injection, where the constitution of the next injection to be tested was chosen after assessing the results obtained from the previous injection.

Table. Establishing regeneration conditions. Effect of injection of different volumes of regeneration solutions A to C on the magnitude of binding, in RU, of oligonucleotide 1 to ECP and myoglobin in chip A, and on regeneration of the dextran-ligand surface in each cell of the chip. Magnitude of binding is calculated as the change of the sensorgram, in RU, from before injection of probe to 80 seconds after injection (columns 2 and 4). Regeneration is assessed by change in the baseline sensorgram from before injection to after regeneration (columns 3 and 5). The aim is to establish reproducible magnitudes of binding with little change in the baseline sensorgram. The results represent a step-wise evolution of the constitution of the regeneration injection, where the constitution of the next regeneration injection (see section 3.5, Chapter 3 for constitution of solutions A, B and C) to be tested was chosen after assessing the results obtained from the previous regeneration injection. Injections 12-20 are repeated injections of the same volume of the same regeneration solution to verify its reproducibility. Conclusions drawn from these data are discussed below, and the same data are displayed in graphs in the Figure, to allow easy identification of trends.

Regeneration injection (volume of regeneration solution)	Magnitude of binding of probe to ECP (RU) following different regeneration injections	Change in baseline ECP sensorgram from before injection of probe to after regeneration (RU)	Magnitude of binding of probe to myoglobin (RU) following different regeneration injections	Change in baseline myoglobin sensorgram from before injection of probe to after regeneration (RU)
injection 1 (10 µl A)	92.7	-149.1	1.7	-68.3
injection 2 (5 µl A)	115.0	-35.4	-0.4	0.7
injection 3 (1 µl A)	106.3	-13.3	-3.2	-4.3
injection 4 (1 µl B)	94.8	19.0	-1.2	-3.2
injection 5 (5 µl B)	76.8	-21.1	-0.5	3.9
injection 6 (5 µl B)	87.6	0.3	-1.6	-2.2
injection 7 (4 µl B)	80.6	6.2	-0.3	1.0
injection 8 (5 µl B)	64.3	-10.4	0.5	7.5
injection 9 (10 µl C)	23.8	-10.0	-1.9	-20.0
injection 10 (2 µl C)	19.1	-9.7	0.1	-12.3
injection 11 (1 µl C)	24.2	3.3	-1.2	-10.6
injection 12 (2 µl C)	21.9	-4.6	1.4	-9.3
injection 13 (2 µl C)	17.9	-4.2	-1.8	-6.8
injection 14 (2 µl C)	19.4	0.3	0.8	0.2
injection 15 (2 µl C)	17.5	-0.5	-1.4	-5.1
injection 16 (2 µl C)	20.0	1.7	-1.2	-2.5
injection 17 (2 µl C)	20.0	4.7	-2.4	-2.0
injection 18 (2 µl C)	18.4	-3.0	0.8	-6.3
injection 19 (2 µl C)	17.5	2.8	0.3	-1.8
injection 20 (2 µl C)	16.4	3.9	2.3	3.0

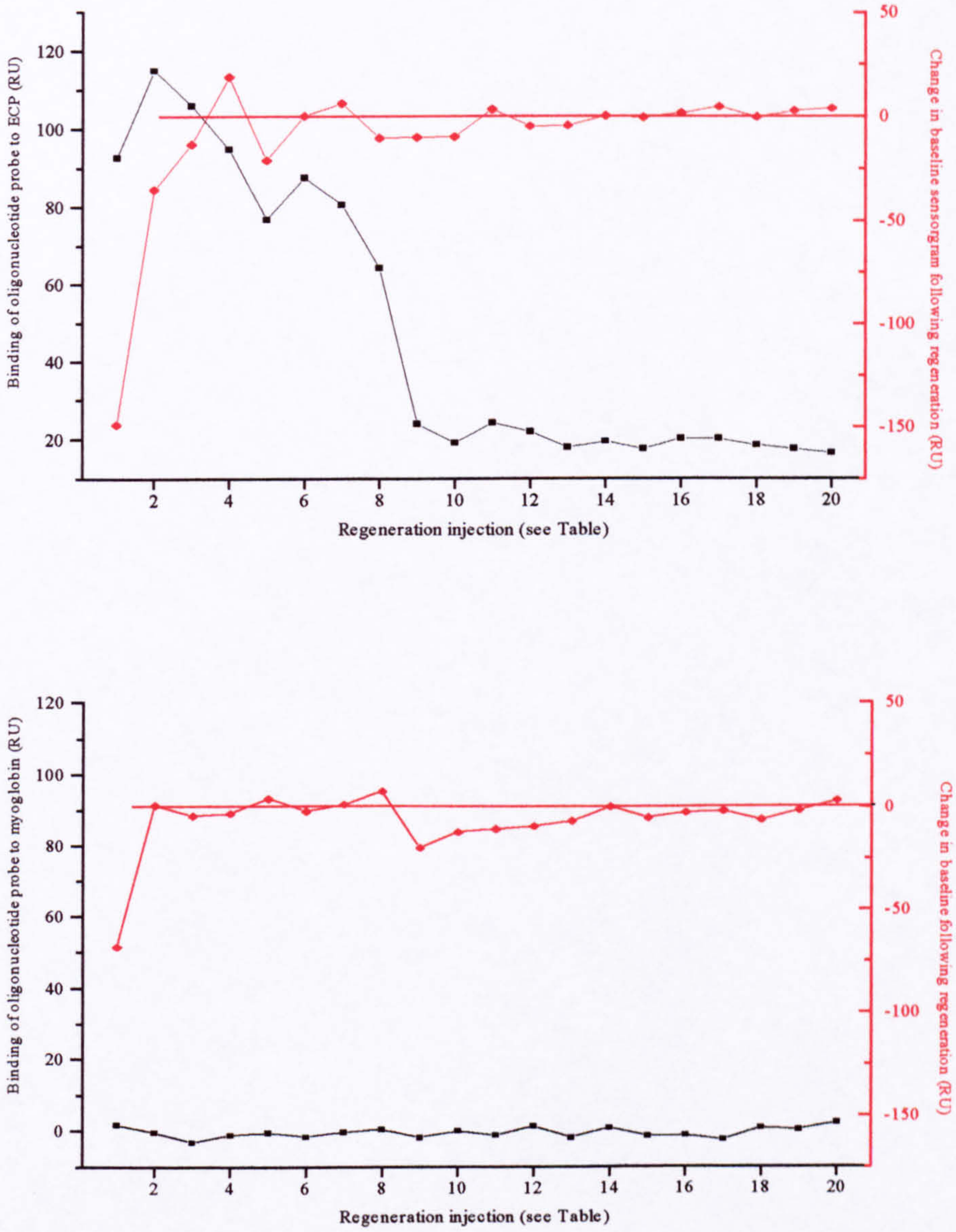

Figure. Establishing regeneration conditions. Effect of different volumes of regeneration solutions A to C (regeneration injections 1-20, see Table) on the magnitude of binding (displayed in black in RU) of oligonucleotide 1 to ECP (above) and myoglobin (below), and on regeneration of the dextran-ligand surface, as assessed by change in the sensorgram from before injection of probe to after regeneration (displayed in red in RU). The data plotted in these graphs are also displayed in the Table: the graphs allow easy identification of trends, particularly the approximately exponential decay in magnitude of binding of probe to ECP with successive bindings, at least until regeneration solution C is used (starting at regeneration injection 9), while the numerical data in the Table explain conclusions drawn below. Regeneration injections 12-20 are repeated injections of the same volume of the same regeneration solution to verify its properties.

The findings in the Table and Figure suggest the following conclusions about the regeneration injections:

- there was an approximately exponential decay in magnitude of binding of probe to ECP (regeneration injections 1-8), at least until regeneration solution C was used (regeneration injections 9-20);

- the smallest injectable quantity (1 μl) of solution A (regeneration injection 3) caused a fall in baseline ECP sensorgram from before injection of probe to after regeneration, suggesting stringent removal of probe bound to ECP in the previous cycle and possibly removal of ECP from dextran, but despite this apparently stringent regeneration, there was still a reduction in magnitude of subsequent probe binding to ECP;

- 5 μl of solution B (regeneration injection 8) caused a fall in baseline ECP sensorgram from before injection of probe to after regeneration, but 4 μl (regeneration injection 7) caused a rise in baseline, suggesting inadequate regeneration of the dextran-ECP surface;

- 10 μl of solution C (regeneration injection 9) caused a fall in baseline ECP sensorgram from before injection of probe to after regeneration, suggesting stringent removal of probe bound to ECP in the previous cycle and possibly removal of ECP from dextran, but despite this apparently stringent regeneration, there was still a reduction in magnitude of subsequent probe binding to ECP, and

- 2 μl of solution C (regeneration injections 12-20) produced reproducible oligonucleotide binding to ECP and little change in the baseline sensorgram (mean

binding to ECP 18.8 RU, SD 1.7; mean change in baseline ECP sensorgram from before injection of probe to after regeneration 0.4 RU, SD 3.3). Furthermore, the magnitude of 'binding' to the control protein, myoglobin, varied little, and there were also only small changes in the baseline sensorgram (mean 'binding' to myoglobin -0.1 RU, SD 1.6; mean change in baseline myoglobin sensorgram from before injection of probe to after regeneration -3.4 RU, SD 3.8).

It was hypothesised that the decay in the magnitude of oligonucleotide probe binding to ECP with each successive binding indicated that either some probe was left bound to ECP after each regeneration injection, or that ECP poorly bound to the dextran matrix was shed during initial injections, or a combination of the two.

Alternatively, the decay in the magnitude of oligonucleotide probe binding to ECP with successive binding might have been caused by a constituent of the running buffer. To exclude the possibility that EDTA in the running buffer, HBS, was stripping Zn^{2+} from ECP and so altering its affinity for the probe, two experiments to replenish the putatively chelated Zn^{2+} were performed:

- a 10 µl bolus of 10 µM zinc chloride (BDH) was injected, followed by a change in the running buffer to HBS without EDTA, and

- similarly, the running buffer was changed to HBS without EDTA but containing additional 10 µM $ZnCl_2$.

Neither experiment had an effect on the underlying decay in magnitude of successive bindings of oligonucleotide probe to ECP, which suggested that EDTA within the running buffer was not stripping Zn^{2+} from ECP to cause this decay.

No matter the cause, the decay in magnitude of oligonucleotide probe binding to ECP was exponential and a sufficiently flat portion of the curve could be used to compare bindings of different probes, particularly if the four probes were bound in succession, i.e. antisense 1, antisense 2, antisense 3 and then sense, and then repeated in cycles in different order.

Thus, 2 μl of solution C was chosen as the regeneration injection and HBS was used as the running buffer.

Appendix II

Protocol for staining of frozen sections with haematoxylin and eosin

1. Stain sections by immersion in a bath of Mayer's haematoxylin (Sigma Chemical Company) for five minutes.
2. 'Blue' sections by immersion in a bath of tap water for 2 minutes.
3. Stain sections by immersion, for two minutes, in a bath of a 1 % (w/v) solution of eosin (Sigma Chemical Company) in a 95 % (v/v) solution of alcohol (BDH) in distilled water.
4. Dehydrate sections by immersion, for two minutes, in successive baths of solutions of 95 % (v/v) alcohol in distilled water, twice, and then absolute alcohol, twice.
5. Finally, immerse sections in baths of xylene (BDH) for two minutes, twice, and air dry sections for fifteen minutes.

Apply a single drop of Ralmount (Sigma Chemical Company), cover with a coverslip (Sigma Chemical Company) and leave overnight.

Appendix III

Quantitation of immunohistochemical staining for activated NFκB

Table I. Number of hits counted per mm^2 using a Lennox graticule on sections of *inflamed* bowel immunostained for activated NFκB (+ve) and the negative control with PBS substituted for the primary antibody (-ve). In patients with CD, the differences between these counts (Δ) are displayed in a scattergram in Figure 9, Chapter 5.

Patient	Diagnosis	Inflammatory score#	Number of positive cells per mm^2 of tissue								
			lamina propria			submucosa			muscle		
			+ve	-ve	Δ	+ve	-ve	Δ	+ve	-ve	Δ
1	CD	10	132	7	125	53	7	46	46	0	46
2	CD	10	0	5	0*	0	0	0	349	9	340
3	CD	2	29	3	26	15	10	5	31	0	31
4	CD	9	263	11	252	60	5	55	35	0	35
5	CD	5	68	0	68	158	0	158	96	0	96
6	CD	9	128	8	120	174	15	159	103	2	101
7	CD	4	147	10	137	31	12	19	51	0	51
8	CD	3	41	2	39	0	0	0	26	2	24
9	CD	9	102	2	100	82	5	77	84	0	84
10	CD	8	114	5	109	91	3	88	87	2	85
11	CD	10	208	6	202	60	31	29	6	8	0*
12	CD	2	39	2	37	73	0	73	53	0	53
13	CD	8	333	0	333	-	-	-	285	0	285
14	UC	-	82	12	70	69	14	55	5	0	5
15	UC	-	50	8	42	-	-	-	15	2	13
16	Wegener's	-	220	35	185	-	-	-	-	-	-
17	Diverticulitis	-	106	13	93	-	-	-	83	9	74

*where the count on the control (-ve) section was greater than the count on the section stained with the primary antibody (+ve), a value of 0 was allocated for the difference between them (Δ).

#inflammatory score of the inflamed specimens. Non-inflamed specimens were obtained from patients 1, 2, 4, 6 and 12, and had inflammatory scores of 0.

Table II. Number of hits counted per mm^2 using a Lennox graticule on sections of *non-inflamed* bowel immunostained for activated NFκB (+ve) and the negative control with PBS substituted for the primary antibody (-ve). The differences between these counts (Δ) are displayed in a scattergram in Figure 9, Chapter 5.

patient	diagnosis	Number of positive cells per mm^3 of tissue								
		lamina propria			submucosa			muscle		
		+ve	-ve	Δ	+ve	-ve	Δ	+ve	-ve	Δ
1	CD	53	6	47	29	0	29	8	0	8
2	CD	108	5	103	175	25	150	-	-	-
4	CD	90	8	82	27	0	27	0	0	0
6	CD	37	12	25	63	0	63	29	0	29
10	CD	8	3	5	43	3	40	26	0	26

Table III. Number of hits counted per mm^2 using a Lennox graticule on sections of bowel from control patients immunostained for activated NFκB (+ve) and the negative control with PBS substituted for the primary antibody (-ve). The differences between these counts (Δ) are displayed in a scattergram in Figure 9, Chapter 5.

control patient	diagnosis	Number of positive cells per mm^3 of tissue								
		lamina propria			submucosa			muscle		
		+ve	-ve	Δ	+ve	-ve	Δ	+ve	-ve	Δ
1	carcinoma	85	0	85	6	8	0*	21	0	21
2	carcinoma	15	9	6	7	12	0*	0	0	0
3	carcinoma	29	11	18	29	0	29	3	0	3
4	carcinoma	52	4	48	32	3	29	3	0	3
5	carcinoma	53	0	53	3	0	3	53	0	53
6	carcinoma	32	16	16	11	16	0*	8	0	8
7	carcinoma	53	0	53	32	3	29	0	0	0
8	carcinoma	5	0	5	2	0	2	0	0	0
9	carcinoma	33	4	29	12	2	10	5	1	4
10	carcinoma	5	0	5	0	0	0	0	0	0
11	carcinoma	9	6	3	8	3	5	3	0	3

*where the count on the control (-ve) was greater than the count with the primary antibody (+ve), a value of 0 was allocated for the difference between them (Δ).

Appendix IV

Reproducibility of counts of immunohistochemical staining

Table. Assessment of reproducibility of counts of cells immunostaining positive for activated NFκB.

	first count (cells mm)^2	**second count (cells mm)^2**	**difference between counts**	**difference as % of mean count**
patient 1 lamina propria	116	126	10	8.3
patient 1 submucosa	50	48	2	4.1
patient 1 muscle	48	52	4	8
patient 5 lamina propria	85	77	7	8.6
patient 5 submucosa	154	143	11	7.4
patient 5 muscle	93	98	5	5.2
patient 6 lamina propria	128	122	6	4.8
patient 6 submucosa	151	162	11	7.0
patient 6 muscle	106	99	7	6.8
			mean	6.7
			standard deviation	1.6

Appendix V

Calculated hydrophobicity scores for oligonucleotide probes

Table. Hydrophobicity scores calculated from sequences for oligonucleotide antisense and sense probes used in previous publications. Publications were chosen using a Medline search for publications using oligonucleotide ISH on frozen sections of intestinal tract, and only those publications that included the sequence of oligonucleotide probes were included.

Publication	target mRNA	Probe type	
		antisense	sense
Kontakou M et al (291)	interferon γ	9	11
		11	6
		3	14
	TNFα	8	5
		7	6
		5	9
	IL-6	12	3
		12	4
		10	4
Beckett CG et al (289)	IL-4	12	6
		13	4
		11	6
	IL-10	9	7
		6	9
		11	2
		13	4
Limb et al(279)	IL-1β	9	9
		7	6
		5	7
mean (SD)		9.1 (3.0)	6.4 (2.9)

Appendix VI

Mean nucleotide base content of the human genome

Table. Mean percentage nucleotide base content of human liver, sperm and thymus (294).

	% nucleotide base composition			
	A	**T**	**G**	**C**
liver	30.3	30.3	19.5	19.9
sperm	30.7	31.2	19.3	18.8
thymus	30.9	29.4	19.9	19.8

References

1. Sen R, Baltimore D. Multiple nuclear factors interact with the immunoglobulin enhancer sequences. Cell 1986;46:705-716.

2. Sen R, Baltimore D. Inducibility of κ immunoglobulin enhancer-binding protein NFκB by a posttranslational mechanism. Cell 1986;47:921-928.

3. Baeuerle PA, Henkel T. Function and activation of NFκB in the immune system. Annu Rev Immunol 1994;12:141-179.

4. Blank V, Kourilsky P, Israel A. NFκB and related proteins: Rel/dorsal homologies meet ankyrin-like repeats. Trends Biochem Sci 1992;17:135-140.

5. Baldwin AS. The NFκB and IκB proteins: new discoveries and insights. Annu Rev Immunol 1996;14:649-681.

6. Grilli M, Chiu JJ, Lenardo MJ. NFκB and Rel: participants in a multiform transcriptional regulatory system. Int Rev Cytol 1993;143:1-62.

7. Rice NR, MacKichan ML, Israel A. The precursor of NFκB p50 has IκB-like functions. Cell 1993;71:243-253.

8. Neri A, Chang CC, Lombardi L, Salina M, Corradini P, Maiolo AT, Chaganti RS, Dalla FR. B-cell lymphoma-associated chromosomal translocation involves candidate oncogene lyt-10, homologous to NFκB p50. Cell 1992;67:1075-1087.

9. Ryseck R, Bull P, Takamiya M, Bours V, Siebenlist U, Dobranszki P, Bravo R. Rel B, a new Rel family transcription activator that can interact with p50 NFκB. Mol Cell Biol 1992;12:674-684.

10. Doerre S, Sista P, Sun SC, Ballard DW, Greene WC. The c-rel proto-oncogene product represses NFκB p65-mediated transcriptional activation of the long terminal repeat of type 1 human immunodeficiency virus. Proc Natl Acad Sci U S A 1993;90:1023-1027.

11. Baeuerle PA, Baltimore D. IκB: a specific inhibitor of the NFκB transcription factor. Science 1988;242:540-546.

12. Henkel T, Zabel U, van Zee K, Muller JM, Fanning E, Baeuerle PA. Intramolecular masking of the nuclear location signal and dimerisation domain in the precursor for the p50 NFκB subunit. Cell 1992;68:1121-1133.

13. Zabel U, Baeuerle PA. Purified human IκB can rapidly dissociate the complex of the NFκB transcription factor with its cognate DNA. Cell 1990;61:255-265.

14. Wen W, Meinkoth J, Tsien R, Taylor S. Identification of a signal for rapid export of proteins from the nucleus. Cell 1995;82:463-473.

15. Liou HC, Sha WC, Scott ML, Baltimore D. Sequential induction of NFκB/Rel family proteins during B-cell terminal differentiation. Mol Cell Biol 1994;14:5349-5359.

16. Haskill S, Beg AA, Tompkins S, Morris JS, Yurochko AD, Sampson-Johannes A, Mondal K, Ralph P, Baldwin AS. Characterization of an immediate-early gene induced in adherent monocytes that encodes IκB-like activity. Cell 1991;65:1281-1289.

17. Thompson JE, Phillips RJ, Erdjument-Bromage H, Tempst P, Ghosh S. IκBβ regulates the persistent response in a biphasic activation of NFκB. Cell 1995;80:573-582.

18. Inoue J, Kerr LD, Kakizuka A, Verma IM. IκB gamma, a 70-kD protein, identical to the C-terminal half of p110 NFκB: a new member of the IκB family. Cell 1992;68:1109-1120.

19. Baeuerle PA, Baltimore D. Activation of DNA-binding activity in an apparently cytoplasmic precursor of the NFκB transcription factor. Cell 1988;53:211-217.

20. Henkel T, Machleidt T, Alkalay I, Kronke M, Ben-Neriah Y, Baeuerle PA. Rapid proteolysis of IκBα is necessary for activation of transcription factor NFκB. Nature 1993;365:182-185.

21. Palombella VJ, Rando OJ, Goldberg AL, Maniatis T. The ubiquitin-proteasome pathway is required for processing the NFκB1 precursor protein and the activation of NFκB. Cell 1994;78:773-785.

22. Scherer DC, Brockman JA, Chen Z, Maniatis T, Ballard DW. Signal-induced degradation of IκB a requires site-specific ubiquitination. Proc Natl Acad Sci U S A 1995;92:11259-11263.

23. Li CC, Dai RM, Longo DL. Inactivation of NFκB inhibitor IκBα: ubiquitin-dependent proteolysis and its degradation product. Biochem Biophys Res Comm 1995;215:292-301.

24. DiDonato JA, Mercurio F, Karin M. Phosphorylation of IκBα precedes but is not sufficient for its dissociation from NFκB. Mol Cell Biol 1995;15:1302-1311.

25. Traenckner EB, Pahl HL, Henkel T, Schmidt KN, Wilk S, Baeuerle PA. Phosphorylation of human IκBα on serines 32 and 36 controls IκBα proteolysis and NFκB activation in response to diverse stimuli. EMBO J 1995;14:2876-2883.

26. Chen Z, Hagler J, Palombella VJ, Melandri F, Scherer D, Ballard D, Maniatis T. Signal-induced site-specific phosphorylation targets IκBα to the ubiquitin-proteasome pathway. Genes Devel 1995;9:1586-1597.

27. Kumar A, Haque J, Lacoste J, Hiscott J, Williams BR. Double-stranded RNA-dependent protein kinase activates transcription factor NFκB by phosphorylating IκB. Proc Natl Acad Sci U S A 1994;91:6288-6292.

28. Maran A, Maitra RK, Kumar A, Dong B, Xiao W, Li G, Williams BR, Torrence PF, Silverman RH. Blockage of NFκB signaling by selective ablation of an mRNA target by 2-5A antisense chimeras. Science 1994;265:789-792.

29. Barroga CF, Stevenson JK, Schwarz EM, Verma IM. Constitutive phosphorylation of IκBα by casein kinase II. Proc Natl Acad Sci U S A 1995;92:7637-7641.

30. Janosch P, Schellerer M, Seitz T. Characterisation of IκB kinases: IκBα is not phosphorylated by Raf-1 or protein kinase C isozymes, but is a casein kinase II substrate. Mol Cell Biol 1996;271:13868-13874.

31. Malinin NK, Boldin MP, Wallach D. MAP3K-related kinase involved in NFκB induction by TNF, CD95 and IL-1. Nature 1997;385:540-544.

32. Schreck R, Rieber P, Baeuerle PA. Reactive oxygen intermediates as apparently widely used messengers in the activation of the NFκB transcription factor and HIV-1. EMBO J 1991;10:2247-2258.

33. Schreck R, Albermann K, Baeuerle PA. NFκB: an oxidative stress-responsive transcription factor of eukaryotic cells (a review). Free Radic Res Comm 1992;17:221-237.

34. Schreck R, Meier B, Mannel DN, Droge W, Baeuerle PA. Dithiocarbamates as potent inhibitors of NFκB activation in intact cells. J Exp Med 1992;175:1181-1194.

35. Brennan P, O'Neill LA. Effects of oxidants and antioxidants on NFκB activation in three different cell lines: evidence against a universal hypothesis involving oxygen radicals. Biochim Biophys Acta 1995;1260:167-175.

36. Suzuki YJ, Mizuno M, Packer L. Transient overexpression of catalase does not inhibit TNF- or PMA-induced NFκB activation. Biochem Biophys Res Comm 1995;210:537-541.

37. Brown K, Park S, Kanno T, Franzoso G, Siebenlist U. Mutual regulation of the transcriptional activator NFκB and its inhibitor, IκBα. Proc Natl Acad Sci U S A 1993;90:2532-2536.

38. Sun SC, Ganchi PA, Ballard DW, Greene WC. NFκB controls expression of inhibitor IκB: evidence for an inducible autoregulatory pathway. Science 1993;259:1912-1921.

39. de Martin R, Vanhove B, Cheng Q, Hofer E, Csizmadia V, Winkler H, Bach FH. Cytokine-inducible expression in endothelial cells of an IκB-like gene is regulated by NFκB. EMBO J 1993;12:2773-2779.

40. Hohmann H, Remy R, Scheidereit C, van Loon APMG. Maintenance of NFκB activity is dependent on protein synthesis and the continuous presence of external stimuli. Mol Cell Biol 1991;11:259-266.

41. Mercurio F, Didonato J, Rosette C, Karin M. Molecular cloning and characterisation of a novel Rel/ NFκB family member displaying structural and functional homology to NFκB p50/p105. DNA Cell Biol 1992;11:523-537.

42. Ten RM, Paya CV, Israel N, Le BO, Mattei MG, Virelizier JL, Kourilsky P, Israel A. The characterisation of the promoter encoding the gene encoding the p50 subunit of NFκB indicates that it participates in its own regulation. EMBO J 192;11:195-203.

43. Hannink M, Temin HM. Structure and autoregulation of the c-rel promoter. Oncogene 1990;5:1843-1850.

44. Gerdes HH, Rosa P, Phillips E, Baeuerle PA, Frank R, Argos P, Huttner WB. The primary structure of human secretogranin II, a widespread tyrosine-sulfated secretory granule protein that exhibits low pH-and calcium-induced aggregation. J Biol Chem 1989;264:12009-12015.

45. Nabel G, Baltimore D. An inducible transcription factor activates expression of human immunodeficiency virus in T-cells. Nature 1987;326:711-713.

46. Sambucetti LC, Cherrington JM, Wilkinson GW, Mocarski ES. NFκB activation of the cytomegalovirus enhancer is mediated by a viral transactivator and by T-cell stimulation. EMBO J 1989;8:4251-4258.

47. Williams JL, Garcia J, Harrich D, Pearson L, Wu F, Gaynor R. Lymphoid specific gene expression of the adenovirus early region 3 promoter is mediated by NFκB binding motifs. EMBO J 1990;9:4435-4442.

48. Kanno M, Fromental C, Staub A, Ruffenach F, Davidson I, Chambon P. The SV40 TC-II (κB) and the related H-2Kb enhansons exhibit different cell type specific and inducible proto-enhancer activities, but the SV40 core sequence and the AP-2 binding site have no enhanson properties. EMBO J 1989;8:4205-4214.

49. Jamieson C, Mauxion F, Sen R. Identification of a functional NFκB binding site in the murine T-cell receptor β2 locus. J Exp Med 1989;170:1737-1743.

50. Israel A, Le-Bail O, Hatat D, Piette J, Kieran M, Logeat F, Wallach D, Fellous M, Kourilsky P. TNF stimulates expression of mouse MHC class I genes by inducing an NFκB-like enhancer binding activity which displaces constitutive factors. EMBO J 1989;8:3793-3800.

51. Blanar MA, Burkly LC, Flavell RA. NFκB binds within a region required for B-cell-specific expression of major histocompatibility complex class II gene E α δ. Mol Cell Biol 1989;9:844-846.

52. Moll T, Czyz M, Holzmuller H, Hofer-Warbinek R, Wagner E, Winkler H, Bach FH, Hofer E. Regulation of the tissue factor promoter in endothelial cells. Binding of NFκB-, AP-1-, and Sp1-like transcription factors. J Biol Chem 1995;270:3849-3857.

53. Whelan J, Ghersa P, Hooft van Huijsduijnen R, Gray J, Chandra G, Talabot F, DeLamarter JF. An NFκB-like factor is essential but not sufficient for cytokine induction of endothelial leukocyte adhesion molecule-1 gene transcription. Nucleic Acids Res 1991;19:2645-2653.

54. Ahmad M, Marui N, Alexander RW, Medford RM. Cell type-specific transactivation of the VCAM-1 promoter through an NFκB enhancer motif. J Biol Chem 1995;270:8976-8983.

55. Ledebur HC, Parks TP. Transcriptional regulation of the intercellular adhesion molecule-1 gene by inflammatory cytokines in human endothelial cells. Essential roles of a variant NFκB site and p65 homodimers. J Biol Chem 1995;270:933-943.

56. Visvanathan KV, Goodbourn S. Double-stranded RNA activates binding of NFκB to an inducible element in the human β interferon promoter. EMBO J 1989;8:1129-1138.

57. Schreck R, Zorbas H, Winnacker EL, Baeuerle PA. The NFκB transcription factor induces DNA bending which is modulated by its 65-kD subunit. Nucleic Acids Res 1990;18:6497-6502.

58. Dunn SM, Coles LS, Lang RK, Gerondakis S, Vadas MA, Shannon MF. Requirement for NFκB p65 and NF-IL6 binding elements in the tumour necrosis factor response region of the granulocyte colony-stimulating factor promoter. Blood 1994;83:2469-2479.

59. Nishizawa M, Nagata S. Regulatory elements responsible for inducible expression of the granulocyte colony-stimulating factor gene in macrophages. Mol Cell Biol 1990;10:2002-2011.

60. Lenardo MJ, Kuang A, Gifford A, Baltimore D. NFκB protein purification from bovine spleen: nucleotide stimulation and binding site specificity. Proc Natl Acad Sci U S A 1988;85:8825-8829.

61. Shimizu H, Mitomo K, Watanabe T, Okamoto S, Yamamoto K. Involvement of a NFκB-like transcription factor in the activation of the interleukin-6 gene by inflammatory lymphokines. Mol Cell Biol 1990;10:561-568.

62. Mukaida N, Okamoto S, Ishikawa Y, Matsushima K. Molecular mechanism of interleukin-8 gene expression. J Leukoc Biol 1994;56:554-558.

63. Shakhov AN, Collart MA, Vassalli P, Nedospasov SA, Jongeneel CV. κB-type enhancers are involved in lipopolysaccharide-mediated transcriptional activation of the tumour necrosis factor α gene in primary macrophages. J Exp Med 1990;171:35-47.

64. Messer G, Weiss EH, Baeuerle PA. Tumour necrosis factor β (TNFβ) induces binding of the NFκB transcription factor to a high-affinity κB element in the TNFβ promoter. Cytokine 1990;2:389-397.

65. Xie QW, Kashiwabara Y, Nathan C. Role of transcription factor NFκB/Rel in induction of nitric oxide synthase. J Biol Chem 1994;269:4705-4708.

66. Zipfel PF, Irving SG, Kelly K, Siebenlist U. Complexity of the primary genetic response to mitogenic activation of human T-cells. Mol Cell Biol 1989;9:1041-1048.

67. Lenardo MJ, Baltimore D. NFκB: a pleiotropic mediator of inducible and tissue-specific gene control. Cell 1989;58:227-229.

68. Jain J, Valge-Archer VE, Sinskey AJ, Rao A. The AP-1 site at -150 bp, but not the NFκB site, is likely to represent the major target of protein kinase C in the interleukin-2 promoter. J Exp Med 1992;175:853-862.

69. Durand DB, Shaw JP, Bush MR, Replogle RE, Belagaje R, Crabtree GR. Characterisation of antigen receptor response elements within the interleukin-2 enhancer. Mol Cell Biol 1988;8:1715-1724.

70. Muegge K, Williams TM, Kant J, Karin M, Chiu R, Schmidt A, Siebenlist U, Young HA, Durum SK. Interleukin-1 costimulatory activity on the interleukin-2 promoter via AP-1. Science 1989;246:249-251.

71. Hoyos B, Ballard DW, Bohnlein E, Siekevitz M, Greene WC. κB-specific DNA binding proteins: role in the regulation of human interleukin-2 gene expression. Science 1989;244:457-460.

72. Granelli-Piperno A, Nolan P. Nuclear transcription factors that bind to elements of the IL-2 promoter. Induction requirements in primary human T-cells. J Immunol 1991;147:2734-2739.

73. Fraser JD, Irving BA, Crabtree GR, Weiss A. Regulation of interleukin-2 gene enhancer activity by the T-cell accessory molecule CD28. Science 1991;251:313-316.

74. Leung K, Nabel GJ. HTLV-1 transactivator induces interleukin-2 receptor expression through an NFκB-like factor. Nature 1988;333:776-778.

75. Bohnlein E, Lowenthal JW, Siekevitz M, Ballard DW, Franza BR, Greene WC. The same inducible nuclear proteins regulates mitogen activation of both the interleukin-2 receptor-α gene and type 1 HIV. Cell 1988;53:827-836.

76. Lin BB, Cross SL, Halden NF, Roman DG, Toledano MB, Leonard WJ. Delineation of an enhancer-like positive regulatory element in the interleukin-2 receptor α-chain gene. Mol Cell Biol 1990;10:850-853.

77. Lowenthal JW, Ballard DW, Bogerd H, Bohnlein E, Greene WC. Tumour necrosis factor α activation of the IL-2 receptor a gene involves the induction of κB-specific DNA binding proteins. J Immunol 1989;142:3121-3128.

78. Miyamoto S, Chiao PJ, Verma IM. Enhanced IκB a degradation is responsible for constitutive NFκB activity in mature murine B-cell lines. Mol Cell Biol 1994;14:3276-3282.

79. Lee H, Arsura M, Wu M, Duyao M, Buckler A, Sonenshein G. Role of rel-related factors in control of *c-myc* gene transcription in receptor-mediated apoptosis of the murine B cell WEHI 231 line. J Exp Med 1995;181:1169-1177.

80. Baldwin AS, Jr., Sharp PA. Two transcription factors, NFκB and H2TF1, interact with a single regulatory sequence in the class I major histocompatibility complex promoter. Proc Natl Acad Sci U S A 1988;85:723-727.

81. Kaltschmidt C, Kaltschmidt B, Neumann H, Wekerle H, Baeuerle PA. Constitutive NFκB activity in neurons. Mol Cell Biol 1994;14:3981-3992.

82. Sheppard A, McQuillan J, Iademarco M, Dean D. Control of vascular cell adhesion molecule-1 gene promoter activity during neural differentiation. J Biol Chem 1995;270:3710-3719.

83. Osborn L, Kunkel S, Nabel GJ. Tumour necrosis factor α and interleukin 1 stimulate the human immunodeficiency virus enhancer by activation of NFκB. Proc Natl Acad Sci U S A 1989;86:2336-2340.

84. Hazan U, Thomas D, Alcami J, Bachelerie F, Israel N, Yssel H, Virelizier JL, Arenzana-Seisdedos F. Stimulation of a human T-cell clone with anti-CD3 or tumour necrosis factor induces NFκB translocation but not human immunodeficiency virus 1 enhancer-dependent transcription. Proc Natl Acad Sci U S A 1990;87:7861-7865.

85. Hohmann HP, Remy R, Poschl B, van Loon AP. Tumour necrosis factors α and β bind to the same two types of tumour necrosis factor receptors and maximally activate the transcription factor NFκB at low receptor occupancy and within minutes after receptor binding. J Biol Chem 1990;265:15183-15188.

86. Novak TJ, Chen D, Rothenberg EV. Interleukin-1 synergy with phosphoinositide pathway agonists for induction of interleukin-2 gene expression: molecular basis of costimulation. Mol Cell Biol 1990;10:6325-6334.

87. Mauxion F, Jamieson C, Yoshida M, Arai K, Sen R. Comparison of constitutive and inducible transcriptional enhancement mediated by κB-related sequences: modulation of activity in B cells by human T-cell leukemia virus type I tax gene. Proc Natl Acad Sci U S A 1991;88:2141-2145.

88. Roulston A, Beauparlant P, Rice N, Hiscott J. Chronic human immunodeficiency virus type 1 infection stimulates distinct NFκB/Rel DNA binding activities in myelomonoblastic cells. J Virol 1993;67:5235-5246.

89. Shurman L, Sen R, Bergman Y. Adenovirus E1A products activate the Ig κ chain enhancer in fibroblasts. A possible involvement of the NFκB binding site. J Immunol 1989;143:3806-3812.

90. Chirillo P, Falco M, Puri PL, Artini M, Balsano C, Levrero M, Natoli G. Hepatitis B virus pX activates NFκB-dependent transcription through a Raf-independent pathway. J Virol 1996;70:641-646.

91. Laherty CD, Hu HM, Opipari AW, Wang F, Dixit VM. The Epstein-Barr virus LMP1 gene product induces A20 zinc finger protein expression by activating NFκB. J Biol Chem 1992;267:24157-24160.

92. Rattner A, Korner M, Rosen H, Baeuerle PA, Citri Y. NFκB activates proenkephalin transcription in T-lymphocytes. Mol Cell Biol 1991;11:1017-1022.

93. Bressler P, Pantaleo G, Demaria A, Fauci AS. Anti-CD2 receptor antibodies activate the HIV long terminal repeat in T-lymphocytes. J Immunol 1991;147:2290-2294.

94. Stein B, Kramer M, Rahmsdorf HJ, Ponta H, Herrlich P. UV-induced transcription from the human immunodeficiency virus type 1 (HIV-1) long terminal repeat and UV-induced secretion of an extracellular factor that induces HIV-1 transcription in non-irradiated cells. J Virol 1989;63:4540-4544.

95. Schreck R, Rieber P, Baeuerle PA. Reactive oxygen intermediates as apparently widely used messengers in the activation of the NFκB transcription factor and HIV-1. EMBO J 1991;10:2247-2258.

96. Mathias S, Dressler KA, Kolesnick RN. Characterisation of a ceramide-activated protein kinase: stimulation by tumour necrosis factor α. Proc Natl Acad Sci U S A 1991;88:10009-10013.

97. Dobrowsky RT, Hannun YA. Ceramide stimulates a cytosolic protein phosphatase. J Biol Chem 1992;267:5048-5051.

98. Goldfeld AE, Strominger JL, Doyle C. Human tumour necrosis factor α gene regulation in phorbol ester stimulated T- and B-cell lines. J Exp Med 1991;174:73-81.

99. Leitman DC, Mackow ER, Williams T, Baxter JD, West BL. The core promoter region of the tumour necrosis factor α gene confers phorbol ester responsiveness to upstream transcriptional activators. Mol Cell Biol 1992;12:1352-1356.

100. Goldfeld AE, Doyle C, Maniatis T. Human tumour necrosis factor α gene regulation by virus and lipopolysaccharide. Proc Natl Acad Sci U S A 1990;87:9769-9773.

101. Ziegler-Heitbrock HW, Sternsdorf T, Liese J, Belohradsky B, Weber C, Wedel A, Schreck R, Baeuerle P, Strobel M. Pyrrolidine dithiocarbamate inhibits NFκB mobilisation and TNF production in human monocytes. J Immunol 1993;151:6986-6993.

102. Berliner JA, Navab M, Fogelman AM, Frank JS, Demer LL, Edwards PA, Watson AD, Lusis AJ. Atherosclerosis: basic mechanisms. Oxidation, inflammation and genetics. Circulation 1995;91:2488-2496.

103. Liao F, Andalibi A, Qiao JH, Allayee H, Fogelman AM, Lusis AJ. Genetic evidence for a common pathway mediating oxidative stress, inflammatory gene induction and aortic fatty streak formation in mice. J Clin Invest 1994;94:877-884.

104. Nakajima T, Kitajima I, Shin H, Takasaki I, Shigeta K, Abeyama K, Yamashita Y, Tokioka T, Soejima Y, Maruyama I. Involvement of NFκB activation in thrombin-induced human vascular smooth muscle cell proliferation. Biochem Biophys Res Comm 1994;204:950-958.

105. Brand K, Page S, Rogler G, Bartsch A, Brandl R, Kneuchl R, Page M, Kaltschmidt C, Baeuerle PA, Neumeier D. Activated transcription factor NFκB is present in the atherosclerotic lesion. J Clin Invest 1996;97:1715-1722.

106. Marok R, Winyard PG, Coumbe A, Kus ML, Gaffney K, Blades S, Mapp PI, Morris CJ, Blake DR, Kaltschmidt C, Baeuerle PA. Activation of the transcription factor NFκB in human inflamed synovial tissue. Arthritis Rheum 1996;39:583-591.

107. Behl C, Davis JB, Lesley R, Schubert D. Hydrogen peroxide mediates amyloid β protein toxicity. Cell 1994;77:817-827.

108. Dewhurst S, Embretson JE, Anderson DC, Mullins JI, Fultz PN. Sequence analysis and acute pathogenicity of molecularly cloned SIVSMM-PBj14. Nature 1990;345:636-640.

109. Anderson MG, Clements JE. Comparison of the transcriptional activity of the long terminal repeats of simian immunodeficiency viruses SIVmac251 and SIVmac239 in T-cell lines and macrophage cell lines. J Virol 1991;65:51-60.

110. Novembre FJ, Hirsch VM, McClure HM, Johnson PR. Molecular diversity of SIVsmm/PBj and a cognate variant, SIVsmm/PGg. J Med Primatol 1991;20:188-192.

111. Garcia JA, Wu FK, Mitsuyasu R, Gaynor RB. Interactions of cellular proteins involved in the transcriptional regulation of the human immunodeficiency virus. EMBO J 1987;6:3761-3770.

112. Kaufman JD, Valandra G, Roderiquez G, Bushar G, Giri C, Norcross MA. Phorbol ester enhances human immunodeficiency virus-promoted gene expression and acts on a repeated 10-base-pair functional enhancer element. Mol Cell Biol 1987;7:3759-3766.

113. MacMicking JD, Nathan C, Hom G, Chartrain N, Fletcher DS, Trumbauer M, Stevens K, Xie QW, Sokol K, Hutchinson N, *et al.* Altered responses to bacterial infection and endotoxic shock in mice lacking inducible nitric oxide synthase. Cell 1995;81:641-650.

114. Pfeffer K, Matsuyama T, Kundig TM, Wakeham A, Kishihara K, Shahinian A, Wiegmann K, Ohashi PS, Kronke M, Mak TW. Mice deficient for the 55 KD tumour necrosis factor receptor are resistant to endotoxic shock, yet succumb to *L. monocytogenes* infection. Cell 1993;73:457-467.

115. Siebenlist U, Franzoso G, Brown K. Structure, regulation and function of NFκB. Ann Rev Cell Biol 1994;10:405-455.

116. Gilmore TD, Koedood M, Piffat KA, White DW. Rel/ NFκB/IκB proteins and cancer. Oncogene 1996;13:1367-1378.

117. Ohno H, Takimoto G, McKeithan TW. The candidate proto-oncogene bcl-3 is related to genes implicated in cell lineage determination and cell cycle control. Cell 1990;60:991-997.

118. Beauparlant P, Kwan I, Bitar R, Chou P, Koromilas AE, Sonenberg N, Hiscott J. Disruption of IκB α regulation by antisense RNA expression leads to malignant transformation. Oncogene 1994;9:3189-3197.

119. Kitajima I, Shinohara T, Bilakovics J, Brown DA, Xu X, Nerenberg M. Ablation of transplanted HTLV-I Tax-transformed tumors in mice by antisense inhibition of NFκB. Science 1992;258:1792-1795.

120. Beg AA, Baltimore D. An essential role for NFκB in preventing TNFα-induced cell death. Science 1996;274:782-784.

121. Wang CY, Mayo MW, Baldwin AS, Jr. TNF- and cancer therapy-induced apoptosis: potentiation by inhibition of NFκB. Science 1996;274:784-787.

122. Beg AA, Sha WC, Bronson RT, Ghosh S, Baltimore D. Embryonic lethality and liver degeneration in mice lacking the RelA component of NFκB. Nature 1995;376:167-170.

123. Neurath MF, Pettersson S, Meyer zum Buschenfelde K. Local administration of antisense phosphorothioate oligonucleotides to the p65 subunit of NFκB abrogates established experimental colitis in mice. Nat Med 1996;2:998-1004.

124. Conner EM, Brand S, Grisham MB. Inhibition of a chronic granulomatous colitis by a selective proteasome inhibitor: antagonist of NFκB activation. Gastroenterology 1996;110:A887

125. Ray A, Prefontaine KE. Physical association and functional antagonism between the p65 subunit of transcription factor NFκB and the glucocorticoid receptor. Proc Natl Acad Sci U S A 1994;91:752-756.

126. Caldenhoven E, Liden J, Wissink S, Van de Stolpe A, Raaijmakers J, Koenderman L, Okret S, Gustafsson JA, van der Saag PT. Negative cross-talk between RelA and the glucocorticoid receptor: a possible mechanism for the antiinflammatory action of glucocorticoids. Mol Endocrinol 1995;9:401-412.

127. Auphan N, DiDonato JA, Rosette C, Helmberg A, Karin M. Immunosuppression by glucocorticoids: inhibition of NFκB activity through induction of IκB synthesis. Science 1995;270:286-290.

128. Scheinman RI, Cogswell PC, Lofquist AK, Baldwin AS, Jr. Role of transcriptional activation of IκBα in mediation of immunosuppression by glucocorticoids. Science 1995;270:283-286.

129. Frantz B, Nordby EC, Bren G, Steffan N, Paya CV, Kincaid RL, Tocci MJ, O'Keefe SJ, O'Neill EA. Calcineurin acts in synergy with PMA to inactivate IκB/MAD3, an inhibitor of NFκB. EMBO J 1994;13:861-870.

130. Venkataraman L, Burakoff SJ, Sen R. FK506 inhibits antigen receptor-mediated induction of c-rel in B and T lymphoid cells. J Exp Med 1995;181:1091-1099.

131. Kopp E, Ghosh S. Inhibition of NFκB by sodium salicylate and aspirin. Science 1994;265:956-959.

132. Weber C, Erl W, Pietsch A, Weber PC. Aspirin inhibits NFκB mobilisation and monocyte adhesion in stimulated human endothelial cells. Circulation 1995;91:1914-1917.

133. Barve S, Joshi-Barve S, Talwalker R, McClain CJ, Varilek GW. Mesalamine (5ASA) and the antioxidant vitamin E, inhibit interleukin-1 mediated activation of NFκB in CaCo-2 cells. Gastroenterology 1995;108:A777

134. Yang JP, Merin JP, Nakano T, Kato T, Kitade Y, Okamoto T. Inhibition of the DNA-binding activity of NFκB by gold compounds *in vitro*. FEBS Lett 1995;361:89-96.

135. Novak U, Paradiso L. Identification of proteins in DNA-protein complexes after blotting of EMSA gels. Biotechniques 1995;19:54-55.

136. Munkholm P, Langholz E, Nielsen OH, Kreiner S, Binder V. Incidence and prevalence of Crohn's disease in the county of Copenhagen, 1962-87: a sixfold increase in incidence. Scand J Gastroenterol 1992;27:609-614.

137. Roth MP, Petersen GM, McElree C, Vadheim CM, Panish JF, Rotter JI. Familial empiric risk estimates of inflammatory bowel disease in Ashkenazi Jews. Gastroenterology 1989;96:1016-1020.

138. Tysk C, Lindberg E, Jarnerot G, Floderus-Myrhed B. Ulcerative colitis and Crohn's disease in an unselected population of monozygotic and dizygotic twins. A study of heritability and the influence of smoking. Gut 1988;29:990-996.

139. Toyoda H, Wang SJ, Yang HY, Redford A, Magalong D, Tyan D, McElree CK, Pressman SR, Shanahan F, Targan SR, *et-al.* Distinct associations of HLA class II genes with inflammatory bowel disease. Gastroenterology 1993;104:741-748.

140. Reinshagen M, Loeliger C, Kuehnl P, Weiss U, Manfras BJ, Adler G, Boehm BO. HLA class II gene frequencies in Crohn's disease: a population based analysis in Germany. Gut 1996;38:538-542.

141. Hugot JP, Laurent-Puig P, Gower-Rousseau C, Olson JM, Lee JC, Beaugerie L, Naom I, Dupas JL, Van-Gossum A, Orholm M, Bonaiti-Pellie C, Weissenbach J, Mathew CG, Lennard-Jones JE, Cortot A, Colombel JF, Thomas G. Mapping of a susceptibility locus for Crohn's disease on chromosome 16. Nature 1996;379:821-823.

142. Satsangi J, Parkes M, Louis E, Hashimoto L, Kato N, Welsh K, Terwilliger JD, Lathrop GM, Bell JI, Jewell DP. Two stage genome-wide search in inflammatory bowel disease provides evidence for susceptibility loci on chromosomes 3, 7 and 12. Nat Genet 1996;14:199-202.

143. Crohn BB, Ginzburg L, Oppenheimer GD. Regional ileitis. A pathologic and clinical entity. J Am Med Assoc 1932;99:1323-1329.

144. Gent AE, Hellier MD, Grace RH, Swarbrick ET, Coggon D. Inflammatory bowel disease and domestic hygiene in infancy. Lancet 1994;343:766-767.

145. Kobayashi K, Blaser MJ, Brown WR. Immunohistochemical examination for *Mycobacteria* in intestinal tissues from patients with Crohn's disease. Gastroenterology 1989;96:1009-1015.

146. Sanderson JD, Moss MT, Tizard ML, Hermon-Taylor J. *Mycobacterium paratuberculosis* DNA in Crohn's disease tissue. Gut 1992;33:890-896.

147. Kobayashi K, Brown WR, Brennan PJ, Blaser MJ. Serum antibodies to mycobacterial antigens in active Crohn's disease. Gastroenterology 1988;94:1404-1411.

148. Thayer WR, Jr., Coutu JA, Chiodini RJ, Van-Kruiningen HJ, Merkal RS. Possible role of *mycobacteria* in inflammatory bowel disease. II. Mycobacterial antibodies in Crohn's disease. Dig Dis Sci 1984;29:1080-1085.

149. Prantera C, Kohn A, Mangiarotti R, Andreoli A, Luzi C. Antimycobacterial therapy in Crohn's disease: results of a controlled, double-blind trial with a multiple antibiotic regimen. Am J Gastroenterol 1994;89:513-518.

150. Lewin J, Dhillon AP, Sim R, Mazure G, Pounder RE, Wakefield AJ. Persistent measles virus infection of the intestine: confirmation by immunogold electron microscopy. Gut 1995;36:564-569.

151. Wakefield AJ, Sawyerr AM, Dhillon AP, Pittilo RM, Rowles PM, Lewis AA, Pounder RE. Pathogenesis of Crohn's disease: multifocal gastrointestinal infarction. Lancet 1989;ii:1057-1062.

152. Wakefield AJ, Sankey EA, Dhillon AP, Sawyerr AM, More L, Sim R, Pittilo RM, Rowles PM, Hudson M, Lewis AA, *et-al*. Granulomatous vasculitis in Crohn's disease. Gastroenterology 1991;100:1279-1287.

153. Wakefield AJ, Pittilo RM, Sim R, Cosby SL, Stephenson JR, Dhillon AP, Pounder RE. Evidence of persistent measles virus infection in Crohn's disease. J Med Virol 1993;39:345-353.

154. Ekbom A, Wakefield AJ, Zack M, Adami HO. Perinatal measles infection and subsequent Crohn's disease. Lancet 1994;344:508-510.

155. Ekbom A, Daszak P, Kraaz W, Wakefield AJ. Crohn's disease after *in utero* measles virus exposure. Lancet 1996;348:515-517.

156. Thompson NP, Montgomery SM, Pounder RE, Wakefield AJ. Is measles vaccination a risk factor for inflammatory bowel disease? Lancet 1995;345:1071-1074.

157. Sutherland LR, Ramcharan S, Bryant H, Fick G. Effect of cigarette smoking on recurrence of Crohn's disease. Gastroenterology 1990;98:1123-1128.

158. Holdstock G, Savage D, Harman M, Wright R. Should patients with inflammatory bowel disease smoke? BMJ 1994;1984:362

159. Cosnes J, Carbonnel F, Beaugerie L, Le Quintrec Y, Gendre JP. Effects of cigarette smoking on the long-term course of Crohn's disease. Gastroenterology 1996;110:424-431.

160. Breuer-Katschinski BD, Hollander N, Goebell H. Effect of cigarette smoking on the course of Crohn's disease. Eur J Gastroenterol Hepatol 1996;8:225-228.

161. Duffy LC, Zielezny MA, Marshall JR, Weiser MM, Byers TE, Phillips JF, Ogra PL, Graham S. Cigarette smoking and risk of clinical relapse in patients with Crohn's disease. Am J Prev Med 1990;6:161-166.

162. Lindberg E, Tysk C, Andersson K, Jarnerot G. Smoking and inflammatory bowel disease. A case control study. Gut 1988;29:352-357.

163. Vessey M, Jewell D, Smith A, Yeates D, McPherson K. Chronic inflammatory bowel disease, cigarette smoking, and use of oral contraceptives: findings in a large cohort study of women of childbearing age. BMJ 1986;292:526-528.

164. Brooke BN. What is ulcerative colitis? Lancet 1953;i:1220-1225.

165. Fujimura Y, Hosobe M, Kihara T. Ultrastructural study of M cells from colonic lymphoid nodules obtained by colonoscopic biopsy. Dig Dis Sci 1992;37:1089-1098.

166. Solcia E, Paulli M, Silini E, Fiocca R, Finzi G, Kindl S, Boveri E, Bosi F, Cornaggia M, Capella C, *et al.* Cathepsin E in antigen-presenting Langerhans and interdigitating reticulum cells. Its possible role in antigen processing. Eur J Histochem 1993;37:19-26.

167. Rutgeerts P, Goboes K, Peeters M, Hiele M, Penninckx F, Aerts R, Kerremans R, Vantrappen G. Effect of faecal stream diversion on recurrence of Crohn's disease in the neoterminal ileum. Lancet 1991;338:771-774.

168. Rutgeerts P, Geboes K, Vantrappen K, Kerremans R, Coenegrachts JL, Coremans G. Natural history of recurrent Crohn's disease at the ileocolonic anastamosis after curative surgery. Gut 1984;25:665-672.

169. Makiyama K, Bennett MK, Jewell DP. Endoscopic appearances of the rectal mucosa of patients with Crohn's disease visualised with a magnifying colonoscope. Gut 1984;25:337-340.

170. Rickert RR, Carter HW. The "early" ulcerative lesion of Crohn's disease: correlative light- and scanning electron-microscopic studies. J Clin Gastroenterol 1980;2:11-19.

171. Allison MC, Hamilton-Dutoit SJ, Dhillon AP, Pounder RP. The value of rectal biopsy in distinguishing self-limited colitis from early inflammatory bowel disease. QJM 1987;248:985-995.

172. Fujimura Y, Kamoi R, Iida M. Pathogenesis of aphthoid ulcers in Crohn's disease: correlative findings by magnifying colonoscopy, electron microscopy, and immunohistochemistry. Gut 1996;38:724-732.

173. Korelitz BI, Sommers SC. Rectal biopsy in patients with Crohn's disease. Normal mucosa on sigmoidoscopic examination. JAMA 1977;237:2742-2744.

174. Sommers SC, Korelitz BI. Duodenal cell counts and histopathology in Crohn's disease. In: Pena AS, Weterman IT, Booth CC, Strober W, eds. Recent advances in Crohn's disease. First Ed. The Hague: Martinus Nijhoff, 1981:47-51.

175. Bookman MA, Bull DM. Characteristics of isolated intestinal mucosal lymphoid cells in inflammatory bowel disease. Gastroenterology 1979;77:503-510.

176. MacDermott RP, Bragdon MJ, Thurmond RD. Peripheral blood mononuclear cells from patients with inflammatory bowel disease exhibit normal function in the allogeneic and autologous mixed leukocyte reaction and cell-mediated lympholysis. Gastroenterology 1984;86:476-484.

177. MacDermott RP, Nash GS, Auer IO, Shlien R, Lewis BS, Madassery J, Nahm MH. Alterations in serum immunoglobulin G subclasses in patients with ulcerative colitis and Crohn's disease. Gastroenterology 1989;96:764-768.

178. Keren DF, Appelman HD, Dobbins WO, Wells JJ, Whisenant B, Foley J, Dieterle R, Geisinger K. Correlation of histopathologic evidence of disease activity with the presence of immunoglobulin-containing cells in the colons of patients with inflammatory bowel disease. Hum Pathol 1984;15:757-763.

179. Rosekrans PC, Meijer CJ, van der Wal AM, Cornelisse CJ, Lindeman J. Immunoglobulin containing cells in inflammatory bowel disease of the colon: a morphometric and immunohistochemical study. Gut 1980;21:941-947.

180. Roche JK, Fiocchi C, Youngman K. Sensitisation to epithelial antigens in chronic mucosal inflammatory disease. Characterisation of human intestinal mucosa-derived mononuclear cells reactive with purified epithelial cell-associated components *in vitro*. J Clin Invest 1985;75:522-530.

181. Fiocchi C, Roche JK, Michener WM. High prevalence of antibodies to intestinal epithelial antigens in patients with inflammatory bowel disease and their relatives. Ann Intern Med 1989;110:786-794.

182. Das KM, Dubin R, Nagai T. Isolation and characterisation of colonic tissue-bound antibodies from patients with idiopathic ulcerative colitis. Proc Natl Acad Sci U S A 1978;75:4528-4532.

183. Das KM, Squillante L, Robertson FM. Amplified expression of intercellular adhesion molecule-1 and M(r) 40K protein by DLD-1 colon tumour cells by interferon γ. Cell Immunol 1993;147:215-221.

184. Mandal A, Dasgupta A, Jeffers L, Squillante L, Hyder S, Reddy R, Schiff E, Das KM. Autoantibodies in sclerosing cholangitis against a shared peptide in biliary and colon epithelium. Gastroenterology 1994;106:185-192.

185. Saxon A, Shanahan F, Landers C, Ganz T, Targan S. A distinct subset of antineutrophil cytoplasmic antibodies is associated with inflammatory bowel disease. J Allergy Clin Immunol 1990;86:202-210.

186. Duerr RH, Targan SR, Landers CJ, Sutherland LR, Shanahan F. Antineutrophil cytoplasmic antibodies in ulcerative colitis. Comparison with other colitides/diarrhoeal illnesses. Gastroenterology 1991;100:1590-1596.

187. Colombel JF, Reumaux D, Duthilleul P, Noel LH, Gower-Rousseau C, Paris JC, Cortot A. Antineutrophil cytoplasmic autoantibodies in inflammatory bowel diseases. Gastroenterol Clin Biol 1992;16:656-660.

188. Cambridge G, Rampton DS, Stevens TR, McCarthy DA, Kamm M, Leaker B. Antineutrophil antibodies in inflammatory bowel disease: prevalence and diagnostic role. Gut 1992;33:668-674.

189. Seibold F, Slametschka D, Gregor M, Weber P. Neutrophil autoantibodies: a genetic marker in primary sclerosing cholangitis and ulcerative colitis. Gastroenterology 1994;107:532-536.

190. Lee JC, Lennard-Jones JE, Cambridge G. Antineutrophil antibodies in familial inflammatory bowel disease. Gastroenterology 1995;108:428-433.

191. Shanahan F, Duerr RH, Rotter JI, Yang H, Sutherland LR, McElree C, Landers CJ, Targan SR. Neutrophil autoantibodies in ulcerative colitis: familial aggregation and genetic heterogeneity. Gastroenterology 1992;103:456-461.

192. Hirata I, Berrebi G, Austin LL, Keren DF, Dobbins WO. Immunohistological characterisation of intraepithelial and lamina propria lymphocytes in control ileum and colon and in inflammatory bowel disease. Dig Dis Sci 1986;31:593-603.

193. Selby WS, Janossy G, Bofill M, Jewell DP. Intestinal lymphocyte subpopulations in inflammatory bowel disease: an analysis by immunohistological and cell isolation techniques. Gut 1984;25:32-40.

194. Harvey J, Jones DB, Wright DH. Leucocyte common antigen expression on T-cells in normal and inflamed human gut. Immunology 1989;68:13-17.

195. MacDonald TT, Hutchings P, Choy MY, Murch S, Cooke A. Tumour necrosis factor α and interferon-γ production measured at the single cell level in normal and inflamed human intestine. Clin Exp Immunol 1990;81:301-305.

196. Allison MC, Poulter LW, Dhillon AP, Pounder RE. Immunohistological studies of surface antigen on colonic lymphoid cells in normal and inflamed mucosa. Comparison of follicular and lamina propria lymphocytes. Gastroenterology 1990;99:421-430.

197. Pallone F, Fais S, Squarcia O, Biancone L, Pozzilli P, Boirivant M. Activation of peripheral blood and intestinal lamina propria lymphocytes in Crohn's disease. *In vivo* state of activation and *in vitro* response to stimulation as defined by the expression of early activation antigens. Gut 1987;28:745-753.

198. Schreiber S, MacDermott RP, Raedler A, Pinnau R, Bertovich MJ, Nash GS. Increased activation of isolated intestinal lamina propria mononuclear cells in inflammatory bowel disease. Gastroenterology 1991;101:1020-1030.

199. Kusugami K, Youngman KR, West GA, Fiocchi C. Intestinal immune reactivity to interleukin-2 differs among Crohn's disease, ulcerative colitis, and controls. Gastroenterology 1989;97:1-9.

200. Soderstrom K, Bucht A, Halapi E, Gronberg A, Magnusson I, Kiessling R. Increased frequency of abnormal γδ T cells in blood of patients with inflammatory bowel diseases. J Immunol 1996;156:2331-2339.

201. Fukushima K, Masuda T, Ohtani H, Sasaki I, Funayama Y, Matsuno S, Nagura H. Immunohistochemical characterisation, distribution, and ultrastructure of lymphocyte populations in inflammatory bowel disease. Gastroenterology 1991;101:670-678.

202. Meuret G, Bitzi A, Hammer B. Macrophage turnover in Crohn's disease and ulcerative colitis. Gastroenterology 1978;74:501-503.

203. Rugtveit J, Brandtzaeg P, Halstensen TS, Fausa O, Scott H. Increased macrophage subset in inflammatory bowel disease: apparent recruitment from peripheral blood monocytes. Gut 1994;35:669-674.

204. Allison MC, Cornwall S, Poulter LW, Dhillon AP, Pounder RE. Macrophage heterogeneity in normal colonic mucosa and in inflammatory bowel disease. Gut 1988;29:1531-1538.

205. Simmonds NJ, Allen RE, Stevens TR, Van-Someren RN, Blake DR, Rampton DS. Chemiluminescence assay of mucosal reactive oxygen metabolites in inflammatory bowel disease. Gastroenterology 1992;103:186-196.

206. Rachmilewitz D, Stamler JS, Bachwich D, Karmeli F, Ackerman Z, Podolsky DK. Enhanced colonic nitric oxide generation and nitric oxide synthase activity in ulcerative colitis and Crohn's disease. Gut 1995;36:718-723.

207. Singer II, Kawka DW, Scott S, Weidner JR, Mumford RA, Riehl TE, Stenson WF. Expression of inducible nitric oxide synthase and nitrotyrosine in colonic epithelium in inflammatory bowel disease. Gastroenterology 1996;111:871-885.

208. Buffinton GD, Doe WF. Depleted mucosal antioxidant defences in inflammatory bowel disease. Free Radic Biol Med 1995;19:911-918.

209. Gionchetti P, Guarnieri C, Campieri M, Belluzzi A, Brignola C, Iannone P, Miglioli M, Barbara L. Scavenger effect of sulfasalazine, 5-aminosalicylic acid, and olsalazine on superoxide radical generation. Dig Dis Sci 1991;36:174-178.

210. Greenfield SM, Punchard NA, Teare JP, Thompson RPH. Review article: the mode of action of the aminosalicylates in inflammatory bowel disease. Aliment Pharmacol Ther 1993;7:369-383.

211. Dvorak AM, Monahan RA, Osage JE, Dickersin GR. Crohn's disease: transmission electron microscopic studies II. Immunologic inflammatory response. Alterations of mast cells, basophils, eosinophils, and the microvasculature. Hum Pathol 1980;11:606-619.

212. Dubucquoi S, Janin A, Klein O, Desreumaux P, Quandalle P, Cortot A, Capron M, Colombel JF. Activated eosinophils and interleukin-5 expression in early recurrence of Crohn's disease. Gut 1995;37:242-246.

213. Gleich GJ, Frigas E, Loering DA, Wassom DL, Steinmuller D. Cytotoxic properties of the eosinophil major basic protein. J Immunol 1979;123:2925-2927.

214. Dinarello CA. Interleukin-1 and its biologically related cytokines. Adv Immunol 1989;44:153-161.

215. Miura M, Hiwatashi N. Cytokine production in inflammatory bowel disease. J Clin Lab Immunol 1985;18:81-86.

216. Satsangi J, Wolstencroft RA, Cason J, Ainley CC, Dumonde DC, Thompson RPH. Interleukin-1 in Crohn's disease. Clin Exp Immunol 1987;67:594-605.

217. Nakamura M, Saito H, Kasanuki J, Tamura Y, Yoshida S. Cytokine production in patients with inflammatory bowel disease. Gut 1992;33:933-937.

218. Mazlam MZ, Hodgson HJ. Peripheral blood monocyte cytokine production and acute phase response in inflammatory bowel disease. Gut 1992;33:773-778.

219. Mahida YR, Wu K, Jewell DP. Enhanced production of interleukin-1β by mononuclear cells isolated from mucosa with active ulcerative colitis of Crohn's disease. Gut 1989;30:835-838.

220. Matsumoto T, Kitano A, Nakamura S, Oshitani N, Obata A, Hiki M, Hashimura H, Okawa K, Kobayashi K, Nagura H. Possible role of vascular endothelial cells in immune responses in colonic mucosa examined immunocytochemically in subjects with and without ulcerative colitis. Clin Exp Immunol 1989;78:424-430.

221. Cappello M, Keshav S, Prince C, Jewell DP, Gordon S. Detection of mRNAs for macrophage products in inflammatory bowel disease by *in situ* hybridisation. Gut 1992;33:1214-1219.

222. Youngman KR, Simon PL, West GA, Cominelli F, Rachmilewitz D, Klein JS, Fiocchi C. Localisation of intestinal interleukin-1 activity and protein and gene expression to lamina propria cells. Gastroenterology 1993;104:749-758.

223. Gionchetti P, Campieri M, Belluzi A, Paganelli GM, Bertinelli E, Ferretto M, Lauri A, Biasco G, Miglioli M, Barbara L. Macrophage subpopulations and interleukin-1β tissue levels in pelvic ileal pouches. Eur J Gastroenterol Hepatol 1994;6:217-222.

224. Isaacs KL, Sartor RB, Haskill S. Cytokine messenger RNA profiles in inflammatory bowel disease mucosa detected by polymerase chain reaction amplification. Gastroenterology 1992;103:1587-1595.

225. Casini-Raggi V, Kam L, Chong YJ, Fiocchi C, Pizarro TT, Cominelli F. Mucosal imbalance of IL-1 and IL-1 receptor antagonist in inflammatory bowel disease. A novel mechanism of chronic intestinal inflammation. J Immunol 1995;154:2434-2440.

226. Mahida YR, Kurlac L, Gallagher A, Hawkey CJ. High circulating concentrations of interleukin-6 in active Crohn's disease but not ulcerative colitis. Gut 1991;32:1531-1534.

227. Stevens C, Walz G, Singaram C, Lipman ML, Zanker B, Muggia A, Antonioli D, Peppercorn MA, Strom TB. Tumour necrosis factor α, interleukin-1β, and interleukin-6 expression in inflammatory bowel disease. Dig Dis Sci 1992;37:818-826.

228. Kusugami K, Fukatsu A, Tanimoto M, Shinoda M, Haruta J, Kuroiwa A, Ina K, Kanayama K, Ando T, Matsuura T, *et-al*. Elevation of interleukin-6 in inflammatory bowel disease is macrophage- and epithelial cell-dependent. Dig Dis Sci 1995;40:949-959.

229. Beutler B, Cerami A. The biology of cachectin/TNF. A primary mediator of the host response. Annu Rev Immunol 1989;7:625-638.

230. Murch SH, Lamkin VA, Savage MO, Walker-Smith JA, MacDonald TT. Serum concentrations of tumour necrosis factor α in childhood chronic inflammatory bowel disease. Gut 1991;32:913-917.

231. Hyams JS, Treem WR, Eddy E, Wyzga N, Moore RE. Tumour necrosis factor α is not elevated in children with inflammatory bowel disease. J Paediatr Gastroenterol Nutr 1991;12:233-236.

232. Hudson M, Gallati H, Ryff JC, Pounder RE, Wakefield AJ. Serum tumour necrosis factor (TNF) and soluble TNF receptors p55 and p75 in Crohn's disease. Gastroenterology 1993;104:A715

233. Braegger CP, Nicholls S, Murch SH, Stephens S, MacDonald TT. Tumour necrosis factor α in stool as a marker of intestinal inflammation. Lancet 1992;339:89-91.

234. Targan SR, Hanauer SB, van-Deventer SJ, Mayer L, Present DH, Braakman T, DeWoody KL, Schaible TF, Rutgeerts PJ. A short-term study of chimeric monoclonal antibody cA2 to tumour necrosis factor α for Crohn's disease. Crohn's Disease cA2 Study Group. N Engl J Med 1997;337:1029-1035.

235. Mullin GE, Maycon ZR, Braun-Elwert L, Cerchia R, James SP, Katz S, Weissman GS, McKinley MJ, Fisher SE. Inflammatory bowel disease mucosal biopsies have specialised lymphokine mRNA profiles. Inflamm Bowel Dis 1996;2:16-26.

236. Fuss IJ, Neurath M, Boirivant M, Klein JS, De-La-Motte C, Strong SA, Fiocchi C, Strober W. Disparate CD4+ lamina propria (LP) lymphokine secretion profiles in inflammatory bowel disease. Crohn's disease LP cells manifest increased secretion of IFN-γ, whereas ulcerative colitis LP cells manifest increased secretion of IL-5. J Immunol 1996;157:1261-1270.

237. Malizia G, Calabrese A, Cottone M, Raimondo M, Trejdosiewicz LK, Smart CJ, Oliva L, Pagliaro L. Expression of leukocyte adhesion molecules by mucosal mononuclear phagocytes in inflammatory bowel disease. Gastroenterology 1991;100:150-159.

238. Ohtani H, Nakamura S, Watanabe Y, Fukushima K, Mizoi T, Kimura M, Hiwatashi N, Nagura H. Light and electron microscopic immunolocalization of endothelial leucocyte adhesion molecule-1 in inflammatory bowel disease. Morphological evidence of active synthesis and secretion into vascular lumen. Virchows Archiv 1992;420:403-409.

239. Koizumi M, King N, Lobb R, Benjamin C, Podolsky DK. Expression of vascular adhesion molecules in inflammatory bowel disease. Gastroenterology 1992;103:840-847.

240. Fiocchi C, Hilfiker ML, Youngman KR, Doerder NC, Finke JH. Interleukin-2 activity of human intestinal mucosa mononuclear cells. Decreased levels in inflammatory bowel disease. Gastroenterology 1984;86:734-742.

241. Mullin GE, Lazenby AJ, Harris ML, Bayless TM, James SP. Increased interleukin-2 messenger RNA in the intestinal mucosal lesions of Crohn's disease but not ulcerative colitis. Gastroenterology 1992;102:1620-1627.

242. Sparano JA, Brandt LJ, Dutcher JP, DuBois JS, Atkins MB. Symptomatic exacerbation of Crohn's disease after treatment with high-dose interleukin-2. Ann Intern Med 1993;118:617-618.

243. James SP. Remission of Crohn's disease after human immunodeficiency virus infection. Gastroenterology 1988;95:1667-1669.

244. Sadlack B, Merz H, Schorle H, Schimpl A, Feller AC, Horak I. Ulcerative colitis-like disease in mice with a disrupted interleukin-2 gene. Cell 1993;75:253-261.

245. Mahida YR, Gallagher A, Kurlak L, Hawkey CJ. Plasma and tissue interleukin-2 receptor levels in inflammatory bowel disease. Clin Exp Immunol 1990;82:75-80.

246. Matsuura T, West GA, Klein JS, Ferraris L, Fiocchi C. Soluble interleukin 2 and CD8 and CD4 receptors in inflammatory bowel disease. Gastroenterology 1992;102:2006-2014.

247. Matsuura T, West GA, Youngman KR, Klein JS, Fiocchi C. Immune activation genes in inflammatory bowel disease. Gastroenterology 1993;104:448-458.

248. Lieberman BY, Fiocchi C, Youngman KR, Sapatnekar WK, Proffitt MR. Interferon-γ production by human intestinal mucosal mononuclear cells. Decreased levels in inflammatory bowel disease. Dig Dis Sci 1988;33:1297-1304.

249. Fais S, Capobianchi MR, Pallone F, Di-Marco P, Boirivant M, Dianzani F, Torsoli A. Spontaneous release of interferon-γ by intestinal lamina propria lymphocytes in Crohn's disease. Kinetics of *in vitro* response to interferon-γ inducers. Gut 1991;32:403-407.

250. Breese E, Braegger CP, Corrigan CJ, Walker-Smith JA, MacDonald TT. Interleukin-2- and interferon-γ-secreting T-cells in normal and diseased human intestinal mucosa. Immunology 1993;78:127-131.

251. Monteleone G, Biancone L, Marasco R, Morrone G, Marasco O, Luzza F, Pallone F. Interleukin-12 is expressed and actively released by Crohn's disease intestinal lamina propria mononuclear cells. Gastroenterology 1997;112:1169-1178.

252. Abbas AK, Murphy KM, Sher A. Functional diversity of helper T-lymphocytes. Nature 1996;383:787-793.

253. Bellezzo JM, Britton RS, Bacon BR, Fox ES. LPS-mediated NFκB activation in rat Kupffer cells can be induced independently of CD14. Am J Physiol 1996;270:956-961.

254. Dubucquoi S, Janin A, Klein O, Desreumaux P, Quandalle P, Cortot A, Capron M, Colombel JF. Activated eosinophils and interleukin-5 expression in early recurrence of Crohn's disease. Gut 1995;37:242-246.

255. Babyatsky MW, Rossiter G, Podolsky DK. Expression of transforming growth factors α and β in colonic mucosa in inflammatory bowel disease. Gastroenterology 1996;110:975-984.

256. Lauritsen K, Laursen LS, Bukhave K, Rask-Madsen J. *In vivo* profiles of eicosanoids in ulcerative colitis, Crohn's colitis, and *Clostridium difficile* colitis. Gastroenterology 1988;95:11-17.

257. Rampton DS, Sladen GE, Youlten LJ. Rectal mucosal prostaglandin E2 release and its relation to disease activity, electrical potential difference and treatment in ulcerative colitis. Gut 1980;21:591-596.

258. Ligumsky M, Karmeli F, Sharon P, Zor U, Cohen F, Rachmilewitz D. Enhanced thromboxane A2 and prostacyclin production by cultured rectal mucosa in ulcerative colitis and its inhibition by steroids and sulfasalazine. Gastroenterology 1981;81:444-449.

259. Sharon P, Stenson WF. Enhanced synthesis of leukotriene B4 by colonic mucosa in inflammatory bowel disease. Gastroenterology 1984;86:453-460.

260. Halstensen TS, Das KM, Brandtzaeg P. Epithelial deposits of immunoglobulin G1 and activated complement colocalise with the M(r) 40 kD putative autoantigen in ulcerative colitis. Gut 1993;34:650-657.

261. Powrie F, Leach MW, Mauze S, Caddle LB, Coffman RL. Phenotypically distinct subsets of CD4+ T cells induce or protect from chronic intestinal inflammation in C.B-17 scid mice. Int Immunol 1993;5:1461-1471.

262. Taurog JD, Richardson JA, Croft JT, Simmons WA, Zhou M, Fernandez-Suciro JL, Balish E, Hammer RE. The germfree state prevents development of gut and joint inflammatory disease in HLA-B27 transgenic rats. J Exp Med 1994;180:2359-2364.

263. Kuhn R, Lohler J, Rennick D, Rajewsky K, Muller W. Interleukin-10-deficient mice develop chronic enterocolitis. Cell 1993;75:263-274.

264. Rath HC, Herfarth HH, Ikeda JS, Grenther WB, Hamm TE, Jr., Balish E, Taurog JD, Hammer RE, Wilson KH, Sartor RB. Normal luminal bacteria, especially *Bacteroides* species, mediate chronic colitis, gastritis, and arthritis in HLA-B27/human β2 microglobulin transgenic rats. J Clin Invest 1996;98:945-953.

265. Ma A, Datta M, Margosian E, Chen J, Horak I. T-cells, but not B cells, are required for bowel inflammation in interleukin-2-deficient mice. J Exp Med 1995;182:1567-1572.

266. Mizoguchi A, Mizoguchi E, Chiba C, Bhan AK. Role of appendix in the development of inflammatory bowel disease in TCR a mutant mice. J Exp Med 1996;184:707-715.

267. Rutgeerts P, D'Haens G, Hiele M, Geboes K, Vantrappen G. Appendectomy protects against ulcerative colitis. Gastroenterology 1994;106:1251-1253.

268. Hermiston ML, Gordon JI. Inflammatory bowel disease and adenomas in mice expressing a dominant negative N-cadherin. Science 1995;270:1203-1207.

269. Meyer R, Hatada EN, Hohmann H, Haiker M, Bartsch C, Rothlisberger U, Lahm H, Schlaeger EJ, van Loom APGM, Scheidereit C. Cloning of the DNA-binding subunit of human NFκB: the level of its mRNA is strongly regulated by phorbol ester or tumour necrosis factor α. Proc Natl Acad Sci U S A 1991;88:966-970.

270. Beg AA, Baldwin AS. The IκB proteins: multifunctional regulators of Rel/ NFκB transcription factors. Genes Devel 1998;7:2064-2070.

271. Higgins CF, Peltz SW, Jacobson A. Turnover of mRNA in prokaryotes and lower eukaryotes. Curr Opin Genet Dev 1992;2:739-747.

272. Wilkinson DG. The theory and practice of *in situ* hybridisation. In: Wilkinson DG, ed. *In Situ* Hybridization, A Practical Approach. First Ed. Oxford: Oxford University Press, 1992:1-13.

273. Brooks PJ, Kaplitt MG, Kleopoulos SP, Funabashi T, Mobbs CV, Pfaff CW. Detection of mRNA and low-abundance heteronuclear RNA with single-stranded DNA probes produced by amplified primer extension labelling. J Histochem Cytochem 1993;41:1761-1763.

274. Lichter P, Cremer T, Borden J, Manuelidis L, Ward DC. Delineation of individual human chromosomes in metaphase and interphase cells by *in situ* suppression hybridisation using recombinant DNA libraries. Hum Genet 1988;80:224-234.

275. Lewis ML, Sherman TG, Watson SJ. *In situ* hybridisation histochemistry with synthetic oligonucleotides: strategies and methods. Peptides 1985;6:75-82.

276. Cox KH, Deleon DV, Angerer LM, Angerer RC. Detection of mRNAs in sea urchin embryos by *in situ* hybridisation using asymmetric RNA probes. Dev Biol 1984;101:485-502.

277. Diaz MO, Barsacchi-Pilone G, Mahon KA, Gall JG. Transcripts of both strands of a satellite DNA occur on lampbrush chromosome loops of the newt notophthalmus. Cell 1981;24:649-659.

278. Stahl LW, Eakin TJ, Baskin DG. Selection of oligonucleotide probes for detection of mRNA isoforms. J Histochem Cytochem 1993;41:1735-1740.

279. Limb GA, Early O, Jones SE, Leroy F, Chignell AH, Dumonde DC. Expression of mRNA coding for TNFα, IL-1β and IL-6 by cells infiltrating retinal membranes. Graefes Arch Clin Exp Ophthalmol 1994;232:646-651.

280. Pringle JH, Primrose L, Kind CN, Talbot IC, Lauder I. *In-situ* hybridisation demonstration of poly-adenylated RNA sequences in formalin-fixed paraffin sections using a biotinylated oligonucleotide poly-d(T) probe. J Pathol 1989;158:279-286.

281. Hamid Q, Azzawi M, Ying S, Moqbel R, Wardlaw AJ, Corrigan CJ, Bradley B, Durham SR, Collins JV, Jeffery PK, Quint DJ, Kay AB. Expression of mRNA for interleukin-5 in mucosal bronchial biopsies from asthma. J Clin Invest 1991;87:1541-1546.

282. Weller PF. The immunobiology of eosinophils. New Engl J Med 1991;324:1110-1118.

283. Spry CJF. Methods: eosinophil structure, constituents and metabolism. In: Eosinophils. A Comprehensive Review, and Guide to the Scientific and Medical Literature. First Ed. Oxford: Oxford University Press, 1994:30-64.

284. Lendrum AC. The staining of eosinophil polymorphs and enterochromaffin cells in histological sections. J Pathol Bacteriol 1944;56:441

285. Patterson S, Gross J, Webster AD. DNA probes bind non-specifically to eosinophils during *in situ* hybridisation: carbol chromotrope blocks binding to eosinophils but does not inhibit hybridisation to specific nucleotide sequences. J Virol Methods 1989;23:105-109.

286. Fox CH, Kotler D, Tierney A, Wilson CS, Fauci AS. Detection of HIV-1 RNA in the lamina propria of patients with AIDS and gastrointestinal disease. J Infect Dis 1989;159:467-471.

287. Kontakou M, Przemioslo RT, Sturgess RP, Limb AG, Ciclitira PJ. Expression of tumour necrosis factor α, interleukin-6, and interleukin-2 mRNA in the jejunum of patients with coeliac disease. Scand J Gastroenterol 1995;30:456-463.

288. Goldberg PA, Herbst F, Beckett CG, Martelli B, Kontakou M, Talbot IC, Ciclitira PJ, Nicholls RJ. Leucocyte typing, cytokine expression, and epithelial turnover in the ileal pouch in patients with ulcerative colitis and familial adenomatous polyposis. Gut 1996;38:549-553.

289. Beckett CG, Dell'Olio D, Kontakou M, Przemioslo RT, Rosen-Bronsen S, Ciclitira PJ. Analysis of interleukin-4 and interleukin-10 and their association with the lymphocytic infiltrate in the small intestine of patients with coeliac disease. Gut 1996;39:818-823.

290. Kontakou M, Sturgess RP, Przemioslo RT, Limb GA, Nelufer JM, Ciclitira PJ. Detection of interferon-γ mRNA in the mucosa of patients with coeliac disease by *in situ* hybridisation. Gut 1994;35:1037-1041.

291. Kontakou M, Przemioslo RT, Sturgess RP, Limb GA, Ellis HJ, Day P, Ciclitira PJ. Cytokine mRNA expression in the mucosa of treated coeliac patients after wheat peptide challenge. Gut 1995;37:52-57.

292. Beckett CG, Dell'Olio D, Ellis HJ, Rosen-Bronsen S, Ciclitira PJ. The detection and localisation of inducible nitric oxide synthase production in the small intestine of patients with coeliac disease. Eur J Gastroenterol Hepatol 1998;10:641-647.

293. Audie JP, Janin A, Porchet N, Copin MC, Gosselin B, Aubert JP. Expression of human mucin genes in respiratory, digestive and reproductive tracts ascertained by *in situ* hybridisation. J Histochem Cytochem 1993;41:1479-1485.

294. Rothwell NV. Chemistry of the gene. In: Rothwell NV, ed. Understanding genetics. A molecular approach. First Ed. New York: Wiley-Liss Inc. 1993:211-234.

295. Barrett DM, Faigel DO, Metz DC, Montone K, Furth EE. *In situ* hybridisation for *Helicobacter pylori* in gastric mucosal biopsy specimens: quantitative evaluation of test performances in comparison with the CLO test and thiazine stain. J Clin Laborat Anal 1997;11:374-379.

296. Freeman TC, Howard A, Bentsen TS, Legon S, Walters JR. Cellular and regional expression of transcripts of the plasma membrane calcium pump PMCA1 in rabbit intestine. Am J Physiol 1995;269:126-131.

297. Yamaguchi K, Nalesnik MA, Michalopoulos GK. Hepatocyte growth factor mRNA in human liver cirrhosis as evidenced by *in situ* hybridisation. Scand J Gastroenterol 1996;31:921-927.

298. Myatt N, Coghill G, Morrison K, Jones D, Cree IA. Detection of tumour necrosis factor α in sarcoidosis and tuberculosis granulomas using *in situ* hybridisation. J Clin Pathol 1994;47:423-426.

299. Yokota K, Matsue H, Shibaki A, Kawashima T, Kobayashi H, Ohkawara A. Identification of mRNA-rich keratinocytes in the basal/suprabasal layers of psoriatic skin. J Dermatol 1996;23:858-862.

300. Ohno I, Lea RG, Flanders KC, Clark DA, Banwatt D, Dolovich J, Denburg J, Harley CB, Gauldie J, Jordana M. Eosinophils in chronically inflamed human upper airway tissues express transforming growth factor β 1 gene. J Clin Invest 1992;89:1662-1668.

301. Wantzin GL, Philip P, Killmann SA. Cytoplasmic labelling of eosinophils with tritiated thymidine triphosphate. Biomedicine 1979;31:10-11.

302. Mezey E, Hoffman BJ, Harta G, Palkovits M, Northup J. Potential problems in using [35S]-dATP-tailed oligonucleotides for detecting mRNAs in certain cells of the immune system. J Histochem Cytochem 1994;42:1277-1283.

303. Garrett KL, Grounds MD, Beilharz MW. Nonspecific binding of nucleic acid probes to Paneth cells in the gastrointestinal tract with *in situ* hybridisation. J Histochem Cytochem 1992;40:1613-1618.

304. Venge P. The eosinophil in inflammation. In: Venge P, Lindbom A, eds. Inflammation. Basic mechanisms, tissue injuring principles and clinical models. First Ed. Stockholm: Almqvist & Wiskell International, 1985:85-103.

305. Peterson CGB, Jornvall H, Venge P. Purification and characterisation of eosinophil cationic protein from normal human eosinophils. Eur J Haematol 1988;40:415-423.

306. Stenberg E, Persson B, Roos H, Urbaniczky C. Quantitative determination of surface concentration of protein with surface plasmon resonance by using radiolabelled proteins. J Colloid Interface Sci 1991;143:513-526.

307. Lofas S, Johnsson B. A novel hydrogel matrix on gold surfaces in surface plasmon resonance sensors for fast and efficient covalent immobilisation of ligands. J Chem Soc 1990;21:1526-1528.

308. Righetti PG, Caravaggio T. Isoelectric Points and Molecular Weights of proteins: a table. J Chromatog 1976;127:1-28.

309. Alam SM, Travers PJ, Wung JL, Nasholds W, Redpath S, Jameson SC, Gascoigne NR. T-cell receptor affinity and thymocyte positive selection. Nature 1996;381:616-620.

310. Huber CG, Oefner PJ, Guenther KB. High-resolution liquid chromatography of oligonucleotides on nonporous alkylated styrene-divinylbenzene copolymers. Anal Biochem 1993;212:351-358.

311. Kaltschmidt C, Kaltschmidt B, Henkel T, Stockinger H, Baeuerle PA. Selective recognition of the activated form of transcription factor NFκB by a monoclonal antibody. Biol Chem Hoppe-Seyler 1995;376:9-16.

312. Zabel U, Henkel T, Silva MS, Baeuerle PA. Nuclear uptake control of NFκB by MAD-3, an IκB protein present in the nucleus. EMBO J 1993;12:201-211.

313. Beesley JE. Blocking of endogenous peroxidase. In: Beesley JE, ed. Immunocytochemistry. A Practical Approach. Oxford: IRL Press at Oxford University Press, 1992:209-215.

314. Huang S, Minassian H, More JD. Application of immunofluorescent staining improved by trypsin digestion. Lab Invest 1976;35:383-391.

315. Gerdes J, Becker MHG, Key G, Cattoretti G. Immunohistological detection of tumour growth fraction (Ki-67 antigen) in formalin-fixed and routinely processed tissues. J Pathol 1992;168:85-87.

316. Saverymuttu SH, Camilleri M, Rees H, Lavender JP, Hodgson HJ, Chadwick VS. Indium^{111}-granulocyte scanning in the assessment of disease extent and disease activity in inflammatory bowel disease. A comparison with colonoscopy, histology, and fecal indium^{111}- granulocyte excretion. Gastroenterology 1986;90:1121-1128.

317. Trojanowski JQ, Obrocka MA, Lee VM. A comparison of eight different chromogen protocols for the demonstration of immunoreactive neurofilaments in rat cerebellum using the peroxidase-antiperoxidase method and monoclonal antibodies. J Histochem Cytochem 1983;31:1217-1223.

318. Murch SH, Braegger CP, Walker-Smith JA, MacDonald TT. Location of tumour necrosis factor α by immunohistochemistry in chronic inflammatory bowel disease. Gut 1993;34:1705-1709.

319. Lennox B. Observations on the accuracy of point counting including a description of a new graticule. J Clin Pathol 1975;28:99-103.

320. Baeuerle PA. The inducible transcription activator NFκB: regulation by distinct protein subunits. Biochim Biophys Acta 1991;1072:63-80.

321. Neurath MF, Pettersson S, Meyer zum Bueschenfelde K, Stober W. Local administration of antisense phosphorothioate oligonucleotides to the p65 subunit of NFκB abrogates established experimental colitis in mice. Nat Med 1996;2:998-1004.

322. Schreiber S, Nikolaus S, Hampe J. Activation of NFκB inflammatory bowel disease. Gut 1998;42:477-484.

323. Goodman MJ, Skinner JM, Truelove SC. Abnormalities in the apparently normal bowel mucosa in Crohn's disease. Lancet 1976;1:275-278.

324. Schurmann G, Betzler M, Herbay T, Mattfeldt T, Moller P. Morphological changes of the enteric nervous system in Crohn's disease. Br J Surg 1988;75:1260-1261.

325. Dvorak AM, Silen W. Differentiation between Crohn's disease and other inflammatory conditions by electron microscopy. Ann Surg 1985;201:53-63.

326. Bishop AE, Polak JM, Bryant MG, Bloom SR, Hamilton S. Abnormalities of vasoactive intestinal polypeptide-containing nerves in Crohn's disease. Gastroenterology 1980;79:853-860.

327. O'Morain C, Bishop AE, McGregor GP, Levi AJ, Bloom SR, Polak JM, Peters TJ. Vasoactive intestinal peptide concentrations and immunocytochemical studies in rectal biopsies from patients with inflammatory bowel disease. Gut 1984;25:57-61.

328. Geboes K, Rutgeerts P, Ectors N, Mebis J, Penninckx F, Vantrappen G, Desmet VJ. Major histocompatibility class II expression on the small intestinal nervous system in Crohn's disease. Gastroenterology 1992;103:439-447.

329. Souza HS, Carvalho ATP, Madi K, Lapa e Silva JR, Elia CS. Phenotypic analysis of intestinal non-inflamed mucosa in Crohn's disease: evidence of mononuclear cell depletion in lamina propria. Eur J Gastro Hepatol 1996;8:563-568.

330. Schuermann GM, Aber-Bishop AE, Facer P, Lee JC, Rampton DS, Dore CJ, Polak JM. Altered expression of cell adhesion molecules in uninvolved gut in inflammatory bowel disease. Clin Exp Immunol 1993;94:341-347.

331. Chen F, Kuhn DC, Sun SC, Gaydos LJ, Demers LM. Dependence and reversal of nitric oxide production on NFκB in silica and lipopolysaccharide-induced macrophages. Biochem Biophys Res Comm 1995;214:839-846.

332. Chen F, Sun SC, Kuh DC, Gaydos LJ, Demers LM. Essential role of NFκB activation in silica-induced inflammatory mediator production in macrophages. Biochem Biophys Res Comm 1995;214:985-992.

333. Camplejohn RS. The measurement of intracellular antigens and DNA by multiparametric flow cytometry. J Microsc 1994;176:1-7.

334. Landberg G, Roos G. Antibodies to proliferating cell nuclear antigen as S-phase probes in flow cytometric cell cycle analysis. Cancer Res 1991;51:4570-4574.

335. Menon SD, Qin S, Guy GR, Tan YH. Differential induction of nuclear NFκB by protein phosphatase inhibitors in primary and transformed human cells. Requirement for both oxidation and phosphorylation in nuclear translocation. J Biol Chem 1993;268:26805-26812.

336. Ormerod MG. Analysis of DNA - general methods. In: Ormerod MG, ed. Flow Cytometry. A Practical Approach. Second Ed. Oxford: Oxford University Press, 1994:119-135.

337. Powell JJ, Harvey RS, Thompson RPH. Microparticles in Crohn's disease-has the dust settled? Gut 1996;39:340-341.

338. Powell JJ, Ainley CC, Harvey RS, Mason IM, Kendall MD, Sankey EA, Dhillon AP, Thompson RPH. Characterisation of inorganic microparticles in pigment cells of human gut associated lymphoid tissue. Gut 1996;38:390-395.